

The background of the cover is a collection of watercolor-style abstract shapes in various colors and patterns. The shapes include solid colors like black, grey, pink, orange, and yellow, as well as patterns such as black dots, black lines, and black Y-shapes. The shapes are scattered across the white background, with some overlapping the dark grey title bar.

# Immune monitoring in thoracic malignancies

Pauline L. de Goeje



# Immune Monitoring in Thoracic Malignancies

Pauline L. de Goeje

The work described in this thesis was conducted at the department of Pulmonary Medicine, Erasmus MC, Rotterdam, The Netherlands

Cover design: Emma de Goeje

Layout: Lara Leijtens | [persoonlijkproefschrift.nl](http://persoonlijkproefschrift.nl)

Print: Ridderprint BV | [www.ridderprint.nl](http://www.ridderprint.nl)

ISBN: 978-94-6375-734-8

All rights reserved. No parts of this thesis may be reproduced, stored in a retrieval system of any nature, or transmitted in any form or by any means, without permission of the author, or when appropriate, of the publishers of the publications.

© 2019 Pauline L. de Goeje

# Immune Monitoring in Thoracic Malignancies

## Immunomonitoren in thoracale maligniteiten

Proefschrift

ter verkrijging van de graad van doctor aan de  
Erasmus Universiteit Rotterdam  
op gezag van de  
rector magnificus

Prof.dr. R.C.M.E. Engels

en volgens besluit van het College voor Promoties.  
De openbare verdediging zal plaatsvinden op

dinsdag 4 februari 2020 om 13.30 uur

Pauline Linda de Goeje  
geboren te Delft

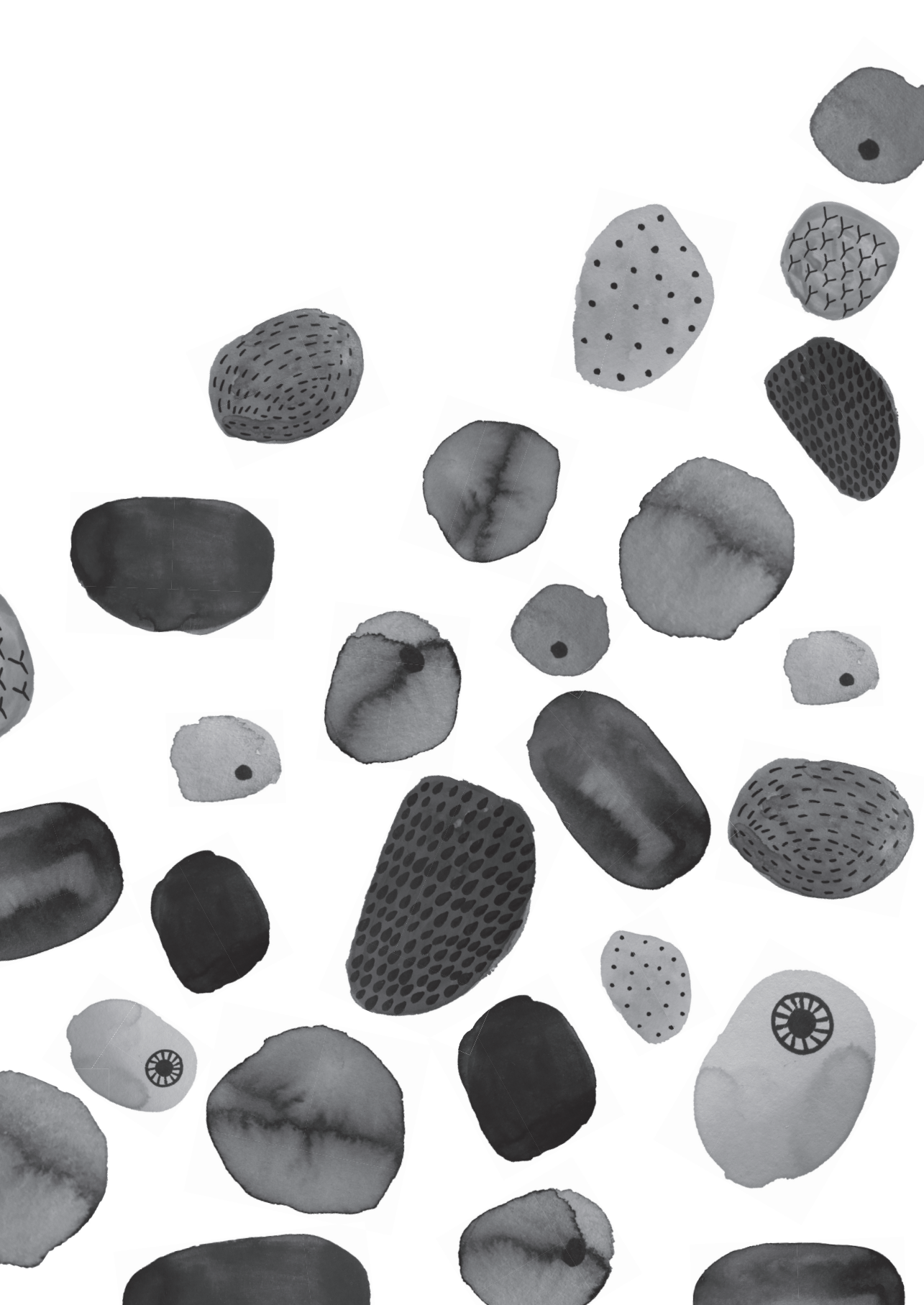
## Promotiecommissie

Promotor(en): Prof.dr. J.G.J.V. Aerts  
Prof.dr. R.W. Hendriks

Overige leden: Prof.dr. A.C. Dingemans  
Prof.dr. P.D. Katsikis  
Prof.dr. E.L.J. Smits

## TABLE OF CONTENTS

Chapter 1	Introduction	6
Chapter 2	Immunoglobulin-like transcript 3 is expressed by myeloid-derived suppressor cells and correlates with survival in patients with non-small cell lung cancer	24
Chapter 3	Stereotactic ablative radiotherapy induces peripheral T-cell activation in early stage lung cancer patients	44
Chapter 4	Induction of peripheral effector CD8 T cell proliferation by paclitaxel/ carboplatin/ bevacizumab in non-small cell lung cancer patients	52
Chapter 5	Predicting survival of lung cancer patients based on their immune profile with a semi-automatic analysis approach	74
Chapter 6	Autologous dendritic cells pulsed with allogeneic tumor cell lysate in mesothelioma: From mouse to human	94
Chapter 7	Autologous dendritic cell therapy in mesothelioma patients enhances frequencies of peripheral CD4 T cells expressing HLA-DR, PD-1 or ICOS	124
Chapter 8	General Discussion	148
Chapter 9	English Summary	164
	Nederlandse Samenvatting	169
	Author affiliations	175
	Dankwoord	179
	PhD Portfolio	183
	About the author	184





# CHAPTER

INTRODUCTION

1

## AN INTRODUCTION TO CANCER

The first description of cancer dates back to around 3000 BC and consisted of a papyrus describing different kinds of tumors and ulcers of the breast for which no treatment existed. At that time, though, it was not called cancer. The Greek physician Hippocrates (460-370 BC) coined the word *carcinos* – meaning crab – to describe tumors, which has later been replaced by the Latin word for crab: *cancer*. Tumors, which are basically lumps of cells in the body, can be benign or malignant. Nowadays, the word cancer is no longer used to describe all tumors; only malignant tumors are defined as cancer.

### Hallmarks of cancer

Various types of cancer exist, depending on the cell of origin. Hanahan and Weinberg in 2000 described six hallmarks of cancer; these were hallmarks that all types of cancer had in common. These included sustaining proliferative signaling, evading growth suppressors, resisting cell death, enabling replicative immortality, inducing angiogenesis, and activating invasion and metastasis [1]. Progressing knowledge has led to a revision of the hallmarks of cancer and four new hallmarks were added in 2011: deregulating cellular energetics, avoiding immune destruction, genome instability and mutation, and tumor-promoting inflammation [2], see figure 1. Together, these hallmarks lead to the development and progression of cancer.

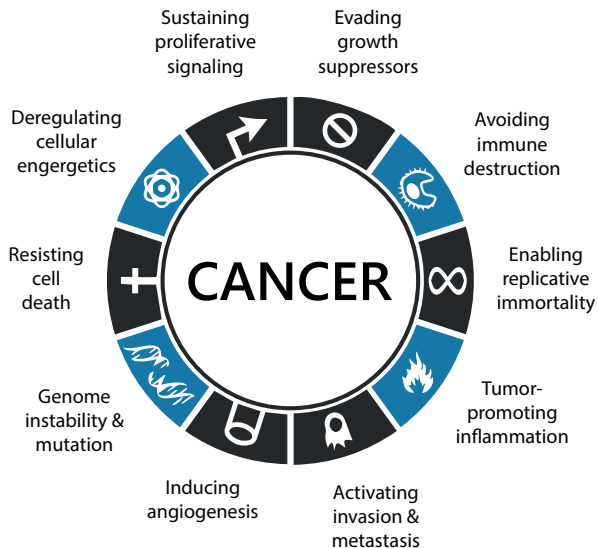


**Figure 1.** The ten hallmarks as defined by Hanahan and Weinberg. Figure adapted from Hanahan & Weinberg, *Cell* 2011. The six hallmarks depicted in black are the hallmarks described in 2000. In 2011, the hallmarks were revisited and four additional hallmarks (depicted in blue) were added.

## Cancer-driving mutations

Normal cells can transform into tumor cells by accumulating several mutations. Examples are mutations in proto-oncogenes and tumor suppressor genes. Proto-oncogenes drive cell proliferation, and upon altered or constitutive activity (*gain of function*) they become oncogenes and may lead to tumor development (hallmark: sustaining proliferative signaling). Examples of oncogenes are *MYC*, a transcription factor inducing cell proliferation, mutated tyrosine kinases of the Ras signaling pathway such as *HRAS*, *KRAS*, and *BRAF*, and growth factor receptors such as epidermal growth factor receptor (EGFR) and vascular endothelial growth factor receptor (VEGFR). Tumor suppressor genes on the other hand prevent cell growth and division, so inactivation or deletion (*loss of function*) of both copies of the tumor suppressor gene can lead to uncontrolled cell division (hallmark: evading growth suppressors). Frequently mutated tumor suppressor genes include *RB1*, encoding retinoblastoma 1, and *TP53*, encoding tumor protein 53. Rb and p53 are both regulators of the cell cycle, preventing the cell from entering the S phase until it is ready to divide [3].

## Stages of cancer

In the early stages of cancer, the tumor is confined to one local site. It becomes malignant once it starts to invade surrounding tissue. When the tumor progresses, individual tumor cells may travel via the lymphatic system to the lymph node and develop into regional a metastasis or travel further to develop metastases at distant organs. These different stages of tumor progression are classified as stage I-IV, in which in general stage I-II represent localized cancer, stage III includes regional metastases and stage IV distant metastases. Survival rates - although greatly varying between cancer types - decrease with each stage, with most cancer patients dying from metastatic disease.

## Cancer treatment

Various cancer treatments have been developed over the years, and the type of treatment depends amongst others on the stage of cancer. When the tumor is locally confined, the tumor is often surgically removed. Radiotherapy is the second treatment option which is often used in early stage tumors, for example when a patient is unfit for surgical treatment or the tumor is in a location that is difficult to reach. Radiotherapy acts via the induction of DNA damage, eventually leading to death of tumor cells. Another class of cancer drugs are chemotherapeutic agents that have been developed since the 1950s and are usually administered systemically to treat cancers that have already spread to lymph nodes or other organs. Chemotherapy affects all dividing cells in the body, and hence has significant side effects. Increased understanding of the molecular changes in cancer cells has led to the development of targeted therapies since the 1970s. These therapies specifically target certain genomic alterations or pathways, such as the oncogene EGFR which is frequently

mutated in lung cancer and thereby driving cancer growth. Inhibiting aberrant EGFR signaling by small molecules can inhibit tumor growth [4]. Lastly, next to direct tumor cell killing as induced by the previously mentioned strategies, immunotherapy has emerged as a new treatment modality over the last decades. Immunotherapy focuses on activating the patient's own immune system to eradicate the tumor, aiming to reverse the hallmarks of evading immune destruction and tumor-promoting inflammation. This treatment strategy is discussed in more detail later in this chapter.

## **THORACIC MALIGNANCIES**

This thesis focuses on thoracic malignancies, which include lung cancer and mesothelioma. Lung cancer has the highest cancer mortality worldwide, with an estimated number of 1.6 million deaths in 2012 [5]. Two main classes of lung cancer are identified: small cell lung cancer, and non-small cell lung cancer. Below, the etiology, prevalence, prognosis and treatment of the two lung cancer subtypes and mesothelioma are discussed.

### **Small cell lung cancer**

Small-cell lung cancer (SCLC) – also referred to as oat-cell carcinoma – was first discovered as being a type of lung cancer in 1926 [6]. It is a specific type of lung cancer with neuroendocrine properties and relatively poorly differentiated cells. This type of lung cancer accounts for 12-15% of all lung cancer cases and is – compared to other subtypes – most strongly associated with smoking. The tumor suppressor genes *RB1* and *TP53* are inactivated in most SCLC cancers. SCLC is characterized by a high mutational burden and minor immune infiltrates. It is highly proliferative and metastasis generally occurs at an early stage, making it a particularly aggressive cancer. The five-year survival rate is around 1-5% [7]. Treatment opportunities have remained equal for several decades, but with increasing insights in the biology and a renewed interest in SCLC research over the last years, it is believed that clinical advancements will be achieved in the coming decade [6].

### **Non-small cell lung cancer**

Non-small cell lung cancer (NSCLC) accounts for ~85% of all lung cancer cases, and can be divided in the subtypes adenocarcinoma, squamous cell carcinoma and large cell carcinoma, depending on the originating cell type. As for SCLC, the main risk factor for NSCLC is smoking, with an estimated ~80% of cases to be caused by smoking. However, a growing proportion of non-smoking NSCLC cases is observed [8]. Treatment of NSCLC depends mainly on cancer stage. In early stage, localized NSCLC, most cancers are either surgically removed, or treated by stereotactic ablative body radiation (SABR), also called stereotactic

body radiation therapy (SBRT). The choice for either of these two treatments is made by the treating physician and the patient and is usually dependent on the overall fitness of the patient and the location of the tumor. Despite the curative intent of these treatments, the majority of patients face a recurrence of the disease, often subsequently progressing to an advanced stage. The majority of patients are diagnosed with an advanced stage disease, when the tumor has already spread to the lymph nodes (regional spread, 22%) or other organs such as liver, bone or brain (distant spread, 57%) [9]. In these advanced stages of NSCLC, patients with specific gene mutations can be treated with targeted therapy (e.g. EGFR, anaplastic lymphoma kinase [ALK] or BRAF inhibitors), but most patients are treated with chemotherapy. In 2015, the first immunotherapy for second-line treatment of NSCLC, the anti-PD1 checkpoint inhibitor pembrolizumab (see below) was approved by the FDA, and approval and use of this and other PD-1/PD-L1 inhibitors has been greatly expanded over the following years. Currently, in 2019, combination of chemotherapy + checkpoint inhibition is the standard first-line treatment for advanced stage NSCLC patients without specific mutations, with low PD-L1 expression. In patients with high PD-L1 expression, either this combination or pembrolizumab monotherapy can be chosen as the preferred treatment.

### **Pleural mesothelioma**

Pleural mesothelioma is a much rarer type of cancer than lung cancer and affects the pleural lining of the lungs. The yearly death rate is 3000 in the US and 5000 in Europe [10]. Mesothelioma is almost exclusively caused by asbestos exposure, with in general a lag time of 20-50 years between exposure and diagnosis. Asbestos use has been banned in many countries, but due to this long incubation time, the incidence is still increasing in most countries. Also, asbestos is still redundantly present in the western world as it is incorporated in buildings, water pipes, etc. Moreover, asbestos is still frequently used in for example Russia, China, Brazil and Kazakhstan [11]. Treatment options for mesothelioma are very limited, and median survival after diagnosis is less than one year [10]. As no known therapeutic targets are present in mesothelioma, patients are usually treated with chemotherapy but with modest improvement of survival. Mesothelioma can also develop from the peritoneum, in which case it is referred to as peritoneal mesothelioma or abdominal mesothelioma.

## **AN INTRODUCTION TO THE IMMUNE SYSTEM**

The immune system protects our body from invading pathogens by distinguishing “self” from “non-self” and triggering immune responses when needed, but is also equipped to fight tumor development and progression. The innate arm of immunity is quick and less specific,

whereas adaptive immunity is slower, highly specific and able to induce 'memory', allowing a stronger and quicker response if the same pathogen is encountered again. Different types of immune cells exist and collaborate to induce an effective immune response, to inhibit immune responses if not needed, and to facilitate tissue repair. Immune cells of the myeloid lineage are mainly involved in innate immunity. These include granulocytes, monocytes and macrophages. Dendritic cells (DC), also from the myeloid lineage, form the bridge between innate and adaptive immunity by sampling from their environment and presenting antigens to T cells. Lymphoid cells include NK cells, T cells, B cells and innate lymphoid cells (ILCs). B cells and T cells are part of adaptive immunity and each cell is specific for one antigen. B cells produce antibodies recognizing the specific antigen (humoral response), while T cells use their T cell receptor to recognize specific antigens presented on major histocompatibility complexes (MHC) of a cell. Cytotoxic T cells (expressing CD8) kill infected or transformed cells presenting the specific antigen that the T cells recognize. T helper cells (expressing CD4) are needed to fully activate and differentiate B cells and cytotoxic T cells. Regulatory T cells on the other hand are suppressing immune responses. T cells are able to greatly expand in numbers once they are activated. They will differentiate from naïve to effector and memory T cell subsets. After the immune response subsides, part of the memory T cells will remain present, ready to respond quickly when the antigen reoccurs [12].

## **THE ROLE OF THE IMMUNE SYSTEM IN CANCER**

Instead of just malignant cells, the tumor consists of a mix of different cell types, apart from tumor cells including stromal cells and immune cells. Together these cells create the tumor microenvironment (TME), of which the composition can greatly influence cancer progression and response to treatment [13]. In the updated version from Hanahan and Weinberg's Hallmarks of cancer in 2011, two hallmarks were added indicating the role of the immune system in the development of cancer: the enabling characteristic of inflammation and the emerging hallmark of evading immune destruction [2]. These hallmarks show the paradoxical role of the immune system in cancer: inflammation enables the tumor to develop (pro-tumor immunity), while the tumor has to evade recognition and killing by the immune system (anti-tumor immunity). Indeed, different immune cells have been known to play opposing roles in relation to cancer. In Table 1, the effect of the presence/ number of various immune cells in the tumor or peripheral blood on the overall or progression free survival of cancer patients are summarized. While for some cell types their effects are clearly positive or negative, for some other cell types some controversy still exists in literature or their effect is dependent on cancer type. This list comprises a summary of meta-analyses and is by all means not complete, as there are many more individual studies describing

links between immune cells and clinical outcome in cancer. An example is innate lymphoid cells (ILCs), which are found to be present in the tumor environment and may contribute to both tumor growth and metastasis as well as anti-tumor immunity [14].

**Table 1.** Effect of immune cells on outcome of cancer patients, summary of meta-analyses

<b>Immune cell</b>	<b>effect on outcome</b>	<b>tumor type</b>	<b>blood/ reference tumor</b>
<b>CD3 T cells</b>	positive	various cancers (overall effect)	tumor Gooden et al. BJC 2011 [15]
	positive	NSCLC	tumor Zeng et al. Oncotarget 2016 [16]; Soo et al. Oncotarget 2018 [17]
	positive	HNSCC	tumor De Ruiten et al. Oncoimmunology 2017 [18]
	positive	gastric cancer	tumor Zheng et al. Oncotarget 2017 [19]
	positive	hepatocellular carcinoma	tumor Yao et al. Sci Rep. 2017 [20]
	no effect	esophageal cancer	tumor Zheng et al. Cell Phys Biochem 2018 [21]
<b>CD4 T cells</b>	positive	NSCLC	tumor Zeng et al. Oncotarget 2016 [16]
	no effect; stromal cells	NSCLC	tumor Soo et al. Oncotarget 2018 [17]
	positive effect		
	questionable / ambiguous	HNSCC	tumor De Ruiten et al. Oncoimmunology 2017 [18]
	no effect	gastric cancer	tumor Zheng et al. Oncotarget 2017 [19]
	no effect on OS; positive on RFS	hepatocellular carcinoma	tumor Yao et al. Sci Rep. 2017 [20]
	no effect	esophageal cancer	tumor Zheng et al. Cell Phys Biochem 2018 [21]
<b>CD8 T cells</b>	positive	various cancers (overall effect)	tumor Gooden et al. BJC 2011 [15]
	positive	triple negative breast cancer	tumor Ibrahim et al. Breast Cancer Res Treat 2014 [22]
	positive	NSCLC	tumor Zeng et al. Oncotarget 2016 [16]
	positive	HNSCC	tumor De Ruiten et al. Oncoimmunology 2017 [18]
	positive	gastric cancer	tumor Zheng et al. Oncotarget 2017 [19]
	positive	hepatocellular carcinoma	tumor Yao et al. Sci Rep. 2017 [20]
	positive	esophageal cancer	tumor Zheng et al. Cell Phys Biochem 2018 [21]

<b>regulatory T cells</b>	negative	breast cancer (overall)	tumor	Jiang et al. BMC Cancer 2015 [23]; Shou et al BMC Cancer. 2016 [24]
	negative	cervical, renal, melanoma, breast, lung	tumor	Shang et al. Sci Rep. 2015 [25]
	negative	NSCLC	tumor	Zeng et al. Oncotarget 2016 [16]
	negative	various cancers (overall effect)	tumor	Shang et al. Sci Rep. 2015 [25]
	negative	hepatocellular carcinoma	tumor	Yao et al. Sci Rep. 2017 [20]
	no effect	various cancers (overall effect)	tumor	Gooden et al. BJC 2011 [15]
	positive	triple negative breast cancer	tumor	Jiang et al. BMC Cancer 2015 [23]
	positive	colorectal, head and neck, esophageal	tumor	Shang et al. Sci Rep. 2015 [25]
<b>B cells</b>	positive	NSCLC	tumor	De Ruiter et al. Oncoimmunology 2017 [18]
	positive	gastric cancer	tumor	Soo et al. Oncotarget 2018 [17]
<b>NK cells</b>	positive	NSCLC	tumor	Zheng et al. Oncotarget 2017 [19]
	positive	gastric cancer	tumor	Soo et al. Oncotarget 2018 [17]
	positive	esophageal cancer	tumor	Zheng et al. Oncotarget 2017 [19]
<b>TAM</b>	negative	NSCLC	tumor	Zheng et al. Cell Phys Biochem 2018 [21]
	positive	lung cancer	tumor	Soo et al. Oncotarget 2018 [17]
<b>M1 macrophages</b>	positive	lung cancer	tumor	Wu et al. Oncotarget 2016 [26]; Soo et al. Oncotarget 2018 [17]
	negative	NSCLC	tumor	Wu et al. Oncotarget 2016 [26]
<b>M2 macrophages</b>	positive	various cancers (overall effect)	tumor	Soo et al. Oncotarget 2018 [17]
	negative	various cancers (overall effect)	tumor	Shen et al. PLoS ONE 2014 [27]
<b>dendritic cells</b>	negative	various cancers (overall effect)	blood	Wang et al. Oncoimmunology 2018 [28]
	negative	NSCLC	blood	Gu et al. Sci Rep. 2015 [29]; Yin et al. Clinics 2015 [30]
<b>neutrophils</b>	negative	renal cell carcinoma	blood	Hu et al. BMJ open 2014 [31]
	negative	pancreatic cancer	blood	Yang et al. World J Gastroenterol 2015 [32]
<b>MDSC</b>	negative	colorectal cancer	blood	Li et al. Int J Cancer 2013 [33]
	negative	various cancers (overall effect)	blood	Templeton et al. J Natl Cancer Inst 2014 [34]
	negative	urinary cancers	blood	Wei et al. PLoS ONE 2014 [35]
	negative	various cancers (overall effect)	blood	Zhou et al. PLoS ONE 2014 [36]
<b>NLR</b>	negative	various cancers (overall effect)	blood	Zhou et al. PLoS ONE 2014 [36]
	positive	various cancers (overall effect)	blood	Nishijima et al. Cancer Treatment Rev 2015 [37]
<b>PLR</b>	positive	various cancers (overall effect)	blood	Nishijima et al. Cancer Treatment Rev 2015 [37]
<b>LMR</b>	positive	various cancers (overall effect)	blood	Nishijima et al. Cancer Treatment Rev 2015 [37]

*TAM = tumor associated macrophage; NLR = neutrophil-lymphocyte ratio; PLR = platelet-lymphocyte ratio; LMR = lymphocyte-monocyte ratio; MDSC = myeloid-derived suppressor cell; NSCLC = non-small cell lung carcinoma; HNSCC = head and neck squamous cell carcinoma*



## The cancer immunity cycle

Besides protecting our bodies against invading pathogens, our immune system also recognizes transformed cells and prevents them from developing into a tumor. This has been described in a model posed by Chen and Mellman in 2013: the cancer immunity cycle (Figure 2) [38]. Cancer cells harbor various alterations compared to their healthy counterparts, which leads to tumor-specific or tumor-associated antigens. These antigens can be picked up by DCs, which upon activation travel to the tumor draining lymph node where they can activate T cells that are specific for that antigen, leading to proliferation and differentiation of T cells. Subsequently the T cell migrates via the blood to the tumor, where the cytotoxic T cells can recognize and kill the tumor cells. On the other hand, tumor cells may also accumulate mutations that increase their capacity to evade recognition by the immune system. They for example downregulate expression of tumor antigens to prevent recognition by the immune system or recruit immune suppressive cells such as regulatory T cells and myeloid-derived suppressor cells (MDSCs) [39] that are able to dampen the immune response.

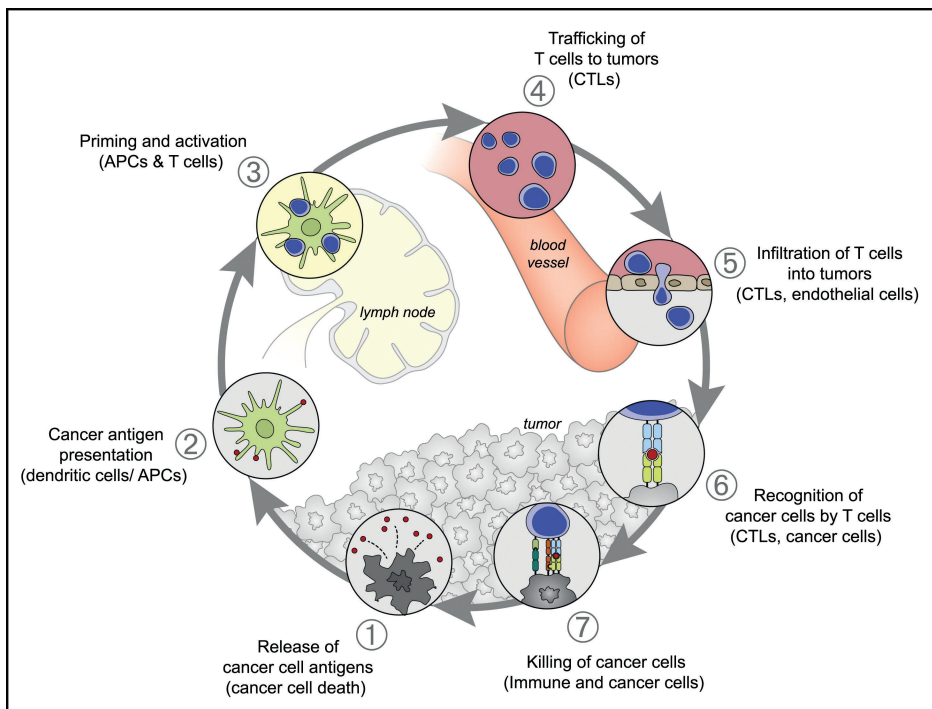


**Figure 2.** The Cancer Immunity Cycle. Reprinted from *Immunity*, Volume 39 issue 1, Chen DS and Mellman I, *Oncology Meets Immunology: The Cancer-Immunity Cycle*, Pages 1-10, Copyright (2013), with permission from Elsevier.

## **Immune surveillance**

The recognition and destruction of transformed cells by our immune system is called immune surveillance. Three different stages of immune surveillance are described, the three E's: elimination, equilibrium and escape. When the immune system recognizes and kills the transformed cells, the tumor is eliminated. However, if some tumor cells remain, they can accumulate additional mutations or other modifications to evade the immune response. In this equilibrium phase, there is a balance between the anti-tumor immune response and the evading capacity of the tumor cells. Over time, tumor cells with a survival benefit will grow out, which eventually may lead to escape, in which the tumor has overcome immune destruction and is able to grow and/or metastasize. Tumors may employ various mechanisms to escape immune destruction. Immune-deserted tumors for example, have prevented induction of a proper anti-tumor immune response by preventing priming or inducing tolerance or immune ignorance. Immune-excluded tumors have created an impenetrable or hostile tumor microenvironment, in which tumor-reactive immune cells cannot infiltrate. Lastly, if immune cells are able to infiltrate the tumor (inflamed tumor), they might be hampered or suppressed by a very immune suppressive microenvironment, caused by the presence of immune suppressive cells or the secretion or expression of various immune suppressive factors such as immune suppressive cytokines or inhibitory ligands.

## **IMMUNOTHERAPIES**

Over the last years, scientific knowledge and interest in the role of the immune system in cancer has greatly expanded. These increasing insights have led to several treatment strategies actively targeting the immune system to combat cancer. Immunotherapeutic strategies can be divided in the following classes: monoclonal antibodies, checkpoint inhibitors, adoptive cell transfer, therapeutic vaccines, and other immunomodulatory compounds such as cytokines.

**Monoclonal antibodies** can be targeted against specific tumor antigens and induce tumor killing via several mechanisms. For example, they may induce antibody-dependent cellular toxicity (ADCC) or deliver an anti-cancer drug specifically to the tumor (antibody-drug conjugate; ADC). Furthermore, monoclonal antibodies might target components of the immune system that may in turn be activated, suppressed or recruited, thereby indirectly targeting the tumor.

**Checkpoint inhibitors** are a class of compounds, which may also be monoclonal antibodies, that inhibit checkpoint molecules on T cells. These checkpoint molecules confer inhibitory signals to the T cell and hence act as a break on their activation. By inhibiting these receptors, T cells can be reinvigorated and thereby enhancing the anti-tumor immune response. Checkpoint inhibitors against cytotoxic T-lymphocyte-associated protein 4 (CTLA-4) and programmed death receptor (PD)-1 were the first to be approved by the FDA and have revolutionized cancer treatment [40-42]. These checkpoint inhibitors are most effective in tumors with a high mutational burden and strong immune infiltration (so called 'hot' tumors) [43-46].

**Adoptive cell transfer** uses immune cells – usually T cells – from a cancer patient, which are expanded and/or modulated *ex vivo* and subsequently transferred back into the patient to boost the immune response. For this treatment strategy, tumor-infiltrating T lymphocytes (TILs) can be used, or T cells with a modified T cell receptor to recognize a certain tumor antigen. Chimeric antigen receptors (CARs) are an example of such modified receptor. These receptors consist of an antigen recognition domain and domains needed for the activation of the T cell. CAR T cells have been very successful in hematological cancers [47, 48].

The strategy of **therapeutic vaccination** aims to induce or boost the immune response against the tumor by exposing the immune system to tumor antigens. For vaccination purposes, whole tumor lysate, peptides or DCs can be used. DCs are the main antigen-presenting cells and can be isolated from blood or cultured *ex vivo* from peripheral blood monocytes. They can be pulsed with peptides, proteins or whole tumor lysate, to present certain antigens on MHC class II or I, the latter via cross-presentation. Our research group has developed a DC vaccination strategy for malignant pleural mesothelioma using monocyte-derived DC pulsed with autologous mesothelioma tumor lysate. As only low numbers of T cells are present in most mesothelioma tumor tissues [49], and DCs are described to be reduced in numbers and functionality in mesothelioma patients [50], this strategy aimed to prime an anti-tumor immune response by delivering activated DCs pulsed with tumor cell lysate. This treatment has been shown to be effective in *in vivo* models [51], and has been shown to be safe in patients [52, 53]. In melanoma and other cancer types DC vaccination has shown promise as well, with strategies employing monocyte-derived DC or blood-derived DC [54-56].

**Other immunomodulatory compounds** include cytokines, for example IL-2 to enhance anti-tumor immune responses in melanoma and renal cell carcinoma [57, 58] and the use of oncolytic viruses that selectively replicate in and kill tumor cells [59].

## **PRECISION MEDICINE AND COMBINATION STRATEGIES**

Immunotherapy has been considered a major breakthrough in the treatment of cancer, with unprecedented responses [40-42]. However, despite long-lasting responses for some patients, the majority of cancer patients does not benefit from treatment with a single checkpoint inhibitor. Due to the heterogeneity and the adaptive ability of cancer, we should aim to target the tumor via multiple hits, sequentially or simultaneously, to further improve response rates and durability of responses. Combination treatment has received a lot of attention recently as becomes evident from published literature [60-64]. Furthermore, there is a dire need for reliable biomarkers that predict response to treatment, which will allow for a better choice of treatment for individual patients. Currently, treatment choices are mostly based on the patient's tumor stage: radiotherapy and surgery for early stage cancers and systemic treatments in advanced stage cancer. The development of targeted therapies has introduced molecular characterization of the tumor to guide treatment strategies: the target mutation or target receptor should be present on the tumor subtype for the treatment to have its effect. For some checkpoint inhibitors, expression of PD-L1 acts as a biomarker, although its clinical value is still debatable [65]. Despite the efforts to find predictive biomarkers in recent years, most treatments are still prescribed with a 'trial-and-error' approach, leading to potentially unnecessary treatments with accompanying side effects. Precision medicine aims to give the right treatment to the right patient, steered by an individual patient's (disease) characteristics. Moreover, as the field moves more and more towards combinatorial treatment strategies, a better understanding of treatment effects and mechanisms of actions is needed to rationally design the most optimal combinations.

## **AIMS AND OUTLINE OF THIS THESIS**

As new medicines are being developed, the number of potential combinations drastically increases. To test all potential combinations in clinical trials is not feasible, and therefore should be guided by solid preclinical data. In this thesis we aimed to increase our understanding of the role of the immune system and its clinical value in patients with thoracic malignancies during treatment. We monitored the effects of several conventional and experimental treatments on the immune profile of patients, and actively exploited the immune system to treat malignant pleural mesothelioma.

To monitor immune modulation by cancer treatment, either tumor or peripheral blood material can be used. Here, we mainly focused on immune cells from peripheral blood, for the following reasons. First, blood samples can be obtained from patients in a minimally

invasive way. This allows for serial collection of patient samples for monitoring responses over time. Blood samples can be obtained even if the tumor is macroscopically absent after treatment. Second, as cancer progresses and metastasizes, it can be regarded as a systemic disease. While tumor biopsies provide information on the local immune response, they are not able to capture the heterogeneity of the tumor and its metastasis, which may differentially respond to treatment [66]. We therefore believe that the peripheral blood represents the general immunological state of a patient and can provide valuable insights into the immune response.

In this thesis, we aimed to increase our understanding of the functional role and clinical value of the immune system and its dynamics in patients with thoracic malignancies, by monitoring immune populations in peripheral blood during treatment.

In **chapter 2**, we focused on an important immune suppressive population present in peripheral blood of cancer patients, of which their function is still largely unknown: MDSC. We studied their clinical value in advanced stage NSCLC patients treated with chemotherapy. Moreover, we further explored potential immune suppressive mechanisms by focusing on the inhibitory receptor immunoglobulin-like transcript (ILT) 3, known for its tolerogenic properties on DC. We assessed expression of ILT3 on MDSC in lung cancer patients with advanced disease before the start of chemotherapy and evaluated its effect on clinical outcome.

In **chapter 3 and 4** we aimed to study the effect of conventional cancer therapies on the peripheral blood immune profile, to address whether these therapies are able to activate or suppress systemic immune activation which may contribute to treatment response. We investigated both activation of T cells, as well as immune-suppressive cell populations. In **chapter 3**, we focused on NSCLC patients with an early stage of disease, who were treated with either surgery or radiotherapy, and assessed treatment effects on the induction of T-cell activation in the early post-treatment period. In **chapter 4** we studied the immune modulatory effects of a chemotherapy/ anti-angiogenesis combination in NSCLC patients with advanced disease and examined whether these were related to clinical outcome.

With advancing techniques such as the increasing number of parameters that can be measured with flow cytometry novel immune cell subpopulations can be identified and cell characteristics, including activation or exhaustion markers, can be analyzed in unprecedented detail. However, the amount of acquired data causes challenges for data analysis. In **chapter 5** we evaluated the use of a novel computational method for the analysis of flow cytometry data for survival prediction, in our cancer immunology setting.

Besides the role of the immune system in responses to conventional therapies, the immune system can be an active target for cancer therapy in emerging immunotherapy strategies. To boost an anti-tumor immune response, DCs can be cultured *ex vivo* and pulsed with tumor lysate. When administered to patients, these activated and mature DCs can induce an anti-tumor immune response. Earlier work by our group on DC vaccination has shown promise as a treatment for mesothelioma. However, the main limitation for scaling up this treatment was the use of autologous tumor material that not always provided sufficient material to pulse the DCs. **Chapter 6** describes a first-in-human trial in which we designed an improved DC immunotherapy for patients with mesothelioma, overcoming this limitation by using allogeneic mesothelioma cell lines. We studied efficacy of this method in mice and assessed safety and feasibility of this therapy in patients.

In **chapter 7** we further investigated the DC immunotherapy approach introduced in chapter 6, by studying immunological changes induced in these patients by treatment, to shed light on the mechanism of action of DC immunotherapy and to identify markers that are suitable for immune monitoring in upcoming DC immunotherapy trials. We asked which immune cell populations alter upon treatment and whether they are related to treatment response. In this study, we aimed to address both broad immune activation, as well as the specificity of the T cells.

The results of chapters 2-7 are summarized and discussed in the context of current literature in **chapter 8**. Furthermore, (clinical) implications and future directions of this research are discussed.

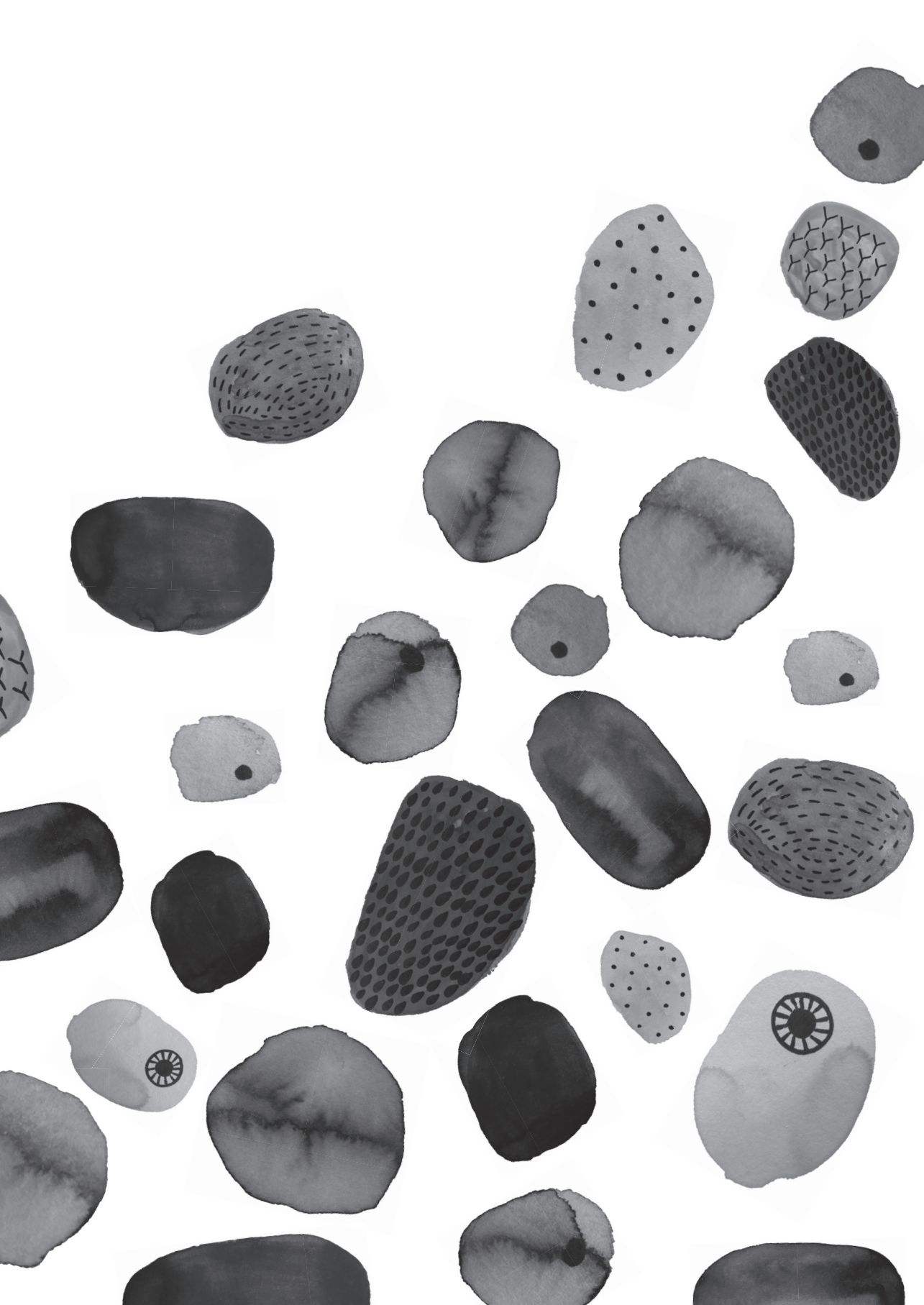
## REFERENCES

1. Hanahan, D. and R.A. Weinberg, *The hallmarks of cancer*. Cell, 2000. **100**(1): p. 57-70.
2. Hanahan, D. and R.A. Weinberg, *Hallmarks of cancer: the next generation*. Cell, 2011. **144**(5): p. 646-74.
3. Weinberg, R.A., *The Biology of Cancer*. 2007: Garland Science, Taylor & Francis Group.
4. Kris, M.G., et al., *Efficacy of gefitinib, an inhibitor of the epidermal growth factor receptor tyrosine kinase, in symptomatic patients with non-small cell lung cancer: a randomized trial*. JAMA, 2003. **290**(16): p. 2149-58.
5. Ferlay, J., et al., *Cancer incidence and mortality worldwide: sources, methods and major patterns in GLOBOCAN 2012*. Int J Cancer, 2015. **136**(5): p. E359-86.
6. Gazdar, A.F., P.A. Bunn, and J.D. Minna, *Small-cell lung cancer: what we know, what we need to know and the path forward*. Nat Rev Cancer, 2017. **17**(12): p. 765.
7. Nicholson, A.G., et al., *The International Association for the Study of Lung Cancer Lung Cancer Staging Project: Proposals for the Revision of the Clinical and Pathologic Staging of Small Cell Lung Cancer in the Forthcoming Eighth Edition of the TNM Classification for Lung Cancer*. J Thorac Oncol, 2016. **11**(3): p. 300-11.
8. Cufari, M.E., et al., *Increasing frequency of non-smoking lung cancer: Presentation of patients with early disease to a tertiary institution in the UK*. Eur J Cancer, 2017. **84**: p. 55-59.
9. *SEER 18 Cancer Statistics 2008-2014*. 2 July 2018]; Available from: <https://www.seer.cancer.gov>.
10. Yap, T.A., et al., *Novel insights into mesothelioma biology and implications for therapy*. Nat Rev Cancer, 2017. **17**(8): p. 475-488.
11. Straif, K., et al., *A review of human carcinogens 2014; Part C: metals, arsenic, dusts, and fibres*. The Lancet Oncology, 2009. **10**(5): p. 453-454.
12. Murphey, K. and C. Weaver, *Janeway's Immunobiology, 9th edition*. 2016: Ww Norton & Co.
13. Hanahan, D. and L.M. Coussens, *Accessories to the crime: functions of cells recruited to the tumor microenvironment*. Cancer Cell, 2012. **21**(3): p. 309-22.
14. Chirossone, L., et al., *Natural killer cells and other innate lymphoid cells in cancer*. Nat Rev Immunol, 2018. **18**(11): p. 671-688.
15. Gooden, M.J., et al., *The prognostic influence of tumour-infiltrating lymphocytes in cancer: a systematic review with meta-analysis*. Br J Cancer, 2011. **105**(1): p. 93-103.
16. Zeng, D.Q., et al., *Prognostic and predictive value of tumor-infiltrating lymphocytes for clinical therapeutic research in patients with non-small cell lung cancer*. Oncotarget, 2016. **7**(12): p. 13765-81.
17. Soo, R.A., et al., *Prognostic significance of immune cells in non-small cell lung cancer: meta-analysis*. Oncotarget, 2018. **9**(37): p. 24801-24820.
18. de Ruyter, E.J., et al., *The prognostic role of tumor infiltrating T-lymphocytes in squamous cell carcinoma of the head and neck: A systematic review and meta-analysis*. Oncoimmunology, 2017. **6**(11): p. e1356148.
19. Zheng, X., et al., *Prognostic role of tumor-infiltrating lymphocytes in gastric cancer: a meta-analysis*. Oncotarget, 2017. **8**(34): p. 57386-57398.
20. Yao, W., et al., *The Prognostic Value of Tumor-infiltrating Lymphocytes in Hepatocellular Carcinoma: a Systematic Review and Meta-analysis*. Sci Rep, 2017. **7**(1): p. 7525.
21. Zheng, X., et al., *Prognostic Role of Tumor-Infiltrating Lymphocytes in Esophagus Cancer: a Meta-Analysis*. Cell Physiol Biochem, 2018. **45**(2): p. 720-732.
22. Ibrahim, E.M., et al., *The prognostic value of tumor-infiltrating lymphocytes in triple-negative breast cancer: a meta-analysis*. Breast Cancer Res Treat, 2014. **148**(3): p. 467-76.
23. Jiang, D., et al., *Clinicopathological and prognostic significance of FOXP3+ tumor infiltrating lymphocytes in patients with breast cancer: a meta-analysis*. BMC Cancer, 2015. **15**: p. 727.
24. Shou, J., et al., *Worse outcome in breast cancer with higher tumor-infiltrating FOXP3+ Tregs : a systematic review and meta-analysis*. BMC Cancer, 2016. **16**: p. 687.

25. Shang, B., et al., *Prognostic value of tumor-infiltrating FoxP3+ regulatory T cells in cancers: a systematic review and meta-analysis*. *Sci Rep*, 2015. **5**: p. 15179.
26. Wu, P., et al., *Inverse role of distinct subsets and distribution of macrophage in lung cancer prognosis: a meta-analysis*. *Oncotarget*, 2016. **7**(26): p. 40451-40460.
27. Shen, M., et al., *Tumor-associated neutrophils as a new prognostic factor in cancer: a systematic review and meta-analysis*. *PLoS One*, 2014. **9**(6): p. e98259.
28. Wang, P.-F., et al., *Prognostic role of pretreatment circulating MDSCs in patients with solid malignancies: A meta-analysis of 40 studies*. *Oncol Immunology*, 2018: p. 1-14.
29. Gu, X.B., et al., *Prognostic significance of neutrophil-to-lymphocyte ratio in non-small cell lung cancer: a meta-analysis*. *Sci Rep*, 2015. **5**: p. 12493.
30. Yin, Y., et al., *Prognostic value of the neutrophil to lymphocyte ratio in lung cancer: A meta-analysis*. *Clinics (Sao Paulo)*, 2015. **70**(7): p. 524-30.
31. Hu, K., et al., *Prognostic role of the neutrophil-lymphocyte ratio in renal cell carcinoma: a meta-analysis*. *BMJ Open*, 2015. **5**(4): p. e006404.
32. Yang, J.J., et al., *Prognostic significance of neutrophil to lymphocyte ratio in pancreatic cancer: a meta-analysis*. *World J Gastroenterol*, 2015. **21**(9): p. 2807-15.
33. Li, M.X., et al., *Prognostic role of neutrophil-to-lymphocyte ratio in colorectal cancer: a systematic review and meta-analysis*. *Int J Cancer*, 2014. **134**(10): p. 2403-13.
34. Templeton, A.J., et al., *Prognostic role of neutrophil-to-lymphocyte ratio in solid tumors: a systematic review and meta-analysis*. *J Natl Cancer Inst*, 2014. **106**(6): p. dju124.
35. Wei, Y., Y.Z. Jiang, and W.H. Qian, *Prognostic role of NLR in urinary cancers: a meta-analysis*. *PLoS One*, 2014. **9**(3): p. e92079.
36. Zhou, X., et al., *Prognostic value of PLR in various cancers: a meta-analysis*. *PLoS One*, 2014. **9**(6): p. e101119.
37. Nishijima, T.F., et al., *Prognostic value of lymphocyte-to-monocyte ratio in patients with solid tumors: A systematic review and meta-analysis*. *Cancer Treat Rev*, 2015. **41**(10): p. 971-8.
38. Chen, D.S. and I. Mellman, *Oncology meets immunology: the cancer-immunity cycle*. *Immunity*, 2013. **39**(1): p. 1-10.
39. Gabrilovich, D.I., *Myeloid-Derived Suppressor Cells*. *Cancer Immunol Res*, 2017. **5**(1): p. 3-8.
40. Robert, C., et al., *Ipilimumab plus dacarbazine for previously untreated metastatic melanoma*. *N Engl J Med*, 2011. **364**(26): p. 2517-26.
41. Weber, J.S., et al., *Nivolumab versus chemotherapy in patients with advanced melanoma who progressed after anti-CTLA-4 treatment (CheckMate 037): a randomised, controlled, open-label, phase 3 trial*. *Lancet Oncol*, 2015. **16**(4): p. 375-84.
42. Mok, T.S.K., et al., *Pembrolizumab versus chemotherapy for previously untreated, PD-L1-expressing, locally advanced or metastatic non-small-cell lung cancer (KEYNOTE-042): a randomised, open-label, controlled, phase 3 trial*. *Lancet*, 2019. **393**(10183): p. 1819-1830.
43. Yarchoan, M., A. Hopkins, and E.M. Jaffee, *Tumor Mutational Burden and Response Rate to PD-1 Inhibition*. *N Engl J Med*, 2017. **377**(25): p. 2500-2501.
44. Samstein, R.M., et al., *Tumor mutational load predicts survival after immunotherapy across multiple cancer types*. *Nat Genet*, 2019. **51**(2): p. 202-206.
45. Gajewski, T.F., et al., *Cancer Immunotherapy Targets Based on Understanding the T Cell-Inflamed Versus Non-T Cell-Inflamed Tumor Microenvironment*. *Adv Exp Med Biol*, 2017. **1036**: p. 19-31.
46. Van Allen, E.M., et al., *Genomic correlates of response to CTLA-4 blockade in metastatic melanoma*. *Science*, 2015. **350**(6257): p. 207-211.
47. Neelapu, S.S., et al., *Axicabtagene Ciloleucel CAR T-Cell Therapy in Refractory Large B-Cell Lymphoma*. *N Engl J Med*, 2017. **377**(26): p. 2531-2544.
48. Maude, S.L., et al., *Chimeric antigen receptor T cells for sustained remissions in leukemia*. *N Engl J Med*, 2014. **371**(16): p. 1507-17.
49. Coussens, L.M., L. Zitvogel, and A.K. Palucka, *Neutralizing tumor-promoting chronic inflammation: a magic bullet?* *Science*, 2013. **339**(6117): p. 286-91.
50. Cornwall, S.M., et al., *Human mesothelioma induces defects in dendritic cell numbers and antigen-processing function which predict survival outcomes*. *Oncoimmunology*, 2016. **5**(2): p. e1082028.



51. Hegmans, J.P., et al., *Immunotherapy of murine malignant mesothelioma using tumor lysate-pulsed dendritic cells*. *Am J Respir Crit Care Med*, 2005. **171**(10): p. 1168-77.
52. Cornelissen, R., et al., *Extended Tumor Control after Dendritic Cell Vaccination with Low-Dose Cyclophosphamide as Adjuvant Treatment in Patients with Malignant Pleural Mesothelioma*. *Am J Respir Crit Care Med*, 2016. **193**(9): p. 1023-31.
53. Hegmans, J.P., et al., *Consolidative dendritic cell-based immunotherapy elicits cytotoxicity against malignant mesothelioma*. *Am J Respir Crit Care Med*, 2010. **181**(12): p. 1383-90.
54. Aarntzen, E.H., et al., *Vaccination with mRNA-electroporated dendritic cells induces robust tumor antigen-specific CD4+ and CD8+ T cells responses in stage III and IV melanoma patients*. *Clin Cancer Res*, 2012. **18**(19): p. 5460-70.
55. Bol, K.F., et al., *Favorable overall survival in stage III melanoma patients after adjuvant dendritic cell vaccination*. *Oncoimmunology*, 2016. **5**(1): p. e1057673.
56. Schreiberl, G., et al., *Effective Clinical Responses in Metastatic Melanoma Patients after Vaccination with Primary Myeloid Dendritic Cells*. *Clin Cancer Res*, 2016. **22**(9): p. 2155-66.
57. Clark, J.I., et al., *Impact of Sequencing Targeted Therapies With High-dose Interleukin-2 Immunotherapy: An Analysis of Outcome and Survival of Patients With Metastatic Renal Cell Carcinoma From an On-going Observational IL-2 Clinical Trial: PROCLAIM(SM)*. *Clin Genitourin Cancer*, 2017. **15**(1): p. 31-41 e4.
58. Rosenberg, S.A., et al., *Treatment of 283 consecutive patients with metastatic melanoma or renal cell cancer using high-dose bolus interleukin 2*. *JAMA*, 1994. **271**(12): p. 907-13.
59. Kaufman, H.L., F.J. Kohlhapp, and A. Zloza, *Oncolytic viruses: a new class of immunotherapy drugs*. *Nat Rev Drug Discov*, 2015. **14**(9): p. 642-62.
60. Horn, L., et al., *First-Line Atezolizumab plus Chemotherapy in Extensive-Stage Small-Cell Lung Cancer*. *N Engl J Med*, 2018. **379**(23): p. 2220-2229.
61. Gandhi, L., et al., *Pembrolizumab plus Chemotherapy in Metastatic Non-Small-Cell Lung Cancer*. *N Engl J Med*, 2018. **378**(22): p. 2078-2092.
62. Paz-Ares, L., et al., *Pembrolizumab plus Chemotherapy for Squamous Non-Small-Cell Lung Cancer*. *N Engl J Med*, 2018. **379**(21): p. 2040-2051.
63. Hellmann, M.D., et al., *Nivolumab plus Ipilimumab in Lung Cancer with a High Tumor Mutational Burden*. *N Engl J Med*, 2018. **378**(22): p. 2093-2104.
64. Forde, P.M., et al., *Neoadjuvant PD-1 Blockade in Resectable Lung Cancer*. *N Engl J Med*, 2018. **378**(21): p. 1976-1986.
65. Remon, J., N. Chaput, and D. Planchard, *Predictive biomarkers for programmed death-1/programmed death ligand immune checkpoint inhibitors in nonsmall cell lung cancer*. *Curr Opin Oncol*, 2016. **28**(2): p. 122-9.
66. Reuben, A., et al., *Genomic and immune heterogeneity are associated with differential responses to therapy in melanoma*. *NPJ Genom Med*, 2017. **2**.



# CHAPTER

# 2

## **IMMUNOGLOBULIN-LIKE TRANSCRIPT 3 IS EXPRESSED BY MYELOID-DERIVED SUPPRESSOR CELLS AND CORRELATES WITH SURVIVAL IN PATIENTS WITH NON-SMALL CELL LUNG CANCER**

Pauline L. de Goeje, Koen Bezemer, Marlies E. Heuvers,  
Anne-Marie C. Dingemans, Harry J.M. Groen, Egbert F. Smit,  
Henk C. Hoogsteden, Rudi W. Hendriks, Joachim G.J.V. Aerts,  
Joost P.J.J. Hegmans

*Oncolimmunology. 2015 Mar 19;4(7):e1014242. eCollection  
2015 Jul.*

## ABSTRACT

Myeloid-derived suppressor cells (MDSC) play an important role in immune suppression and are elevated under pathological conditions such as cancer and chronic inflammation. They comprise a heterogeneous population of immature myeloid cells that exert their immune suppressive function via a variety of mechanisms. Immunoglobulin-like transcript 3 (ILT3) is a receptor bearing immunoreceptor tyrosine-based inhibition motifs (ITIM), that can be expressed on antigen presenting cells and is an important regulator of dendritic cell tolerance. ILT3 exists in a membrane-bound and a soluble form and can interact with a still unidentified ligand on T cells and thereby induce T cell anergy, Tregs or T suppressor cells. In this report, we analyzed freshly isolated mononuclear cell fraction from peripheral blood of 105 patients with non-small cell lung cancer and 20 healthy controls and demonstrate for the first time that ILT3 is expressed on MDSC. We show that increased levels of circulating monocytic MDSC and polymorphonuclear MDSC correlate with reduced survival. On the basis of ILT3 cell surface expression, an ILT3<sup>low</sup> and ILT3<sup>high</sup> population of PMN-MDSC could be distinguished. Interestingly, in line with the immune suppressive function of ILT3 on dendritic cells, patients with increased proportions of PMN-MDSC and an increased fraction of the ILT3<sup>high</sup> subset had a shorter median survival than patients with elevated PMN-MDSC and a smaller ILT3<sup>high</sup> fraction. ILT3 expressed on MDSC might reflect a previously unknown mechanism by which this cell population induces immune suppression and could therefore be an attractive target for immune intervention.

## INTRODUCTION

The immune system influences lung cancer pathogenesis, progression, and response to therapy and thereby strongly contributes to the prognosis of the disease [1]. The influence of the immune system is, however, paradoxical, as the different components can either inhibit tumor growth or promote immune evasion and cancer progression [2]. In the latter process, myeloid-derived suppressor cells (MDSC) are an important contributor [3].

MDSC are a heterogeneous population of immature myeloid cells that accumulate in blood, lymphoid organs and tumor tissue under several pathologic conditions, including cancer [3, 4]. MDSC are generally characterized by being CD33 and CD11b positive and HLA-DR low or negative [5]. This population can be divided in two subgroups with different morphology. Monocytic (MO-)MDSC are mononuclear and CD14 positive, whereas granulocytic or polymorphonuclear (PMN-)MDSC are CD14 negative [3, 5]. Both populations contribute to tumor immune escape by inducing immune suppression and tolerance through a variety of mechanisms, such as production of nitric oxide and reactive oxygen species, arginine and cysteine depletion and induction of regulatory T cells [6-9]. However, their regulation and dynamics are poorly understood, especially in humans [10].

An important mediator in the induction of immune tolerance is the immunoglobulin-like transcript (ILT) 3 (also described as LILRB4, CD85k, LIR-5), which is expressed on monocytes and antigen-presenting cells (APCs) such as macrophages and dendritic cells (DCs) [11, 12]. ILT3 expression marks tolerogenic DCs and has been reported to be elevated in APCs of cancer patients [13, 14] and decreased in autoimmune diseases [15, 16]. ILT3 is believed to signal via its immunoreceptor tyrosine-based inhibitory motifs (ITIMs). These motifs are known to inhibit NF- $\kappa$ B activation and transcription of costimulatory molecules and thereby render the cell tolerogenic [17]. The two extracellular Ig-like domains of ILT3 most likely contain ligand binding sites; however, the nature of the ligand is still unknown [12, 17-19]. Membrane-bound ILT3 interacts with T cells in a cell-to-cell contact dependent manner and induces immune suppression or tolerance by inducing anergy in CD4<sup>+</sup> T cells, suppressing the differentiation of IFN- $\gamma$  producing CD8<sup>+</sup> T cells, inhibiting T cell proliferation and induction of regulatory T cells (Tregs) and alloantigen-specific CD8<sup>+</sup> T suppressor cells (Ts) [17, 20]. Moreover, a soluble form of ILT3 (sILT3) resulting from alternative splicing, has been described to interact with T cells and induce anergy [21]. CD68<sup>+</sup> tumor associated macrophages are the major source of sILT3 [21, 22].

Earlier we have shown that MDSC are elevated in treatment-naïve stage IV non-small cell lung carcinoma (NSCLC) patients [23]. Because MDSC have the ability to induce immune

suppression, we hypothesized that ILT3 expression could be part of a yet unidentified mechanism by which MDSCs mediate immune escape. Therefore, we aimed to assess expression of ILT3 on MDSC in lung cancer patients with advanced disease before the start of chemotherapy and evaluate its effect on clinical outcome.

## RESULTS

### Characteristics of study subjects

In this study, 118 stage IV NSCLC patients participating in the NVALT12 study were included. Of 13 patients, blood samples were not available for processing within 6 hours after the samples were taken and were excluded from further analysis. Table 1 shows the characteristics of the 105 NSCLC study participants and 20 healthy controls (HC) that were included in our analyses. The patient characteristics of this study cohort were similar to the total NVALT12 population [23], therefore no selection bias was introduced.

**Table 1.** characteristics of study subjects

	Healthy controls	NSCLC patients
Number of subjects	20	105
Age (years) (Mean $\pm$ SD)	54 $\pm$ 7.5	61 $\pm$ 8.3
<b>Gender (%)</b>		
Male	4 (20)	53 (50.5)
Female	16 (80)	52 (49.5)
<b>WHO performance score (%)</b>		
0	20 (100)	51 (49)
1		50 (48)
2		3 (3)
<b>Histologic subtype (%)</b>		
Adenocarcinoma		87 (84)
Large cell carcinoma		17 (16)

### Both MO-MDSC and PMN-MDSC are elevated in stage IV NSCLC patients

The two MDSC subsets - MO-MDSC and PMN-MDSC - were assessed in the peripheral blood of stage IV NSCLC patients and healthy controls by flow cytometric analysis of freshly obtained peripheral blood mononuclear cells (PBMC). The gating strategy for the two populations is presented in Figure 1A and was performed as previously described [23]. First, mature granulocytes were excluded based on their CD16<sup>++</sup> expression [5, 24]. Then, MO-MDSC were characterized as CD11b<sup>+</sup> CD14<sup>+</sup> HLA-DR<sup>-</sup> CD33<sup>+</sup> CD15<sup>+</sup>, whereas PMN-MDSC were characterized as CD11b<sup>+</sup> CD14<sup>-</sup> HLA-DR<sup>-</sup> CD33<sup>+</sup> CD15<sup>+</sup>.

As reported earlier by our group, MDSC are elevated in NSCLC patients [23]. Accordingly, in the cohort used in this study, the frequencies of both MO-MDSC and PMN-MDSC in peripheral blood were significantly higher in patients than in healthy controls, as shown in Figure 1B.

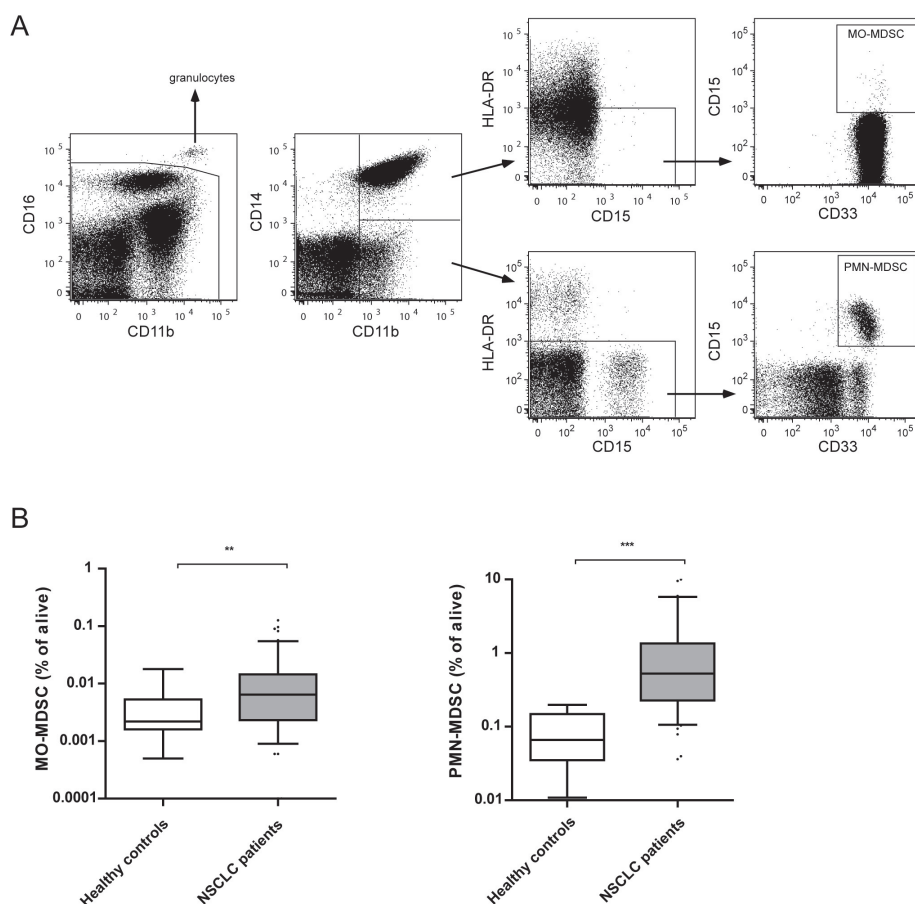


**Figure 1.** Circulating MO-MDSC and PMN-MDSC are increased in NSCLC patients. A. Flow cytometry was performed on freshly isolated PBMC from NSCLC patients and healthy controls. Gating strategy for determination of circulating MO-MDSC and PMN-MDSC is depicted in this figure. After gating the live cells, CD16<sup>high</sup> cells were excluded. MO-MDSC were characterized as CD14<sup>+</sup>CD11b<sup>+</sup>HLA-DR<sup>low</sup>CD15<sup>+</sup> and PMN-MDSC were characterized as CD14<sup>+</sup>CD11b<sup>+</sup>HLA-DR<sup>low</sup>CD15<sup>+</sup>. MDSC levels were determined as frequency of alive. B. Frequency of both MO-MDSC and PMN-MDSC in PBMC was significantly higher in NSCLC patients than in healthy controls. \*\*  $p < 0.01$ ; \*\*\*  $p < 0.001$ ; Mann-Whitney U test.

### ILT3 is expressed by subpopulations of MDSC

ILT3 expression could be detected on both PMN-MDSC and MO-MDSC (Figure 2A). In contrast to MO-MDSC, which showed a homogeneous high expression of ILT3 (right panel),

PMN-MDSC comprised two subsets of high and low ILT3 expression (left panel). Figure 2B shows ILT3 expression on PMN-MDSC of four different patients, compared to their CD11b<sup>-</sup>CD14<sup>-</sup> cells (mainly lymphocytes) and CD11b<sup>+</sup>CD14<sup>+</sup> cells (mainly monocytes). Whereas the lymphocytes were consistently negative for ILT3 (mean fluorescence intensity (MFI) = 53), monocytes showed high and homogeneous ILT3 expression (median MFI = 7399). The expression of ILT3 on PMN-MDSC was intermediate and showed two peaks in most patients, although the distribution over ILT3<sup>high</sup> (MFI >10<sup>3</sup>) and ILT3<sup>low</sup> (MFI <10<sup>3</sup>) fractions varied extensively between patients (percentage of ILT3<sup>high</sup> cells varied between 0.2% and 92.9%). In contrast to PMN-MDSC, virtually all MO-MDSC were positive for ILT3 with a homogeneous expression of the marker, which was slightly but significantly lower than expression in the monocyte population (MFI = 6275,  $p < 0.001$ ).

### **The ILT3<sup>high</sup> fraction of PMN-MDSC is increased in lung cancer patients and is not correlated with T and B cell frequencies or monocytes**

The proportions of ILT3<sup>high</sup> PMN-MDSC within the total PMN-MDSC population varied considerably between patients. As shown in Figure 3A, the fraction of ILT3<sup>high</sup> of PMN-MDSC was significantly higher in NSCLC patients (39%, SD 24%) compared to healthy controls (12%, SD 10%;  $p < 0.0001$ ). The proportion of ILT3<sup>high</sup> PMN-MDSC did not correlate with the proportion of PMN-MDSC (Figure 3B). To investigate whether the ILT3<sup>high</sup> fraction of PMN-MDSC had an effect on, or was affected by, other immunological cell populations, we analyzed T cells, the CD4<sup>+</sup>/CD8<sup>+</sup> T cell ratio, B cells and monocytes. No statistically significant correlations were found for the ILT3<sup>high</sup> fraction of PMN-MDSC with proportions of B cells, T cells, the CD4<sup>+</sup>/CD8<sup>+</sup> ratio and monocytes in NSCLC patients. Furthermore, no correlation with MO-MDSC existed (Figure 3B). Analyses with absolute numbers of these cell populations gave similar results (data not shown).

### **Soluble ILT3 is elevated in serum of NSCLC patients and does not correlate with immunological cell populations**

It has been described that besides membrane-bound ILT3, also soluble ILT3 (sILT3) can have immune suppressive effects [21]. In multiple types of cancer, sILT3 is present in the serum of patients and is able to strongly abolish T cell responses against tumor antigens [21, 22]. To test whether sILT3 is present in the serum of the NSCLC patients, sILT3 levels were quantified by ELISA in a pilot of 30 randomly chosen NSCLC patients and 8 healthy controls. Figure 4A demonstrates that sILT3 was present in the serum of NSCLC patients and that the levels of sILT3 were significantly higher ( $p = 0.03$ ) compared to the levels of sILT3 in healthy controls. We hypothesized that soluble ILT3 might be produced by ILT3 expressing MDSC. However, no correlation was found between the serum levels of sILT3 and the proportions of ILT3<sup>high</sup> cells in the PMN-MDSC population (Figure 4B). Furthermore, sILT3 was not correlated



with the mean fluorescence intensity (MFI) values of surface ILT3 on monocytes or MDSC populations (data not shown). To check whether sILT3 levels were related to the peripheral immune profile of the patients, we assessed the correlation between sILT3 serum levels and peripheral immune cell proportions in the patient cohort. No significant correlations were found between the levels of sILT3 and the frequency PMN-MDSC and MO-MDSC, T cells, the CD4<sup>+</sup>/CD8<sup>+</sup> ratio, B cells and monocytes (Figure 4C).

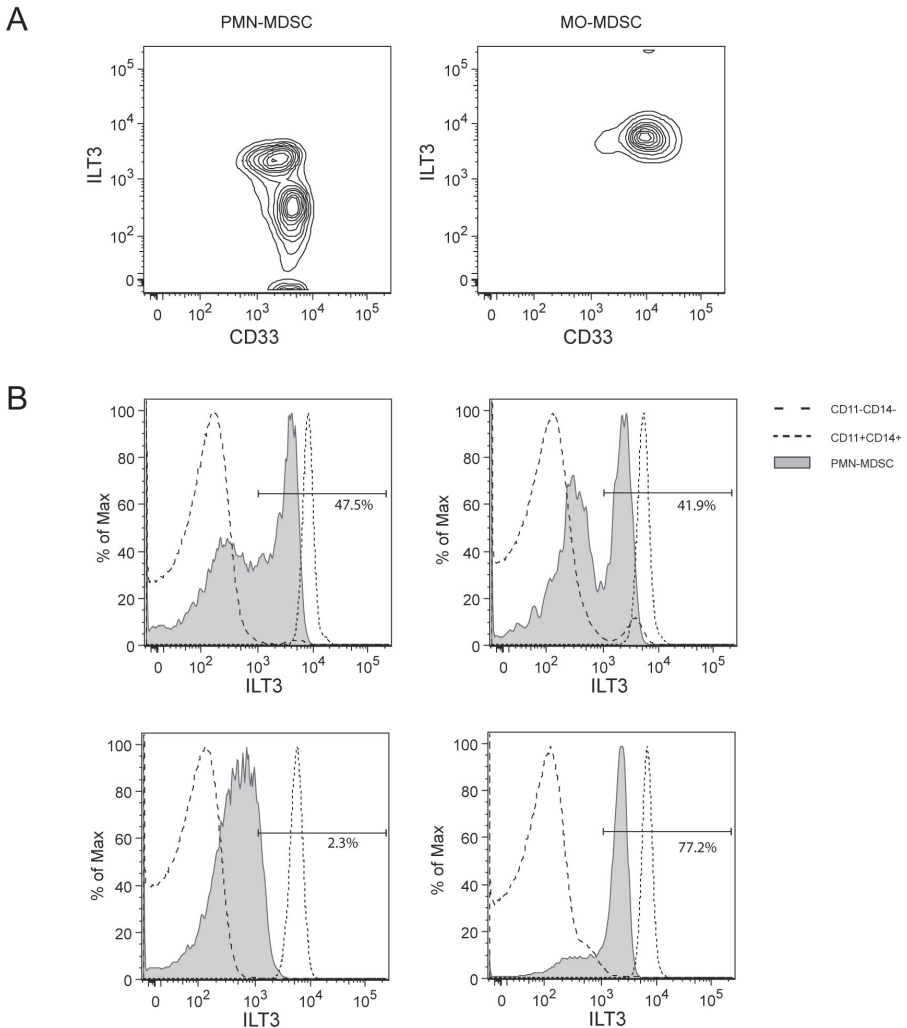


**Figure 2.** ILT3 expression on MDSC. A. Flow cytometric data of a representative patient, displayed as density plot based on ILT3 and CD33 expression. Left panel: PMN-MDSC, right panel: MO-MDSC. B. Histograms of 4 different patients with ILT3 expression of PMN-MDSCs (shaded) compared to the expression within the CD11b<sup>-</sup>CD14<sup>-</sup> population (dashed line, mainly lymphocytes) and CD11b<sup>+</sup>CD14<sup>+</sup> population (dotted line, mainly monocytes). Proportions of ILT3<sup>high</sup> fraction are displayed as percentage of PMN-MDSC.

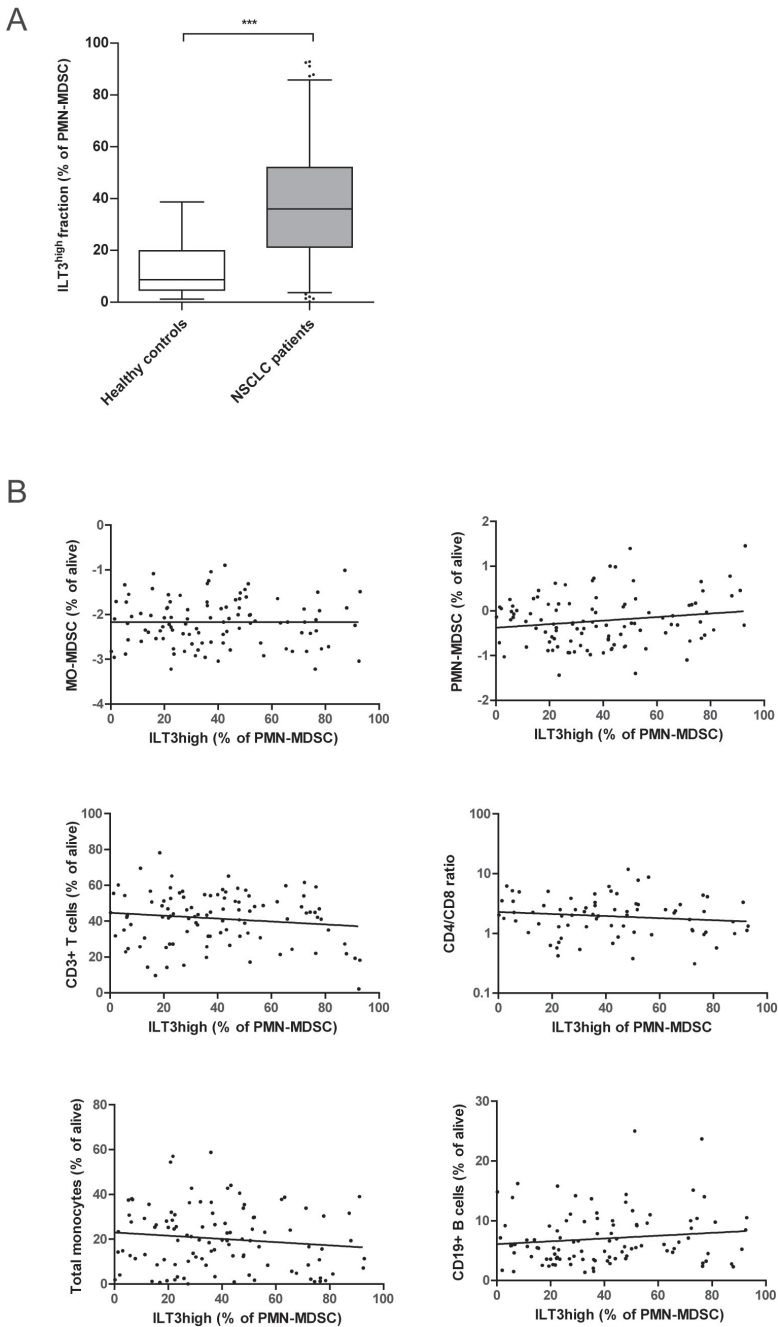


**Figure 3.** ILT3<sup>high</sup> proportion of PMN-MDSC in NSCLC patients. A. ILT3<sup>high</sup> proportions of PMN-MDSC were significantly higher in NSCLC patients than in healthy controls. \*\*\*  $p < 0.001$ , Student's *t* test. B. In NSCLC patients, correlations between the proportion of ILT3<sup>high</sup> PMN-MDSC and various immune subsets were analyzed with the Spearman rho test. None of the tests revealed a significant correlation ( $p > 0.05$  in all analyses).

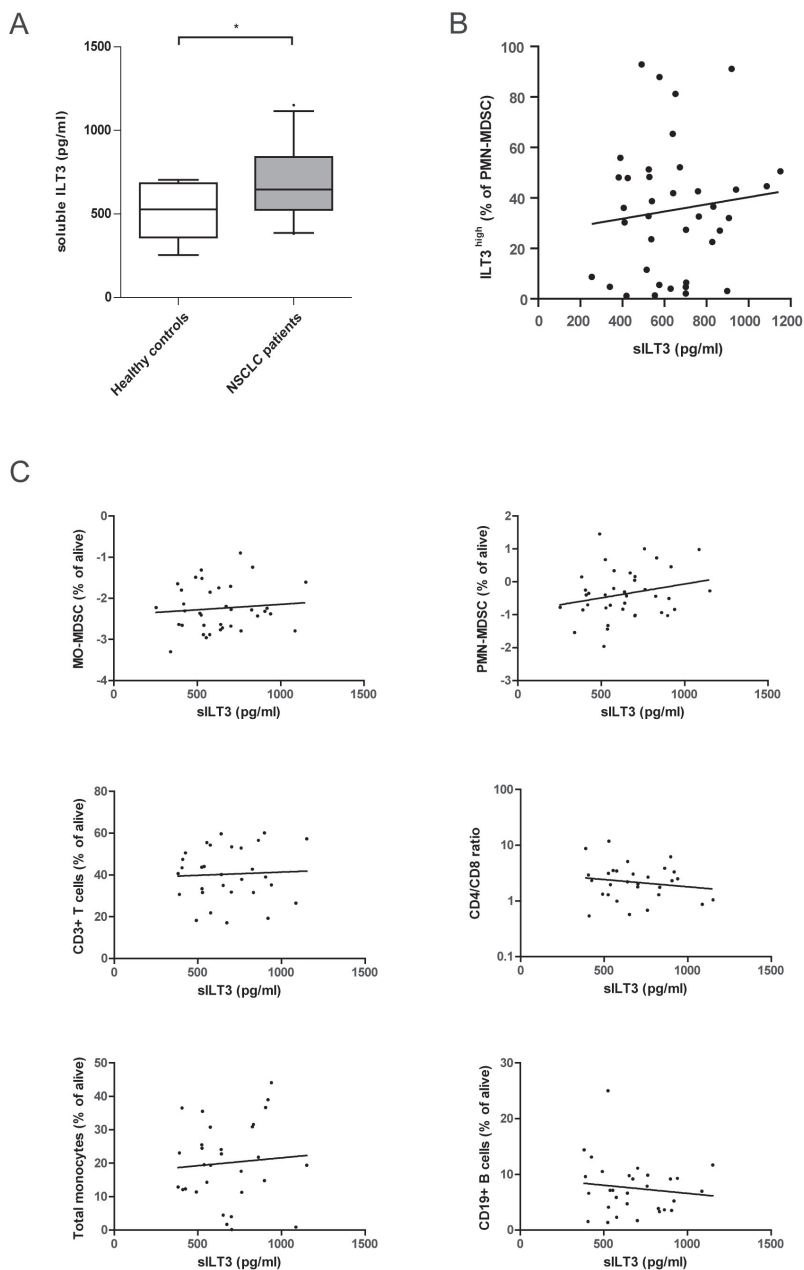


**Figure 4.** Serum sILT3 in NSCLC patients Figure 5: ILT3<sup>high</sup> proportion of PMN-MDSC in NSCLC patients. A. Soluble ILT3 was measured by ELISA in serum samples of healthy controls (n=8) and stage IV NSCLC patients (n=30). Levels were significantly higher in NSCLC patients compared to healthy controls. \* p<0.05, Student's t test. B. sILT3 levels of NSCLC patients did not correlate with the fraction of ILT3<sup>high</sup> cells of PMN-MDSC (Spearman's rho test). C. In NSCLC patients, correlations between level of sILT3 in serum and various immune subsets were analyzed with the Spearman rho test. None of the tests revealed a significant correlation (p>0.05 in all analyses).

## Increased proportions of circulating MDSC correlate with a poorer outcome in NSCLC patients

For various types of cancer, it has been shown that higher levels of MDSC correlate with reduced survival of patients [25, 26]. To validate this effect in our patient cohort, patients were divided into two groups, based on the proportions of MDSC. Values that were higher than the mean + 2 standard deviations of healthy controls were considered to be elevated. In this way, we identified patients with elevated PMN-MDSC and patients with elevated MO-MDSC. In accordance with reported findings [25, 26], patients with elevated proportions of PMN-MDSCs had a significantly shorter survival than patients with low proportions of PMN-MDSC ( $p=0.017$ ). Likewise, patients with elevated proportions of MO-MDSC had a significantly shorter survival than patients with low MO-MDSC values ( $p=0.007$ ). The survival curves are shown in Figure 5A and B. Of note, proportions of PMN-MDSC and MO-MDSC were significantly correlated ( $p<0.001$ ; not shown).

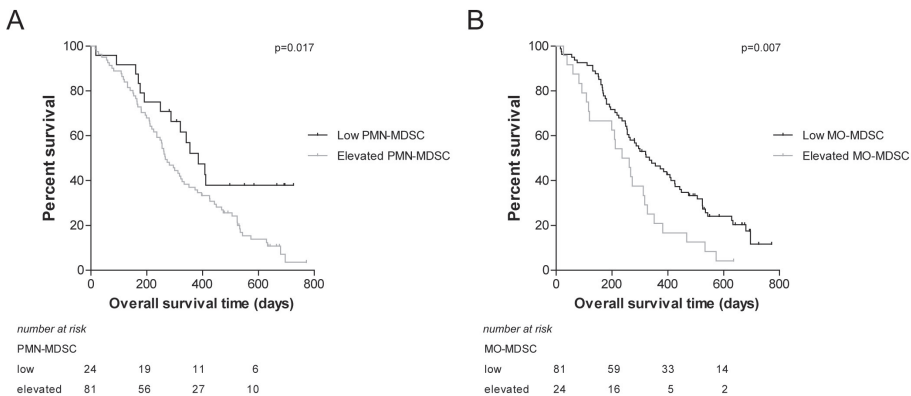


**Figure 5.** Survival curves of NSCLC patient groups based on frequency of MDSC. Survival curves of NSCLC patients divided into two groups, based on the mean value + 2SD of healthy controls. A. Survival curve of patients with elevated versus low PMN-MDSC levels B. Survival curve of patients with elevated or low MO-MDSC levels.

## The $ILT3^{high}$ fraction of PMN-MDSC correlates with a poorer outcome in NSCLC patients

To assess if  $ILT3^{high}$  expression on PMN-MDSC influenced clinical outcome, NSCLC patients were divided in two groups based on the percentages of  $ILT3^{high}$  cells of PMN-MDSC, in the same way as with proportions of MDSC. Figure 6A shows a slightly shorter overall survival for patients with a higher percentage of  $ILT3^{high}$  PMN-MDSC, although this did not reach statistical significance ( $p=0.15$ ). However, it is conceivable that the impact of high  $ILT3$  expression on PMN-MDSC is limited in patients with low proportions of these cells. Therefore, we performed a sub analysis on the group of patients with the highest levels of

PMN-MDSC (above median; Figure 6B). We found a significant negative correlation with overall survival ( $p=0.023$ , Figure 6C). In contrast, in patients with low proportions of MDSC, the percentage of ILT3<sup>high</sup> cells did not influence overall survival (Figure 6D). Analysis on progression free survival showed similar results, but only the effect of MO-MDSC level reached statistical significance (data not shown). Serum levels of sILT3 were not correlated with survival (data not shown).

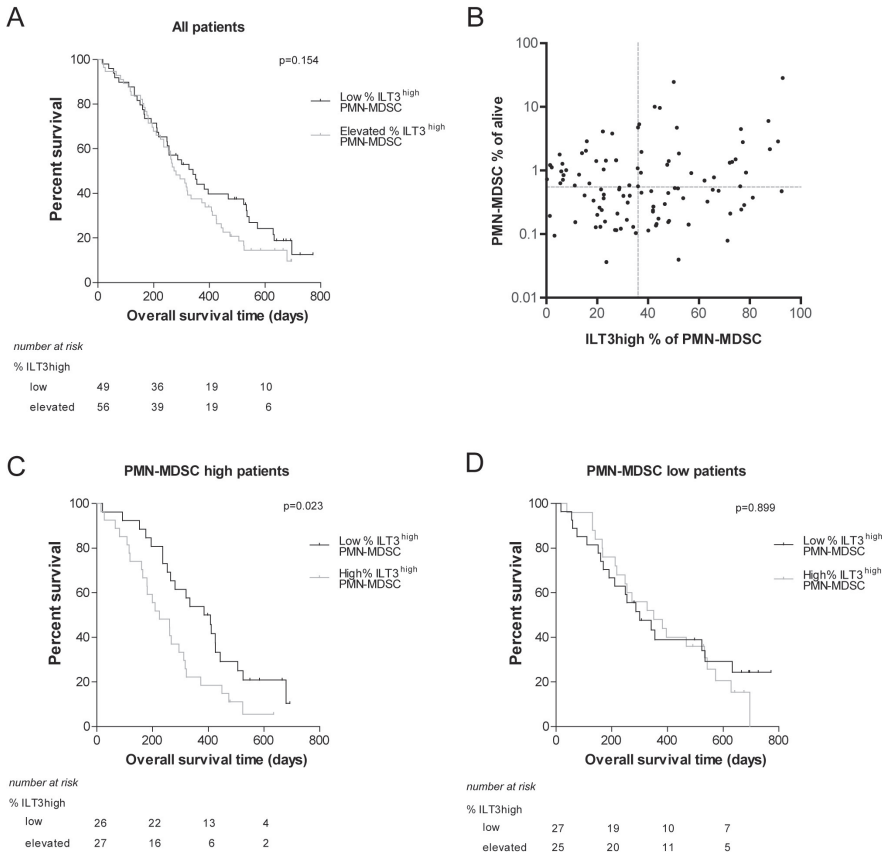


**Figure 6.** NSCLC patient survival based on ILT3 fractions of MDSC. A. Patients with an elevated percentage of ILT3<sup>high</sup> PMN-MDSC versus patients with low percentage of ILT3<sup>high</sup> PMN-MDSC. Survival curves were not significantly different. B. No correlation was found between the level of total PMN-MDSC and the percentage of ILT3<sup>high</sup> PMN-MDSC (Spearman's rho;  $p=0.38$ ). For the curves in Figure C and D, patients were divided based on the frequency of PMN-MDSC and the percentage of ILT3<sup>high</sup> PMN-MDSC. Cut off values were at median value of all patients to create equally sized groups. C. In patients with high levels of PMN-MDSC, the fraction of ILT3<sup>high</sup> cells correlated significantly with overall survival. D. In patients with low levels of PMN-MDSC, the percentage of ILT3<sup>high</sup> PMN-MDSC did not significantly contribute to overall survival. The curves were compared with a log-rank test, stratified for treatment arm. *PBMC* = peripheral blood mononuclear cells. *MO-MDSC* = monocytic myeloid-derived suppressor cells. *PMN-MDSC* = polymorphonuclear myeloid-derived suppressor cells.

## DISCUSSION

This is the first study showing that the immune suppressive molecule ILT3 is expressed by MDSC. In recent years, MDSC have received a lot of attention for their immune suppressive role in cancer, which they can execute through a diversity of mechanisms, such as arginase-1 and iNOS expression and oxidative stress [27]. Given that MDSCs are a heterogeneous population of immature cells, these mechanisms are likely to be differentially employed by the different subsets of MDSC and dependent on the context of the microenvironment. With the demonstration of ILT3 expression on the cell membrane of MDSC, we describe a, for MDSC previously unknown pathway, that MDSC might use to execute their immune suppressive function. The heterogeneity of MDSC is further demonstrated by our finding that ILT3 is not expressed on all circulating MDSC of lung cancer patients, but on MO-MDSC and a subset of PMN-MDSC only.

Little is known about MDSC under physiological conditions. In healthy individuals, immature myeloid cells with the same phenotype as MDSC are continuously generated in the bone marrow, where they differentiate into mature myeloid cells before entering the circulation. Under pathological conditions they can be released from the bone marrow before maturation. However, in mice it has been described that MDSC are also present in the liver during physiological conditions and are thought to play a pivotal role in maintaining homeostasis [28]. So, the function of MDSC is probably different in healthy controls compared to cancer patients. It has been described that MDSC of diseased mice have an increased capacity to suppress T cell proliferation compared with MDSC of normal mice [28]. This is supported by the finding that MDSC from healthy controls show a decreased expression of immune suppressive molecules compared with MDSC from cancer patients [29]. Likewise, in a previous study we showed that arginase-1 is expressed in PBMC in much larger amounts in lung cancer patients than in healthy controls [23, 30]. Our finding that ILT3 is upregulated on MDSC of NSCLC patients is in agreement with functional differences with regard to immune suppression by MDSC in NSCLC patients and healthy controls.

ILT3 expression on DC is of critical importance in the induction of tolerance [31, 32]. ILT3 can be induced on APCs by cytokines such as IL-10, interferon (IFN)- $\alpha$  and IFN- $\beta$  and by interaction with CD8<sup>+</sup> T suppressor cells (Ts) [33, 34]. Other inducers of ILT3 on APC are vitamin D3 analogs, COX-1/2 inhibitors, and tryptophan depletion in the environment, resulting in T cell non-responsiveness and tolerance [18, 33, 35]. Intracellular signaling via the ITIMs of ILT3 induces tolerance in DCs via downregulation of the NF $\kappa$ B pathway and plays an inhibitory role in antigen presentation [36]. However, these signaling pathways are not likely to play an important role in ILT3 expressing MDSC, since MDSC are not classical APC

and are defined by low HLA-DR expression. Therefore, ILT3 induced immune suppression by MDSC is not likely to exert its effectiveness via co-stimulation or antigen presentation as holds true for DCs. However, extracellular signaling by membrane bound ILT3 as well as sILT3 has been shown to induce immune suppressive CD8<sup>+</sup> T suppressor cells and CD4<sup>+</sup> Tregs [18, 19]. MDSC might therefore use this extracellular signaling pathway to exert their immune suppressive function, as indeed this cell population is known to induce Tregs and T cell anergy.

In this study we did not find a correlation between ILT3 expression on MDSC and the proportion of T cells in PBMC. However, functionality of these T cells was not assessed in this study. Given that MDSC might induce anergy in T cells or induce Tregs from naïve T cells, functionality rather than number of T cells could be diminished by ILT3<sup>+</sup> MDSC and should be investigated in further studies. Unfortunately, the amount of blood collected from each patient in combination with the low levels and phenotypic instability of the MDSC populations did not allow for functional studies to compare the ILT3<sup>high</sup> and ILT3<sup>low</sup> PMN-MDSC subsets or the comparison with suppressive capacity of MO-MDSC.

The clinical relevance of both membrane-bound and soluble ILT3 has been demonstrated in studies of different cancer types. In B-CLL, myeloid leukemia, pancreatic and gastric cancer, membrane-bound ILT3 is expressed on tumor cells and in B-CLL its expression on tumor cells is associated with aggressive growth [13, 37, 38]. Elevated expression on DCs was found in colorectal cancer patients when compared to healthy controls [14]. Moreover, strong infiltration of CD68<sup>+</sup> ILT3<sup>high</sup> macrophages has been demonstrated in lymph nodes containing metastatic carcinoma cells [22]. Also, sILT3 is elevated in serum of melanoma, colorectal and pancreatic carcinoma patients [21, 22]. In contrast, in SLE and autoimmune thyroid disease, where in contrast to cancer the immune system is over activated, ILT3 expression is decreased on DCs of patients [15, 39] and in multiple sclerosis, ILT3 was reported to be decreased on circulating monocytes [16]. In line with these results, we found elevated sILT3 levels and a higher percentage of ILT3<sup>+</sup> PMN-MDSC in NSCLC patients, which indicates a role for this molecule in tumor pathogenesis or progression, most likely via stimulating tumor immune escape. In this cohort of stage IV NSCLC patients, the detrimental effect of the presence of elevated proportions of circulating MO-MDSC and PMN-MDSC was confirmed, as elevated proportions of MDSC were correlated with a decreased overall survival. We were unable to demonstrate a significant effect of the percentage of ILT3<sup>high</sup> PMN-MDSC on clinical outcome for the whole patient population, although the mean survival time was shorter in patients with elevated ILT3<sup>high</sup> PMN-MDSC (Figure 6A). However, when patients with PMN-MDSC proportions above median were selected, an elevated percentage of ILT3<sup>high</sup> PMN-MDSC was correlated with reduced survival. This finding

supports our hypothesis that ILT3 expression on MDSC plays a role in immune suppression, but only in patients with higher proportions of PMN-MDSC its influence is large enough to be detected in survival analyses. In contrast to PMN-MDSC, all MO-MDSC expressed ILT3 on their membrane. Given that the frequency of MO-MDSC in peripheral blood was very low but still rendered a significant correlation with overall survival, MO-MDSC might be a stronger immune suppressor than PMN-MDSC in stage IV NSCLC patients. Although we did not provide evidence for this, one might speculate that this could be due to the constitutive expression of ILT3 on MO-MDSC. Moreover, the proportion of ILT3<sup>high</sup> PMN-MDSC did not correlate with the proportions of other immunological cell types, thereby indicating that its clinical value is not a reflection of an altered balance in the rest of the immune system, but rather might exert a tumor promoting function, either via altering functionality of the immune cells rather than cell numbers, or by acting locally on tumor progression or immune escape. The absence of evidence for clinical relevance of the level of sILT3 in serum in this study might be due to the small size of serum samples measured, although the lack of any correlation with circulating immune cell populations provided no further indication of its role in peripheral blood. sILT3 might however function more locally, since it has been shown to be produced by tumor associated CD68<sup>+</sup> macrophages [21]. Given that sILT3 levels did not correlate with the expression level on circulating MDSC or monocytes, it is not likely that sILT3 is produced in the periphery in high amounts, but might rather reflect the local immune composition and a suppressive microenvironment.

Taken together, our results show that ILT3 is expressed on MDSC and indicate that this effects the clinical outcome. The relevance of ILT3 in cancer patients is supported by results from literature [14, 37, 38] and therefore further investigation of its mode of action on MDSC should be performed. Yet, it is debatable that ILT3 on its own would determine the immune suppressive status of MDSC. Rather, the sum of all immune suppressive mechanisms and their relative contribution to the activity of MDSC, will determine the extent of its unfavorable effects in cancer patients.

MDSC play an important role in mediating immune suppression and therefore represent a significant hurdle to successful immunotherapy in NSCLC [2]. Therefore, combining immunotherapeutic approaches with MDSC inhibiting drugs like gemcitabine or VEGF blockers to elicit more potent anticancer effects, is a promising development.

To our knowledge this is the first study that demonstrates the expression of ILT3 on human MDSC. Future studies will underscore the importance of this molecule on MDSC in other experimental or clinical settings.



## MATERIAL AND METHODS

### Study population

The patients in this study were participating in the NVALT12 study (trial number NCT01171170), a randomized phase II multicentre study on the effect of a nitroglycerin patch or placebo in patients with stage IV NSCLC treated with carboplatin, paclitaxel and bevacizumab. Patients in the NVALT12 study were diagnosed with stage IV non-squamous NSCLC and were not eligible for treatment with curative intent. Disease stage was determined in accordance with the American Joint Committee on Cancer (AJCC). Blood samples were collected before start of treatment and analysed by flow cytometry. In this study, 118 patients were included for analysis of ILT3 expression. Twenty age-matched healthy controls (HC) (mean age 54 years) with no history of malignancies and/or autoimmune diseases were enrolled in the study. Written consent was obtained from all individuals before blood sampling and the study was approved by the ethical committee of the Erasmus Medical Center (MEC-2012-048 (HC) and CCMO: NL33442.042.10 (NSCLC patients)).

### Isolation of PBMC

PBMC were isolated using a Ficoll-Hypaque (GE Healthcare, Diegem, Belgium) density gradient. Blood was supplemented to 50 mL with phosphate buffered saline (PBS, Gibco, Breda, The Netherlands) before layering onto the Ficoll-Hypaque. After centrifugation of 20 minutes at 1200xg, PBMC were collected from the plasma-Ficoll interphase. Cells were washed twice with 50 mL PBS and counted prior to further analysis. In previous research, we demonstrated that MDSC levels remain constant in the first six hours, but decrease significantly when stored for a longer time [23]. Therefore, flow cytometry on PBMC was performed immediately and within six hours after blood was collected.

### Flow cytometry

PBMC were stained with the following conjugated monoclonal antibodies: anti-CD15 PE, anti-CD16 PERCP-Cy5.5, anti-CD33 PE-Cy7, anti-CD11b APC, anti-HLA-DR APC-Cy7 (all from BD Biosciences), anti-CD14 PE-Texas-Red (Invitrogen, Breda, The Netherlands), anti-ILT3 FITC (R&D Systems) and a live/dead marker 4',6-diamidino-2-phenylindole (DAPI, Molecular Probes, Eugene, OR, USA) to analyze MDSC. Staining with anti-CD4 FITC, anti-CD8 APC, (all from BD Biosciences), anti-CD3 APC-eFluor 780 (eBioscience, San Diego, CA, USA), and DAPI was performed for the analysis of T cells.

Cells were washed with FACS buffer (PBS, 0.25% BSA, 5 mM EDTA, 0.05% NaN<sub>3</sub>) and stained for 30 min at 4°C with the above-mentioned antibodies, appropriately diluted in FACS buffer

supplemented with 2% normal human serum. Flow cytometry was performed on a LSRII flow cytometer (BD Biosciences) and data were analyzed with FlowJo software (Tree Star).

MDSC were characterized as previously described [23]. In the MDSC staining, the CD16 marker was used to exclude mature granulocytes based on their CD16<sup>++</sup> expression, as has been considered important for MDSC purity [5, 24]. PMN-MDSC were characterized as CD11b<sup>+</sup> CD14<sup>-</sup> HLA-DR<sup>-</sup> CD33<sup>+</sup> CD15<sup>+</sup> and MO-MDSC were characterized as CD11b<sup>+</sup> CD14<sup>+</sup> HLA-DR<sup>-</sup> CD33<sup>+</sup> CD15<sup>+</sup>. Total monocytes were characterized as being CD11b<sup>+</sup> CD14<sup>+</sup>. In the lymphocyte staining, T cells were characterized as CD3<sup>+</sup> and divided into a CD4<sup>+</sup> CD8<sup>-</sup> (CD4<sup>+</sup> T cells) and a CD4<sup>-</sup> CD8<sup>+</sup> (CD8<sup>+</sup> T cells) subset. B cells were characterized as CD19<sup>+</sup> cells.

### **Measurement of soluble ILT3 in serum**

For quantitative detection of ILT3 in serum, a commercially available enzyme-linked immunosorbent assay (ELISA) was used according to manufacturer's specifications (Cusabio biotech.). All samples were assayed in duplicate and quantified using a standard curve. The detection range was from 31.2-2000 pg/ml.

### **Statistical analysis**

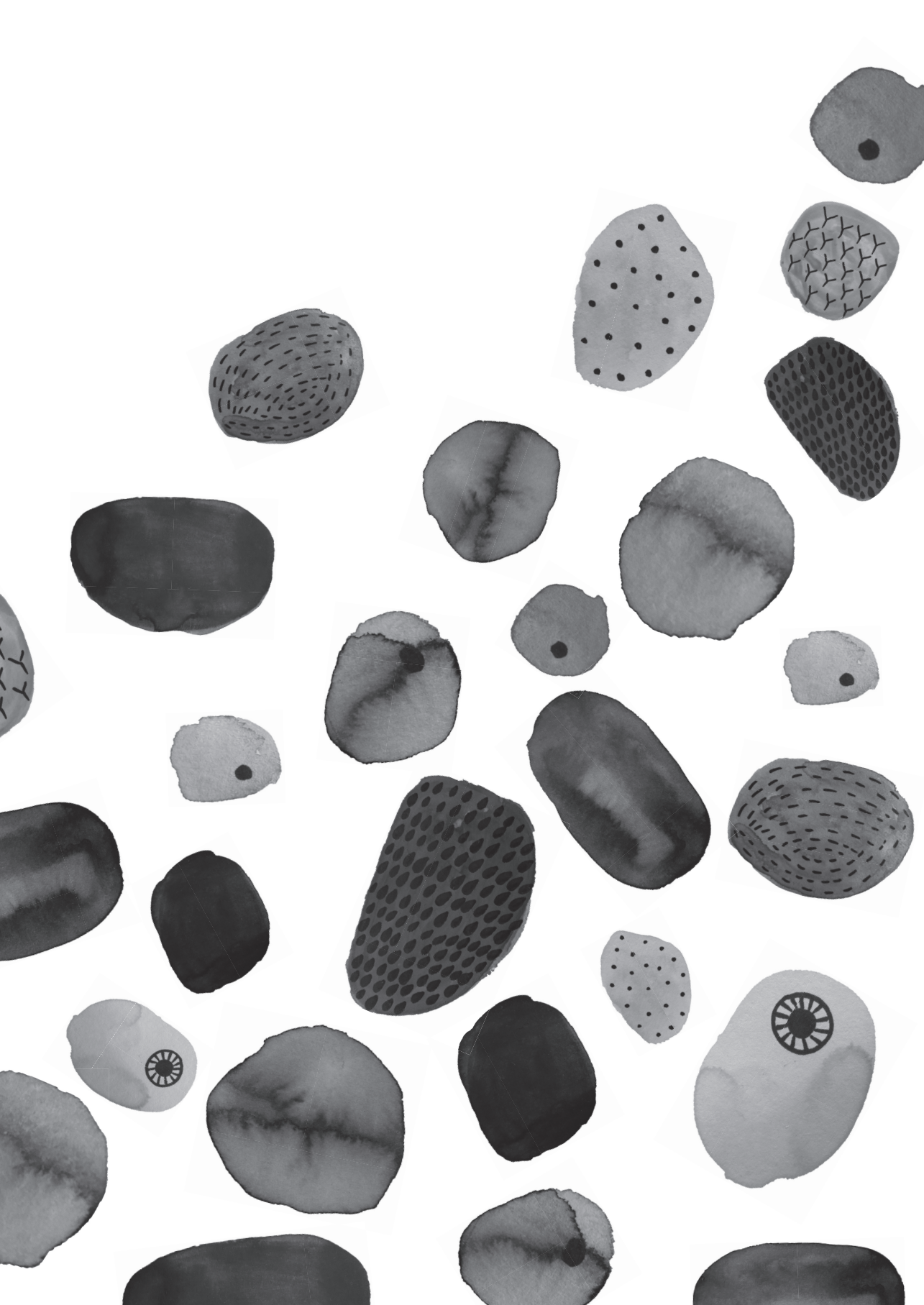
Differences between healthy controls and lung cancer patients were evaluated by Mann-Whitney *U* test. Correlations were assessed by using the Spearman's rho correlation test. The effects of sizes of immunological cell populations and expression levels of ILT3 on survival were assessed with a log-rank (Mantel-Cox) test. In these analyses, patients were stratified for treatment group. Statistical analysis was performed using the statistical program SPSS (version 21.0, SPSS Inc., Chicago, USA). All p-values were two-sided and p-values below the conventional level of significance ( $p < 0.05$ ) were considered statistically significant. Figures were made in GraphPad Prism (version 5.0, GraphPad Software, San Diego, CA, USA).

## REFERENCES

1. Bremnes, R.M., et al., *The role of tumor-infiltrating immune cells and chronic inflammation at the tumor site on cancer development, progression, and prognosis: emphasis on non-small cell lung cancer*. J Thorac Oncol, 2011. **6**(4): p. 824-33.
2. Heuvers, M.E., et al., *Patient-tailored modulation of the immune system may revolutionize future lung cancer treatment*. BMC Cancer, 2012. **12**: p. 580.
3. Jiang, J.W., W.J. Guo, and X.H. Liang, *Phenotypes, accumulation, and functions of myeloid-derived suppressor cells and associated treatment strategies in cancer patients*. Human Immunology, 2014. **75**(11): p. 1128-1137.
4. Ortiz, M.L., et al., *Myeloid-derived suppressor cells in the development of lung cancer*. Cancer Immunol Res, 2014. **2**(1): p. 50-8.
5. Damuzzo, V., et al., *Complexity and challenges in defining myeloid-derived suppressor cells*. Cytometry B Clin Cytom, 2014.
6. Youn, J.I. and D.I. Gabrilovich, *The biology of myeloid-derived suppressor cells: the blessing and the curse of morphological and functional heterogeneity*. Eur J Immunol, 2010. **40**(11): p. 2969-75.
7. Gabrilovich, D.I., S. Ostrand-Rosenberg, and V. Bronte, *Coordinated regulation of myeloid cells by tumours*. Nat Rev Immunol, 2012. **12**(4): p. 253-68.
8. Filipazzi, P., V. Huber, and L. Rivoltini, *Phenotype, function and clinical implications of myeloid-derived suppressor cells in cancer patients*. Cancer Immunol Immunother, 2012. **61**(2): p. 255-63.
9. Buijs, N., et al., *The Role of a Disturbed Arginine/NO Metabolism in the Onset of Cancer Cachexia: A Working Hypothesis*. Current Medicinal Chemistry, 2012. **19**(31): p. 5278-5286.
10. Condamine, T. and D.I. Gabrilovich, *Molecular mechanisms regulating myeloid-derived suppressor cell differentiation and function*. Trends Immunol, 2011. **32**(1): p. 19-25.
11. Colonna, M., et al., *A novel family of Ig-like receptors for HLA class I molecules that modulate function of lymphoid and myeloid cells*. J Leukoc Biol, 1999. **66**(3): p. 375-81.
12. Cheng, H., et al., *Crystal structure of leukocyte Ig-like receptor LILRB4 (ILT3/LIR-5/CD85k): a myeloid inhibitory receptor involved in immune tolerance*. J Biol Chem, 2011. **286**(20): p. 18013-25.
13. Colovai, A.I., et al., *Expression of inhibitory receptor ILT3 on neoplastic B cells is associated with lymphoid tissue involvement in chronic lymphocytic leukemia*. Cytometry B Clin Cytom, 2007. **72**(5): p. 354-62.
14. Orsini, G., et al., *Quantification of Blood Dendritic Cells in Colorectal Cancer Patients During the Course of Disease*. Pathol Oncol Res, 2013. **20**(2): p. 267-276.
15. Leskela, S., et al., *Plasmacytoid dendritic cells in patients with autoimmune thyroid disease*. J Clin Endocrinol Metab, 2013. **98**(7): p. 2822-33.
16. Jensen, M.A., et al., *Immunoglobulin-like transcript 3, an inhibitor of T cell activation, is reduced on blood monocytes during multiple sclerosis relapses and is induced by interferon beta-1b*. Mult Scler, 2010. **16**(1): p. 30-8.
17. Suci-Foca, N. and R. Cortesini, *Central role of ILT3 in the T suppressor cell cascade*. Cell Immunol, 2007. **248**(1): p. 59-67.
18. Kim-Schulze, S., et al., *Recombinant Ig-like transcript 3-Fc modulates T cell responses via induction of Th energy and differentiation of CD8+ T suppressor cells*. J Immunol, 2006. **176**(5): p. 2790-8.
19. Vlad, G. and N. Suci-Foca, *Induction of antigen-specific human T suppressor cells by membrane and soluble ILT3*. Experimental and Molecular Pathology, 2012. **93**(3): p. 294-301.
20. Vlad, G., et al., *Membrane and soluble ILT3 are critical to the generation of T suppressor cells and induction of immunological tolerance*. Int Rev Immunol, 2010. **29**(2): p. 119-32.
21. Cortesini, R., *Pancreas cancer and the role of soluble immunoglobulin-like transcript 3 (ILT3)*. JOP, 2007. **8**(6): p. 697-703.
22. Suci-Foca, N., et al., *Soluble Ig-like transcript 3 inhibits tumor allograft rejection in humanized SCID mice and T cell responses in cancer patients*. J Immunol, 2007. **178**(11): p. 7432-41.
23. Heuvers, M.E., et al., *Arginase-1 mRNA expression correlates with myeloid-derived suppressor cell levels in peripheral blood of NSCLC patients*. Lung Cancer, 2013. **81**(3): p. 468-74.

24. Rodriguez, P.C., et al., *Arginase I-producing myeloid-derived suppressor cells in renal cell carcinoma are a subpopulation of activated granulocytes*. *Cancer Res*, 2009. **69**(4): p. 1553-60.
25. Gabitass, R.F., et al., *Elevated myeloid-derived suppressor cells in pancreatic, esophageal and gastric cancer are an independent prognostic factor and are associated with significant elevation of the Th2 cytokine interleukin-13*. *Cancer Immunol Immunother*, 2011. **60**(10): p. 1419-30.
26. Jordan, K.R., et al., *Myeloid-derived suppressor cells are associated with disease progression and decreased overall survival in advanced-stage melanoma patients*. *Cancer Immunol Immunother*, 2013. **62**(11): p. 1711-22.
27. Poschke, I. and R. Kiessling, *On the armament and appearances of human myeloid-derived suppressor cells*. *Clin Immunol*, 2012. **144**(3): p. 250-68.
28. Chen, S., et al., *Immunosuppressive functions of hepatic myeloid-derived suppressor cells of normal mice and in a murine model of chronic hepatitis B virus*. *Clin Exp Immunol*, 2011. **166**(1): p. 134-42.
29. Ochoa, A.C., et al., *Arginase, prostaglandins, and myeloid-derived suppressor cells in renal cell carcinoma*. *Clin Cancer Res*, 2007. **13**(2 Pt 2): p. 721s-726s.
30. Liu, C.Y., et al., *Population alterations of L-arginase- and inducible nitric oxide synthase-expressed CD11b+/CD14(-)/CD15+/CD33+ myeloid-derived suppressor cells and CD8+ T lymphocytes in patients with advanced-stage non-small cell lung cancer*. *J Cancer Res Clin Oncol*, 2010. **136**(1): p. 35-45.
31. Chang, C.C., et al., *Tolerization of dendritic cells by T(S) cells: the crucial role of inhibitory receptors ILT3 and ILT4*. *Nat Immunol*, 2002. **3**(3): p. 237-43.
32. Ge, G., et al., *Induction of CD4+ CD25+ Foxp3+ T regulatory cells by dendritic cells derived from ILT3 lentivirus-transduced human CD34+ cells*. *Transpl Immunol*, 2012. **26**(1): p. 19-26.
33. Vlad, G. and N. Suci-Foca, *Induction of antigen-specific human T suppressor cells by membrane and soluble ILT3*. *Exp Mol Pathol*, 2012.
34. Vlad, G., R. Cortesini, and N. Suci-Foca, *CD8+ T suppressor cells and the ILT3 master switch*. *Hum Immunol*, 2008. **69**(11): p. 681-6.
35. Waschbisch, A., et al., *Interferon Beta and vitamin d synergize to induce immunoregulatory receptors on peripheral blood monocytes of multiple sclerosis patients*. *PLoS One*, 2014. **9**(12): p. e115488.
36. Cella, M., et al., *A novel inhibitory receptor (ILT3) expressed on monocytes, macrophages, and dendritic cells involved in antigen processing*. *J Exp Med*, 1997. **185**(10): p. 1743-51.
37. Zhang, Y., et al., *Expression of immunoglobulin-like transcript (ILT)2 and ILT3 in human gastric cancer and its clinical significance*. *Mol Med Rep*, 2012. **5**(4): p. 910-6.
38. Dobrowolska, H., et al., *Expression of immune inhibitory receptor ILT3 in acute myeloid leukemia with monocytic differentiation*. *Cytometry B Clin Cytom*, 2013. **84**(1): p. 21-9.
39. Jensen, M.A., et al., *Functional genetic polymorphisms in ILT3 are associated with decreased surface expression on dendritic cells and increased serum cytokines in lupus patients*. *Ann Rheum Dis*, 2013. **72**(4): p. 596-601.





# CHAPTER

## **STEREOTACTIC ABLATIVE RADIOTHERAPY INDUCES PERIPHERAL T-CELL ACTIVATION IN EARLY STAGE LUNG CANCER PATIENTS**

Pauline L. de Goeje, Egbert F. Smit, Cynthia Waasdorp,  
Merel T.B. Schram, Margaretha E.H. Kaijen-Lambers, Koen  
Bezemer, Mark de Mol, Koen J. Hartemink, Joost J.M.E.  
Nuyttens, Alexander P.W.M. Maat, Joost P.J.J. Hegmans, Rudi  
W. Hendriks, Suresh Senan, Joachim G.J.V. Aerts

*Published in:*

*Am J Respir Crit Care Med. 2017 Nov 1;196(9):1224-1227.*

*doi: 10.1164/rccm.201610-2178LE.*

# 3

Both surgery and stereotactic ablative body radiotherapy (SABR) are guideline-specified treatments for early stage non-small cell lung cancer (NSCLC). However, despite curative treatment approaches, patients may develop disease recurrences which are often incurable [1]. Immune infiltration of the tumor is correlated to survival, and depending on the immune cell types present, either has a positive (immune activating cells) or negative (immune suppressive cells) prognostic value [2]. Radiotherapy has both been reported to suppress and activate the immune system. This depends most likely on the dose and, as part of the effects are caused by dying tumor cells, also by tumor type and stage [3]. NSCLC is known to suppress the immune system [4], and tumor removal by itself might therefore also have an immune stimulatory effect. We hypothesized that the two treatment options (SABR or surgery) would differentially affect the immune response in early stage NSCLC. Here, we assessed the effects on the induction of T-cell activation in the early post-treatment period. Some of the results of these studies have been previously reported in the form of an abstract [5].

Blood samples were collected from 23 histological or cytological proven early stage (cT1-T2aN0M0) NSCLC patients who underwent surgery (n=13) or SABR in 3 to 8 fractions (n=10), as determined by the treating physician (ClinicalTrials.gov identifier NCT02488850). All patients signed informed consent before inclusion in the study. Peripheral blood mononuclear cells (PBMC) were isolated at baseline, and at four time points during the first six weeks after treatment. PBMC were stained with antibodies against T-cell subset and activation markers and analyzed by flow cytometry. Flow cytometry procedures, 4h cell stimulation with phorbol-12-myristate-13-acetate and ionomycin and cytokine stainings have been described previously [6]. Linear mixed effects models using maximum likelihood with patient-specific random effects were used to determine changes in immune populations. Normality of the residuals was checked and if needed, transformation of the data was applied. Statistical analyses were performed in R for windows, version 3.2.3. Figures were generated in GraphPad Prism 5.

In both groups the proportions of total CD4 and CD8 T-cells within PBMC did not substantially change over the first 6 weeks of treatment. Likewise, proportions of different T-cell subsets, including  $\gamma\delta$ -T-cells, NKT-cells and naïve and memory T-cells remained stable over time, where regulatory T-cell proportions increased from 5% to 6% of CD4 on average (not shown). To determine the activation status of the T-cells, we assessed expression of CD69, CD25, PD-1, CTLA4 and the proliferation marker Ki67, likely reflecting relevant effector cells [7]. We did not observe changes over time in CD69, CD25 and CTLA4. However, the fractions of proliferating (Ki67<sup>+</sup>) and PD-1 expressing T-cells increased significantly after SABR ( $p < 0.001$  for both Ki67<sup>+</sup> FoxP3-CD4<sup>+</sup> non-regulatory T-cells and Ki67<sup>+</sup> CD8 T-cells,



$p=0.032$  and  $p=0.029$  for PD-1<sup>+</sup> CD4 and CD8 T-cells, respectively)(Figure 1). In the surgery group, smaller but significant changes were seen in Ki67<sup>+</sup> proportions. The interaction term of time and group, however, showed that there was a significant difference in kinetics of Ki67<sup>+</sup> CD8 T-cells between the two treatments ( $p<0.001$ ), but did not reach significance for Ki67<sup>+</sup>CD4 T-cells. No significant changes in PD-1<sup>+</sup> proportions were observed in the surgery group. PD-1 is upregulated on T-cells upon recognition of the cognate antigen, and can be indicative of either activation or exhaustion of T-cells [2]. To assess whether the PD-1<sup>+</sup> T-cells in the peripheral blood of these patients were functionally active or exhausted, we analyzed their interferon  $\gamma$  (IFN $\gamma$ ) production. Figure 2A shows that in PD-1<sup>+</sup> CD4 and CD8 T-cells, the fractions of IFN $\gamma$ -producing cells were larger than in the PD-1<sup>-</sup> T-cell populations ( $p<0.001$  for both CD4 and CD8 T-cells), indicating that the PD-1<sup>+</sup> cells are more functionally active than the PD-1<sup>-</sup> T-cells. Moreover, in four of nine SABR-treated patients (one patient had a non-evaluable sample at baseline), PD-1<sup>+</sup> proportions increased with at least >4%. Figure 2B shows that in these four patients, the increase in PD1<sup>+</sup> T-cells coincided with an increase in proportions of IFN $\gamma$ <sup>+</sup> T-cells, again supporting that in early stage NSCLC patients, PD-1 expression is indicative of increased T-cell functionality rather than exhaustion. Of note, the only surgery-treated patient that showed an increase in PD1<sup>+</sup> T-cells, also showed an increase in IFN $\gamma$ <sup>+</sup> T-cells (not shown).

In this non-randomized observational study, we showed that SABR induced peripheral blood T-cell activation in a major subgroup of patients with early stage lung cancer, whereas after surgery, only a minor and temporary increase in proliferation was induced. The T-cell response to SABR was mainly characterized by an increased PD-1 expression and proliferation, while earlier activation markers did not detectably increase in peripheral blood. No evidence of superiority of either of the two treatments with respect to clinical outcome has been published as of today [8]. In our study, with a median follow up time of 712 days, the recurrence rates were similar (surgery: 2 out of 13, SABR: 3 out of 10), whereby the small sample size does not allow for statistical evaluation. The observed immune activation after SABR, however, can potentially be beneficial in several combination treatment strategies. Firstly, PD-1 is upregulated on T-cells after cognate antigen recognition, and acts as a checkpoint for T-cells by negatively modulating the immune response upon binding of its ligand. Blockade of this receptor-ligand interaction prolongs the immune response and has been shown to improve clinical outcome in NSCLC significantly [9].

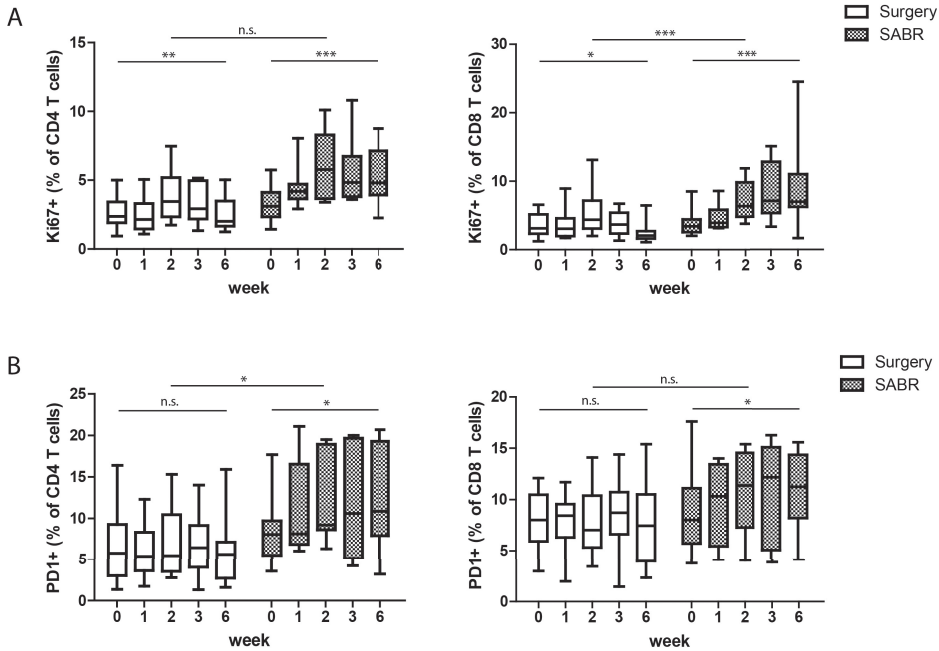


**Figure 1.** T-cell proliferation and PD-1 expression after surgery or SABR in early stage NSCLC patients. Ki67 positive proportions of FoxP3<sup>-</sup> non-regulatory CD4 T-cells and CD8 T-cells (A) and PD-1 positive proportions of CD4 and CD8 T-cells (B) at baseline and during the first six weeks after treatment with either surgery (n=13) or SABR (n=10) were determined by flow cytometry. Changes over time were assessed per group with linear mixed effects models with patient-specific random effects. Differences in kinetics between the two groups (A) were assessed by the time\*group interaction term. \*\*\* =  $p < 0.001$ ; \*\* =  $p < 0.01$ ; \* =  $p < 0.05$ ; n.s. = not significant.

Our findings that SABR induces T-cell activation and concomitant PD-1 expression suggests that the combination of SABR with an inhibitor of the PD-1/PD-L1 axis, may be an interesting treatment strategy, particularly as it is known that PD-L1 is upregulated on tumor cells and myeloid cells in response to IFN $\gamma$ , which we found to be increased simultaneously. Secondly, combinations of surgery and radiotherapy treatment are sometimes administered in the context of post-surgical adjuvant radiotherapy [10]. In light of our results, a superior outcome might be achieved when radiotherapy is administered prior to surgery as a neo-adjuvant immune activating therapy. In fact, a phase II clinical trial is currently recruiting to evaluate this hypothesis [11]. In conclusion, SABR induces systemic T-cell activation, characterized by PD1 expression in a major fraction of patients, while surgery does not. These findings argue for combining SABR with checkpoint inhibitors or other immunotherapies with or without surgery. Furthermore, it would be of interest to incorporate immune-monitoring, which may be expanded with additional activation markers [7], in upcoming (clinical) studies.

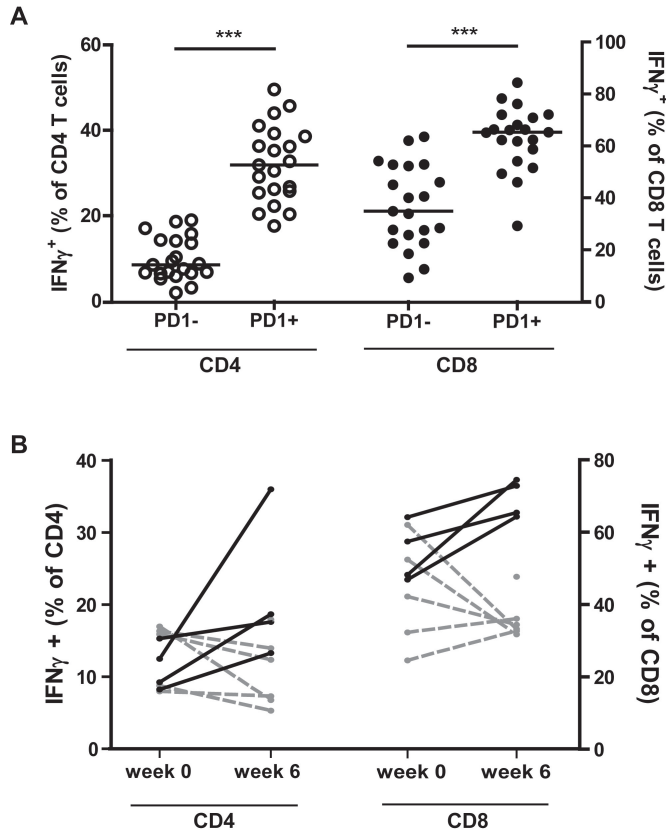


**Figure 2.** Intracellular IFN $\gamma$  expression after *in vitro* stimulation of peripheral blood T-cells. A. Intracellular IFN $\gamma$  expression in PD1<sup>+</sup> and PD1<sup>-</sup> fractions of T-cells of NSCLC patients. \*\*\* =  $p > 0.001$  (Wilcoxon signed rank test). B. Changes in IFN $\gamma$ -producing T-cells in NSCLC patients 6 weeks after SABR. Two groups of patients are depicted, the patients that showed an increase in PD-1 positive T-cells 6 weeks after treatment (black solid lines) versus the patients that do not show an increase in PD-1 positive T-cells (grey dashed lines).

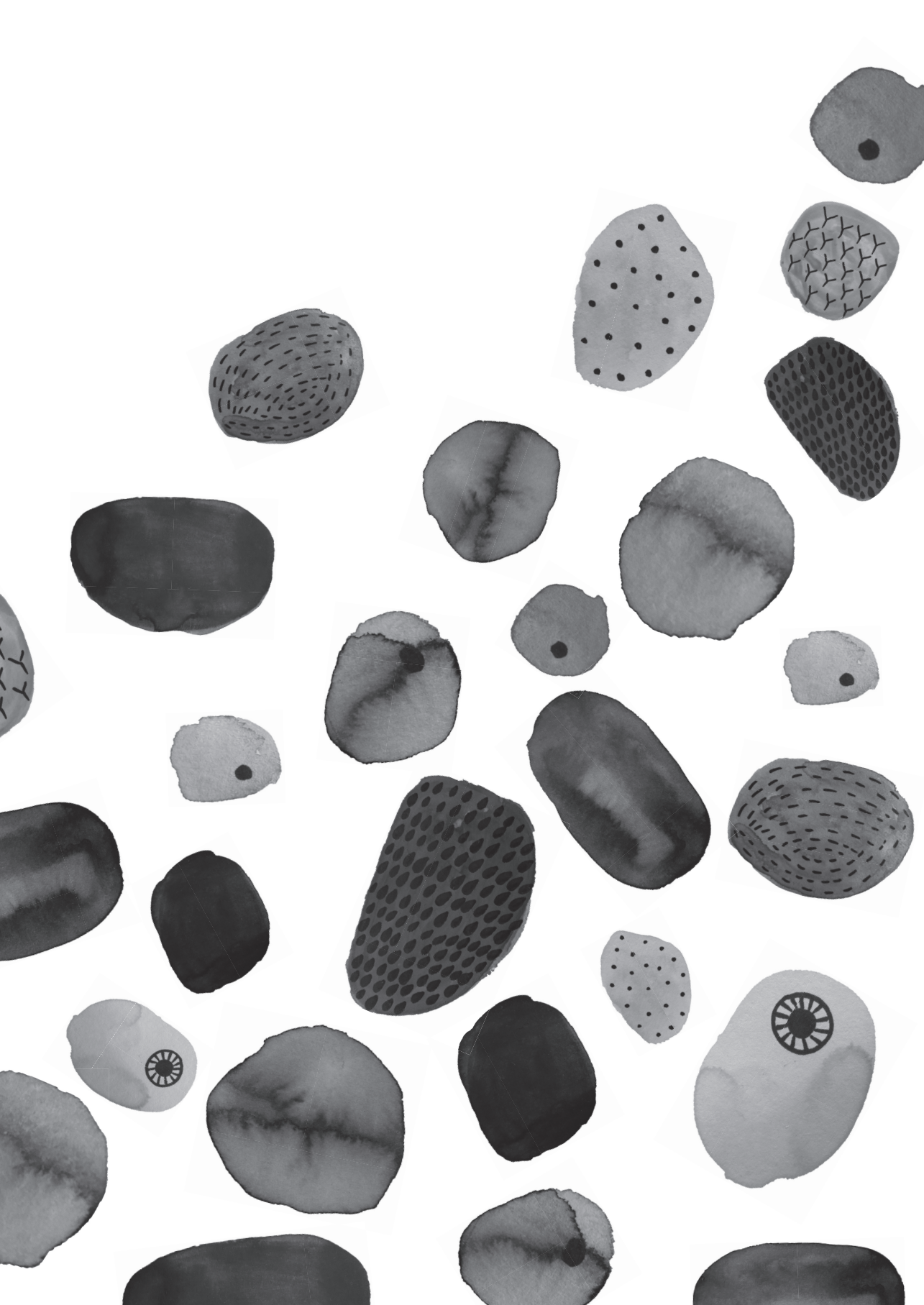
## ACKNOWLEDGEMENTS

First of all, we thank all patients for their participation in this study. Furthermore, we thank K.A.L. Mauff for statistical assistance.

## REFERENCES

1. Hung, J.J., et al., *Post-recurrence survival in completely resected stage I non-small cell lung cancer with local recurrence*. Thorax, 2009. **64**(3): p. 192-6.
2. Remark, R., et al., *The non-small cell lung cancer immune contexture. A major determinant of tumor characteristics and patient outcome*. Am J Respir Crit Care Med, 2015. **191**(4): p. 377-90.
3. Deloch, L., et al., *Modern Radiotherapy Concepts and the Impact of Radiation on Immune Activation*. Front Oncol, 2016. **6**: p. 141.
4. Motz, G.T. and G. Coukos, *Deciphering and reversing tumor immune suppression*. Immunity, 2013. **39**(1): p. 61-73.
5. Aerts, J.G. *Immune Activation in Early Stage Non-Small Cell Lung Cancer (NSCLC) following Stereotactic Ablative Radiotherapy (SABR) and Surgery (ID 2123)*. in *16th World Conference on Lung Cancer*. 2015. Denver.
6. Paats, M.S., et al., *Systemic CD4+ and CD8+ T-cell cytokine profiles correlate with GOLD stage in stable COPD*. Eur Respir J, 2012. **40**(2): p. 330-7.
7. Miller, J.D., et al., *Human effector and memory CD8+ T cell responses to smallpox and yellow fever vaccines*. Immunity, 2008. **28**(5): p. 710-22.
8. Chang, J.Y., et al., *Stereotactic ablative radiotherapy versus lobectomy for operable stage I non-small-cell lung cancer: a pooled analysis of two randomised trials*. Lancet Oncol, 2015. **16**(6): p. 630-7.
9. Brahmer, J., et al., *Nivolumab versus Docetaxel in Advanced Squamous-Cell Non-Small-Cell Lung Cancer*. N Engl J Med, 2015. **373**(2): p. 123-35.
10. Pechoux, C.L., et al., *Role of adjuvant radiotherapy in completely resected non-small-cell lung cancer*. EJC Suppl, 2013. **11**(2): p. 123-30.
11. Safi, S., et al., *A randomized phase II study of radiation induced immune boost in operable non-small cell lung cancer (RadImmune trial)*. BMC Cancer, 2015. **15**: p. 988.





# CHAPTER

## **INDUCTION OF PERIPHERAL EFFECTOR CD8 T CELL PROLIFERATION BY PACLITAXEL/ CARBOPLATIN/ BEVACIZUMAB IN NON-SMALL CELL LUNG CANCER PATIENTS**

Pauline L. de Goeje, Myrthe Poncin, Koen Bezemer,  
Margaretha E.H. Kajjen-Lambers, Harry J. Groen, Egbert  
F. Smit, Anne-Marie C. Dingemans, André Kunert, Rudi W.  
Hendriks, Joachim G.J.V. Aerts

*Published in:*

*Clin Cancer Res. 2019 Apr 1;25(7):2219-2227. doi:  
10.1158/1078-0432.CCR-18-2243. Epub 2019 Jan 14.*

4

## STATEMENT OF TRANSLATIONAL RELEVANCE

To rationally combine checkpoint inhibition and conventional treatment modalities in advanced NSCLC, a better understanding of the immunomodulatory effect of conventional treatments is required. In this study, increased proliferation of peripheral blood CD8 effector T cells was observed after treatment of stage IV NSCLC patients with paclitaxel/carboplatin/bevacizumab. Proliferating CD8 T cells expressed higher levels of PD-1 and CTLA-4. Since similar populations have been found to be associated with response to checkpoint inhibition, these results suggest that paclitaxel/carboplatin/bevacizumab treatment induces an immune profile reflecting sensitivity for checkpoint inhibition.

## ABSTRACT

**Introduction:** Chemotherapy has long been the standard treatment for advanced stage non-small cell lung cancer (NSCLC), but checkpoint inhibitors are now approved for use in several patient groups and combinations. To design optimal combination strategies, a better understanding of the immune modulatory capacities of conventional treatments is needed. Therefore, we investigated the immune-modulatory effects of paclitaxel/carboplatin/bevacizumab (PCB), focusing on immune populations associated with response to checkpoint inhibitors in peripheral blood.

**Methods:** 223 stage IV NSCLC patients, enrolled in the NVALT12 study, received PCB, with or without nitroglycerin patch. Peripheral blood was collected at baseline and after the first and second treatment cycle. Proportions of T cells, B cells, and monocytes were determined by flow cytometry. Furthermore, several subsets of T cells and the expression of Ki67 and co-inhibitory receptors on these subsets were determined.

**Results:** Whereas proliferation of CD4 T cells remained stable following treatment, proliferation of peripheral blood CD8 T cells was significantly increased, particularly in the effector memory and CD45RA<sup>+</sup> effector subsets. The proliferating CD8 T cells more highly expressed PD-1 and CTLA-4 compared to non-proliferating CD8 T cells. Immunological responders (>2-fold increased proliferation after treatment) did not show an improved progression free or overall survival.

**Conclusions:** Paclitaxel/ carboplatin/ bevacizumab induces proliferation of CD8 T cells, consisting of effector cells expressing co-inhibitory checkpoint molecules. Induction of proliferation was not correlated to clinical outcome in the current clinical setting. Our findings provide a rationale for combining PCB with checkpoint inhibition in lung cancer.



## INTRODUCTION

Despite the great progress that has been made in the field of lung cancer treatment over the last decades, non-small cell lung cancer (NSCLC) remains to be responsible for the highest cancer mortality worldwide [1]. Current treatments for metastasized NSCLC consist of platinum-based chemotherapy, specific therapies targeting genetic abnormalities, and checkpoint inhibition. Checkpoint inhibitors targeting programmed death receptor (PD)-1 or PD-ligand 1 (PD-L1) are now a cornerstone in the treatment of NSCLC: PD-1 inhibitors nivolumab and pembrolizumab, and PD-L1 inhibitors durvalumab and atezolizumab are all FDA approved treatments under certain conditions for patients with NSCLC in different stages of the disease [2-6]. For first-line treatment in NSCLC, pembrolizumab is FDA approved as single treatment for patients with >50% PD-L1-positive tumor cells and in combination with pemetrexed/carboplatin for non-squamous NSCLC regardless of PD-L1 status [7, 8]. Recently, the IM150 study was the first phase III study showing improved survival with first line treatment of a PD-L1 inhibitor in an unselected group of patients. Here, combined treatment of atezolizumab with paclitaxel/carboplatin/bevacizumab (PCB) performed better than PCB alone and was FDA approved recently [9]. As a result, the question now arising is whether the addition of chemotherapy treatment increases the response to checkpoint inhibitors. It is therefore important to understand the immune modulatory effects of chemotherapy.

In previous reports on the immune modulatory effects of chemotherapy, contradictory results were obtained. For example, Ramakrishnan and colleagues found an increased CD8<sup>+</sup> T cell infiltration after treatment with carboplatin/paclitaxel in various mouse models [10]. On the other hand, Pfirschke and colleagues did not observe any induced CD8 T cell responses after treatment with paclitaxel in mouse models, in contrast to treatment with oxaliplatin/cyclophosphamide. Indeed, variable effects on several immune cell populations have been described for different chemotherapeutic treatments, as reviewed by Galuzzi et al. [11].

Monitoring chemotherapy-induced changes requires sequential patient samples. While the availability of tumor biopsies of metastasized NSCLC is limited, peripheral blood is relatively easy and non-invasive to obtain. Furthermore, peripheral blood immune populations have been shown to have predictive or prognostic value in several studies [12]. Recently, Ki67 expression of CD8 T cells has been suggested as biomarker for response to checkpoint inhibition in both melanoma and NSCLC [13, 14]. In the current study, we investigated the peripheral blood immune profile of patients with metastasized NSCLC during treatment with the PCB chemotherapy combination, with a focus on immune populations that have been reported to be associated with response to checkpoint inhibition. We used multiplex

flow cytometry as a method to assess (surface) protein expression on a single cell level, allowing assessment of specific immune populations and their activation status. We aimed to identify populations that are affected by the chemotherapy/bevacizumab combination and might act as a catalyst for response to immunotherapy treatment.

## **MATERIALS AND METHODS**

### **Study population**

The patients in this study were all enrolled in the NVALT12 study (trial number NCT01171170), a randomized phase II multicenter study on the effect of a nitroglycerin patch or placebo in patients with stage IV NSCLC treated with PCB. Details of the study are described elsewhere [15]. In short, 223 non-squamous NSCLC patients were included who were all diagnosed with stage IV disease and were not eligible for treatment with curative intent. Patients were treatment-naïve and received PCB every three weeks for three cycles. Nine patients did not start treatment; these patients were excluded from the analysis. The same dose of paclitaxel (175 mg/m<sup>2</sup>) and carboplatin (AUC=6) was administered to each patient and no major dose adjustments were made after the first cycle. Bevacizumab was continued every three weeks until progression. This study had two treatment arms: a control arm with patients only receiving the PCB combination, and an experimental arm in which a nitroglycerin patch was applied for five consecutive days around the day of chemotherapy administration. Written consent was obtained from all individuals before blood sampling and the study was approved by the Dutch Central Committee on Research Involving Human Subjects (CCMO: NL33442.042.10). The study was conducted in accordance with the ethical standards of the institutional and national research committee and with the 1964 Helsinki Declaration and its later amendments.

### **Peripheral blood processing**

For the exploratory objectives of this study, peripheral blood was collected from patients on the day of the first, second and third cycle of treatment, prior to treatment administration. These samples correspond to week 0, week 3 and week 6 from start of therapy. Twenty mL of blood was drawn in EDTA tubes and processed within six hours of blood collection. Peripheral blood mononuclear cells (PBMC) were isolated via standard density-gradient centrifugation using Ficoll-Hypaque (GE Healthcare, Diegem, Belgium). One million cells were used for flow cytometry staining of myeloid-derived suppressor cells (MDSC). The remaining cells were cryopreserved in 10% dimethyl sulfoxide (Sigma-Aldrich, St Louis, Mo), 40% fetal calf serum (Gibco) and RPMI (Invitrogen, Molecular Probes, Waltham, Mass) until further use.

## Flow cytometry

Three different flow cytometry stainings were performed on the PBMC samples: one myeloid staining (performed on fresh material), a T cell staining and an intracellular cytokine staining (both performed on cryopreserved samples). Prior to the intracellular cytokine staining, cells were stimulated for 4 hours at 37°C with phorbol 12-myristate 13-acetate (PMA) and ionomycin (both from Sigma-Aldrich, USA), supplemented with GolgiStop (BD Biosciences, USA) [16]. The antibodies used for the three stainings are listed in Supplementary Table S1. First, extracellular markers were stained for 30 minutes at 4°C. Subsequently, cells were fixed and permeabilized with FoxP3 transcription factor fix/perm mix (eBioscience) (T cell staining) or fixed with 2% PFA and permeabilized with 0.5% saponin (intracellular cytokine staining). Next, intracellular markers were stained for 60 minutes at 4°C. FoxP3, Ki67, CTLA-4, Granzyme B and IFN $\gamma$  were stained intracellular. All other markers were included in the extracellular staining. To identify dead cells, 4',6-diamidino-2-phenylindole (DAPI, Molecular Probes) (myeloid staining) or LIVE/DEAD™ fixable aqua dead cell stain kit (Invitrogen) (T cell and intracellular cytokine staining) were used. Data were acquired using an LSR II flow cytometer equipped with three lasers and analyzed using FlowJo (Tree Star, Inc., USA). FMO controls were used for gating where appropriate.

## Statistical analysis

Statistical analyses were performed in R version 3.4.2 for windows (The R Foundation for Statistical Computing) and by Prism 5 (GraphPad).  $P < 0.05$  was considered statistically significant. Changes of immune populations over time were tested against baseline, using the Wilcoxon signed rank test, taking into account paired samples. Multiple comparison correction was applied by adjusting the  $\alpha$ :  $p < 0.025$  was considered as significant in case of two comparisons (i.e. week 3 vs week 0 and week 6 vs week 0). The bar graphs show median values with error bars representing the interquartile range. Survival of different patient subpopulations was displayed using Kaplan Meier curves and tested using a log-rank test. Tumor lesion measurements for RECIST1.1 responses were used as a measure of total tumor burden. Total tumor diameter was determined as the sum of the diameters of target lesions measured on computed tomography (CT) scans.

# RESULTS

## Patient characteristics

In this study, we analyzed peripheral blood samples of patients that were enrolled in the NVALT12 study, the details of which are previously published [15]. For immune monitoring analysis, we used data of all patients whose blood was collected and processed for both

week 0 and at least one of the later time points (week 3 and week 6), which resulted in a total of 131 patients with paired samples. No significant differences in baseline immune populations or clinical outcome were observed between these 131 patients and the patients from whom only a baseline sample was available, ruling out a 'lost to follow-up' bias (Supplementary Table S2). 68 patients received standard PCB combination therapy in the control arm of the study, and 63 patients received an additional nitroglycerin patch with the aim to dilate blood vessels to increase chemotherapy efficacy in the experimental arm (Supplementary Table S3). However, the experimental arm did not improve progression free survival (PFS) or overall survival (OS) (see ref [15]). We first checked whether there were any differences in the dynamics of major immune populations between the two treatment arms. After the second treatment cycle (week 6 after start of treatment) no significant differences were seen between the proportions of T cells, the CD4/CD8 T cell ratio, the proportions of myeloid cells, and the proportions of B cells (Supplementary Table S3). Because no differences in clinical outcome (PFS and OS) between the two treatment arms were reported and because our data did not indicate any effects on immune dynamics, we decided to pool the two treatment arms for the remaining analyses.

### **Chemotherapy in NSCLC patients results in increased proportions of T cells**

We assessed whether any major PBMC populations were changed within the first six weeks after the start of treatment. Absolute number of total PBMC did not change over time (Supplementary Figure S1). At week 6, the proportions of T cells were significantly increased compared to baseline values (median 46.3% vs. 42% of PBMC,  $p=0.001$ , Wilcoxon signed rank test; Figure 1). As T cells play an important role in anti-tumor immunity, we further explored the chemotherapy-induced changes in peripheral blood T cells by assessing the relative fractions of CD8 T cells (cytotoxic T lymphocytes; CTLs), non-regulatory CD4 T cells (T helper cells) and regulatory T cells (Tregs). The proportions of these subsets within the total T cell population remained stable over time (Supplementary Figure S2). As the staining protocol for myeloid cells was expanded to include the marker CD16 after inclusion of the first 40 patients, this allowed us to additionally characterize three monocyte subsets in 95 patients. These analyses revealed a relative increase in non-classical monocytes and intermediate monocytes and a decrease in classical monocytes (Supplementary Figure S3).

### **Proportions of Ki67<sup>+</sup> cells within the CD8, but not within the CD4 T cell population increase after chemotherapy treatment**

Because we observed an increase in the proportions of total T cells, we assessed the proportions of proliferating (Ki67<sup>+</sup>) cells within the T cell subsets. An increase in the proportions of proliferating cells was observed specifically in the CD8<sup>+</sup> T cells ( $p=0.004$  at

week 3 and  $p < 0.001$  at week 6, compared to baseline; Figure 2B). A transient decrease was seen in the proportions of Ki67<sup>+</sup> Tregs at week 3 ( $p = 0.003$ , compared to baseline), returning to baseline levels at week 6. No changes in the proliferation of non-regulatory CD4 T cells were observed.

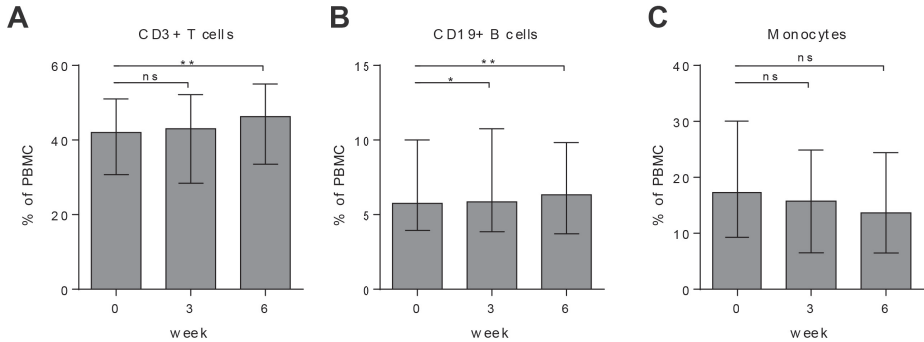


**Figure 1.** Proportions of major leukocyte populations in NSCLC patients treated with chemotherapy. Proportions of CD3<sup>+</sup> T cells (A), CD19<sup>+</sup> B cells (B) and monocytes (C) in PBMC of NSCLC patients treated with PCB before start (week 0), after the first (week 3) and second (week 6) cycle of chemotherapy, as determined by flow cytometric analysis. Bars represent median values with interquartile range. \*  $p < 0.025$  \*\*  $p < 0.005$  \*\*\*  $p < 0.0005$  ( $\alpha$  level adjusted for multiple comparisons; Wilcoxon signed rank test)

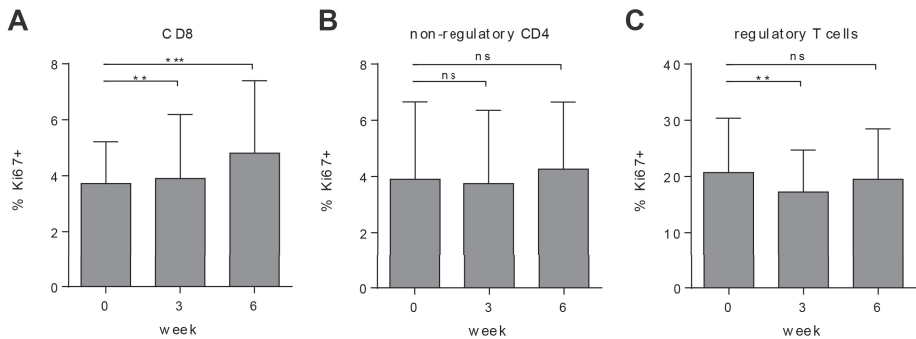


**Figure 2.** Changes in the proliferation of T cell subsets in peripheral blood of NSCLC patients treated with chemotherapy. Ki67 expression was assessed as marker of proliferation on CD8 T cells (A), FoxP3<sup>-</sup> non-regulatory CD4 T cells (B) and FoxP3<sup>+</sup> regulatory CD4 T cells (C) by flow cytometry of PBMC samples before treatment (week 0) and 3 and 6 weeks after start of treatment. Ki67<sup>+</sup> T cells are depicted as percentage of the parent population. \*\*  $p < 0.005$ , \*\*\*  $p < 0.0005$ , ns = not significant (Wilcoxon-signed rank test)

### Increased proliferation occurs mainly in effector CD8 T cells

Next, we asked whether the increase in proliferation of CD8 T cells could be attributed to a specific maturation subset. To this end, we identified fractions of CD45RA<sup>+</sup>CCR7<sup>+</sup> naive T cells ( $T_N$ ), CD45RA<sup>+</sup>CCR7<sup>+</sup> central memory T cells ( $T_{CM}$ ), CD45RA<sup>+</sup>CCR7<sup>-</sup> effector memory T cells ( $T_{EM}$ ) and CD45RA<sup>+</sup>CCR7<sup>-</sup> effector T cells ( $T_{EMRA}$ ), as shown in Figure 3A. Proportions of Ki67<sup>+</sup> CD8 T cells were increased in all four subsets at week 6 compared to baseline. The largest proportions of Ki67<sup>+</sup> T cells were present within the CD8  $T_{EM}$  subset. Both  $T_{EM}$  and  $T_{EMRA}$  CD8 showed a clear increase of the Ki67<sup>+</sup> fraction starting at week 3 ( $T_{EM}$   $p=0.007$ ;  $T_{EMRA}$   $p<0.001$ ). These results indicate that mainly the effector CD8 T cells respond to chemotherapy with an increased capacity for proliferation.

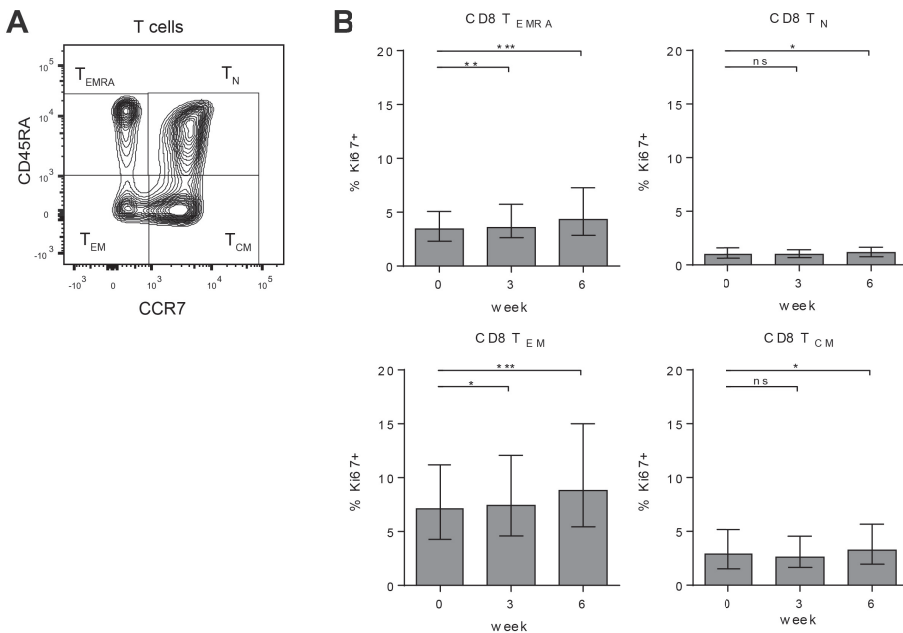


**Figure 3.** Changes in Ki67<sup>+</sup> proportions within maturation stages of CD8 T cells. A) The different maturation stages for CD8 T cells were determined by flow cytometry using the markers CD45RA and CCR7, defining the following subsets: naive ( $T_N$ : CD45RA<sup>+</sup>CCR7<sup>+</sup>), central memory ( $T_{CM}$ : CD45RA<sup>+</sup>CCR7<sup>+</sup>), effector memory ( $T_{EM}$ : CD45RA<sup>+</sup>CCR7<sup>-</sup>) and CD45RA<sup>+</sup> effector ( $T_{EMRA}$ : CD45RA<sup>+</sup>CCR7<sup>-</sup>). B) Ki67<sup>+</sup> proportions of T cell maturation subsets as defined in panel A. Ki67<sup>+</sup> T cells are depicted as percentage of the parent population. \*  $p<0.025$ , \*\*  $p<0.005$ , \*\*\*  $p<0.0005$ , ns = not significant (Wilcoxon-signed rank test)

### Proliferating CD8 T cells have higher expression of co-inhibitory receptors

To further investigate the phenotype of the proliferating effector CD8 T cells, we determined the expression of PD-1 and cytotoxic T-lymphocyte-associated antigen-4 (CTLA-4). These two well-known co-inhibitory receptors can be targeted by checkpoint inhibitors

currently approved for treatment of several cancer types. Figure 4 shows the expression of these surface markers in CD8 T<sub>EM</sub> cells. Similar results for CD8 T<sub>EMRA</sub> cells were obtained (Supplementary Figure S4). Proliferating CD8 T<sub>EM</sub> showed higher proportions of PD-1<sup>+</sup> cells than non-proliferating CD8 T<sub>EM</sub>. At week 3, a small decrease was seen in the proportions of PD1<sup>+</sup> T cells (Figure 4A). Furthermore, within the PD-1-positive fraction, mean fluorescence intensity (MFI) values indicated a higher per cell expression level of PD-1 in proliferating versus non-proliferating cells (Figure 4B). Expression of CTLA-4 was generally low in peripheral blood T cells. However, expression of CTLA-4 was higher in Ki67<sup>+</sup>PD-1<sup>+</sup> CD8 T cells than in CD8 T cells that were single positive for either Ki67 or PD-1 (Figure 4C).

In summary, these findings show that proliferation of CD8<sup>+</sup> T cells is associated with higher expression of the co-inhibitory receptors PD-1 and CTLA-4 over the 6 weeks period evaluated.

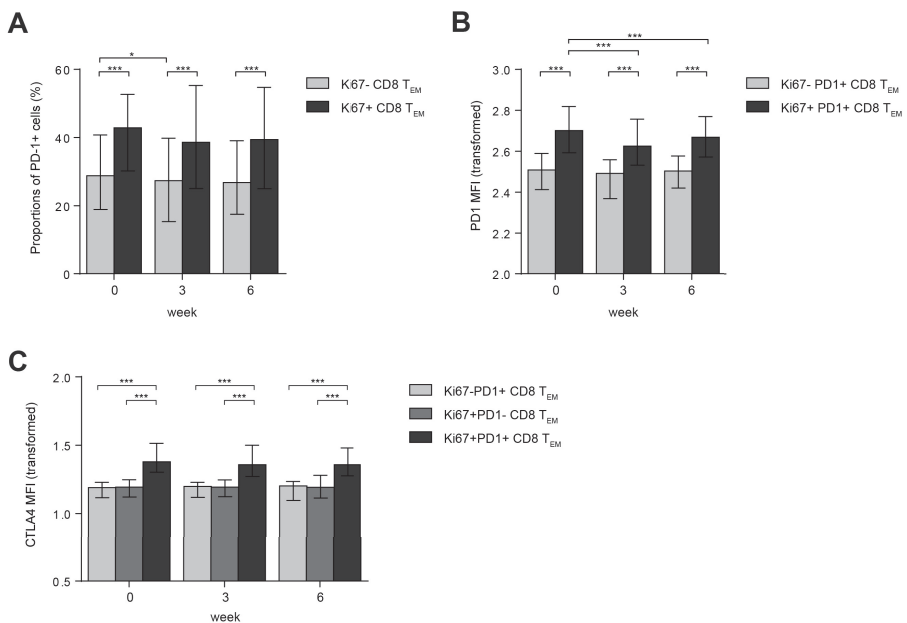


**Figure 4.** Co-inhibitory receptor expression on proliferating CD8 T<sub>EM</sub> cells in peripheral blood of chemotherapy-treated NSCLC patients. A) Proportions of PD1<sup>+</sup> cells within Ki67<sup>-</sup> and Ki67<sup>+</sup> CD8 T<sub>EM</sub> populations over time. B) PD-1 expression on Ki67<sup>-</sup> and Ki67<sup>+</sup> PD-1<sup>+</sup> CD8 T<sub>EM</sub> cells over time, as depicted by mean fluorescent intensity (MFI). The MFI value is presented as biexponentially transformed value. C) Expression of CTLA-4 CD8 T<sub>EM</sub> subsets as defined by PD1 and Ki67 expression over time. Biexponentially transformed MFI value is depicted. In all graphs, the bars show median values with the interquartile range depicted by the error bars. \*  $p < 0.025$ , \*\*  $p < 0.005$ , \*\*\*  $p < 0.0005$  (Wilcoxon-signed rank test)

### **Increased proliferation of CD8 T cells in peripheral blood of NSCLC patients after chemotherapy treatment does not correlate with clinical response**

To investigate whether the observed increase in proliferation of effector CD8 T cells correlated with the clinical outcome of these patients, we defined immunological responders (iR) as the patients in whom an increase in the proportions of Ki67<sup>+</sup> CD8 T cells at week 3 or week 6 of at least a two-fold was observed ( $n=35$ ). Immunological non-responders (iNR) were defined as patients who showed no increase at either week 3 or week 6 (fold change  $<1$ ;  $n=31$ ). These cut-off values were chosen based on the distribution of the data as seen from figure 5A, and closely resemble the 25% and 75% percentiles to provide groups that show distinct Ki67 dynamics with at least 30 patients per group. No significant differences in both PFS and OS were observed between the iR and iNR patient groups (Figure 5B). Notably, also baseline proportions of Ki67<sup>+</sup> CD8 T cells did not correlate with survival ( $\beta = 1.01$ , 95%CI 0.98-1.04; Cox regression). The proportions of PD1<sup>+</sup> cells were equal in proliferating T<sub>EM</sub> from iR and iNR patients (Figure 5C), but the per-cell expression levels of both PD1 and CTLA-4 decreased over time in iR, but not in iNR patients (Figure 5D and 5E).

Huang et al. [13] have shown that in melanoma patients treated with a PD-1 inhibitor, increased proportions of Ki67<sup>+</sup> CD8 T cells were correlated with clinical outcome, but only when combined with total tumor burden into a Ki67<sup>+</sup>CD8/tumor burden ratio. Therefore, we calculated the ratio of Ki67<sup>+</sup> of CD8 T cells over the tumor burden, estimated by the total tumor diameter defined during RECIST1.1 response evaluation. In this cohort of PCB-treated NSCLC patients, we did not detect a difference in OS between patients with a high or low Ki67<sup>+</sup>CD8/tumor burden ratio (Supplementary Figure S5).

### **Proliferation of CD8 T cells is correlated with proportions of MDSCs**

Besides immune activating cell populations, we analyzed two main immune suppressive cell populations, Tregs and myeloid-derived suppressor cells (MDSC), in the peripheral blood. Neither the proportions of FoxP3<sup>+</sup> Tregs (as shown in Figure 1B), nor the expression of PD-1 and CTLA-4 on Tregs (Supplementary Figure S6) changed over time. In contrast, granulocytic MDSC, characterized by expression of CD33, CD11b, CD15 and a lack of expression of CD14 and HLA-DR, were elevated 3 weeks after start of treatment, but returned to baseline levels by week 6, in both iR and iNR patients (Figure 6A). Proportions of monocytic MDSC (CD33<sup>+</sup>CD11b<sup>+</sup>HLA-DR<sup>+</sup>CD14<sup>+</sup>CD15<sup>-</sup>) did not change over time (data not shown). The fraction of proliferating CD8 T cells was significantly correlated to the proportion of granulocytic MDSC, but not monocytic MDSC in the peripheral blood (spearman  $\rho = 0.27$ ,  $p < 0.001$ , Figure 6B), suggesting a balance between the immune suppressive and immune activating components within patients. No differential PFS was observed between patients with a high and patients with a low Ki67<sup>+</sup>CD8 T cells/ MDSC ratio (Figure 6C).



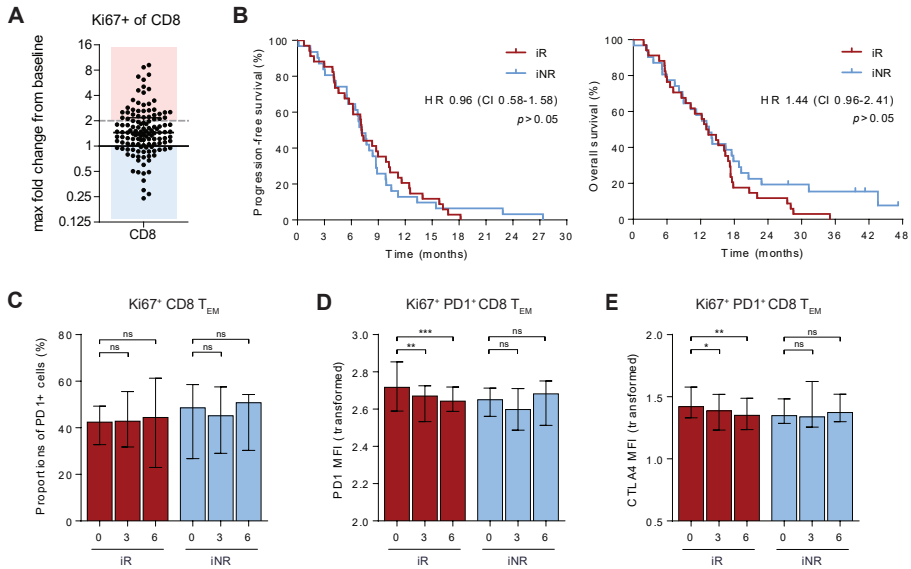


**Figure 5.** Comparison between immunological responders and immunological non-responders A) Immunological responders (iR; indicated in the red rectangle) were defined as patients with an increase in Ki67<sup>+</sup> CD8 T cells of at least two-fold compared to baseline at week 3 or week 6. Immunological non-responders (iNR; indicated in the blue rectangle) were patients who had a fold-change from baseline <1 at both week 3 and week 6. 35 patients were defined as iR and 31 patients were defined as iNR. B) Kaplan Meier plots of progression-free (left) and overall (right) survival of iR and iNR patients. Curves were compared with a log-rank test, which resulted in a  $p$  value >0.05 (not significant). HR = Hazard ratio. C) Proportions of PD1<sup>+</sup> cells within Ki67<sup>-</sup> and Ki67<sup>+</sup> CD8 T<sub>EM</sub> populations over time in iR patients (red) and iNR patients (blue) as defined in figure 5A. D) PD-1 expression on Ki67<sup>-</sup> and Ki67<sup>+</sup> PD1<sup>+</sup> CD8 T<sub>EM</sub> cells over time in iR patients (red) and iNR patients (blue), as depicted by mean fluorescent intensity (MFI). The MFI value is presented as biexponentially transformed value. E) CTLA-4 expression on Ki67<sup>-</sup>PD1<sup>+</sup> CD8 T<sub>EM</sub> cells at week 0, 3 and 6 in iR patients (red) and iNR patients (blue). Biexponentially transformed MFI value is depicted. In panel C-E, bars depict median values with the interquartile range. \*  $p < 0.025$ , \*\*  $p < 0.005$ , \*\*\*  $p < 0.0005$  (Wilcoxon signed rank test)

Taken together, although proliferation of CD8 T cells was correlated with proportions of MDSCs, we did not observe a correlation of the Ki67<sup>+</sup>CD8 T cells/MDSC ratio with PFS.

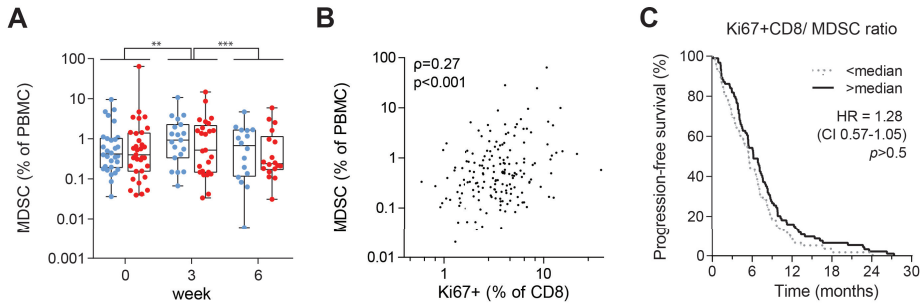


**Figure 6.** Myeloid-derived suppressor cells in chemotherapy-treated NSCLC patients are correlated with proliferation of CD8 T cells. A) Proportion of granulocytic MDSC (CD33<sup>+</sup>CD11b<sup>+</sup>CD14<sup>+</sup>CD15<sup>+</sup>H-LA-DR<sup>+</sup>) of PBMC as measured by flow cytometry at three different time points before and during treatment with chemotherapy. iR patients are shown in red, iNR patients in blue (as defined in Figure 5A). B) Spearman correlation between the proportion of proliferating (Ki67<sup>+</sup>) CD8 T cells and the proportion of MDSC. C). Kaplan Meier curves for progression-free survival of patients with a Ki67<sup>+</sup>CD8/MDSC ratio higher or lower than the median value. \*\*  $p<0.005$ , \*\*\*  $p<0.0005$  (Wilcoxon signed rank test)

## DISCUSSION

In this study, we found that the PCB chemotherapy combination increased proliferation of peripheral blood CD8<sup>+</sup> T cells in stage IV NSCLC patients. The proliferating CD8 T cells were mainly of the effector phenotype and expressed higher levels of the co-inhibitory receptors PD-1 and CTLA-4 than did their non-proliferating counterparts. The increased proliferation, however, had no significant impact on the prognosis of patients.

Two recently published studies showed an increased proliferation of CD8 effector T cells during treatment with PD-1/PD-L1 inhibitors in melanoma [13] and in NSCLC [14], which was suggested to be associated with an improved response to the PD-1 checkpoint inhibition therapy. The relatively high expression of PD-1 and CTLA-4 and the effector phenotype of proliferating CD8 T cells in our study, are similar to those published studies, indicating the involvement of the same effector T cell population. Consequently, our findings implicate that the increased proliferation that was previously reported after PD-1/PD-L1 inhibition, is not specific for response to immunotherapy, but can be induced by PCB as well.

Although in melanoma, a higher Ki67<sup>+</sup> CD8 T cells to tumor burden ratio was associated with improved response to checkpoint inhibitors [13], in our current study no correlation was observed between the increased proliferation in CD8 T cells (either alone or in combination with tumor burden) and response to chemotherapy. In this study, no time points beyond 6 weeks were available for analysis, so any delayed effects of immune modulation which

could have affected clinical outcomes were not assessed. In this context, it is of note that it was reported that in response to checkpoint inhibition, Ki67<sup>+</sup> CD8 T cells peaked after three or six weeks in most patients (13). Even though no correlation with clinical outcome was found in patients treated with PCB, it is conceivable that the increase in Ki67<sup>+</sup> CD8 T cells in combination with a decrease in tumor burden in a subgroup of patients, leads to an immune signature (a high Ki67<sup>+</sup>CD8/tumor burden ratio) that signifies susceptibility to checkpoint inhibition. Nevertheless, without additional treatment these T cells are not effective in prolonging survival. This may partly be ascribed to PD-L1 expression by tumor cells or other cells in the tumor micro-environment, which can efficiently inhibit the proliferating PD-1<sup>+</sup> effector T cells, thereby precluding effective tumor cell killing. Furthermore, T cells might be hampered to enter the tumor, either by physical constraints – e.g. dense tumor stroma – or by intra-tumoral immune suppressive factors [17-19]. While peripheral blood offers the ideal compartment for sequential immune monitoring, to ensure that our findings of an increased immune activation in PBMCs actively contributes to an improved immune response within the tumor, our findings require additional validation in paired tumor biopsies.

The importance of a systemic immune response for tumor eradication has been shown by Spitzer et al. [20], which indicates that peripheral blood immune subsets are clinically relevant for cancer treatment. Moreover, it was shown that a particular subset of proliferating CD4 effector memory T cells was important to prevent recurrences. Since we did not detect induction of proliferation in CD4 T cell subsets after chemotherapy, it might be that the proliferating CD8 T cells lack T cell help needed to be fully equipped to attack the tumor. In the studies monitoring patients on checkpoint inhibition, CD4 T cell proliferation was increased, although to a lesser extent than the CD8 T cells.

One factor that was not addressed in this study, is the specificity of the proliferating CD8 T cells. It has been reported in literature that the PD-1<sup>+</sup> T cell fraction is enriched for tumor-specific T cells [21], which suggests that the increased proliferation mainly occurring in the PD1<sup>+</sup> fraction, might be enriched for tumor specific T cells. However, currently we cannot draw any conclusions about the specificity of the proliferating CD8 T cells induced after PCB in comparison with checkpoint inhibition.

We have previously reported that higher numbers of MDSC were correlated with a poorer OS in the same cohort of NSCLC patients [22]. Here, we show that the proportions of Ki67<sup>+</sup> CD8 T cells were correlated with the proportions of MDSCs in peripheral blood of advanced stage NSCLC patients, suggesting a negative feedback loop of immune suppression in case of increased proliferation of CD8 T cells. This correlation might also contribute to the lack of improved clinical outcome in patients that exhibit an induction of CD8 T cells proliferation.

Furthermore, no correlations with clinical outcomes were found for any other myeloid cell populations, including monocyte subsets, or Treg (not shown).

Our findings of an induced CD8 effector cell proliferation are of particular interest given the recently reported positive phase III study comparing the same chemotherapy/ bevacizumab combination and atezolizumab versus PCB alone [9]. Since a positive result was reported for the first time in an unselected (for PD-L1 expression) patient population using this combination strategy, this might indicate a beneficial effect of the combination of checkpoint inhibition with chemotherapy/ bevacizumab, compared to checkpoint inhibition alone. Based on our data we cannot determine the differential role of the different agents. Certainly for anti-VEGF agents, like bevacizumab, data are available for its potential immune modulatory effect [23, 24].

Our finding that PCB increases proportions of proliferating CD8 T cells, which have been reported to correlate to response to checkpoint inhibition in relation to tumor burden [13], supports the hypothesis that chemotherapy, in this case combined with an anti-vascular endothelial growth factor (VEGF) antibody, may increase responsiveness to PD-(L)1 checkpoint inhibition. Furthermore, the relatively frequent expression of PD-1 on these proliferating CD8 T cells after therapy that we reported, highlights the potential of combined treatment of PCB with anti-PD-1 or anti-PD-L1 therapy. Due to their expression of PD-1, inhibition of the PD-1/ PD-L1 axis could reinvigorate these CD8 T cells to an effective immune response, especially since they are mainly of the effector phenotype. Although limited, the decreased per-cell expression of PD-1 after chemotherapy in immunological responders might point to a further increased susceptibility to treatment during later time points. This would be supported by the reported finding that T cells with intermediate PD1 expression are most sensitive to anti-PD-1 treatment [25].

Future studies will have to confirm whether the combination of chemotherapy and checkpoint blockade represents an effective combination, compared to checkpoint inhibition alone. To date, no clinical trials in NSCLC patients have directly compared these two arms. This study warrants further investigation into this combination strategy, in which Ki67<sup>+</sup> CD8 T cells need to be re-evaluated as potential predictive biomarkers.

## ACKNOWLEDGEMENTS

The authors would like to thank Vincent van der Noort, PhD for study data management and Eric Boersma, PhD for statistical assistance.

## REFERENCES

1. Ferlay, J., et al., *Cancer incidence and mortality worldwide: sources, methods and major patterns in GLOBOCAN 2012*. Int J Cancer, 2015. **136**(5): p. E359-86.
2. Herbst, R.S., et al., *Pembrolizumab versus docetaxel for previously treated, PD-L1-positive, advanced non-small-cell lung cancer (KEYNOTE-010): a randomised controlled trial*. Lancet, 2016. **387**(10027): p. 1540-50.
3. Pai-Scherf, L., et al., *FDA Approval Summary: Pembrolizumab for Treatment of Metastatic Non-Small Cell Lung Cancer: First-Line Therapy and Beyond*. Oncologist, 2017. **22**(11): p. 1392-1399.
4. Kazandjian, D., et al., *FDA Approval Summary: Nivolumab for the Treatment of Metastatic Non-Small Cell Lung Cancer With Progression On or After Platinum-Based Chemotherapy*. Oncologist, 2016. **21**(5): p. 634-42.
5. Antonia, S.J., et al., *Durvalumab after Chemoradiotherapy in Stage III Non-Small-Cell Lung Cancer*. N Engl J Med, 2017. **377**(20): p. 1919-1929.
6. Lievens, L.A., et al., *Checkpoint Blockade in Lung Cancer and Mesothelioma*. Am J Respir Crit Care Med, 2017. **196**(3): p. 274-282.
7. Reck, M., et al., *Pembrolizumab versus Chemotherapy for PD-L1-Positive Non-Small-Cell Lung Cancer*. N Engl J Med, 2016. **375**(19): p. 1823-1833.
8. Langer, C.J., et al., *Carboplatin and pemetrexed with or without pembrolizumab for advanced, non-squamous non-small-cell lung cancer: a randomised, phase 2 cohort of the open-label KEYNOTE-021 study*. Lancet Oncol, 2016. **17**(11): p. 1497-1508.
9. 2017, E.I.O.C., *ESMO IO 2017 Press Release: First Line Combination Therapy Improves Progression-Free Survival In Advanced Lung Cancer*. 2017, ESMO Immuno Oncology Congress 2017.
10. Ramakrishnan, R., et al., *Chemotherapy enhances tumor cell susceptibility to CTL-mediated killing during cancer immunotherapy in mice*. J Clin Invest, 2010. **120**(4): p. 1111-24.
11. Galluzzi, L., et al., *Immunological Effects of Conventional Chemotherapy and Targeted Anticancer Agents*. Cancer Cell, 2015. **28**(6): p. 690-714.
12. Weide, B., et al., *Immunologic correlates in the course of treatment with immunomodulating antibodies*. Semin Oncol, 2015. **42**(3): p. 448-58.
13. Huang, A.C., et al., *T-cell invigoration to tumour burden ratio associated with anti-PD-1 response*. Nature, 2017. **545**(7652): p. 60-65.
14. Kamphorst, A.O., et al., *Proliferation of PD-1+ CD8 T cells in peripheral blood after PD-1-targeted therapy in lung cancer patients*. Proc Natl Acad Sci U S A, 2017. **114**(19): p. 4993-4998.
15. Dingemans, A.M., et al., *A randomized phase II study comparing paclitaxel-carboplatin-bevacizumab with or without nitroglycerin patches in patients with stage IV nonsquamous nonsmall-cell lung cancer: NVALT12 (NCT01171170)dagger*. Ann Oncol, 2015. **26**(11): p. 2286-93.
16. Paats, M.S., et al., *Systemic CD4+ and CD8+ T-cell cytokine profiles correlate with GOLD stage in stable COPD*. Eur Respir J, 2012. **40**(2): p. 330-7.
17. Motz, G.T., et al., *Tumor endothelium FasL establishes a selective immune barrier promoting tolerance in tumors*. Nat Med, 2014. **20**(6): p. 607-15.
18. Turley, S.J., V. Cremasco, and J.L. Astarita, *Immunological hallmarks of stromal cells in the tumour microenvironment*. Nat Rev Immunol, 2015. **15**(11): p. 669-82.
19. Salmon, H., et al., *Matrix architecture defines the preferential localization and migration of T cells into the stroma of human lung tumors*. J Clin Invest, 2012. **122**(3): p. 899-910.
20. Spitzer, M.H., et al., *Systemic Immunity Is Required for Effective Cancer Immunotherapy*. Cell, 2017. **168**(3): p. 487-502 e15.
21. Gros, A., et al., *Prospective identification of neoantigen-specific lymphocytes in the peripheral blood of melanoma patients*. Nat Med, 2016. **22**(4): p. 433-8.
22. de Goeje, P.L., et al., *Immunoglobulin-like transcript 3 is expressed by myeloid-derived suppressor cells and correlates with survival in patients with non-small cell lung cancer*. Oncoimmunology, 2015. **4**(7): p. e1014242.

23. Martino, E.C., et al., *Immune-modulating effects of bevacizumab in metastatic non-small-cell lung cancer patients*. *Cell Death Discov*, 2016. **2**: p. 16025.
24. Elamin, Y.Y., et al., *Immune effects of bevacizumab: killing two birds with one stone*. *Cancer Microenviron*, 2015. **8**(1): p. 15-21.
25. Chen, D.S. and I. Mellman, *Elements of cancer immunity and the cancer-immune set point*. *Nature*, 2017. **541**(7637): p. 321-330.

**SUPPLEMENTARY DATA****Supplementary Table S1.** Antibodies used for flow cytometry staining.

<b>Antibody</b>	<b>Intracellular/ extracellular</b>	<b>Manufacturer</b>
<b>Myeloid staining</b>		
anti-CD15 PE	Extracellular	BD Biosciences
anti-CD16 PerCP-Cy5.5	Extracellular	BD Biosciences
anti-CD33 PE-Cy7	Extracellular	BD Biosciences
anti-CD11b APC	Extracellular	BD Biosciences
anti-HLA-DR APC-Cy7	Extracellular	BD Biosciences
anti-CD14 PE-Texas-Red	Extracellular	Invitrogen
anti-ILT3 FITC	Extracellular	R&D Systems
<b>T cell staining (direct)</b>		
anti-CCR7 FITC	Extracellular	R&D systems
anti-CD25 PE Cy7	Extracellular	eBioscience
anti-CD3 APC-eFluor780	Extracellular	eBioscience
anti-CD8 AF700	Extracellular	eBioscience
anti-CD45RA PE Texas Red	Extracellular	Invitrogen
anti-CD19 PerCPCy5.5	Extracellular	BD Biosciences
anti-CD14 PerCPCy5.5	Extracellular	BD Biosciences
anti-CD16 PerCPCy5.5	Extracellular	BD Biosciences
anti-CD4 BV786	Extracellular	BD Biosciences
anti-CD28 BV605	Extracellular	BD Biosciences
anti-PD1 BV711	Extracellular	BD Biosciences
anti-FoxP3 PE	Intracellular	eBioscience
anti-Ki67 APC	Intracellular	eBioscience
anti-CTLA4 BV421	Intracellular	BD Biosciences
<b>Intracellular cytokine staining</b>		
anti-CD3 APC-eFluor780	Extracellular	eBioscience
anti-CD8 AF700	Extracellular	eBioscience
anti-CD45RA PE Texas Red	Extracellular	Invitrogen
anti-CD69 FITC	Extracellular	BD Biosciences
anti-CD4 BV786	Extracellular	BD Biosciences
anti-PD1 BV711	Extracellular	BD Biosciences
anti-Granzyme B PE	Intracellular	Invitrogen
anti-IFN $\gamma$ APC	Intracellular	BD Biosciences

**Supplementary Table S2.** Clinical and immunological Characteristics of lost-to-follow up patients versus patients

	<b>Study Pt (N=131)</b>	<b>Lost FU (N=92)</b>	<b>p-value</b>
Clinical response CR/PR/SD/PD (n)	2/56/55/12	1/30/31/8	0.97
T cells (% of PBMC)	35.7 (25.2-44.5)	44.5 (35.7-29.9)	0.16
CD4/ CD8 ratio	1.4 (0.8-2.1)	2.1 (1.4-0.7)	0.63
Myeloid cells (% of PBMC)	19 (11.1-33.2)	33.2 (19-10.4)	0.27
B cells (% of PBMC)	6.9 (4-10.7)	10.7 (6.9-3.6)	0.09
Naïve (% of T cells)	26.2 (14.5-39.2)	39.2 (26.2-13.2)	0.19
Central memory (% of T cells)	22 (15.6-27.6)	27.6 (22-10.3)	0.56
Effector memory (% of T cells)	24.7 (17.3-33)	33 (24.7-18.3)	0.96
CD45RA+ Effector memory (% of T cells)	17 (8.5-30.5)	30.5 (17-11.3)	0.08

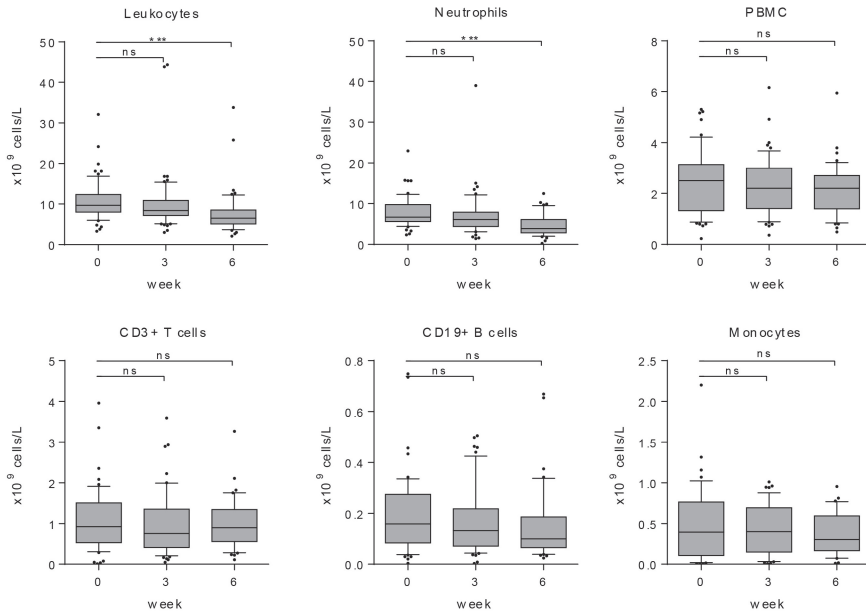
Values of immune populations represent medians and interquartile range between brackets; p-value for clinical response is tested with chi-square test; p-value for immune populations is from Mann-Whitney U test; CR = complete response; PR = partial response, SD = stable disease, PD = progressive disease

**Supplementary Table S3.** Patient data of patients whose blood was received for at least two time points. Patient characteristics, clinical response and immune populations after treatment.

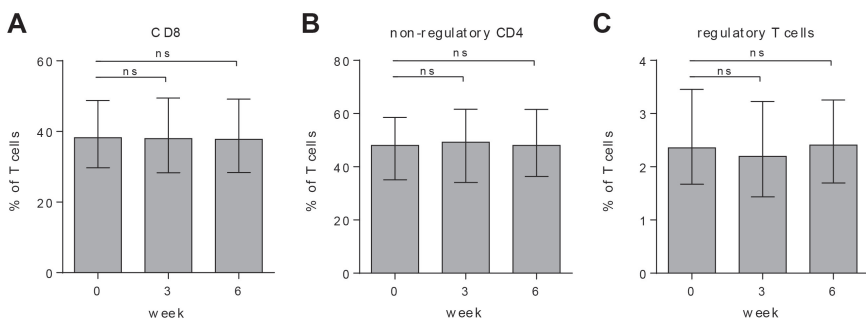
	<b>Arm A (PCB) (n=68)</b>	<b>Arm B (PCB + N) (n=63)</b>	<b>Total (n=131)</b>
<b>Clinical response*</b>			
Complete response	1 (1.5%)	1 (1.6%)	2 (1.5%)
Partial response	35 (51.5%)	21 (33.3%)	56 (42.7%)
Stable disease	25 (36.8%)	30 (47.6%)	55 (42.0%)
Progressive disease	3 (4.4%)	9 (14.3%)	12 (9.2%)
Not evaluable	4 (5.9%)	2 (3.2%)	6 (4.6%)
<b>Immune populations after treatment (week 6)</b>			
	<b>Median (IQ range)</b>		<b>Mann-Whitney</b>
% T cells	47.7 (34.3-56.7)	43.7 (33.5-52.7)	N.S.
CD4/CD8 ratio	2.6 (1.4-3.5)	1.8 (1.2-2.9)	N.S.
% myeloid cells	17.0 (7.4-24.9)	17.4 (8.4-29.5)	N.S.
% B cells	5.9 (3.6-8.9)	7.5 (4.4-10.2)	N.S.
<b>Immune populations after treatment (week 3)</b>			
	<b>Median (IQ range)</b>		<b>Mann-Whitney</b>
% T cells	42.5 (28.1-52.1)	43.2 (29.9-51.0)	N.S.
CD4/CD8 ratio	2.2 (1.2-3.6)	1.7 (1.3-2.7)	N.S.
% myeloid cells	18.0 (7.6-27.7)	20.4 (9.4-28.4)	N.S.
% B cells	5.4 (3.5-10.6)	6.2 (4.1-10.6)	N.S.

\* as defined by RECIST1.1; PCB=paclitaxel/carboplatin/bevacizumab, N = nitroglycerin patch, IQ range = inter quartile range

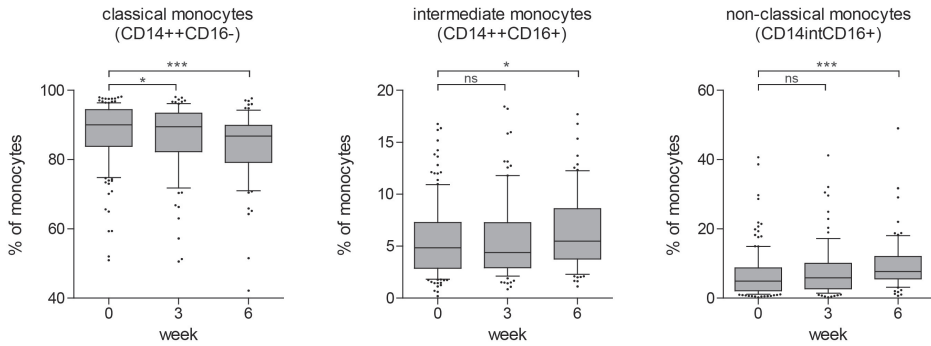




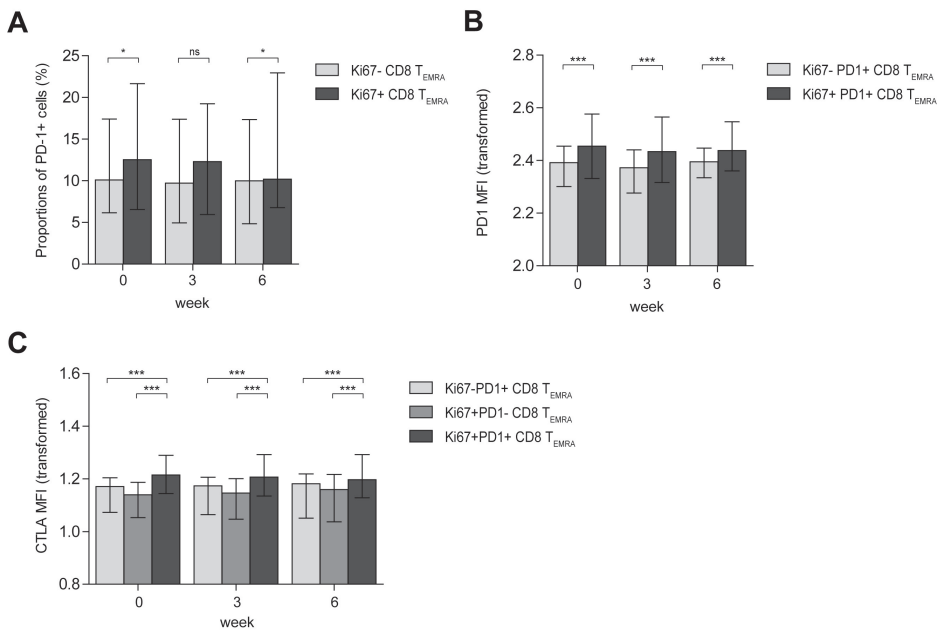
**Supplementary Figure S1.** Absolute numbers of immune cells per liter peripheral blood of NSCLC patients treated with chemotherapy. Absolute leukocytes, neutrophils, PBMC (leukocytes–neutrophils), T cells, B cells and monocytes were determined at baseline (week 0) and after the first (week 3) and second (week 6) cycle of chemotherapy. Data are shown from a subgroup of patients of whose absolute white blood cell counts were determined on the same day as the PBMC flow cytometry analysis ( $n=74$ ). \*\*\*  $p < 0.001$ ; ns = not significant (Wilcoxon signed rank test)



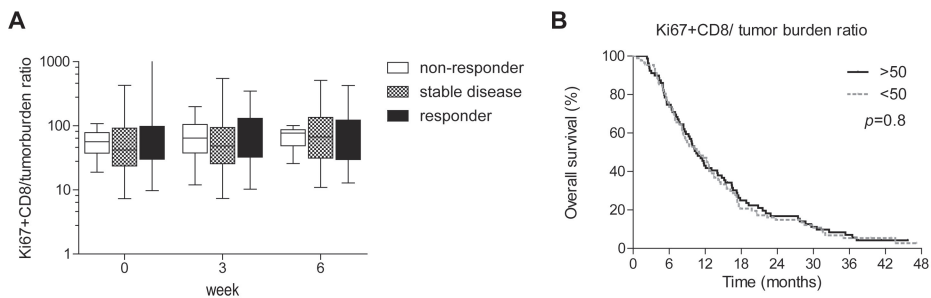
**Supplementary Figure S2.** Proportions of major T cell subsets in NSCLC patients treated with chemotherapy. Proportions of CD8<sup>+</sup> T cells (A), non-regulatory CD4<sup>+</sup> T cells (B) and regulatory CD4<sup>+</sup> T cells (C) in PBMC T cells of NSCLC patients treated with PCB before start (week 0), after the first (week 3) and second (week 6) cycle of chemotherapy, as determined by flow cytometric analysis. Bars represent median values with interquartile range. \*  $p < 0.025$  \*\*  $p < 0.005$  \*\*\*  $p < 0.0005$  ( $\alpha$  level adjusted for multiple comparisons; Wilcoxon signed rank test)



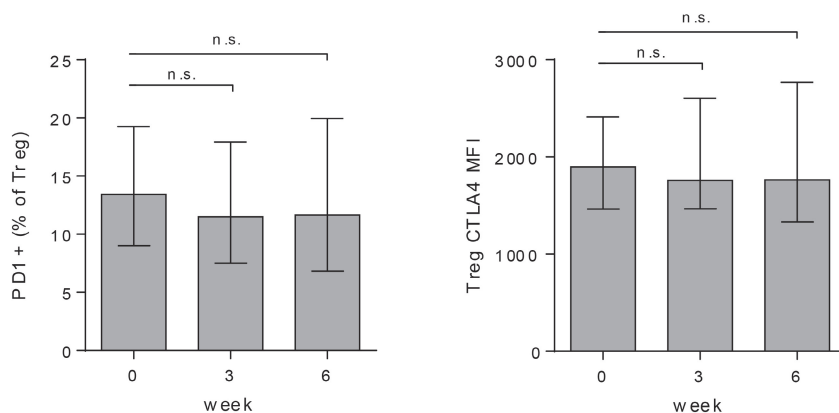
**Supplementary Figure S3.** Monocyte subsets in peripheral blood of NSCLC patients treated with chemotherapy. Proportions of classical (CD14++CD16-), intermediate (CD14++CD16+) and non-classical (CD14intCD16+) monocytes before (week 0), and after the first (week 3) and second (week 6) chemotherapy cycle, as defined in a subset of patients ( $n=97$ ). Box plot whiskers depict the 10-90% range. \*  $p < 0.05$ , \*\*\*  $p < 0.001$ , ns = not significant (Wilcoxon signed rank test)



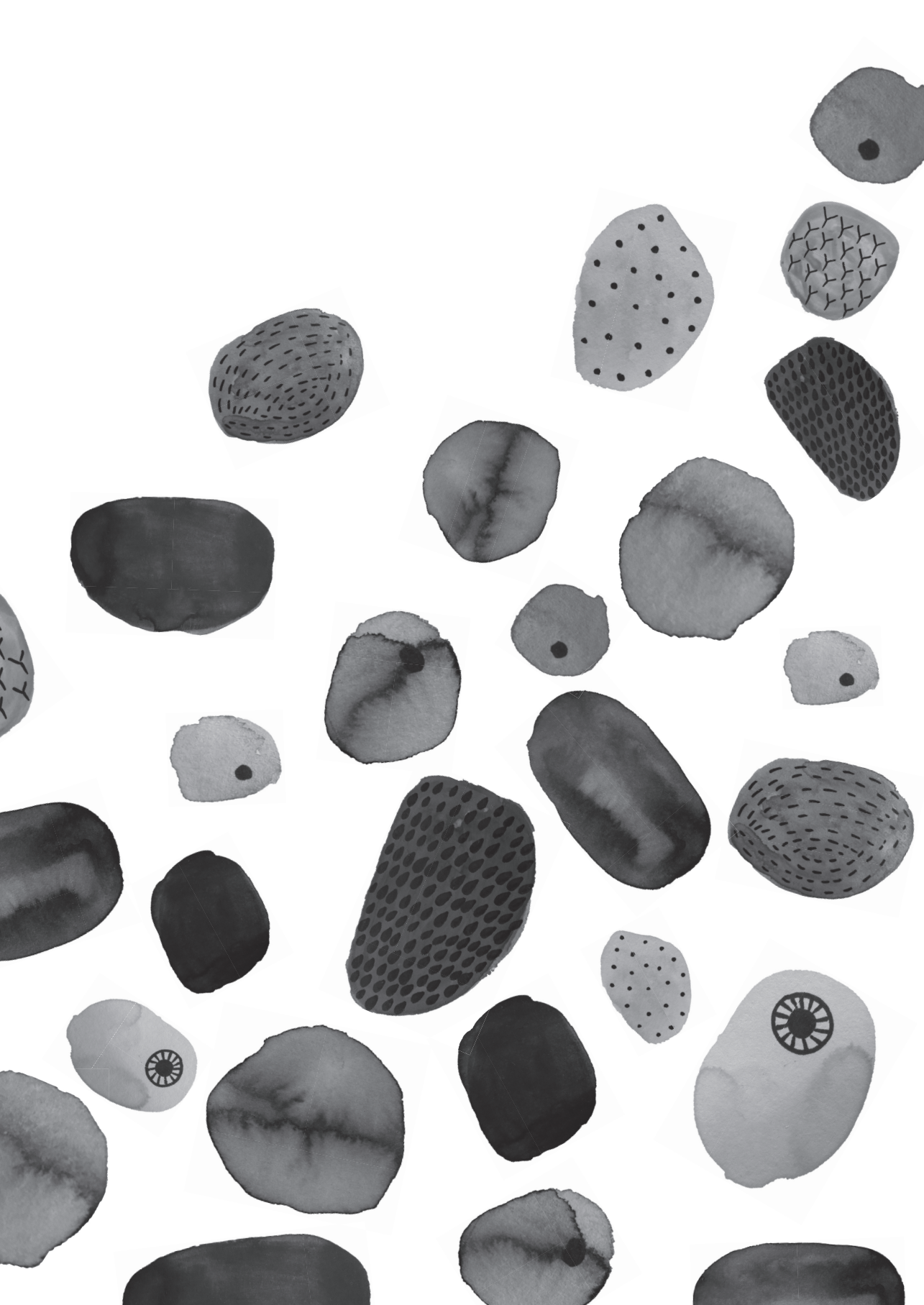
**Supplementary Figure S4.** Co-inhibitory receptor expression on proliferating CD8 T<sub>EMRA</sub> cells in peripheral blood of chemotherapy-treated NSCLC patients. A) Proportions of PD1+ cells within Ki67- and Ki67+ CD8 T<sub>EMRA</sub> populations over time. B) PD-1 expression on Ki67- and Ki67+ PD1+ CD8 T<sub>EMRA</sub> cells over time, as depicted by mean fluorescent intensity (MFI). The MFI value is presented as biexponentially transformed value. C) Expression of CTLA-4 CD8 T<sub>EMRA</sub> subsets as defined by PD1 and Ki67 expression over time. Biexponentially transformed MFI value is depicted. In all graphs, the bars show median values with the interquartile range depicted by the error bars. \*  $p < 0.05$ , \*\*  $p < 0.01$ , \*\*\*  $p < 0.001$  (Wilcoxon-signed rank test)



**Supplementary Figure S5.** Ki67<sup>+</sup> CD8<sup>+</sup>/ tumor burden ratio in NSCLC patients in relation to clinical outcome. The Ki67<sup>+</sup> CD8<sup>+</sup>/tumor burden ratio was calculated by dividing the percentage of Ki67<sup>+</sup> cells of CD8<sup>+</sup> T cells, by the total tumor diameter before treatment. Total tumor diameter was determined as the sum of the diameters of target lesions measured on computed tomography (CT) scans. A) The Ki67<sup>+</sup>CD8<sup>+</sup>/tumor burden ratio in non-responders, stable disease patients and responders (both partial and complete), as defined by RECIST criteria. B) Overall survival of patients with a Ki67<sup>+</sup>CD8<sup>+</sup>/tumor burden ratio >50 ( $n=79$ ) and <50 ( $n=87$ ). Kaplan Meier curves were compared with a log-rank test, which showed no significant difference.



**Supplementary Figure S6.** PD1 and CTLA4 expression on Tregs. Fraction of PD1<sup>+</sup> Tregs (left) and CTLA4 MFI of Tregs (right) as determined by flow cytometry in patients at week 0, 3 and 6.



# CHAPTER

## **PREDICTING SURVIVAL OF LUNG CANCER PATIENTS BASED ON THEIR IMMUNE PROFILE WITH A SEMI- AUTOMATIC ANALYSIS APPROACH**

Pauline L. de Goeje, Sofie Van Gassen, Myrthe Poncin, Rudi  
W. Hendriks, Joachim G.J.V. Aerts, Yvan Saey

*Manuscript in preparation*

# 5

## ABSTRACT

Over the last decades, the role of the immune system in the development and treatment of cancer has been more and more recognized and understood. Various individual immune populations have been shown to be associated with treatment response or survival outcome, but the clinical value differs for the different cancer types, stages and treatments. We hypothesized that a combination of immune populations can be used to predict survival of non-small cell lung cancer (NSCLC) patients. To analyze multiple immune populations derived from complex flow cytometry data, we used a semi-automatic analysis pipeline FloReMi, which has recently been developed. In this study, we assessed the feasibility of this method for our research question by applying the pipeline on a study with 180 stage IV NSCLC patients receiving chemotherapy treatment. Peripheral blood samples were collected and immune populations were examined using three flow cytometry panels with 12-16 markers each. Population frequencies and expression levels were extracted from these data and a random survival forest model was trained and evaluated using five-fold cross validation. The feature extraction from the FloReMi pipeline was compared to manually obtained features and showed a good correlation (average  $\rho = 0.81$ ). A total of 63,423 features were extracted from the flow cytometry data in the FloReMi pipeline. The feature selection step selected 37-41 features to be used in the prediction model. The RSF model had an error rate of 0.421, which was lower than the error rate of the random survival forest model trained with manually obtained features (0.472). The model did give a significant prediction of overall survival ( $p = 9.6 \cdot 10^{-4}$ ). The top feature found with the FloReMi analysis was the frequency of HLA-DR<sup>+</sup>CD33<sup>+</sup> population. In conclusion, semi-automatic gating with FloReMi is a feasible way to extract an exhaustive number of features from flow cytometry data. Although prediction of survival based on the selected features was statistically significant, in contrast to a model based on manually obtained features, the accuracy of prediction is too low to be of clinical significance. Therefore, this method is more suitable for explorative research than to develop clinically applicable prediction rules. The selected features derived from this pipeline require further investigation and validation to assess their clinical value.

## INTRODUCTION

The immune system plays an important role in the development of cancer and in the response to cancer therapy [1]. There has been an increasing number of immunotherapies that harness the immune system to fight cancer, which have been FDA approved for treatment against various kinds of cancers [2], but also conventional therapies have been reported to rely heavily on the patients' immune system for their effect [1, 3]. One of the cancer types in which immunotherapy has been successfully implemented over the last decade, is non-small cell lung cancer (NSCLC). However, only a minority of patients benefits from long-term responses, so a better tailoring of treatments to the right patient is needed. Several immune populations have been described to correlate with survival in various types of cancer, either in the tumor microenvironment or in the peripheral blood. While some markers are either favorable or unfavorable in several cancer types, many immune populations rendered contradictory results in literature, which might be either dependent on tumor type, or other (sometimes unknown) factors [4]. In NSCLC, various immune populations present in the local tumor microenvironment, have been reported to have prognostic value, as reviewed elsewhere [5, 6]. In peripheral blood, elevated proportions of myeloid-derived suppressor cells have been reported to be associated with a reduced survival [7, 8]. Naïve regulatory T cells in peripheral blood are also associated with a worse survival, while terminally differentiated regulatory T cells are associated with an improved survival [9].

To predict survival of cancer patients or their response to therapy with the goal to facilitate personalized medicine, it is likely that a combination of known biomarkers will give the most accurate prediction. For example, as has been shown in melanoma, the increase in Ki67 expressing PD1-positive CD8 T cells, solely did not predict response to PD-1 inhibition. However, combined with tumor burden, the Ki67<sup>+</sup>CD8/tumor burden ratio was significantly associated with survival [10]. We hypothesized that the immune profile of non-small cell lung cancer patients, comprising a combination of immune markers, can predict survival and may be used to personalize cancer treatment.

The most frequently used sample type to study the immune profile of patients is the peripheral blood, which is easily accessible and can be obtained sequentially to monitor dynamics of immune populations. Flow cytometry is the most common technique to define various immune cells, using various markers at the same time at the single cell level. Due to technical developments, the number of fluorochromes that can be measured at the same time is increasing, which leads to the generation of increasingly complex data. Moreover, with the introduction of CyTOF that makes use of mass spectrometry to distinguish different

isotopes instead of fluorescence, even more markers (currently up to 50) can be measured per cell. Manual analysis of these data becomes very labor intensive, and in addition is prone to researcher bias. (Semi)-automatic data analysis will become indispensable in future research using flow cytometry. Currently, various (semi)-automatic pipelines are being developed [11], but are not yet commonly used in the (tumor) immunology field. In this study, we used and evaluated a recently developed pipeline (FloReMi) [12] to predict survival in a cohort of NSCLC patients, based on their immune profile as determined by flow cytometry on peripheral blood samples. We evaluated whether the use of this pipeline can reliably define various immune populations, and whether this provides a useful prediction model for personalized medicine when used with a clinical trial cohort of about two hundred patients.

## **MATERIAL AND METHODS**

### **Patient samples**

The patients in this study were participating in the NVALT12 study (trial number NCT01171170), a randomized Phase II multicenter study on the effect of a nitroglycerin patch or placebo in patients with stage IV NSCLC treated with carboplatin, paclitaxel, and bevacizumab. Patients in the NVALT12 study were diagnosed with stage IV non-squamous NSCLC and were not eligible for treatment with curative intent. Disease stage was determined in accordance with the American Joint Committee on Cancer (AJCC). Further details of the study are described elsewhere [13]. Blood samples were collected before the start of treatment and peripheral blood mononuclear cells (PBMC) were isolated using standard density gradient procedure. Written consent was obtained from all individuals before blood sampling and the study was approved by CCMO: NL33442.042.10). Patient characteristics that were collected and used in the current study were age, sex, smoking status (current smoker, ex-smoker and non-smoker) and WHO performance score.

### **Flow cytometry data acquisition**

Three different stainings were performed on the PBMC samples, which are described in **Chapter 4** [14]. Flow cytometry data was acquired on an LSR II (BD Biosciences) with three lasers. Application settings were used to calibrate the fluorescence signals on each measurement day. Manual gating was performed in FlowJo version X (FlowJo, LCC).

### **FloReMi analysis pipeline**

We used the FloReMi pipeline as described in van Gassen et al. [12] with some adjustments for the current dataset. All analyses were performed in R version 3.3.2 for windows. Below,



the four steps of the FloReMi pipeline are described: preprocessing, feature extraction, feature selection and survival prediction.

## Preprocessing

During preprocessing, only good quality events were selected from the fcs files, by selecting only those events that were recorded during stable flow. To this end, thresholds were set for each sample as the average flow  $\pm X$  events/s with  $X=100$  as default, adjusted manually for individual samples when necessary based on visual analysis. Moreover, margin events on the FSC and SSC channels were removed. The values of the fluorescence channels were compensated using the compensation matrix derived from the BD FACSDiva software, as calculated based on compensation controls, and subsequently transformed with biexponential transformation. With manual gates generated in FlowJo, a population of single live cells (MDSC staining) or single live T cells (T cell stainings) was selected as starting population for feature extraction.

## Feature extraction

For a selection of markers (see Table 1, column 2) gates were created automatically based on one-dimensional histograms using the deGate function of the flowDensity package. For each of these markers, an optimal threshold was determined, which divided cells into a positive and a negative population. All automatically determined thresholds were visualized and manually checked. Where needed, manual adjustments to the thresholds were implemented. Features were created using the flowType function of the flowType package: for each staining, populations were defined by combining all possible combinations of marker values (positive, negative or neutral), extracting both frequency of the populations, as well as the MFI value of all markers (table 1 column 2 and 3) as features. Whether thresholds were set for certain markers or not, was determined based on their expression profile: if a clear positive and negative population could be distinguished, or if an FMO control could be used to define the threshold, the marker was used with a split to create a positive and negative populations. For markers with a more gradual expression profile, the expression was only included as MFI value. For the markers Ki67 and PD1 in staining A, thresholds were set based on the 99.5 percentile of isotype controls. Furthermore, based on variance between samples (determined by visual inspection of the histograms), a threshold was set for each sample individually, or for a whole batch of samples measured on the same day using aggregated data.

**Table 1.** Markers used for feature extraction in FloReMi pipeline.

<b>Staining</b>	<b>Markers for splits and MFI</b>	<b>Markers for MFI only</b>
<b>A</b>	CCR7, FoxP3, CD45RA, PD1, CD4, Ki67, CD8	CD25, CTLA4, CD28, CD3
<b>B</b>	CD69, Granzyme B, CD45RA, CD4, IFN $\gamma$ and CD8	PD1, CD3
<b>C</b>	FSC-A, SSC-A, CD14, CD33, CD11b, HLA-DR, CD15	

### Feature selection

For the feature selection step, a Cox proportional hazards model was applied for all individual features, determining the strength of their association with overall survival. Then, all features were sorted based on either the p-value or the concordance index from these individual Cox proportional-hazards models (both sorting methods were evaluated during optimization of the model). Features were selected starting from the feature with the lowest p-value or the highest concordance index, only selecting features that had a correlation coefficient (Pearson  $r$ )  $< 0.2$  for correlation with already selected features. The first 5000 features of the sorted feature list were evaluated for feature selection.

### Survival prediction

For survival prediction, a random survival forest (RSF) model was trained used using the `rfsrc` function of the `randomForestSRC` R package. The number of trees was set to 500 and missing data (caused by missing MFI values for ‘empty’ population, or by samples on which not all three stainings were performed due to insufficient cell numbers) were imputed using the on-the-fly random imputation strategy implemented in the `rfsrc` library [15].

### Cross validation

To evaluate the performance of the model, we performed a five-fold cross-validation. In contrast to the original pipeline [12], the feature selection step was included in the cross-validation. This means that feature selection was performed only on the train data within the five folds, preventing selection of features based on their predictive value on the complete data, including the validation set, which would lead to a bias. The trained RSF model was evaluated on the five validation sets, which resulted in a predicted survival score for each patient in the validation set. We evaluated the predictive value of the individual folds using their error rate. This error rate was calculated in the `rfsrc` function and is calculated as  $1 - C$ , with  $C$  being Harrell’s concordance index [16]. To evaluate overall performance of the cross-validation, a Cox regression was performed on the complete dataset, using the predicted survival score as single variable to predict actual survival. Concordance index and p-value were used as performance measure of this Cox regression model.

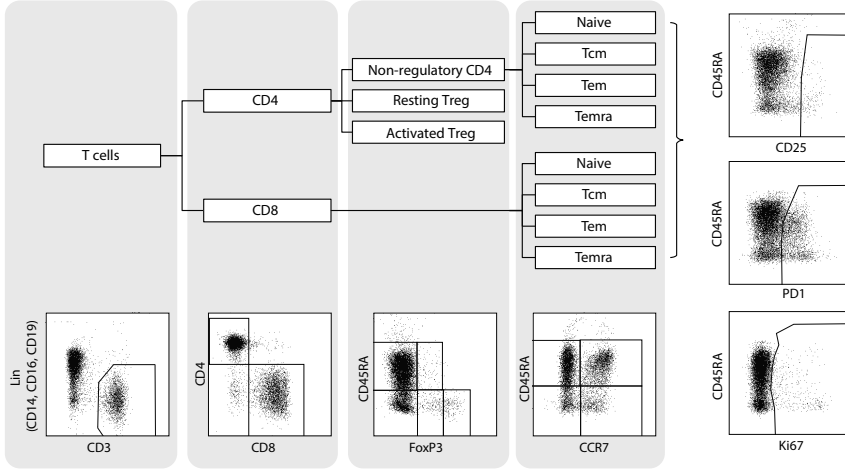
## RESULTS

### **FloReMi-derived features are strongly correlated with manually defined populations**

Flow cytometry data were obtained from peripheral blood samples of 190 stage IV non-squamous NSCLC patients. The raw fcs files were analyzed with two different methods: the (semi-)automatic analysis pipeline FloReMi (as described in van Gassen et al [12]), and manual gating in FlowJo as the golden standard. Our first aim was to compare the features that were extracted with the FloReMi pipeline, with the manually defined features. For this aim we focused on stainings A and B, because for these stainings, a substantial number of populations was manually gated (in contrast, staining C was used to define MDSC only). The manual gating strategy for these panels are shown in figure 1, which led to the identification of 44 and 49 populations in staining A and B, respectively. In the FloReMi analysis pipeline, the preprocessing step included quality control of the samples and selection of the start population. On average 3.4% ( $\pm$  3.1%) of events were removed from the sample in the quality control step, based on an unstable flow or values outside of the outer margins. A start population for further analysis was used, based on the manual gates for T cells in both stainings. All events that passed quality control and that were within the start population gate, were used for the subsequent step of the pipeline: feature extraction. During this step, 26,244 and 6,561 features were extracted from panel A and B, respectively. These features consisted of the proportions of all defined populations within the start population, and additionally the MFI values of all markers on each of these populations, as defined by the markers in table 1. To assess the reliability of the automatically extracted features in the FloReMi pipeline, we calculated the correlation between the manually gated populations and the corresponding features from the FloReMi analysis and found a mean Spearman  $\rho$  value of 0.81 ( $\pm$  0.19). Figure 2 shows the correlation between some of the automatically defined and manually gated populations, as an example. In general, larger populations correlated more strongly than the (very) small populations. From these results, we concluded that using the FloReMi pipeline, reliable features can be extracted from raw flow cytometry data.

## Staining A

pre-gating on single cells (based on FSC-H and FSC-A), and death-marker negative cells



## Staining B

pre-gating on single cells (based on FSC-H and FSC-A), and death-marker negative cells

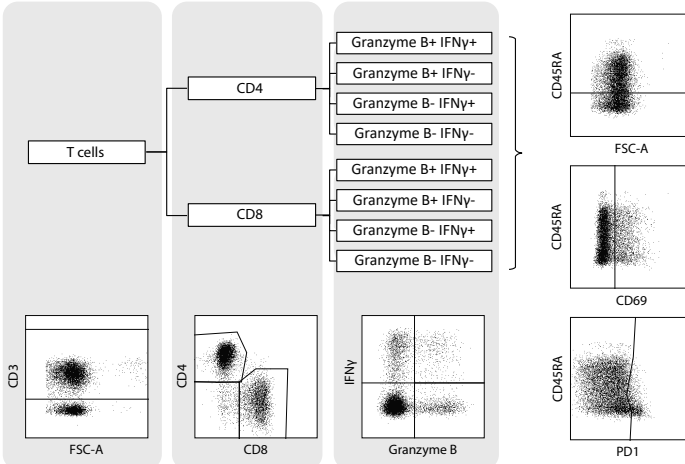


**Figure 1.** Manual gating of immune populations in T cell stainings A and B. A) Staining A was performed on cells immediately after thawing. After pre-gating on live cells and single cells (based on FSC-A and FSC-H), T cells were gated as CD3<sup>+</sup>Lin<sup>-</sup> cells. Next, CD4<sup>+</sup> and CD8<sup>+</sup> T cells were gated. CD4 T cells were subdivided based on their CD45RA and FoxP3 expression according to Miyara et al. (Immunity 2013), with activated Tregs gated as FoxP3<sup>high</sup>CD45RA<sup>-</sup>; resting Tregs as FoxP3<sup>int</sup>CD45RA<sup>+</sup>. All other CD4<sup>+</sup> T cells together were identified as non-regulatory CD4 T cells. Non-regulatory CD4 T cells and CD8 T cells were further gated based on their CD45RA and CCR7 expression into naïve (CD45RA<sup>-</sup>CCR7<sup>+</sup>), central memory (T<sub>CM</sub><sup>+</sup>: CD45RA<sup>-</sup>CCR7<sup>+</sup>), effector memory (T<sub>EM</sub><sup>+</sup>: CD45RA<sup>-</sup>CCR7<sup>-</sup>) and CD45RA<sup>+</sup> effector (T<sub>EMRA</sub><sup>+</sup>: CD45RA<sup>+</sup>CCR7<sup>-</sup>) cells using Boolean gates. On all populations, the proportions of CD25<sup>+</sup>, PD1<sup>+</sup> and Ki67<sup>+</sup> cells were assessed. B). Before staining, cells were stimulated for 4 hours with PMA/ionomycin. After pre-gating on live cells and single cells (based on FSC-A and FSC-H), T cells were gated as CD3<sup>+</sup> cells. Next, CD4<sup>+</sup> and CD8<sup>+</sup> T cells were gated. Using boolean gates, the proportions of Granzyme B and IFNγ-positive and negative populations were determined on both CD4 and CD8 T cell subsets. Of each of the combined populations, proportions of CD45RA<sup>+</sup>, CD69<sup>+</sup> and PD1<sup>+</sup> cells were assessed.

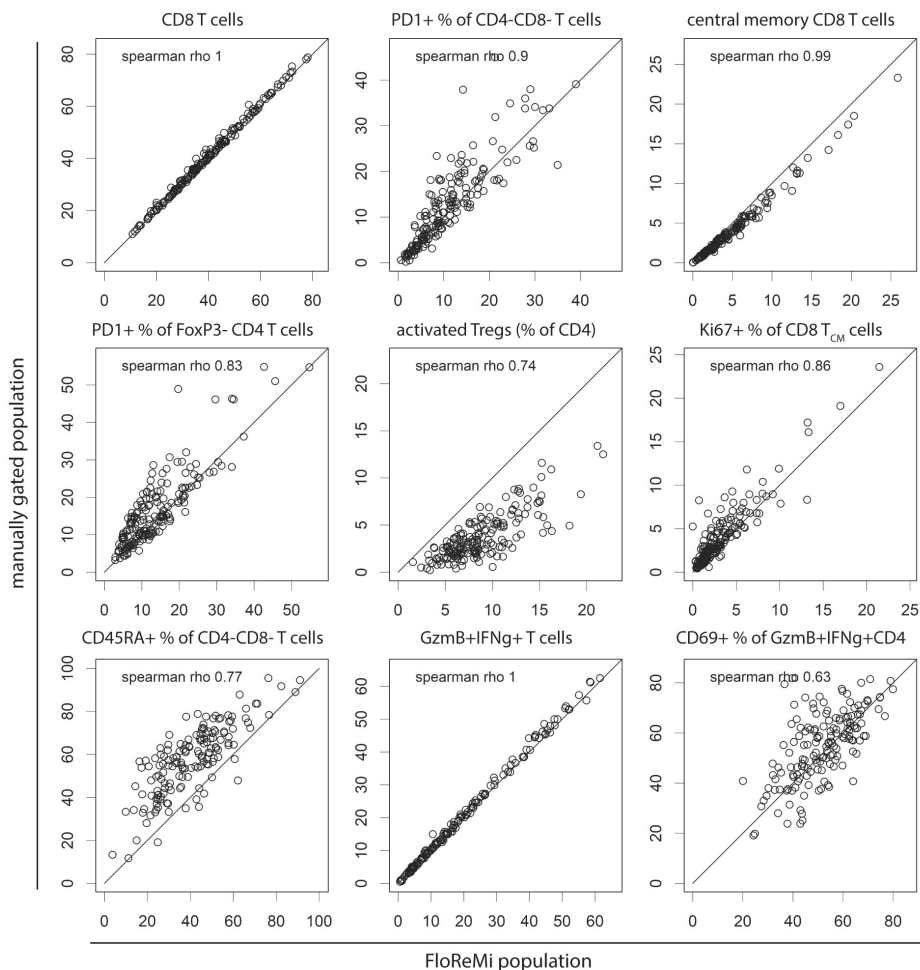


**Figure 2.** Correlations between manual gating and automatic gating in the FloReMi pipeline. A selection of manually gated populations, and their corresponding FloReMi populations. For proportions of marker-positive cells within specific population, the two corresponding FloReMi populations were divided by each other (for example PD1<sup>+</sup>CD4<sup>-</sup>CD8<sup>-</sup> cells divided by all CD4<sup>-</sup>CD8<sup>-</sup> cell to calculate percentage PD1<sup>+</sup> cells within the CD4<sup>-</sup>CD8<sup>-</sup> population). The top two rows are populations from staining A, the bottom row are populations from staining B. The numbers on the axes represent percentages. The Spearman  $\rho$  correlation of both populations was calculated for all baseline patient samples (n=190).

### Prediction model for survival in NSCLC patients using flow cytometry features

For the prediction model, we used the extracted features from the three stainings (A, B and C). Staining B was performed on a stimulated and an unstimulated sample for each patient, and features derived from both samples, as well as the difference between the two samples, were included. Additionally, some of the features based on clinical/ patient



characteristics collected in the clinical trial were included: age, sex, smoking status (current smoker, ex-smoker and non-smoker), WHO performance score and treatment arm. The total number of features before feature selection was  $26,244 (A) + 3 \cdot 6561 (B) + 17,496 (C) + 5 (\text{clinical}) = 63,428$ .

An RSF model was trained and evaluated using five-fold cross-validation: data of four folds (80%) were used for feature selection and to train the model, which was evaluated using the data of the fifth fold. This was repeated five times, using each of the folds once for evaluation. In the same way, cross-validation was performed for an RSF model using the features from manual gating instead (frequencies and MFIs as shown in figure 1). The predicted score for both models was plotted against the actual overall survival time in figure 3. The correlation between the predicted and actual survival time was evaluated with a cox model using the predicted score as variable for actual OS. Strikingly, while the predicted score was not significantly associated with the actual overall survival in the model using features from manual gating ( $p=0.97$ ), the predicted score of the FloReMi model was significantly associated with the actual overall survival ( $p=9.6 \cdot 10^{-4}$ ). The model evaluation of the cross-validation of both models is summarized in table 3. An error rate for each fold of CV was calculated, and the average and range are displayed. An error rate of 0 represents a perfect prediction, whereas a random prediction would result in an error rate of 0.5. The number of selected features differed per fold. Both the concordance index and the p-value were derived from the Cox regression using the predicted scores. From these results, we concluded that the FloReMi pipeline can achieve a significant predictive value in lung cancer patients, but that this prediction is only marginally better than random.

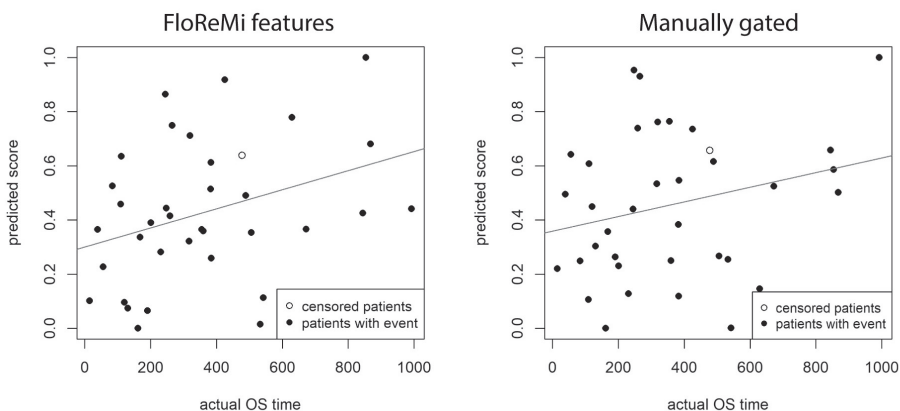


**Figure 3.** Correlation between RSF prediction from cross-validation and actual survival data. Actual OS time is displayed as number of days. An RSF model was trained using the automatically extracted features from the FloReMi pipeline (left) and using the features derived from manual gating in FlowJo (right).

**Table 2.** Results of the final model and prediction on the holdout data.

	<b>FloReMi RSF model</b>	<b>RSF model with manual features</b>
<b>Error rate</b>	0.421 (0.38-0.48)	0.472 (0.35-0.55)
<b>Number of features</b>	43.2 (37-51)	16.6 (15-18)
<b>Cox regression p-value</b>	9.6E-4	0.971
<b>Cox concordance index</b>	0.58	0.49

**Table 3.** Selected features.

#	<b>feature</b>	<b>subset</b>	<b>staining</b>
1	% of cells	CD33+HLA-DR-	C
2	CD45RA MFI	CD69-GzmB-CD8-	B difference
3	CD14 MFI	CD14+CD33-CD11b+	C
4	median FSC-A	CD14-CD11b-HLA-DR+CD15+	C
5	CD14 MFI	CD33+CD11b-HLA-DR-CD15-	C
6	% of cells	FoxP3+CD45RA-PD1-CD4-CD8+	A
7	CD25 MFI	CCR7-CD45RA-CD4-Ki67+CD8-	A
8	CD8 MFI	CCR7-FoxP3-CD45RA+PD1+CD4-CD8-	A
9	HLA-DR MFI	FSC-A+SSC-A-CD14-CD33+CD11b+HLA-DR+CD15-	C
10	median FSC-A	SSC-A+CD33-CD11b+HLA-DR+CD15-	C
11	PD1 MFI	CD69-CD4+CD8-	B difference
12	CD25 MFI	CCR7+FoxP3+CD4-Ki67+CD8+	A
13	FoxP3 MFI	CCR7+CD45RA-PD1-Ki67+CD8+	A
14	CD45RA MFI	CCR7-FoxP3+CD45RA-PD1-CD4+CD8+	A
15	HLA-DR MFI	FSC-A+SSC-A-CD14-CD33+CD11b-	C
16	CTLA4 MFI	FoxP3-CD45RA-PD1-CD4+Ki67+CD8+	A
17	CD33 MFI	SSC-A-CD15+	C
18	GzmB MFI	CD69-IFNg+CD8+	B difference
19	CD3 MFI	CD69+GzmB-CD45RA-CD4-CD8-	B unstimulated
20	HLA-DR MFI	FSC-A+SSC-A+CD14-CD33-CD11b-HLA-DR+	C
21	median SSC-A	FSC-A+SSC-A+CD14-CD33-CD11b-CD15+	C
22	CTLA4 MFI	CCR7-FoxP3+CD4-Ki67+CD8+	A
23	median SSC-A	FSC-A-SSC-A-CD33-CD11b-CD15-	C
24	median FSC-A	FSC-A-SSC-A-CD33-CD11b+HLA-DR-CD15+	C
25	CD33 MFI	CD14+CD33-HLA-DR-	C
26	CD11b MFI	FSC-A-CD33-CD11b-HLA-DR-	C
27	median FSC-A	FSC-A-CD14-CD11b+HLA-DR-CD15-	C
28	HLA-DR MFI	FSC-A+CD14-CD11b+CD15-	C
29	CD69 MFI	CD69+CD4+IFNg-CD8+	B stimulated
30	PD1 MFI	GzmB+IFNg+	B difference
31	CCR7 MFI	CCR7+FoxP3-CD45RA+PD1+Ki67+	A
32	HLA-DR MFI	FSC-A-HLA-DR-	C
33	CD3 MFI	CD45RA-IFNg+CD8-	B difference
34	CD11b MFI	FSC-A+SSC-A-	C
35	FoxP3 MFI	CCR7-FoxP3+CD4+Ki67-CD8+	A
36	PD1 MFI	CCR7-CD45RA-Ki67+	A



37	FoxP3 MFI	CCR7+FoxP3+PD1+Ki67-CD8+	A
38	CD4 MFI	CD69+GzmB+CD45RA-IFNg-CD8-	B stimulated
39	CD8 MFI	CD69-CD4-	B difference
40	CD4 MFI	CCR7-FoxP3+CD45RA+CD8+	A
41	PD1 MFI	CCR7+FoxP3-CD45RA+PD1+CD4+Ki67+	A
42	PD1 MFI	GzmB-CD45RA-CD4-CD8-	B difference
43	CD11b MFI	FSC-A-SSC-A-CD11b-HLA-DR+CD15+	C
44	CD45RA MFI	CD69-GzmB+CD4+IFNg-	B difference
45	CD45RA MFI	CD45RA+PD1+CD4+Ki67+	A
46	CD15 MFI	SSC-A+CD14+CD33+HLA-DR-CD15+	C
47	CD25 MFI	CCR7-CD45RA+PD1-CD4+CD8+	A
48	CD45RA MFI	CD69-GzmB+CD45RA-CD4-	B difference
49	HLA-DR MFI	FSC-A-SSC-A+CD14+CD33+HLA-DR-CD15-	C
50	CD14 MFI	FSC-A-CD14+CD33-CD11b-HLA-DR+	C
51	CD8 MFI	FoxP3+CD45RA+PD1-CD4+Ki67+CD8-	A

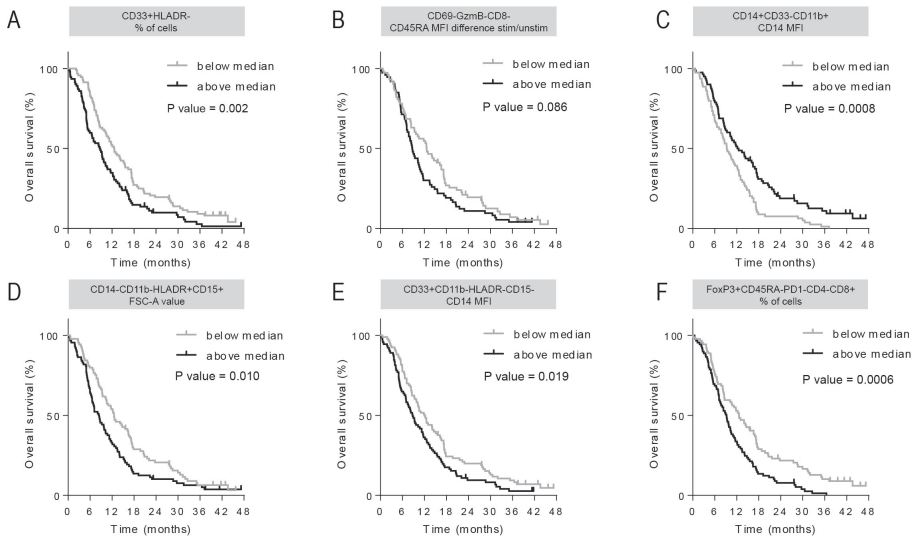


**Figure 4.** Survival of patients based on individual FloReMi selected features. A-E show the top 6 selected features (see table 3). Patient groups were split on the median value of the feature, and the curves were compared with a log-rank test.

### Survival analysis of individual selected features

From a biological viewpoint, it is valuable to know which features contribute to a significant prediction of overall survival. Since the five folds of cross-validation each led to a different set of features, we performed a feature selection step on all samples for a final selection of features, which are listed in table 3. To assess the clinical value of the resulting FloReMi features with a conventional statistical analysis method, we compared survival of patients based on the top six selected features, in which two patient groups with above or below



median value for the feature were compared. Five of the top six selected features showed a significant difference between the patient groups (Figure 4).

## DISCUSSION

Flow cytometry panels are becoming increasingly complex as the technique advances, leading to generation of large amounts of high-dimensional data. With manual analysis of these data, only two markers can be analyzed at the same time, which can be labor-intensive, subjective and inefficient when working with large marker panels. Various computational models are being developed to overcome these problems, with the objective of visualization and/ or computation of flow cytometric data, as reviewed in [11]. The FloReMi pipeline is one example of these newly developed tools and is aimed specifically to predict survival of patients using features extracted from flow cytometry data, which fitted our research question and patient cohort. Here, we used this pipeline for the first time on a dataset other than the dataset used for development of the pipeline, to assess the value of this analysis method for predicting survival of cancer patients based on their immune profile. We showed that feature extraction using semi-automatic gating produces reliable features in an unbiased manner. Subsequent survival prediction using these features provided a significant prediction, although only marginally better than random.

The FloReMi pipeline consists of four steps: pre-processing, feature extraction, feature selection and survival prediction, which can be used independently. After pre-processing to ensure quality of the data, feature extraction generated an exhaustive number of immune populations based on cutoffs to define positive and negative populations for each marker. Although by using cutoffs, information on the continuous variable is lost, this does correspond to 'gating' in manual analysis, which makes the generated populations comparable to manually obtained populations and interpretable. Indeed, a high correlation was found with the manually defined populations. Moreover, expression level values are included in additional features derived from MFI values of each marker for every population. The feature extraction step could therefore be useful in future studies to automate analysis of extensive marker panels in studies with large numbers of samples.

In the feature selection and survival prediction steps, features are first sorted based on their association with outcome in the train data. The most informative features are selected without including features that are correlated to other selected feature, to reduce redundancy. This led to a manageable list of selected features (around 40), that were used to train a survival model. From a biological view point, it is interesting to review this list of

selected features. We have shown previously that myeloid-derived suppressor cells (MDSC) are associated with survival in this cohort of patients [7]. Therefore, we hypothesized that amongst others, MDSC-related features would be selected and provide predictive value in the survival model.

The first selected feature that had the strongest correlation to survival in the training data, was the percentage of CD33<sup>+</sup>HLA-DR<sup>-</sup> cells of total PBMC in staining C. This feature partly overlaps with our definition of MDSC (which are CD33<sup>+</sup>HLA-DR<sup>-</sup>, but additionally also CD11b<sup>+</sup>, and CD14<sup>+</sup> or CD15<sup>+</sup> depending on the MDSC subset) [7], but has also been reported as a broader definition of MDSC in combination with the absence of lineage marker expression [17, 18]. The second selected feature was the difference in CD45RA expression between the stimulated and unstimulated condition CD69<sup>-</sup>GzmB<sup>-</sup>CD8<sup>-</sup> cells. This feature is more difficult to interpret, as overall CD45RA expression does not differ between the stimulated and unstimulated condition, but rather the size of the CD69<sup>-</sup> T cell population, likely affecting the CD45RA MFI (data not shown). In general, features consisting of an MFI on a certain population do not always have a clear biological meaning, especially when it concerns an MFI feature of a population negative for that marker (for example feature #8 in table 3). Due to the exclusion of features based on their correlation with other selected features, better known or interpretable features might be excluded if they are lower on the sorted list. Further investigation into the (biological or technical) relation between the correlated features would be worthwhile to discover the most biologically relevant features. For example, instead of excluding the majority of features, feature clustering could be used in which an average cluster value could be used in the survival model.

The overall performance of the survival model was only marginally better than random. However, using only the manually obtained features, no predictive value was generated at all. This does suggest that the FloReMi pipeline is able to improve survival prediction by using the flow cytometric data to its maximal extent, including features that would otherwise not been manually gated for.

There are several possible explanations for the low performance of the survival prediction in this study. Firstly, there might be limited predictive value in the peripheral blood immune profile of NSCLC patients. However, the potential of the immune profile as prognostic marker has been shown by the immunoscore as developed in colorectal cancer [19]. Here, a combined score of immune populations in the local tumor environment had strong prognostic value and was used to classify patients in different risk groups. The prognostic value of immune populations in peripheral blood is less definite, but several immune populations have been shown to be associated with survival in NSCLC [20, 21]. Whereas

log-rank tests evaluate the association of certain markers with survival in a group of patients, this is arguably not sufficient to indeed predict survival of an individual patient. The top feature discovered with the FloReMi pipeline, HLA-DR CD33<sup>+</sup> cells, has a similarly strong association with survival as the previously published MDSC [7], which suggests that this method is not inferior to manual survival analysis.

Secondly, even though the analysis pipeline is an unbiased approach to data analysis, the choice of markers in the flow cytometry panel is still a manual procedure which will introduce some bias. In our study design, we tried to create panels containing the most relevant markers focused on T cells or myeloid-derived suppressor cells based on literature. Still, the number of markers to be included in a single staining is limited, and therefore these stainings might not have captured all relevant immune parameters for survival prediction in NSCLC. In contrast, gene expression analysis would represent a more unbiased approach, which has been employed by some other groups in NSCLC [22, 23] and other cancer types [24-26]. The drawback of RNA sequencing, however, is the lack of information on protein levels.

Thirdly, feature selection using features sorted on their p-value derived from individual association with survival, will render some false positive findings. The most strongly associated features are selected, but no threshold is used as how strong this association (p value or effect size) should be before inclusion in the selected feature list. In contrast to the first reported use of the pipeline, we here have included feature selection within the cross-validation. In the original report, a leave-one-out cross-validation provided a concordance index of 0.99, but in this analysis the features were preselected on outcome for the whole dataset. Final evaluation of the holdout set provided a concordance index of 0.67 equaling an error rate of 0.33, which has been reached here in the best performing folds as well. The disadvantage of selecting features within the cross-validation is the prolonged calculation time, as feature selection calculation is relatively time-consuming compared to fitting the RSF model. Therefore, further improvements to the feature selection step should take into account calculation time as a relevant factor next to interpretability of results.

Lastly, survival models for patients based solely on their peripheral blood immune profile would be unlikely to reach a predictive value close to 1, as there are a myriad of factors influencing survival of cancer patients. Therefore, the FloReMi method would be more valuable as an explorative tool to discover populations that are associated with patient survival, by investigating the selected feature list.

In summary, the semi-automatic analysis pipeline of flow cytometry data can be used to analyze high-dimensional flow cytometry data derived from peripheral blood of NSCLC patients to extract large amounts of features, which can be used for any kind of further analysis. Survival prediction using these features can potentially generate biological and clinical value, although this should be further investigated in another clinical dataset with known clinical value. The selected features in this study, could be interesting targets for further investigation on their clinical value in NSCLC patients.

## REFERENCES

1. Zitvogel, L., et al., *Immunological aspects of cancer chemotherapy*. Nat Rev Immunol, 2008. **8**(1): p. 59-73.
2. Gong, J., et al., *Development of PD-1 and PD-L1 inhibitors as a form of cancer immunotherapy: a comprehensive review of registration trials and future considerations*. J Immunother Cancer, 2018. **6**(1): p. 8.
3. Galluzzi, L., et al., *Immunological Effects of Conventional Chemotherapy and Targeted Anticancer Agents*. Cancer Cell, 2015. **28**(6): p. 690-714.
4. Fridman, W.H., et al., *The immune contexture in human tumours: impact on clinical outcome*. Nat Rev Cancer, 2012. **12**(4): p. 298-306.
5. Remark, R., et al., *The non-small cell lung cancer immune contexture. A major determinant of tumor characteristics and patient outcome*. Am J Respir Crit Care Med, 2015. **191**(4): p. 377-90.
6. Anichini, A., et al., *The non-small cell lung cancer immune landscape: emerging complexity, prognostic relevance and prospective significance in the context of immunotherapy*. Cancer Immunol Immunother, 2018. **67**(6): p. 1011-1022.
7. de Goeje, P.L., et al., *Immunoglobulin-like transcript 3 is expressed by myeloid-derived suppressor cells and correlates with survival in patients with non-small cell lung cancer*. Oncoimmunology, 2015. **4**(7): p. e1014242.
8. Vetsika, E.K., et al., *A circulating subpopulation of monocytic myeloid-derived suppressor cells as an independent prognostic/predictive factor in untreated non-small lung cancer patients*. J Immunol Res, 2014. **2014**: p. 659294.
9. Kotsakis, A., et al., *Prognostic value of circulating regulatory T cell subsets in untreated non-small cell lung cancer patients*. Sci Rep, 2016. **6**: p. 39247.
10. Huang, A.C., et al., *T-cell invigoration to tumour burden ratio associated with anti-PD-1 response*. Nature, 2017. **545**(7652): p. 60-65.
11. Saeys, Y., S.V. Gassen, and B.N. Lambrecht, *Computational flow cytometry: helping to make sense of high-dimensional immunology data*. Nat Rev Immunol, 2016. **16**(7): p. 449-62.
12. Van Gassen, S., et al., *FloReMi: Flow density survival regression using minimal feature redundancy*. Cytometry A, 2016. **89**(1): p. 22-9.
13. Dingemans, A.M., et al., *A randomized phase II study comparing paclitaxel-carboplatin-bevacizumab with or without nitroglycerin patches in patients with stage IV nonsquamous nonsmall-cell lung cancer: NVALT12 (NCT01171170)dagger*. Ann Oncol, 2015. **26**(11): p. 2286-93.
14. de Goeje, P.L., et al., *Induction of Peripheral Effector CD8 T-cell Proliferation by Combination of Paclitaxel, Carboplatin, and Bevacizumab in Non-small Cell Lung Cancer Patients*. Clin Cancer Res, 2019. **25**(7): p. 2219-2227.
15. Tang, F. and H. Ishwaran, *Random Forest Missing Data Algorithms*. Stat Anal Data Min, 2017. **10**(6): p. 363-377.
16. Harrell, F.E., Jr., et al., *Evaluating the yield of medical tests*. JAMA, 1982. **247**(18): p. 2543-6.
17. Shen, P., et al., *Increased circulating Lin(-/low) CD33(+) HLA-DR(-) myeloid-derived suppressor cells in hepatocellular carcinoma patients*. Hepatol Res, 2014. **44**(6): p. 639-50.
18. Verschoor, C.P., et al., *Blood CD33(+)HLA-DR(-) myeloid-derived suppressor cells are increased with age and a history of cancer*. J Leukoc Biol, 2013. **93**(4): p. 633-7.
19. Pages, F., et al., *International validation of the consensus Immunoscore for the classification of colon cancer: a prognostic and accuracy study*. Lancet, 2018.
20. Catacchio, I., et al., *Immune Prophets of Lung Cancer: The Prognostic and Predictive Landscape of Cellular and Molecular Immune Markers*. Transl Oncol, 2018. **11**(3): p. 825-835.
21. Qi, L., et al., *Deconvolution of the gene expression profiles of valuable banked blood specimens for studying the prognostic values of altered peripheral immune cell proportions in cancer patients*. PLoS One, 2014. **9**(6): p. e100934.
22. Kossenkov, A.V., et al., *Peripheral immune cell gene expression predicts survival of patients with non-small cell lung cancer*. PLoS One, 2012. **7**(3): p. e34392.



23. Zander, T., et al., *Blood-based gene expression signatures in non-small cell lung cancer*. Clin Cancer Res, 2011. **17**(10): p. 3360-7.
24. Chen, Y.C., et al., *Peripheral immune cell gene expression changes in advanced non-small cell lung cancer patients treated with first line combination chemotherapy*. PLoS One, 2013. **8**(2): p. e57053.
25. Wang, L., et al., *A robust blood gene expression-based prognostic model for castration-resistant prostate cancer*. BMC Med, 2015. **13**: p. 201.
26. Wolf, B., et al., *Gene expression profile of peripheral blood lymphocytes from renal cell carcinoma patients treated with IL-2, interferon-alpha and dendritic cell vaccine*. PLoS One, 2012. **7**(12): p. e50221.

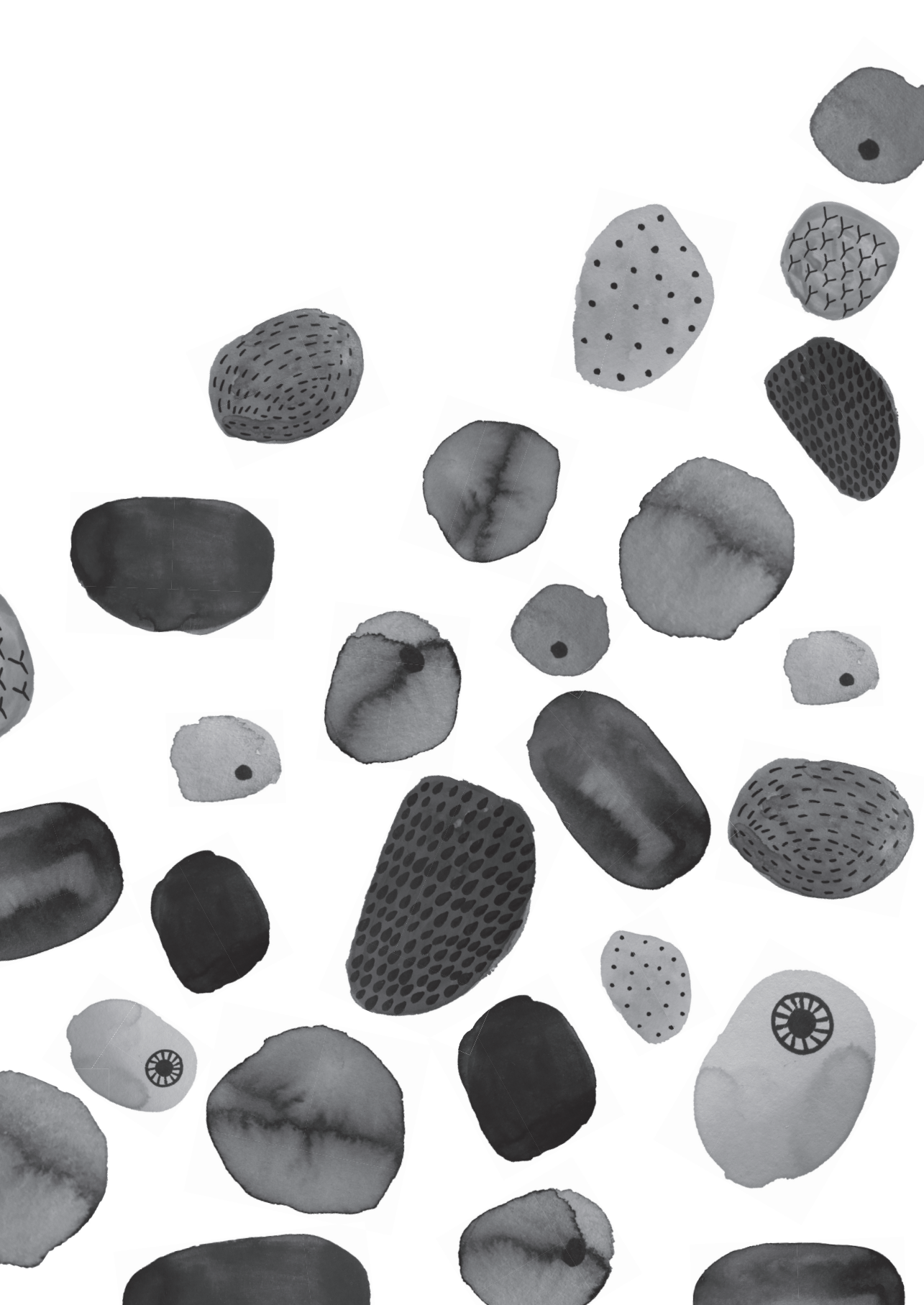
## SUPPLEMENTARY DATA

**Supplementary table 1.** Antibodies used for flow cytometry

Marker	Fluorochrome	Company	Catalog #
<b>Staining A: T cells (immediately stained)</b>			
CCR7	FITC	R&D systems	FAB197F
CD14	PerCPy5.5	BD Biosciences	550787
CD16	PerCPy5.5	BD Biosciences	560717
CD19	PerCPy5.5	BD Biosciences	561295
CD25	PE Cy7	eBioscience	25-0259-42
CD28	BV605	BD Biosciences	562976
CD3	APC-eF780	eBioscience	47-0038(-42)
CD4	BV786	BD Biosciences	563877
CD45RA	PE Texas Red	Invitrogen	MHCD45RA17
CD8	AF700	eBioscience	56-0088-42
CTLA4	BV421	BD Biosciences	562743
FoxP3	PE	eBioscience	12-4777(-42)
Ki67	APC	eBioscience	17-5699(-42)
PD1	BV711	BD Biosciences	564017
LIVE/DEAD™ fixable aqua dead cell stain	BV510	Invitrogen	L34966
<b>Staining B: T cells (stimulated)</b>			
CD3	APC-eF780	eBioscience	47-0038(-42)
CD4	BV786	BD Biosciences	563877
CD45RA	PE Texas Red	Invitrogen	MHCD45RA17
CD69	FITC	BD Biosciences	555530
CD8	AF700	eBioscience	56-0088-42
GzmB	PE	Invitrogen	MHGB04
IFN $\gamma$	APC	BD Biosciences	554702
PD1	BV711	BD Biosciences	564017
LIVE/DEAD™ fixable aqua dead cell stain	BV510	Invitrogen	L34966
<b>Staining C: Myeloid cells</b>			
CD11b	APC	BD Biosciences	340937
CD14	PE-Texas Red	Invitrogen	MHCD1417
CD15	PE	BD Biosciences	555402
CD16	PerCP-Cy5.5	BD Biosciences	560717
CD33	PE-Cy7	BD Biosciences	333946
HLA-DR	APC-Cy7	BD Biosciences	335796
ILT3	FITC	R&D systems	AF2425
DAPI	Measured in BV421	Invitrogen	D1306

**Supplementary Table 2.** Number of features extracted from each staining and per patient

	T cell staining A	T cell staining B	MDSC staining
Number of markers to split	7	6	7
Number of markers for MFI	11	8	7
Features per sample	26,244	6,561	17,496
Features per patient	26,244	19,683	17,496





# CHAPTER

# 6

## **AUTOLOGOUS DENDRITIC CELLS PULSED WITH ALLOGENEIC TUMOR CELL LYSATE IN MESOTHELIOMA: FROM MOUSE TO HUMAN**

Joachim G.J.V. Aertst†, Pauline L. de Goejet, Robin Cornelissen, Margaretha E.H. Kajjen-Lambers, Koen Bezemer, Cor H. van der Leest, Niken M. Mahaweni, André Kunert, Ferry A.L.M. Eskens, Cynthia Waasdorp, Eric Braakman, Bronno van der Holt, Arnold G. Vulto, Rudi W. Hendriks, Joost P.J.J. Hegmans\*, Henk C. Hoogsteden\*.

† These authors contributed equally as first authors

\* These authors contributed equally as senior authors

*Clin Cancer Res.* 2018 Feb 15;24(4):766-776. doi: 10.1158/1078-0432.CCR-17-2522. Epub 2017 Dec 12.

## **STATEMENT OF TRANSLATIONAL RELEVANCE**

Malignant pleural mesothelioma is a highly lethal neoplasm for which new treatment options, like immunotherapy, are urgently needed. Early results from studies investigating checkpoint inhibitors show either no efficacy (anti CTLA-4) or a temporary beneficial effect in a minority of patients (anti PD-1). This is ascribed to the absence of a tumor-directed T-cell response. Previously, we demonstrated that autologous tumor lysate-pulsed dendritic cell immunotherapy increased T cell response towards malignant mesothelioma. However, the use of autologous tumor material hampers implementation in large clinical trials, which might be overcome by using allogeneic tumor cell lines as tumor antigen source. Here, we present a translational study that provides the basis for allogeneic lysate loaded DC immunotherapy. First, we show efficacy of this strategy in a murine mesothelioma model. Subsequently, we established clinical grade human mesothelioma cell lines to pulse autologous DC from 9 patients in a first-in-human trial. We show that this treatment is safe and feasible in mesothelioma patients. Our findings pave the way for clinical application of dendritic cell immunotherapy in mesothelioma to be evaluated in phase III clinical trials.

## ABSTRACT

**Purpose:** Mesothelioma has been regarded as a non-immunogenic tumor, which is also shown by the low response rates to treatments targeting the PD-1/PD-L1 axis. Previously, we demonstrated that autologous tumor lysate-pulsed dendritic cell (DC) immunotherapy increased T-cell response towards malignant mesothelioma. However, the use of autologous tumor material hampers implementation in large clinical trials, which might be overcome by using allogeneic tumor cell lines as tumor antigen source. The purpose of this study was to investigate if allogeneic lysate pulsed DC immunotherapy is effective in mice and safe in humans.

**Experimental Design:** Firstly, in two murine mesothelioma models, mice were treated with autologous DCs pulsed with either autologous or allogeneic tumor lysate, or injected with PBS (negative control). Survival and tumor-directed T cell responses of these mice were monitored. Results were taken forward in a first-in-human clinical trial, in which 9 patients were treated with 10, 25 or 50 million DC per vaccination. DC vaccination consisted of autologous monocyte-derived DC pulsed with tumor lysate from 5 mesothelioma cell lines.

**Results:** In mice, allogeneic lysate-pulsed DC immunotherapy induced tumor-specific T cells and led to an increased survival, to a similar extent as DC immunotherapy with autologous tumor lysate. In the first-in-human clinical trial, no dose limiting toxicities were established and radiographic responses were observed. Median PFS was 8.8 months (95% CI 4.1-20.3) and median OS not reached (median follow up 22.8 months).

**Conclusions:** DC immunotherapy with allogeneic tumor lysate is effective in mice and safe and feasible in humans.

## INTRODUCTION

Malignant pleural mesothelioma (MPM) is a highly lethal neoplasm for which new treatment options are urgently needed [1]. Recently reported randomized studies investigating immunotherapy (cytotoxic T-lymphocyte-associated protein 4 (CTLA-4) inhibitor tremelimumab) and molecular targeting (FAK inhibition, defactinib) were found to be negative for the primary endpoint of an increase in overall survival [2, 3]. The phase III MAPS trial targeting angiogenesis (anti-VEGF, bevacizumab) in combination with chemotherapy showed a modest increase in survival [4].

A number of new agents are being tested in early phase studies in MPM, mostly focusing on immunotherapy with checkpoint inhibitors. Initial results have become available on the blockade of programmed death receptor (PD)-1/ programmed death ligand 1 (PD-L1) in MPM showing single agent response rates ranging between 9-25% [5]. Response rates to PD1/PDL1 inhibitors in these ranges have also been found in other solid malignancies, such as non-small cell lung cancer (NSCLC) [6]. As the effect of checkpoint inhibitors is based on reinvigoration of anti-tumor T cell responses, response to therapy is correlated to the presence of tumor infiltrating T cells pretreatment [7]. Also in mesothelioma, an immune infiltrate including T cells is correlated to improved survival [8]. An immunotherapeutic approach aiming to increase the number of tumor-directed T cells, is vaccination. In a recent systematic review on the efficacy of tumor vaccines and cellular immunotherapies it was established that cell-based vaccination has the highest efficacy in complex tumors like NSCLC [9]. Dendritic cell (DC)-based immunotherapy is a potent cell-based immunotherapeutic approach [10, 11], which aims to boost the immune system of cancer patients by enhancing tumor antigen presentation and subsequent activation of tumor-specific (cytotoxic) T cells. DCs are reduced in number in the peripheral blood of mesothelioma patients, and are less functional in terms of activation and antigen presentation compared to healthy controls [12]. Therefore, *ex vivo* DC activation and maturation might improve their immune function and direct them to present tumor associated antigens (TAA). To pulse DCs *ex vivo*, a variety of sources of tumor antigens can be used, such as proteins or peptides, DNA or mRNA in the case of known antigens, or whole tumor cells or tumor lysate, in which undefined antigens are present as well [13].

In previous studies in both murine models and patients with mesothelioma, we have demonstrated that dendritic cell vaccination induces tumor-specific CD8 T cell responses accompanied by promising survival rates [14-16]. In these studies, we have used an autologous tumor lysate as a source to pulse DCs, as vaccination with a broad range of antigens can induce a broad repertoire of anti-tumor T cells and therefore might be more

effective [17]. Two recent publications showed the potential of a polyvalent vaccination to induce a broad range of T cell responses in a setting of long synthetic peptide vaccination in melanoma [18, 19]. For our DC vaccination strategy in mesothelioma, we generated autologous tumor lysate from patients' own tumor material obtained via pleural drainage, tumor resection or biopsies, which was used to pulse DCs. This approach was found to be safe and well tolerated by mesothelioma patients [15, 16]. However, using an autologous whole tumor cell lysate limited the number of patients that could be included due to logistic limitations, such as the amount and quality of the tumor material. This impeded scaling up the treatment for multicenter clinical trials [20].

An alternative source to pulse the DCs with a broad spectrum of antigens, is the use of an allogeneic tumor lysate generated from cell line cultures, which contain TAA [17]. We hypothesized that DC immunotherapy with an allogeneic lysate prepared from tumor cell lines would be able to induce antitumor responses similar to the autologous tumor cell lysate. In this study, we first examined the efficacy of allogeneic tumor lysate DC immunotherapy *in vivo* in two different murine mesothelioma models (CBA/j and BALB/c mice), in which we demonstrated that allogeneic tumor lysate loaded DC immunotherapy was similarly effective in improving survival of mesothelioma-bearing mice as autologous tumor lysate DC immunotherapy. To translate these findings to human, we developed a human allogeneic tumor cell lysate, generated from 5 clinical grade mesothelioma cell lines. In a first-in-human phase I study, patients with mesothelioma were treated with increasing numbers of autologous DCs pulsed with allogeneic lysate. We found that the treatment is safe, induces an anti-tumor immune response, and is associated with radiographic responses and promising overall survival.

## METHODS

### PRECLINICAL:

#### Tumor cell lines culture

The AB1 and AC29 mouse mesothelioma cell lines were kindly provided by Prof. Bruce W.S. Robinson, Queen Elizabeth II Medical Centre, Australia. The AB1 and AC29 cell lines have been derived from malignant mesothelioma after intraperitoneal (i.p.) inoculation of crocidolite asbestos into BALB/c (H-2d) and CBA/j (H-2k) mice, respectively. Both cell lines were obtained in the years 2003–2005, aliquoted and stored at -190°C.

These cell lines were maintained in RPMI 1640 GlutaMax™ supplemented with 50µg/ml gentamycin (all obtained from Invitrogen, Breda, the Netherlands) and 5% fetal bovine

serum (FBS) (HyClone, Thermo Scientific). Tumor cells were cultured from early passages (max. 5 passages following cell line acquisition).

### **Tumor lysate production**

AB1 and AC29 tumor cells were harvested from 80% confluent culture flasks and resuspended at a concentration of  $50 \times 10^6$  cells/ml for AB1 and  $100 \times 10^6$  cells/ml for AC29 in phosphate buffered saline (PBS). Cells were disrupted by five freeze-thaw cycles and subsequent sonication to produce a homogeneous lysate.

### **Isolation and loading of DCs**

As in a murine model, it is not possible to obtain sufficient amount of monocyte-derived DCs from peripheral blood, DCs were obtained from bone marrow culture using a modified version of a previously described procedure [21]. Instead of flushing the femurs and tibias of naïve BALB/c or CBA/j mice for the bone marrow, major leg bones were crushed using a mortar and pestle with addition of approximately 3 mL of RPMI medium. Cells were passed through a 100  $\mu$ m cell strainer, depleted of red blood cells and cultured in DC culture medium, composed of RPMI supplemented with 5% FBS, 50  $\mu$ g/ml gentamycin, 50  $\mu$ M beta-mercaptoethanol (Sigma- Aldrich, Missouri, USA) and 20 ng/ml recombinant murine granulocyte macrophage-colony-stimulating factor (GM-CSF) (gift from prof. Bart Lambrecht). Cells were placed in 90 mm culture dishes (Nunc™) with a total number of  $2 \times 10^6$  cells/10 ml at seeding and incubated at 37° C (Innova Co-170, New Brunswick Scientific) in a humidified atmosphere at 5% CO<sub>2</sub> (day 0). On day 3, the 10 ml of DC culture medium was added. On day 6, 10 ml of the media was replaced by 10 ml fresh DC medium. After 8 days in culture, DCs were pulsed with AB1 (3 tumor cell equivalents per DC) or AC29 (6 AC29 tumor cell equivalents per DC) tumor lysate. After 8 hours, LPS was added to allow full maturation. The next day, DCs were harvested by gentle pipetting and purified by Lympholyte-Mammal (Cedarlane, Hornby, ON, Canada) density gradient centrifugation, washed three times with PBS and resuspended at a concentration of  $1-3 \times 10^6$  viable cells in 500  $\mu$ l PBS.

### **Verification maturation status of DCs**

To verify the purity and maturation of DCs, the cultured cells were assessed with flow cytometry on a FACS LSR II (BD Biosciences). DCs were characterized as CD11c<sup>+</sup>MHC-II<sup>+</sup>. CD40, CD80 and CD86 were used to verify maturation of DCs. The following antibodies with matched isotype controls were used: anti-CD11c-PE Texas Red, anti-MHC class II-Alexa Fluor 700, anti-CD40APC (eBioscience), anti-CD80PerCP-Cy5.5 and anti-CD86PE-Cy7 (BD Biosciences). DAPI, 4',6-diamidino-2-phenylindole (Invitrogen) was used as a viability dye.

### **In vivo survival experiments**

Female BALB/c mice and CBA/j mice (Harlan, Zeist, The Netherlands) were housed at the animal care facility of the Erasmus MC, Rotterdam. The experiment was approved by the local Ethical Committee for Animal Welfare. Experiments were started at 6-8 weeks of age. At day 0, mice were injected intraperitoneally (i.p.) with a  $0.5 \times 10^6$  AB1 tumor cells (BALB/c mice) or  $15 \times 10^6$  AC29 tumor cells (CBA/j mice). The number of tumor cells for these mouse models were titrated to achieve a tumor incidence in untreated mice of at least 80%, with mice generally surviving until at least two weeks after tumor inoculation [14, 22]. At day 7, mice received an i.p. injection with PBS or DCs immunotherapy pulsed with either AB1 tumor lysate or AC29 tumor lysate. 6 mice were used per group.

Each vaccine contained  $1-3 \times 10^6$  DCs, depending on the yield, and equal for all mice within the experiment. Tumor growth, physical well-being, body weight, and the survival were monitored every other day for 70 days after tumor injection.

### **In vitro degranulation assay and flow cytometric analysis**

Splenocytes from PBS treated, DC treated or naive mice were restimulated with tumor cells. 50.000 AC29 or AB1 tumor cells were seeded in a flat bottom 24 wells plate (Costar™, Corning Inc), to which  $1 \times 10^6$  splenocytes were added the next day, together with  $10 \mu\text{g/ml}$  CD107a -FITC (BD Bioscience). After one hour, the protein transport inhibitor Golgi stop™ was added (BD Bioscience). As a positive control, splenocytes were stimulated with 50 ng/ml phorbol 12-myristate 13-acetate (PMA) and 500 ng/ml Ionomycin (Sigma). Unstimulated splenocytes were used as negative control. After 4 hours of incubation at  $37^\circ\text{C}$ , splenocytes were harvested and stained for flow cytometry with anti-CD3-APCCy7, anti-CD8-PE-Cy7, anti-CD44-PerCP-Cy5.5 and anti-CD62L-APC (eBioscience). Fixable Viability Dye eFluor® 506 (eBioscience) was used to exclude dead cells. For staining of intracellular IFN $\gamma$ , cells were fixed with 2% paraformaldehyde and permeabilized with 0,5% saponin, before IFN $\gamma$  was stained intracellularly with anti-IFN $\gamma$ -Pacific Blue (eBioscience).

### **Caspase 3/7 assay**

CD8 $^+$  T cells were isolated from splenocytes from DC treated mice using the CD8 $^+$  Isolation kit (Miltenyi Bioscience). Purified CD8 $^+$  T cells were then co-cultured with AB1 tumor cells or AC29 tumor cells in a 20:1 or 50:1 ratio in a black coated and transparent flat bottom 96 microplate (Greiner). Cell Player™ Caspase 3/7 reagent (Essen Bioscience) was added at 5  $\mu\text{M}$  final concentration per well to detect apoptosis during the co-culture. Cells were cultured in the Incucyte™ FLR (Essen Bioscience) for 4 days at  $37^\circ\text{C}$  in a humidified atmosphere at 5% CO $_2$  and images were captured every 2.5 hours for caspase 3/7 upregulation.

**CLINICAL:****Study design**

In this first-in-human open label non-randomized dose escalation phase I study we enrolled adult patients with mesothelioma. In total, nine MPM patients divided over 3 cohorts (3 patients per cohort) received autologous monocyte-derived DCs (Mo-DC) pulsed with allogeneic tumor cell line lysate. The first cohort received 10 million Mo-DC per vaccination, the second cohort received 25 million Mo-DC per vaccination and the third cohort received 50 million Mo-DC per vaccination. The autologous Mo-DC and the allogeneic tumor cell line lysate used to load the autologous Mo-DC were produced under GMP-certified conditions. The study was approved by the Central Committee on Research involving Human Subjects (NL443300014) as defined by the Medical Research Involving Human Subjects Act. Procedures followed were in accordance with the ethical standards of these committees on human experimentation and with the Helsinki Declaration of 1975, as revised in 2008. The trial is registered within [clinicaltrials.gov](https://clinicaltrials.gov), number NCT02395679.

**Patient selection**

Patients with histologically or cytologically confirmed MPM were eligible to participate in the study. Moreover, patients had to be non-progressive after at least 4 cycles of pemetrexed and platinum containing chemotherapy (as determined by CT). Patients that refused chemotherapy treatment as first line treatment were also eligible. Other inclusion criteria were: measurable disease on CT dimensions according to modified Response Evaluation Criteria In Solid Tumors (RECIST) [23], at least 18 years of age, able to give written informed consent, ambulatory (WHO-ECOG performance status 0 or 1, with an expected survival of at least 3 months), normal organ function and adequate bone marrow reserve (absolute neutrophil count  $> 1.0 \times 10^9/l$ , platelet count  $> 100 \times 10^9/l$ , and Hb  $> 6.0$  mmol/l), a positive DTH skin test (induration  $> 2$ mm after 48 hours) against at least one positive control antigen tetanus toxoid, ability to return to the Erasmus MC for adequate follow-up as required by this protocol, written informed consent according to ICH-GCP, and planned start date of vaccination at least 5 weeks after the last dosage of chemotherapy.

A potential subject who met any of the following criteria was excluded from participation in this study: medical or psychological impediment to probable compliance with the protocol; current use or discontinuation of less than 6 weeks of steroids (or other immunosuppressive agents), with the exception of prophylactic usage of dexamethasone during chemotherapy; prior malignancy except adequately treated basal cell or squamous cell skin cancer, superficial or in-situ cancer of the bladder or other cancer for which the patient has been disease-free for five years; serious concomitant disease or active infections; history of autoimmune disease or organ allografts, or with active acute or chronic infection, including HIV and viral



hepatitis; serious intercurrent chronic or acute illness such as pulmonary (asthma or COPD) or cardiac (NYHA class III or IV) or hepatic disease or other illness considered by the study coordinator to constitute an unwarranted high risk for investigational DC treatment; known allergy to shell fish (may contain KLH); pregnant or lactating women; inadequate peripheral vein access to perform leukapheresis and concomitant participation in another clinical trial.

### **Procedures**

Patients received MesoPher (see below: Production of DC vaccination) via intradermal (i.d.) and intravenous (i.v.) injections with two thirds of the dose i.v. and one third i.d. in 3 biweekly vaccinations, followed by a booster after 3 and 6 months. The combined i.d. and i.v. administration was chosen to induce a systemic immune response, as proposed by Adema et al. [24] and was used in previous phase I trials by our group as well [15, 16]. Cohorts of 3 patients received a dose level to evaluate safety. Within each cohort a patient was required to complete 7 days after the vaccination without toxicities before a new patient was treated. If none of these 3 patients in one cohort had a DLT within 8 weeks of starting the first dose, the next dose level was started.

### **Outcomes**

The primary objective was to determine the safety of the different dose schedules, to establish the recommended dose for further studies. Secondary objectives were antitumor activity according to radiological examinations, immunological profiling and overall survival.

### **Safety evaluation**

Physical examination and hematological and biochemistry assessments were performed weekly. A 12 lead ECG and laboratory testing was performed before the patient could be included in the trial, and before every vaccination. Toxicity was scored according to the NCI-CTCAE version 4.0.

The following toxicities occurring during 8 weeks after the first vaccination, were defined as dose-limiting (DLTs), when considered possibly, probably or definitively related to study medication. Hematological toxicity: thrombocytopenia grade 3 during longer than 7 days or grade 4 or a neutropenia grade 3 during longer than 7 days or grade 4. Non-hematological toxicity: any grade 3/4 toxicity except for diarrhea, nausea, vomiting, hypertension if not adequately treatable, skin toxicity. Immune related toxicity: any grade 4 except for rash and (drug related) fever.

### **Tumor evaluations**

Tumor evaluations were performed every 6 weeks by chest CT preferably using contrast and response was determined according to the modified RECIST. Objective responses had to be confirmed 6 weeks after the initial assessment. Duration of response was from first documented response until disease progression.

### **Immunological evaluations**

Serum samples were collected before start of treatment, on the day of each vaccination, and two weeks after each vaccination. A DTH skin test was performed two weeks after the third vaccination with the lysate, MesoPher, tumor lysate-pulsed DCs without KLH and injection fluid as negative control. DTH reaction was measured 48h after intradermal injection. If a positive reaction was observed, a 3 or 6 mm punch biopsy was taken from the skin induration, and was used immediately for isolation of skin-test infiltrating lymphocytes (SKIL).

### **Rapid expansion of skin-test infiltrating lymphocytes**

Skin biopsies were placed in a 6-wells plate with 3 ml medium consisting of RPMI, 7% normal human serum and low concentrations IL-2 (100 IU/ml) for 7 days. Subsequently T cells were rapidly expanded with a feeder system as described elsewhere [25].

### **Dextramer staining and analysis**

Online prediction algorithms (netCTL: <http://www.cbs.dtu.dk/services/NetCTL/> and netMHCpan: <http://www.cbs.dtu.dk/services/NetMHCpan/>) were used to select HLA-A2 binding mesothelin peptides with high affinity and predicted MHC presentation. Dextramers were ordered from Immudex (Copenhagen, Denmark). Dextramer A: PE-conjugated HLA-A2 dextramer with peptide SLLFLLFSL (mesothelin<sub>20-28</sub>), Dextramer B: APC-conjugated HLA-A2 dextramer with peptide VLPLTVAEV (mesothelin<sub>531-539</sub>). Dextramer staining was performed according to manufacturer's protocol. Anti-CD3-BV711 and anti-CD8-FITC (clone SK1) (BD Biosciences) were used for extracellular staining. DAPI was used as viability dye. Samples were measured on an LSR-II flow cytometer (BD). FMO controls were used to determine dextramer-positive populations.

### **Statistical analysis**

All statistical tests on the murine experiments were performed in GraphPad Prism 5. The size of the first-in-human dose escalation study was based on the standard 3+3 dose escalation design, and therefore we did not perform a further samples size estimation.

### **Production of DC vaccination (MesoPher)**

Eligible patients underwent autologous DC pulsed with allogeneic tumor lysate-based immunotherapy (MesoPher). Allogeneic tumor lysate was produced under GMP-compliant conditions and consists of five unique, clinical grade human MM cell lines, which are patented under patent ID P6038325NL. For the production of MesoPher, Mo-DC were generated from CD14<sup>+</sup> monocytes according to a 10-day culture protocol. CD14<sup>+</sup> monocytes were enriched from patient derived apheresis products by CliniMACS procedure (CD14<sup>+</sup> procedure, Miltenyi). Purity of the CD14<sup>+</sup> monocytes after CliniMACS procedure was >97% and viability was >95% for all MesoPher preparations. Hereafter CD14<sup>+</sup> monocytes were cultured in T225 flasks (100 million cells per flask) in X-VIVO 15 (Lonza) supplemented with 2% NHS (Sanquin) and adhered overnight on 37°C, 5% CO<sub>2</sub>. The following day half of the medium was refreshed with fresh medium supplemented with 2% NHS, and 1000 IU/ml rhGM-CSF (Miltenyi) and 1600 IU/ml rhIL-4 (Miltenyi) were added. Cells were cultured for 3 additional days at 37°C, 5% CO<sub>2</sub>. On the fifth day of culture, immature unpulsed Mo-DC were harvested and reseeded in 6-wells plates (1 million cells/well) in presence of tumor lysate (tumor cell equivalent to DC ratio 1:3), and supplemented with 800 IU/ml rhGM-CSF, 500 IU/ml rhIL-4 and 10 µg/ml VACMUNE KLH (BioSyn). On day 8 of the culture immature pulsed Mo-DC were matured with 5 ng/ml IL-1B, 15 ng/ml IL-6, 20 ng/ml TNF-alpha (all Miltenyi) and 10 µg/ml PGE-2 (Pfizer). On day 10 of the culture, cells were harvested and had to comply with the following quality demands in order to release the batch: sterile, >80% viability, >90% MHC class II<sup>+</sup> CD11c<sup>+</sup> cells and >80% CD80<sup>+</sup> cells of the MHC class II CD11c<sup>+</sup> cells.

## **RESULTS**

### **Allogeneic and autologous tumor lysate-loaded DCs mediate comparable survival in mesothelioma bearing mice**

To investigate whether allogeneic tumor lysate-loaded DCs were as effective as autologous tumor lysate-loaded DCs in improving survival in mesothelioma bearing mice, we set up an *in vivo* experiment using two different mouse models for mesothelioma, as depicted in figure 1A. Mesothelioma was induced in these mice as described previously [26]. These mouse models are different in both mouse strain and aggressiveness of tumor growth and are chosen to assure robustness of the treatment across different models. In short, BALB/c mice were injected with the syngeneic AB1 cell line and CBA/j mice were injected the syngeneic AC29 mesothelioma cell line. Seven days following tumor inoculation, BALB/c mice and CBA/j mice received either PBS (vehicle), autologous tumor lysate pulsed-DC (AB1 for BALB/c and AC29 for CBA/j), or allogeneic tumor lysate pulsed-DC (AC29 for BALB/c and

AB1 for CBA/j). The survival of these mice is depicted in figure 1B. The results show that DC immunotherapy significantly improved survival in tumor bearing mice of both BALB/c and CBA/j mouse strains compared to PBS treated control mice ( $p < 0.05$ ), with no significant differences in efficacy between autologous lysate-loaded and allogeneic lysate-loaded DC immunotherapy.

### **Allogeneic tumor lysate-loaded DCs induce an anti-tumor T cell response in mesothelioma bearing mice**

To demonstrate the induction of a tumor specific T cell response, splenocytes from surviving CBA/j mice were stimulated with tumor cells. Interferon (IFN)  $\gamma$  production was assessed by intracellular cytokine staining and degranulation was assessed by cell surface expression of CD107. IFN $\gamma^+$  and CD107 $^+$  splenic CD8 T cells were increased upon stimulation with tumor cells in DC treated mice, but not untreated mice. No difference was observed between the autologous lysate and allogeneic lysate treatment (figure 2A and 2B). CD8 T cells from all groups were equally capable of IFN $\gamma$  production and degranulation upon PMA/ionomycin stimulation (not shown). This increased CD8 T cell functionality after DC treatment coincided with increased proportions of effector memory (CD44 $^+$ CD62L $^-$ ) CD8 T cells in treated versus untreated mice, at the expense of naïve T cells (figure 2C). To confirm that the induced T cells in these mice were capable of killing tumor cells, we co-cultured splenic CD8 T cells from DC immunotherapy treated and untreated BALB/c mice with AB1 tumor cells. Tumor cell growth was diminished when co-cultured with CD8 T cells from DC immunotherapy-treated mice compared to untreated mice, which was due to increased apoptosis as shown by increased caspase expression (Supplementary figure S1).

Altogether, these results demonstrate that treatment with DCs pulsed with either autologous or allogeneic tumor lysate induce an effective anti-tumor immune response and improve survival in mesothelioma bearing mice.

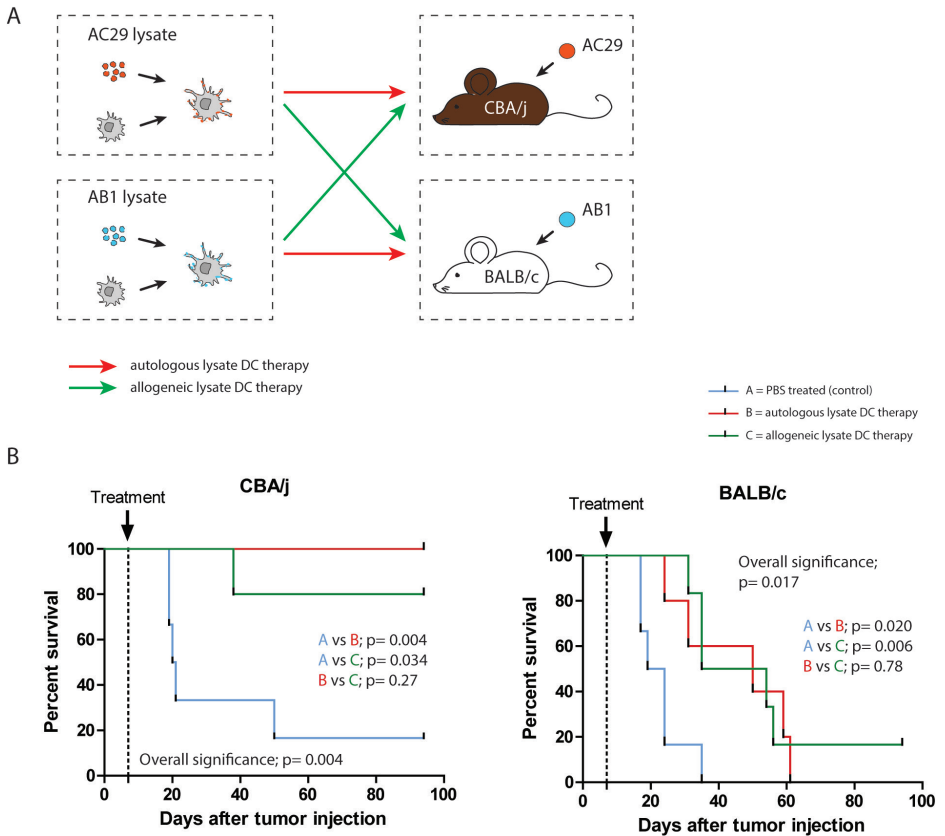


**Figure 1.** Efficacy of allogeneic tumor lysate-pulsed dendritic cell immunotherapy in mesothelioma bearing mice. A) Schematic image of the two mesothelioma mouse models and autologous or allogeneic pulsed dendritic cell immunotherapy. Two different mouse strains were used, CBA/j and BALB/c, inoculated i.p. with their syngeneic mesothelioma cell line (AC29 for CBA/j and AB1 for BALB/c). Syngeneic DCs were cultured from the bone marrow of littermates and pulsed with tumor lysate of either of two tumor cell lines. In the autologous lysate condition, mice were treated with DCs pulsed with the tumor lysate matching their tumor, while in the allogeneic condition, mice were treated with DCs pulsed with the tumor lysate of the allogeneic tumor cell line. B) Survival of mesothelioma bearing mice treated with DC vaccination. 7 days after tumor inoculation, mice were injected i.p. with either PBS (group A, blue), autologous DCs pulsed with autologous tumor cell lysate (group B, red) or autologous DCs pulsed with allogeneic lysate (group C, green). Kaplan Meier curves are shown for the CBA/j mice (top) and BALB/c mice (bottom). Statistical survival difference between the groups was determined using the log-rank test

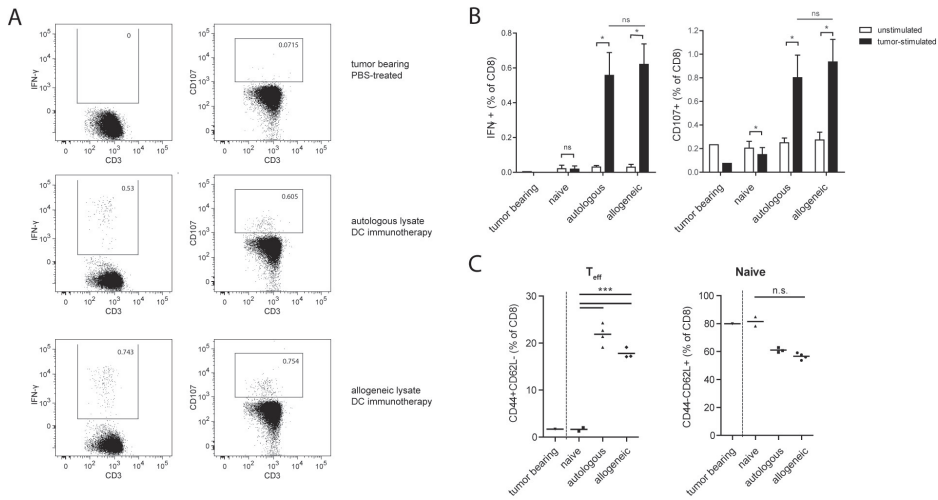


**Figure 2.** DC immunotherapy-induced immunological changes in a murine mesothelioma model. A) Representative flow cytometry plots of IFN $\gamma$  production (left) and CD107 expression (right) in splenic CD8 T cells after co-culture with tumor cells. Splenocytes of surviving CBA/j mice (autologous: n=4, allogeneic: n=3), were isolated when the mice were sacrificed and cultured in the presence of AC29 tumor cells. As controls, both tumor bearing and naïve mice were included (naïve: n=2, tumor-bearing: n=1). B) Quantification of IFN $\gamma$  production (left) and CD107 expression (right) in splenic CD8 T cells, either stimulated with tumor cells or unstimulated. \* = p<0.05 (paired Student's t test for stimulated vs unstimulated, unpaired Student's t test for comparison autologous vs allogeneic treatment) C) Proportions of effector phenotype (CD44<sup>+</sup>CD62L<sup>-</sup>) CD8 T cells (T<sub>eff</sub>, left) and naïve phenotype (CD44<sup>-</sup>CD62L<sup>+</sup>; right) CD8 T cells in splenocytes isolated from treated mice, and tumor bearing and naïve mice as negative controls. \* = p<0.05 (one-way ANOVA).

No dose limiting toxicity was induced by allogeneic tumor lysate pulsed DC immunotherapy in a first-in-human trial targeting mesothelioma

The comparable outcome between autologous lysate-pulsed DC immunotherapy and allogeneic lysate-pulsed DC immunotherapy in our mesothelioma mouse models, led us to initiate a first-in-human phase I clinical trial with allogeneic-lysate pulsed DC immunotherapy (MesoPher). To this end, long-term human mesothelioma cell lines were established from pleural effusion cells isolated from patients with pathologically proven mesothelioma. Lysate of five cell lines was combined to pulse DCs with.

In total, 9 patients were treated according to the predefined treatment schedule between January 2015 and October 2015. Data cut off was in April 2017. Patient characteristics are summarized in table 1. Five patients were treated as maintenance after chemotherapy whilst 4 were treatment naïve. Patients received a vaccination regimen of 3 biweekly vaccinations and a booster vaccination after 3 and 6 months. In 2 out of 9 patients in the highest dose

regimen (patient 7 and 9) no booster vaccination after 6 months could be given due to shortage of DCs to generate 5 vaccinations.

**Table 1.** Patient characteristics

	<b>Patients (N = 9)</b>
Age median (range)	69 (45-79)
<b>Sex</b>	
male	8 (89%)
female	1 (11%)
<b>Histological subtype</b>	
Epithelioid	9 (100%)
Sarcomatoid	0 (0%)
Biphasic	0 (0%)
<b>Stage</b>	
1	0 (0%)
2	1 (11%)
3	5 (56%)
4	3 (33%)
<b>ECOG performance score</b>	
0	7 (78%)
1	2 (22%)
<b>Prior treatment</b>	
Chemotherapy (platinum-based+pemetrexed)	5 (56%)*
Radiotherapy	0 (0%)
Surgery	1 (11%)+
Other	0 (0%)
<b>Response to chemotherapy (if applicable)</b>	
SD	3 (60%)
PR	2 (40%)

\* Chemotherapy consisted of cisplatin or carboplatin, combined with pemetrexed, with a total of 4 (n=4) or 6 (n=1) cycles; † Surgery in this patient consisted of abdominal debulking surgery (this patient had both pleural and abdominal mesothelioma).

Neither predefined dose limiting toxicities nor grade 3 or 4 toxicities were established. A summary of all grade toxicity is presented in table 2, with further specifications of adverse events in table S1. Treatment related adverse events were mild (grade 1 or 2), although present in all patients. These treatment-related adverse events included an induration of the skin related to the intradermal injections in all patients at vaccination 2 and 3 and a grade 1 or 2 fever in all patients after vaccination. This was a transient fever occurring 4-8 hours after vaccination and lasting for maximally 24 hours.

**Table 2:** Toxicities/ adverse events of patients in first-in-human clinical trial

<b>N=9</b>	<b>Any grade, N (%)</b>	<b>Grade 3-4, N (%)</b>
Any AE	9 (100)	0 (0)
Injection site reaction	9 (100)	0 (0)
Fever	9 (100)	0 (0)
Respiratory	6 (67)	0 (0)
Lab abnormalities	8 (89)	0 (0)
Gastrointestinal	1 (11)	0 (0)
Appetite	1 (11)	0 (0)

An immune response was induced in patients after three doses of allogeneic tumor lysate pulsed DC immunotherapy, in which mesothelin-specific T cells could be detected

As readout for a recall response against the vaccine, a DTH skin test was performed 2 weeks after the third vaccination, using a negative control, the lysate only, lysate-pulsed DCs with KLH (MesoPher) lysate-pulsed DCs without KLH. No skin reactions were seen in the negative control or after injection of the lysate only. All 9 patients responded with redness and thickening of the skin 48 hours after injection of MesoPher with KLH. Injection with lysate-pulsed DCs without the adjuvant KLH resulted in a response in 5 out of 9 patients, which all received a dose of at least 25 million DC.

To assess whether in the positive skin reaction, tumor specific T cells could be detected, we isolated T cells from a biopsy of the DTH test skin induration. Mesothelin was chosen as a relevant model-antigen, as all 9 patients in our study had histologically proven mesothelin expression in diagnostic tumor biopsies. Using dextramers against two different mesothelin-epitopes, we assessed reactivity against these epitopes in all HLA-A2 positive patients of which viable T cells were obtained from the skin biopsy. In four out of six evaluable patients, mesothelin-specific T cells could be detected (figure 3). In three of these four patients, T cells against both epitopes were observed, while in one patient (patient 2), T cells against one epitope were detected. These data show that the immune reaction induced by MesoPher contained T cells specific for a relevant tumor-associated antigen, which could be detected in the majority of evaluable patients.



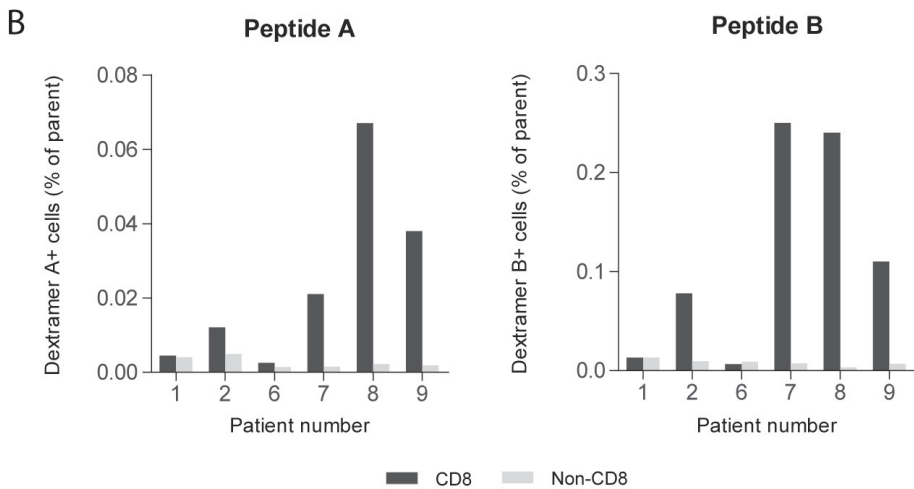
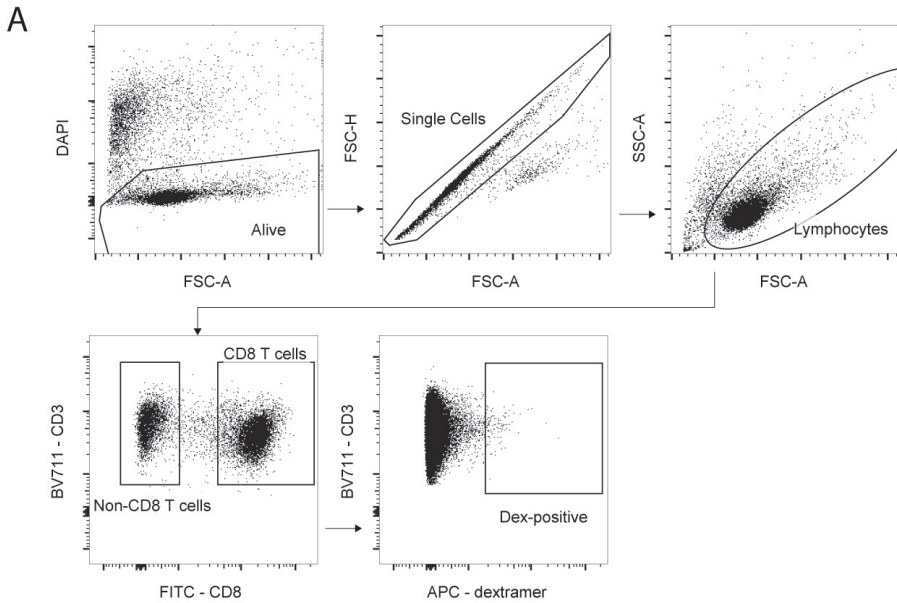


**Figure 3.** Mesothelin-specific CD8 T cells in skin-test infiltrating lymphocytes after injection with allogeneic lysate-pulsed DCs. T cells were isolated from a biopsy of the positive post-treatment DTH test with the vaccine, and expanded in vitro. CD8 T cells specific for two mesothelin-peptides were detected using FCM with peptide-MHC multimers. Results were obtained of all HLA-A2<sup>+</sup> patients of which sufficient T cells could be expanded from the biopsy. A) Gating strategy of dextramer binding CD8 and non-CD8 T cells. B) Quantification of dextramer-binding CD8 T cells. The bars in these graphs represent peptide-MHC binding T cells, as percentage of either CD8 or non-CD8 T cells, whereby the non-CD8 T cells were used as a negative control.

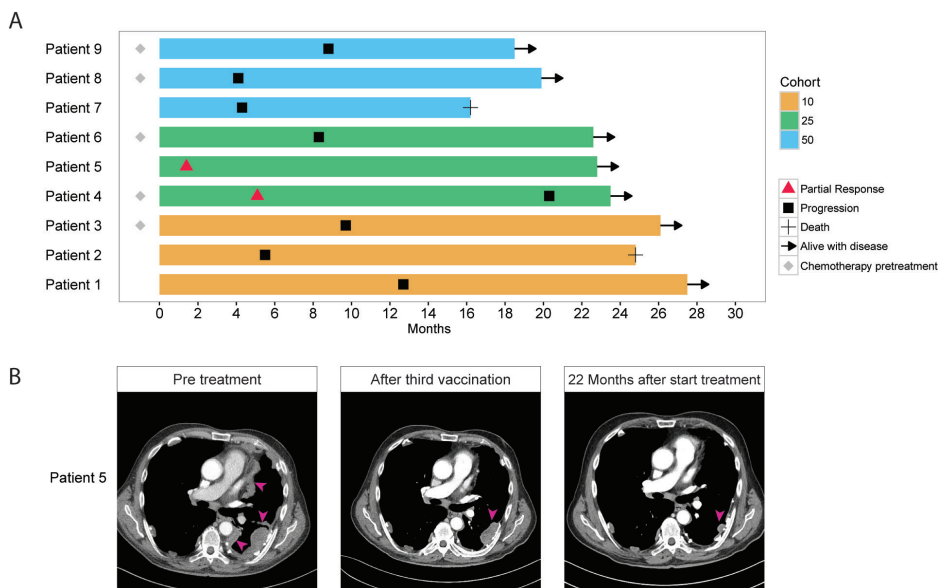


**Figure 4.** Overall survival and RECIST responses after first vaccination. A) Swimmer plot of patients in phase I clinical trial with MesoPher treatment. Overall survival of patients since date of first vaccination is represented by the filled bars. Start and end of RECIST responses are depicted by the red triangles and black squares, respectively. First evaluation of response was after 6 weeks for all patients. Except patient 5 that experienced a partial response, all other patients had stable disease at first evaluation. Patients treated with chemotherapy prior to inclusion in the study are depicted with a grey diamond. The other patients were treatment naïve. B) Pre- and post-vaccination computed tomography (CT) scans of patient 5. CT scans with contrast of the ongoing response of one treatment naïve patient receiving allogeneic lysate-pulsed autologous DC vaccination. Tumor mass is indicated with pink arrows. All lesions were solid. This patient was treatment naïve and received 5 doses of 25 million DCs. Pretreatment tumor burden decreased with 70% after the third vaccination (six weeks after start of treatment) and continued to decrease.

### Radiographic responses and promising overall survival after DC immunotherapy

Response and survival data of all patients are summarized in figure 4A and supplementary figure S2, with now eight of nine patients experiencing progression. In two patients treated both in the 25 million DC cohort, a confirmed partial response was established after the treatment. One patient was pretreated with chemotherapy and one patient treatment naïve. The pretreated patient had a response with a duration of 15 months, while the treatment naïve patient has an ongoing response with a current duration of 21 months. This patient showed a remarkable decrease of total tumor burden of 70% after the third vaccination (Figure 4B and supplementary figure S3). In the other 7 patients, a stable disease was established leading to a disease control rate of 100%. Median overall survival has not been reached, since 7 patients are currently alive after a median follow up of 22.8 months (range,

18.5-27.4 months). Median progression free survival (PFS, defined as time from registration until progression or death, whichever came first) was 8.8 months (95% confidence interval (CI) 4.1-20.3). PFS at 12 months was 33% (95% CI 8%-62%). Treatment beyond progression was started in all but one patient after progression and is described in supplementary table S2. The one patient that did not start treatment beyond progression has a slow progression of the tumor (and not a 30% enlargement from nadir) and is not experiencing clinical deterioration.

## DISCUSSION

We here show that autologous dendritic cell therapy with an allogeneic tumor cell lysate is effective in a murine model of mesothelioma and that a comparable treatment is safe and feasible in patients, with promising clinical activity.

The goal of DC-based immunotherapy is to augment the patient's immune system by means of improving tumor cell recognition by T cells. When using autologous tumor lysate to pulse DCs, a personalized set of antigens is presented to the patients' T cells. Practical limitations in obtaining autologous lysate from patients, led to use of an allogeneic lysate derived from tumor cell lines, which relies on the existence of common tumor antigens that are shared between patients.

In two different murine mesothelioma models, a comparable survival was found between mice receiving allogeneic tumor lysate-pulsed DCs and mice receiving autologous tumor lysate-pulsed DCs. Moreover, our *in vitro* experiments show that in this model a similar functional tumor-specific CD8 T cell response was established, demonstrated by the production of IFN $\gamma$  and degranulation of the CTLs. This indicates that allogeneic tumor lysate is as immunogenic as autologous tumor lysate when used in a DC immunotherapy setting. We cannot rule out the possibility, however, that allogeneic tumor lysate is slightly less effective, since the groups were too small to definitely compare efficacy between the DC treatments with either allogeneic or autologous lysate. Also, unpulsed DC, which are known to have some, but a notably inferior, effect on survival [14], were not included as a separate arm in these experiments. But, most importantly, our findings clearly show efficacy of DC immunotherapy using allogeneic tumor lysate.

The results of our murine experiments led us to initiate a first-in-human clinical trial, which showed that treatment was safe and feasible. The trial was designed as a 3+3 design and no dose limiting or major toxicities were established, even in the highest dose. Two partial

responses were observed in the 25 million cells dose cohort, which indicates that this dose is high enough to induce radiographic responses. Since the yield of monocytes from leukapheresis limited the number of vaccinations that could be given at the 50 million dose cohort, we decided that the dose of 25 million cells was the optimal dose level to be taken forward in further clinical trials. As it was decided to initiate further studies with the 25 million cell dose level, we found it unethical and unnecessary to include further patients in the trial as no additional safety data are to be expected for this dose. In contrast to e.g. targeted therapies where a higher dose is expected to be more effective, since DC immunotherapy relies on the induction of an anti-tumor immune response and expansion of effector cells within the patient, a larger number of DC's is not necessarily needed to induce a stronger immune response [27]. To increase effectivity of DC immunotherapy, it is probably more beneficial to change the microenvironment to facilitate optimal conditions for the expansion and migration of T cells to the tumor. In future studies, it might be of interest to determine effectivity not only by radiographic response, but also by immunological readout, e.g. by monitoring increases in (tumor-specific) CTLs.

Evidence of an immune response induced by vaccination was seen in all patients in the form of a positive response to the DTH skin test after the third vaccination. A DTH response has been shown to correlate with overall survival in a DC vaccination setting in melanoma, although the clinical applicability of this correlation is still largely unclear [28]. At the time of the second or subsequent vaccinations, a similar reaction was observed at the site of intradermal injection. This response did not occur after the first vaccination and thus indicates an induction of a tumor lysate-directed response. Interestingly, in the lowest dose cohort and one of the patients of the second cohort, the DTH response was not present if pulsed DCs without KLH were administered. This finding underlines the importance of an adjuvant to enhance immune activation, especially in lower doses of DC vaccination. On the other hand, the positive skin reaction towards pulsed DCs without the adjuvant KLH in the higher doses proves that this DC vaccination induced a response against the lysate, and not against KLH only. This was also confirmed by the presence of mesothelin-specific T cells in the skin induration. Frequencies of mesothelin-specific T cells in the skin biopsy were very low, which was expected, since the full tumor lysate consists of a broad array of tumor antigens, of which mesothelin was chosen as a relevant candidate. Future studies will have to prove whether assessment of particular tumor antigen-specific T cell responses can be used as a biomarker for clinical responses.

One of the limitations of the study is that in human number of total tumor-specific T cells before and after therapy could not be determined in assays similar to the assays performed in mice, as no viable tumor material was available of the patients. Another limitation of

the study is that this was a selected patient population with only patients who were not progressing after chemotherapy and 4 treatment naïve patients, refusing chemotherapy at that moment.

Although conventional radiographic response criteria may be suboptimal in immunotherapy, as they may not reflect tumor growth optimally [20], we determined objective response rate and progression free survival by modified RECIST criteria [23]. The radiographic partial response in 2 of the 9 patients shows the potency of DC immunotherapy to induce tumor reduction. While in the medical literature, safety of allogeneic lysate pulsed DC immunotherapy has been reported for colorectal cancer [29, 30], melanoma [31, 32], urological cancers [33] and thyroid cancer [34] using doses up to 10 million DC per vaccination, clinical responses in this study are promising compared with previously reported studies. Although none of these studies had efficacy as primary outcome, the reported radiographic responses were stable disease at best in most studies [29, 31, 33-37], with an exception of one complete response in melanoma [32] and one partial response (out of 20) in a MAGE antigen expressing colorectal cancer patient [30].

For melanoma, immunotherapy has been successful over the last decades, which has led to FDA approval of three different checkpoint inhibitors (CTLA4 inhibitor ipilimumab and PD1 inhibitors nivolumab and pembrolizumab) and an oncolytic virus therapy (T-VEC). With the high mutational load of melanoma [38], a broad repertoire of tumor specific T cells can potentially arise [39]. MPM, however, is a poorly immunogenic tumor with a lower mutational burden and lower response rates to e.g. checkpoint inhibitors [5]. The clinical responses, including a 70% tumor reduction at first radiographic assessment in one patient, indicates that that DC immunotherapy is capable to evoke an effective tumor-killing immune response, even in a non-immunogenic tumor type.

In two recent studies in melanoma, vaccination with long synthetic peptides in most cases led to delayed outgrowth of metastases, while the combination with checkpoint inhibitors was very potent to induce partial or complete responses [18, 19]. For mesothelioma, with the potential induction of *de novo* tumor directed immune responses or enhancement of pre-existing responses by DC vaccination, combination therapy of DC vaccination with a checkpoint inhibitor that can reinvigorate this immune response, is anticipated to provide a synergistic effect as well. Indeed, clinical responses towards checkpoint inhibitors were observed in the patients that had received MesoPher previously but ultimately developed disease progression. Out of three patients that received the PD-1 checkpoint inhibitor nivolumab, two showed a partial response and one showed stable disease. Moreover, the use of immunological readouts such as systemic T cell activation, the presence of tumor

antigen-specific T cells or various immune suppressive cells will also aid in determining the best combination approach.

Other immunotherapy approaches are being explored as well for mesothelioma, most of which exploit the tumor-associated antigen mesothelin. These approaches include adoptive T cell transfer with mesothelin-CAR T cells, which might also be given regionally and therefore may overcome a potential T cell homing problem [40]. Other approaches include a chimeric anti-mesothelin antibody involving antibody-dependent cellular cytotoxicity (ADCC) [41] and an immunotoxin-coupled anti-mesothelin antibody approach [42].

The overall survival of patients in this study is promising. However, the number of patients in this trial is too limited to draw firm conclusions. Randomized trials with allogeneic-lysate pulsed dendritic cell immunotherapy in malignant pleural mesothelioma are now warranted to establish efficacy of the current approach. In fact, such a trial is planned to open in 2017.

## **ACKNOWLEDGEMENTS**

The authors would like to thank the department of hematology, the apheresis unit, the pharmacy and the research nurses of the department pulmonary medicine of the Erasmus MC for their support in facilitating the production and delivery of the DC vaccination. The authors also thank dr. Dave Roelen (Leiden University Medical Center) for performing HLA typing of our patients and Jan von der Thüsen (Erasmus MC dept. of Pathology) for the immunostainings of patient biopsies. The human trial was funded by the Dutch Cancer Society (KWF) and ZonMW (grant number 95104006; granted to J. Hegmans) and Amphera b.v. Amphera b.v. is a spin-off company from the Erasmus MC University and had no access to patient related data. All authors had full access to the raw dataset upon request.

## REFERENCES

1. Yap, T.A., et al., *Novel insights into mesothelioma biology and implications for therapy*. Nat Rev Cancer, 2017. **17**(8): p. 475-488.
2. Duff, J. *Verastem Mesothelioma Clinical Trial Stopped Early For Futility*. 2015 [cited 2017 1 May 2017]; Available from: <https://www.mesothelioma.com/news/2015/09/verastem-mesothelioma-clinical-trial-stopped-early-for-futility.htm>.
3. Kindler, H.L., et al. *Tremelimumab as second- or third-line treatment of unresectable malignant mesothelioma (MM): Results from the global, double-blind, placebo-controlled DETERMINE study*. in *J Clin Oncol*. 2016.
4. Zalcman, G., et al., *Bevacizumab for newly diagnosed pleural mesothelioma in the Mesothelioma Avastin Cisplatin Pemetrexed Study (MAPS): a randomised, controlled, open-label, phase 3 trial*. Lancet, 2016. **387**(10026): p. 1405-14.
5. Lievens, L.A., et al., *Checkpoint Blockade in Lung Cancer and Mesothelioma*. Am J Respir Crit Care Med, 2017.
6. Aerts, J.G. and J.P. Hegmans, *Tumor-specific cytotoxic T cells are crucial for efficacy of immunomodulatory antibodies in patients with lung cancer*. Cancer Res, 2013. **73**(8): p. 2381-8.
7. Tumeh, P.C., et al., *PD-1 blockade induces responses by inhibiting adaptive immune resistance*. Nature, 2014. **515**(7528): p. 568-71.
8. Ujiie, H., et al., *The tumoral and stromal immune microenvironment in malignant pleural mesothelioma: A comprehensive analysis reveals prognostic immune markers*. Oncoimmunology, 2015. **4**(6): p. e1009285.
9. Dammeyer, F., et al., *Efficacy of Tumor Vaccines and Cellular Immunotherapies in Non-Small-Cell Lung Cancer: A Systematic Review and Meta-Analysis*. J Clin Oncol, 2016. **34**(26): p. 3204-12.
10. Palucka, K. and J. Banchereau, *Cancer immunotherapy via dendritic cells*. Nat Rev Cancer, 2012. **12**(4): p. 265-77.
11. Steinman, R.M. and M. Dhodapkar, *Active immunization against cancer with dendritic cells: the near future*. Int J Cancer, 2001. **94**(4): p. 459-73.
12. Cornwall, S.M., et al., *Human mesothelioma induces defects in dendritic cell numbers and antigen-processing function which predict survival outcomes*. Oncoimmunology, 2016. **5**(2): p. e1082028.
13. Osada, T., et al., *Dendritic cell-based immunotherapy*. Int Rev Immunol, 2006. **25**(5-6): p. 377-413.
14. Hegmans, J.P., et al., *Immunotherapy of murine malignant mesothelioma using tumor lysate-pulsed dendritic cells*. Am J Respir Crit Care Med, 2005. **171**(10): p. 1168-77.
15. Hegmans, J.P., et al., *Consolidative dendritic cell-based immunotherapy elicits cytotoxicity against malignant mesothelioma*. Am J Respir Crit Care Med, 2010. **181**(12): p. 1383-90.
16. Cornelissen, R., et al., *Extended Tumor Control after Dendritic Cell Vaccination with Low-Dose Cyclophosphamide as Adjuvant Treatment in Patients with Malignant Pleural Mesothelioma*. Am J Respir Crit Care Med, 2016. **193**(9): p. 1023-31.
17. Buonaguro, L., et al., *Translating tumor antigens into cancer vaccines*. Clin Vaccine Immunol, 2011. **18**(1): p. 23-34.
18. Ott, P.A., et al., *An immunogenic personal neoantigen vaccine for patients with melanoma*. Nature, 2017. **547**(7662): p. 217-221.
19. Sahin, U., et al., *Personalized RNA mutanome vaccines mobilize poly-specific therapeutic immunity against cancer*. Nature, 2017. **547**(7662): p. 222-226.
20. Peikert, T. and D.H. Serman, *Harnessing the Power of the Host: Improving Dendritic Cell Vaccines for Malignant Pleural Mesothelioma*. Am J Respir Crit Care Med, 2016. **193**(9): p. 943-5.
21. Lutz, M.B., et al., *An advanced culture method for generating large quantities of highly pure dendritic cells from mouse bone marrow*. J Immunol Methods, 1999. **223**(1): p. 77-92.
22. Veltman, J.D., et al., *Zoledronic acid impairs myeloid differentiation to tumour-associated macrophages in mesothelioma*. Br J Cancer, 2010. **103**(5): p. 629-41.
23. Byrne, M.J. and A.K. Nowak, *Modified RECIST criteria for assessment of response in malignant pleural mesothelioma*. Ann Oncol, 2004. **15**(2): p. 257-60.

24. Adema, G.J., et al., *Migration of dendritic cell based cancer vaccines: in vivo veritas?* *Curr Opin Immunol*, 2005. **17**(2): p. 170-4.
25. Van de Griend, R.J., et al., *Rapid expansion of human cytotoxic T cell clones: growth promotion by a heat-labile serum component and by various types of feeder cells.* *J Immunol Methods*, 1984. **66**(2): p. 285-98.
26. Dammeijer, F., et al., *Depletion of tumor-associated macrophages with a CSF-1R kinase inhibitor enhances antitumor immunity and survival induced by DC immunotherapy.* *Cancer Immunol Res*, 2017.
27. Aarntzen, E.H., et al., *Reducing cell number improves the homing of dendritic cells to lymph nodes upon intradermal vaccination.* *Oncoimmunology*, 2013. **2**(7): p. e24661.
28. Lopez, M.N., et al., *Prolonged survival of dendritic cell-vaccinated melanoma patients correlates with tumor-specific delayed type IV hypersensitivity response and reduction of tumor growth factor beta-expressing T cells.* *J Clin Oncol*, 2009. **27**(6): p. 945-52.
29. Burgdorf, S.K., et al., *Clinical responses in patients with advanced colorectal cancer to a dendritic cell based vaccine.* *Oncol Rep*, 2008. **20**(6): p. 1305-11.
30. Toh, H.C., et al., *Clinical Benefit of Allogeneic Melanoma Cell Lysate-Pulsed Autologous Dendritic Cell Vaccine in MAGE-Positive Colorectal Cancer Patients.* *Clin Cancer Res*, 2009. **15**(24): p. 7726-7736.
31. Trepiakas, R., et al., *Vaccination with autologous dendritic cells pulsed with multiple tumor antigens for treatment of patients with malignant melanoma: results from a phase I/II trial.* *Cytotherapy*, 2010. **12**(6): p. 721-34.
32. Salcedo, M., et al., *Vaccination of melanoma patients using dendritic cells loaded with an allogeneic tumor cell lysate.* *Cancer Immunol Immunother*, 2006. **55**(7): p. 819-29.
33. Pandha, H.S., et al., *Dendritic cell immunotherapy for urological cancers using cryopreserved allogeneic tumour lysate-pulsed cells: a phase I/II study.* *BJU Int*, 2004. **94**(3): p. 412-8.
34. Bachleitner-Hofmann, T., et al., *Pilot trial of autologous dendritic cells loaded with tumor lysate(s) from allogeneic tumor cell lines in patients with metastatic medullary thyroid carcinoma.* *Oncol Rep*, 2009. **21**(6): p. 1585-92.
35. Lee, J.H., et al., *A phase I/IIa study of adjuvant immunotherapy with tumour antigen-pulsed dendritic cells in patients with hepatocellular carcinoma.* *Br J Cancer*, 2015. **113**(12): p. 1666-76.
36. Nestle, F.O., et al., *Vaccination of melanoma patients with peptide- or tumor lysate-pulsed dendritic cells.* *Nat Med*, 1998. **4**(3): p. 328-32.
37. Palucka, A.K., et al., *Dendritic cells loaded with killed allogeneic melanoma cells can induce objective clinical responses and MART-1 specific CD8+ T-cell immunity.* *J Immunother*, 2006. **29**(5): p. 545-57.
38. Alexandrov, L.B., et al., *Signatures of mutational processes in human cancer.* *Nature*, 2013. **500**(7463): p. 415-21.
39. Rizvi, N.A., et al., *Cancer immunology. Mutational landscape determines sensitivity to PD-1 blockade in non-small cell lung cancer.* *Science*, 2015. **348**(6230): p. 124-8.
40. Adusumilli, P.S., et al., *Regional delivery of mesothelin-targeted CAR T cell therapy generates potent and long-lasting CD4-dependent tumor immunity.* *Sci Transl Med*, 2014. **6**(261): p. 261ra151.
41. Hassan, R., et al., *Phase II clinical trial of amatuximab, a chimeric antimesothelin antibody with pemetrexed and cisplatin in advanced unresectable pleural mesothelioma.* *Clin Cancer Res*, 2014. **20**(23): p. 5927-36.
42. Hassan, R., et al., *Major cancer regressions in mesothelioma after treatment with an anti-mesothelin immunotoxin and immune suppression.* *Sci Transl Med*, 2013. **5**(208): p. 208ra147.



## SUPPLEMENTARY DATA

### Supplementary Materials and Methods: Preparation of allogeneic tumor lysate

#### *Mesothelioma tumor cell line establishment*

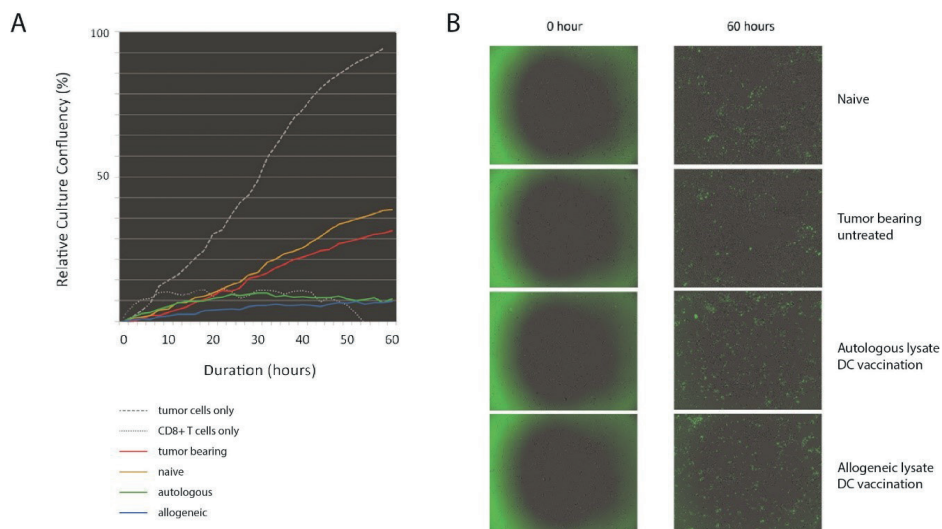
For the production of allogeneic tumor lysate, tumor cell lines were established from pleural effusion cells isolated from different patients with pathologically proven mesothelioma. After signing informed consent, patient pleural effusion was collected under sterile conditions and transported to the cleanroom facility immediately. Pleural fluid was centrifuged (400xg, 15 min, RT) and cells were isolated and cultured in RPMI 1640 + Glutamax (Lonza CAT BE12-702F) supplemented with 10% (v/v) centrifuged pleural effusion supernatant. During the first days of the culture, cells were washed every day to remove non-adherent cells. When culture flasks reached >80% confluency cells were harvested with TrypLe Select (Gibco CAT 12563) and part of the cells were reseeded in new T175 culture flasks. In this way, after several passages, six long-term mesothelioma tumor cell lines were established and patented (Patent ID: P6038325NL).

#### *Production of allogeneic tumor cell lysate*

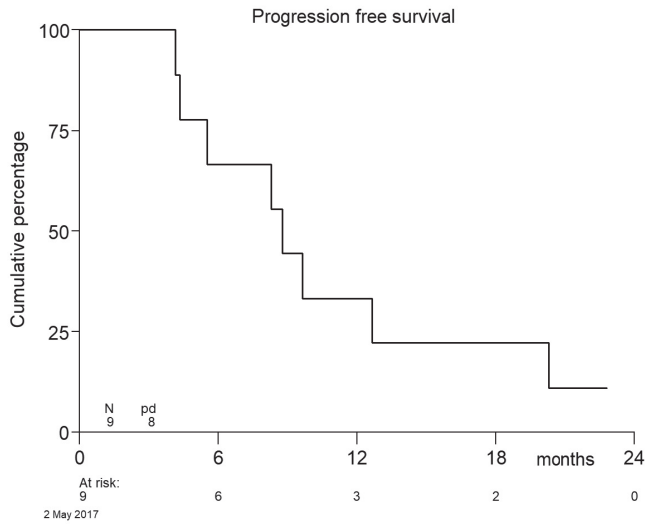
For the production of allogeneic tumor lysate, five of these tumor cell lines were selected based on the diversity in patient (age, sex), clinical (survival, response to therapy) and cellular characteristics of the cell lines (morphology, growth rate). Furthermore, the cell lines met the following criteria: 1) negative results for sterility, mycoplasma and adventitious viruses (Hepatitis B virus [HBV], Hepatitis C virus [HCV], human immunodeficiency virus [HIV type I & II], human T cell lymphotropic virus [HTLV type I&II], and *Treponema pallidum* [syphilis]), 2) diversity of the cell lines in patient-, clinical- and cellular-characteristics (age and sex of the donor, medical history, treatment response, progression-free survival, overall survival, and histological subtype) and 3) guarantee for long term culture. For the production of the lysate, tumor cell lines were cultured in RPMI 1640 + Glutamax (Lonza CAT BE12-702F) supplemented with 2% Normal Human Serum (NHS, Sanquin), upscaled and batches of tumor cells (serial subcultures) were frozen at <-70°C during every harvest procedure (50 million cells/ml). After compliance with the QC assays performed on these serial subcultures (namely Sterility assays [Negative], STR profiling analysis [no difference in short tandem repeats throughout the culture] and volume determination [less than 10% deviation from the theoretical value]), these were pooled per cell line to form five intermediate products. After compliance with the QC assay (Sterility [Negative]), these were pooled to form one large master batch. The large master batch was freeze thawed for 5 cycles and gamma irradiated with 100 Gy to establish the tumor cell lysate. To ensure complete cell lysis QC assays were performed: 1) Colony formation during cell culture (1 ml of tumor cell lysate was placed into culture for 14 days, no colony formation was detected) and 2) Flow cytometric

cell analysis using DCFDA for alive cells and DAPI for dead cells (no alive cells were detected). After compliance of these QC assays, the tumor lysate was aliquoted into cryovials each containing 1,05 ml (52,5 million tumor cell equivalents [TCE]/1,05 ml).

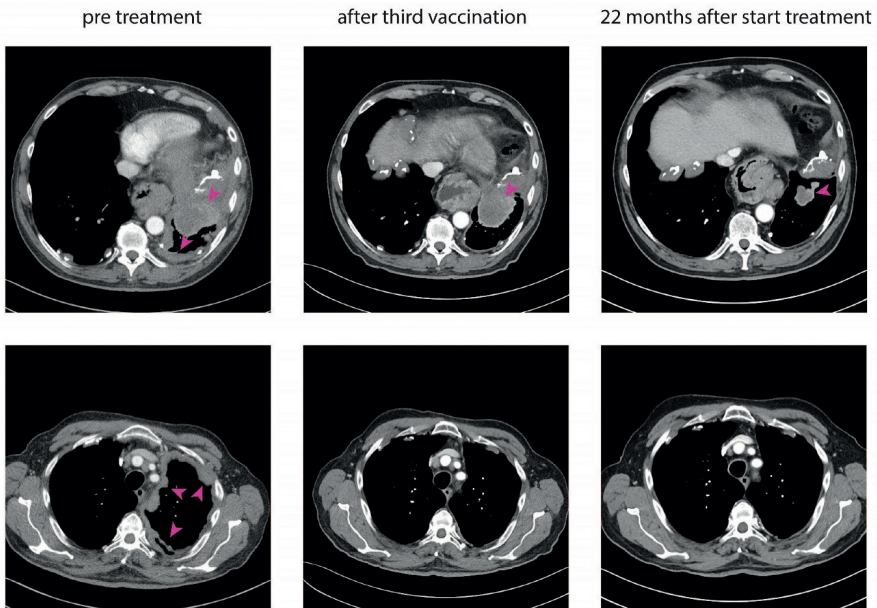
## Supplementary figures and tables



**Supplementary Figure S1.** CD8 T cells from DC immunotherapy treated mice show tumor cell killing capacity. A) AC29 tumor cell growth co-cultured with magnetic activated cell sorted (MACS) splenic CD8 T cells of DC immunotherapy treated and untreated mice. Cells were grown and confluency was measured by an IncuCyte® cell count proliferation assay B) Caspase staining (green) at start and at end (60 hours) of co-culture visualized with fluorescence microscopy in an IncuCyte® apoptosis assay.



**Supplementary Figure S2.** Progression free survival of patients in the first-in-human clinical study. Progression free survival (PFS, defined as time from registration until progression or death, whichever came first) of all nine patients included in the first-in-human trial.



**Supplementary Figure S3:** Pre- and post-vaccination computed tomography (CT) scans of patient 5 at two different heights. CT scans with contrast illustrating ongoing response of patient 5, as in figure 3, at two different heights (upper panels and lower panels). Tumor mass is indicated with pink arrows. This patient was treatment naïve and received 5 doses of 25 million DCs. Pretreatment tumor burden decreased with 70% after the third vaccination (six weeks after start of treatment) and continued to decrease.

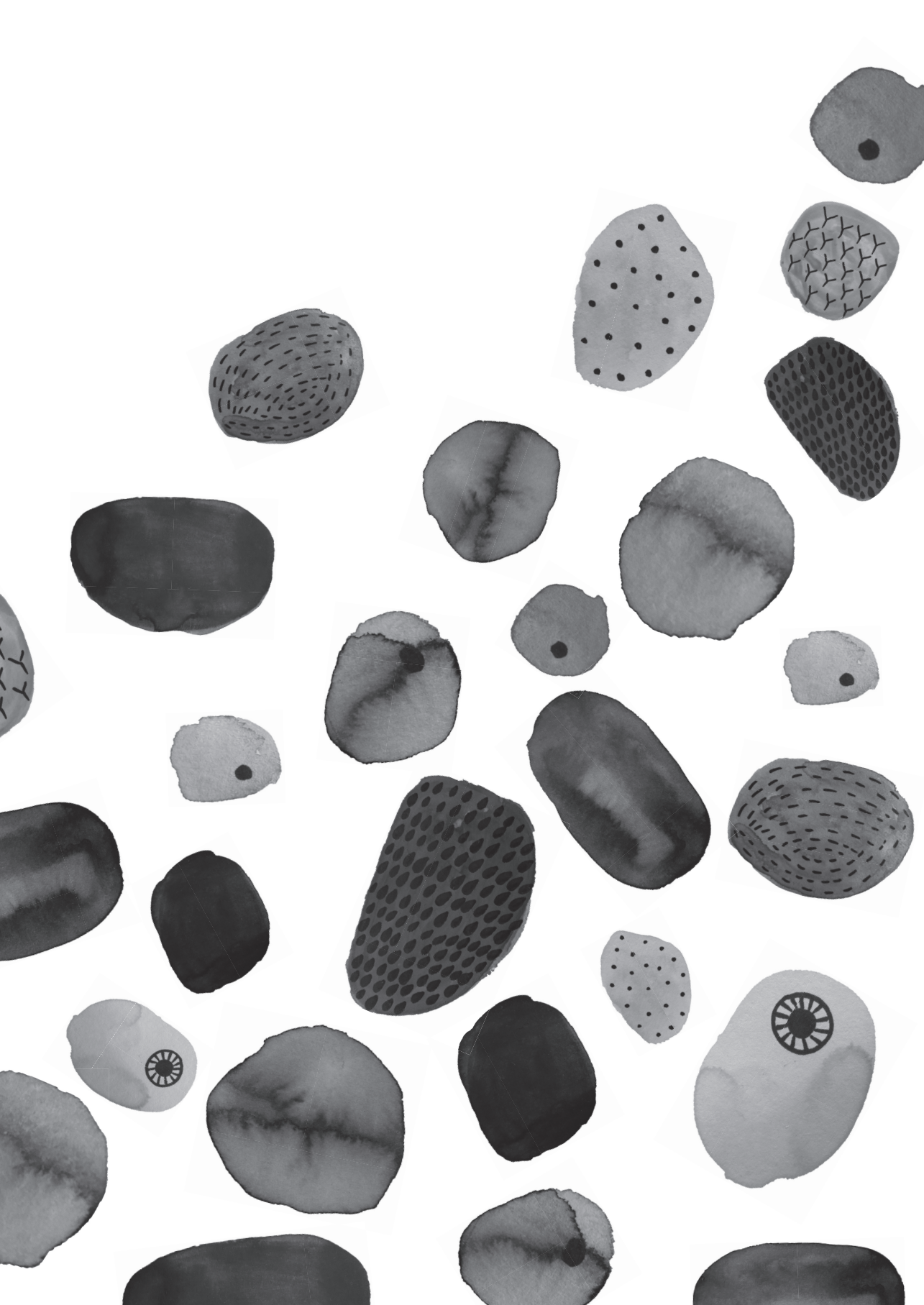
**Supplementary table S1:** specification of all observed grade 1 and 2 respiratory, gastrointestinal and lab abnormalities

<b>N=9</b>	<b>Grade 1 (N)</b>	<b>Grade 2 (N)</b>
Respiratory (n=6)	Cough (4) Dyspnea (3)	
Lab abnormalities (n=8)	Anemia (5) Aspartate aminotransferase increase (3) CPK increase (2) Blood bilirubin increase (2) Alanine aminotransferase increase (1) Alkaline phosphatase increase (1) ANA titer increase (1) LDH increase (1) Creatinine increase (1) Hypernatremia (1) Eosinophil increase (1)	Alanine aminotransferase increase (1) White blood cell count decrease (1)
Gastrointestinal (n=1)	Diarrhea (1)	

**Supplementary table S2:** additional treatment after progression

<b>Patient</b>	<b>Follow up treatment</b>	<b>Best Response</b>
MCV001	none	
MCV002	cisplatin - pemetrexed	SD
MCV003	dendritic cell booster	PD
MCV004	pembrolizumab	not yet evaluated
MCV005	none	
MCV006	nivolumab	SD
MCV007	cisplatin - pemetrexed	PR
MCV008	nivolumab	PR
MCV009	nivolumab	PR





# CHAPTER

# 7

## **AUTOLOGOUS DENDRITIC CELL THERAPY IN MESOTHELIOMA PATIENTS ENHANCES FREQUENCIES OF PERIPHERAL CD4 T CELLS EXPRESSING HLA-DR, PD-1 OR ICOS**

Pauline L. de Goeje†, Yarne Klaver †, Margaretha E.H. Kaijen-Lambers, Anton W. Langerak, Heleen Vroman, André Kunert, Cor H. Lamers, Joachim G.J.V. Aerts, Reno Debets\*, Rudi W. Hendriks\*

† Contributed equally as first authors

\* Contributed equally as senior authors

*Published in:*

*Front Immunol. 2018 Sep 7;9:2034. doi: 10.3389/fimmu.2018.02034. eCollection 2018.*

## ABSTRACT

**Introduction:** Malignant pleural mesothelioma (MPM) is a malignancy with a very poor prognosis for which new treatment options are urgently needed. We have previously shown that dendritic cell (DC) immunotherapy provides a clinically feasible treatment option. In the current study, we set out to assess the immunological changes induced by DC immunotherapy in peripheral blood of MPM patients.

**Methods:** Peripheral blood was collected from nine patients enrolled in a phase I dose escalation study, before and after treatment with DCs that were pulsed with an allogeneic tumor lysate preparation consisting of a mixture of five cultured mesothelioma cell lines. We used immune profiling by multiplex flow cytometry to characterize different populations of immune cells. In particular, we determined frequencies of T cell subsets that showed single and combinatorial expression of multiple markers that signify T cell activation, maturation and inhibition. Therapy-induced T cell reactivity was assessed in peptide/MHC multimer stainings using mesothelin as a prototypic target antigen with confirmed expression in the clinical tumor lysate preparation. T cell receptor (TCR) diversity was evaluated by *TCRB* gene PCR assays.

**Results:** We observed an increase in the numbers of B cells, CD4 and CD8 T cells, but not NK cells at 6 weeks post treatment. The increases in B and T lymphocytes were not accompanied by major changes in T cell reactivity towards mesothelin nor in *TCRB* diversity. Notably, we did observe enhanced proportions of CD4 T cells expressing HLA-DR, PD-1 (at 2 weeks after onset of treatment) and ICOS (6 weeks) and a CD8 T cell population expressing LAG3 (2 weeks).

**Discussion:** DC immunotherapy using allogeneic tumor lysate resulted in enhanced frequencies of B cells and T cells in blood. We did not detect a skewed antigen-reactivity of peripheral CD8 T cells. Interestingly, frequencies of CD4 T cells expressing activation markers and PD-1 were increased. These findings indicate a systemic activation of the adaptive immune response and may guide future immune monitoring studies of DC therapies.



## INTRODUCTION

Malignant pleural mesothelioma (MPM) is a solid tumor of the pleural lining that is strongly related to the exposure to asbestos [1]. Overall survival is poor with a median survival of less than a year, and conventional therapies like chemotherapy and radiotherapy being able to improve survival only by a few months [2]. Immunotherapy has evolved as an important new treatment modality in various kinds of cancer, with checkpoint inhibitors currently being FDA approved as first line therapy for several cancer types. Initial results of clinical studies for MPM with checkpoint inhibitors as second line treatment showed response rates of 9-25% [3].

MPM is characterized by a strong immunosuppressive component, with relatively low numbers of T cells infiltrating the tumor [1, 4]. These low numbers of tumor-infiltrating T cells have prognostic value in MPM [5] and might explain the relatively low response rates to checkpoint inhibitors [1].

Furthermore, in MPM patients dendritic cells (DCs) have been shown to be reduced in numbers and in antigen-processing function compared to healthy controls, which negatively affected survival outcomes [6]. The reduced functionality of DCs is thought to relate to low intra-tumoral T cell numbers. Along these lines, DC vaccination represents a promising therapeutic strategy.

Previously, we have developed a cellular therapy for MPM, consisting of autologous DCs pulsed with autologous tumor lysate with the intention to cover a broad range of tumor antigens [7]. This vaccination strategy was shown to be safe with promising clinical outcomes [7, 8]. However, the availability and quality of tumor material that could be obtained, limited the feasibility of the treatment with DCs loaded with autologous tumor lysate. To overcome this limitation, DC vaccination using allogeneic tumor lysate was developed and tested for safety and feasibility in a phase I clinical trial [9]. Allogeneic tumor lysate derived from five *in vitro* cultured clinical-grade human mesothelioma cell lines was used to pulse autologous DCs and the resulting DC vaccine was administered to patients i.d. and i.v. once every two weeks for three cycles, with a booster vaccination at three and six months after the start of treatment. The study was set up as a dose escalation study with three cohorts of three patients, and each cohort received 10 million, 25 million or 50 million DCs per vaccination, respectively. By circumventing the immunosuppressive tumor immune environment and providing enhanced tumor antigen presentation with DC vaccination, impressive objective responses could be obtained, as exemplified by a tumor reduction of ~70% at 6 weeks post-treatment in one of the patients in this phase-I trial [9].

In the current study we aimed to characterize the immunological changes induced by DC immunotherapy in these nine MPM patients. For a better understanding of the immunological changes induced by DC immunotherapy we monitored peripheral blood, which is the preferred compartment for sequential sampling. We used extensive multiplex flow cytometry with a focus on T cell activation and inhibitory markers and characterized T cell specificity using peptide-MHC multimers to obtain a detailed immune profile and immune dynamics following DC immunotherapy.

## METHODS

### Patients

The nine patients in this study participated in a first-in-human clinical trial as described by Aerts et al [9]. In short, all patients had pathologically-proven MPM and were included in the study at least 6 weeks after their last chemotherapy treatment, or were treatment-naïve if they had refused chemotherapy treatment. After inclusion in the study, patients received leukapheresis, which was used as a source of autologous DCs.

The DCs were prepared as described [9] and pulsed with a lysate, consisting of a mixture of five *in vitro* cultured mesothelioma cell lines. Patients received a total of 3 vaccinations every two weeks and blood samples were obtained at baseline and at week 2, 4, 6 and 8 following initial vaccination. Booster vaccinations were administered at 3 and 6 months [9]. One third of the dose was administered intradermally (i.d.), and two thirds of the dose intravenously (i.v.). As this was a dose escalation study, patients 1-3 received 10 million DCs per vaccination, patients 4-6 received 25 million DCs per vaccination and patients 7-9 received 50 million DCs per vaccination. Patients 7 and 9 did not receive their second booster vaccination due to shortage of patient material. All other patients completed the full treatment scheme (Table S1 in Supplementary Material). For flow cytometry (FCM) analysis, cohort 1 was not included since the collected peripheral blood samples of patients in cohort 1 were immediately processed and stored. For cohort 2 and 3 the protocol was amended to enable absolute immune cell quantification.

### Collection and processing of peripheral blood samples

Ethylene diamine tetra acetic acid (EDTA) anticoagulated peripheral blood was drawn from patients at baseline prior to the first vaccination (week 0), at 2 weeks after the first vaccination, i.e., prior to the second vaccination (week 2) and 2 weeks after the third vaccination at week 6 and analyzed within 6 hours by multiplex FCM. One ml of whole blood was used for multiplex FCM and from the remaining blood, peripheral blood mononuclear

cells (PBMCs) were isolated by standard Ficoll density gradient centrifugation and were stored at -80 °C for further analyses.

### **Multiplex flow cytometric assessment of numbers and phenotype of immune cells**

To enumerate immune cell populations, whole blood (100µl) was stained with the 'absolute numbers' panel (Table S2 in Supplementary Material) and incubated for 15 min at room temperature. Subsequently, 2 ml of lysis buffer (NH<sub>4</sub>Cl: 8,26 mg/ml, KHCO<sub>3</sub>: 1 mg/ml and EDTA: 37µg/ml) was added to the blood and incubated for 15 min at room temperature. Subsequently 100µl of Flow-Count Fluorospheres (Beckman Coulter Inc) was added and samples were measured on a BD LSRFortessa™ flow cytometer. A minimum of 10,000 CD45+ cells were measured to enable clear distinction of defined immune cell populations. Subsequently, data was analyzed with FlowJo version X (FlowJo, LCC) using the gating strategy as exemplified in Figure S1 in Supplementary Material. Values were expressed as cells per microliter. To determine the phenotype of T cells, the T cell maturation, activation, co-inhibitory and co-stimulatory receptors were analyzed on whole blood with different FCM panels (Table S2 in Supplementary Material). 100µl of whole blood was stained with each of the panels and incubated for 15 minutes at room temperature. Subsequently, 2 ml of lysis buffer was added to the blood and after an incubation of 15 minutes at room temperature, the cell suspensions were centrifuged at 450g for 5 minutes, washed and resuspended in buffered 0.1% paraformaldehyde (PFA). A minimum of 30.000 CD3+ cells were measured on the LSRFortessa™ flow cytometer to obtain clearly detectable immune populations. The FCM data were analyzed with FlowJo version X.

### **Determination of mesothelin-specific T cells**

PBMCs were thawed and subsequently T cells were rapidly expanded with a feeder system as described elsewhere [10]. After this rapid expansion protocol, T cells were co-cultured with artificial antigen presenting cells (aAPC) [11] loaded with mesothelin peptide A: SLLFLFLSL (mesothelin<sub>20-28</sub>), or mesothelin peptide B: VLPLTVAEV (mesothelin<sub>531-539</sub>) (Immudex, Copenhagen, Denmark). The aAPC cell line is based on K562 cells, retrovirally transduced with CD80, CD83, and HLA-A2 for optimal antigen presentation and co-stimulation, and enables enrichment of antigen-reactive T cells with protocols optimized in our laboratory [12]. 2.5 x 10<sup>6</sup> aAPC cells/ml were incubated at room temperature for five hours with 10µg/ml peptide and subsequently irradiated (120 Gy). Subsequently, these peptide-loaded aAPC cells were co-cultured with T cells (ratio 1:20) in T cell medium (RPMI Hepes [Lonza] supplemented with 10% human serum [Sanquin, Amsterdam, The Netherlands], 1% L-glutamine and 1% penicillin/streptomycin), 180 IU IL-2 per ml (Chiron, Amsterdam, The Netherlands), and 5 ng IL-15 per ml (Le-Perray-en-Yvelines, France). Mesothelin-driven T cell

expansion was continued for 4 cycles, after which T cells were examined for their binding ability to corresponding mesothelin peptide-HLA-A2 complex multimers. In this study, we performed a maximum of 4 peptide-specific expansion cycles.

Dextramer A: PE-conjugated HLA-A2 dextramer with peptide SLLFLLFSL (mesothelin<sub>20-28</sub>) and dextramer B: APC-conjugated HLA-A2 dextramer with peptide VLPLTVAEV (mesothelin<sub>531-539</sub>) were both ordered from Immudex (Copenhagen, Denmark). Dextramer staining was performed according to manufacturer's protocol. Anti-CD3-BV711 (clone UCHT1) and anti-CD8-FITC (clone SK1) mAbs (both from BD Biosciences) were used together with dextramers for extracellular staining. 4',6-diamidino-2-phenylindole (DAPI) was used as viability dye. Samples were measured on an LSR-II flow cytometer (BD). Fluorescence-minus-one (FMO) controls were used to enable gating and determine dextramer-positive populations.

### **GeneScan T cell clonality analysis**

Cell pellets from PBMC samples were frozen and stored until further use. Genomic DNA was isolated using the AllPrep DNA / RNA Mini kit (QIAGEN, Hilden, Germany) according to manufacturer's instructions. T-cell receptor (TCR) b gene repertoire was measured using commercially available multiplex TCR V $\beta$ -J $\beta$  PCR assays (Invivoscribe, San Diego, CA, USA) as developed and approved by the BIOMED-2 / EuroClonality consortium [13]. GeneScan fragment analysis was done on an ABI 3130 xl instrument (ThermoFisher Scientific) and data were analyzed using PeakScanner software. Data interpretation was based on GeneScan patterns of duplicate PCR results, largely following the EuroClonality guideline [14].

### **DC – PBMC co-cultures**

Mature lysate-pulsed DC (as were used for the DC immunotherapy) were co-cultured with PBMC samples of the same patient. For each patient PBMC samples from week 0, week 2 and week 7 were co-cultured with DCs in a 96-wells plate in a 1:10 ratio, in RPMI supplemented with 10% normal human serum (duplicate cultures). After 24 hours, the supernatant was collected for enzyme-linked immunosorbent assay (ELISA) to determine IFN $\gamma$  (Invitrogen) and the cells were harvested for flow cytometry. For flow cytometric analysis, the cells were stained with the following antibodies: anti-CD3-APC-eF780 and anti-CD8-AlexaFluor700 (eBiosciences), anti-CD4-BV785, anti-CD56-PE-Cy7 and anti-CD69-FITC (BD Biosciences) and anti-CD137-PE (Biolegend).

### **Statistical analyses**

Statistical analyses and graphs were made with GraphPad Prism v5.0. For comparison of changes from baseline measurements, Wilcoxon signed-ranks test was used to test for significance between baseline measurements and other time points. The heatmap was made

in R for windows version 3.4.1 using the package in “gplots” (<https://cran.r-project.org/web/packages/gplots/>). Clustering was performed with a complete agglomeration method, and distance matrix of all variables was computed with Euclidean distance.

## RESULTS

### Numbers of B, CD4 and CD8 T lymphocytes in peripheral blood increase upon vaccination with DCs

We first assessed the absolute numbers of specific lymphocyte subsets ( $CD3^+CD4^+$ ,  $CD3^+CD8^+$ ,  $CD3^-CD19^+$  and  $CD3^-CD56^+$ ) from the six patients treated in the second and third cohort (dosage 25 million and 50 million DC per vaccination), using the gating strategy as shown in Figure S1 in Supplementary Material. Patients showed a significant increase at week 6 (after 3 vaccinations) compared to baseline in (median) numbers of  $CD4^+$  T cells (increase from 522 to 634 cells/ $\mu$ l),  $CD8^+$  T cells (from 256 to 304 cells/ $\mu$ l) and B cells (from 162 to 199 cells/ $\mu$ l), but not Natural Killer (NK) cells (Figure 1). Together, these results are indicative for a potentiation of adaptive immunity in peripheral blood after DC immunotherapy.

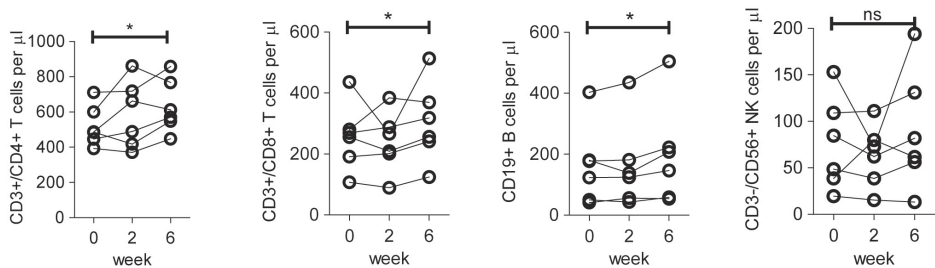


**Figure 1.** Absolute number of lymphocyte subsets in peripheral blood of patients before and after DC immunotherapy. Quantification of absolute numbers of  $CD4^+$  T cells ( $CD45^+/CD3^+/CD4^+$ ),  $CD8^+$  T cells ( $CD45^+/CD3^+/CD8^+$ ), B cells ( $CD45^+/CD3^-/CD19^+$ ), and NK cells ( $CD45^+/CD3^-/CD56^+$ ) in peripheral blood of patients in cohort 2 and 3 on baseline prior to the first vaccination (week 0), 2 weeks after the first vaccination, i.e., prior to the second vaccination (week 2) and 2 weeks after the third vaccination (week 6). Differences between week 0 and week 6 with respect to paired continuous parameters were determined using the exact Wilcoxon signed rank test. \*  $p < 0.05$ ; ns: not significant.

### Lysate-specific and mesothelin-specific T cells are detectable in peripheral blood of mesothelioma patients

Next, we investigated whether the increased numbers of T cells due to DC vaccination harbored vaccine-specific  $CD8^+$  T cells. For three patients, lysate-pulsed DCs were available after completion of the treatment schedule. Co-cultures of PBMC before and after treatment with these lysate-pulsed DC showed an increase in  $CD69$ -positive  $CD4^+$  and  $CD8^+$  T cells,

CD137-positive CD4<sup>+</sup> and CD8<sup>+</sup> T cells, and IFN $\gamma$  secretion after therapy, supporting the induction of a vaccine-specific response (Figure S2 in the Supplementary Material).

To further identify vaccine-specific CD8 T cells in all patients we selected mesothelin as a prototypic antigen based on the following lines of evidence. Firstly, RNA sequencing and western blot data obtained from the mesothelioma cell lines used to generate the lysate preparation validated mesothelin mRNA and protein expression. Secondly, immune histochemistry confirmed the expression of mesothelin in eight out of eight available patient biopsies. Lastly, mesothelin peptide/HLA-A2 complexes with reported immune reactivity [15, 16], (peptide A: SLLFLLFSL and peptide B: VLPLTVAEV) were bound by CD8 T cells derived from patient skin biopsies after challenge with DC vaccine [9], as summarized in Table S2 in Supplementary Material. To determine whether DC therapy would induce changes in the frequency of mesothelin-specific CD8 T cells, we measured the binding of two mesothelin-peptide/HLA-A2 multimers by CD8 T cells in pre- versus post-vaccination peripheral blood samples. To this end, T cell fractions were first propagated using four T cell culture cycles in the presence of mesothelin peptides (A and B). Figures 2A and 2B show flow cytometry plots for one of the two mesothelin epitopes (peptide B) in propagated CD8 T cell fractions from HLA-A2-positive patients (8 out of 9 patients). These analyses show that the frequency of mesothelin-specific CD8 T cells is variable among patients, and already pre-exists in 5 out of 8 HLA-A2 positive patients and does not change significantly upon treatment. Similar data were obtained for a second mesothelin epitope (peptide A; Figure S3 in Supplementary Material) and no correlation was observed between the frequencies of CD8 T cells specific for the two epitopes analyzed (data not shown).

In addition, we studied TCRB diversity of total T cells as a global measure of T cell reactivity via GeneScan TCRB PCR (Figure 2C). While some patients showed dominant peaks (e.g. patient 9), the GeneScan patterns were generally similar in pre-treatment and post-treatment PBMC fractions from the MPM patients, indicating that DC therapy did not induce clonal T cell expansion or selection. Collectively, these findings show that DC vaccination-specific T cells are detectable, but that this is not accompanied by an overall enhancement of frequencies in peripheral blood, nor obvious shifts in T cell TCRB repertoire.

### **Increased frequencies of PD-1, HLA-DR and ICOS positive CD4<sup>+</sup> T cells after DC vaccination.**

We then evaluated changes in frequencies of CD4 or CD8 T cells expressing surface activation, maturation or co-signaling markers and compiled a heatmap of all variables measured by FCM at pre- and post-therapy time points (Figure 3). Hierarchical clustering of samples showed clustering of the different time points per patient for the measured

variables. This demonstrates that intra-individual differences over time are relatively small, compared to inter-individual differences in the immunological variables that were measured.

To further explore immunological parameters that were modulated by DC immunotherapy, we assessed the expression of the various surface markers at multiple time points. Figure 4A-D display the expression of T cell activation, co-inhibitory and co-stimulatory markers that were significantly altered either early after the start of treatment (two weeks after the first vaccination) or later during treatment (two weeks after the third vaccination). In particular, CD4<sup>+</sup> T cells in peripheral blood showed a significant gain of HLA-DR<sup>+</sup> and PD-1<sup>+</sup> T cells (Figure 4A, B) after the first vaccination. After 3 vaccinations, we detected a significant increase of CD278 (inducible T-cell co-stimulator; ICOS) positive CD4<sup>+</sup> T cells compared to baseline (Figure 4D). CD8 T cells did not show any significant increase of these markers, although CD8<sup>+</sup> T cells demonstrated a significant enrichment of CD223<sup>+</sup> (Lymphocyte activation gene-3; LAG-3) T cells (Figure 4C). No significant changes were observed in the following markers on both CD4<sup>+</sup> and CD8<sup>+</sup> T cells: CD25, CD69, CD272 (BTLA), CD137 (4-1BB), CD154 (CD40L), CD134 (OX40); (Figure S4 in Supplementary Material).

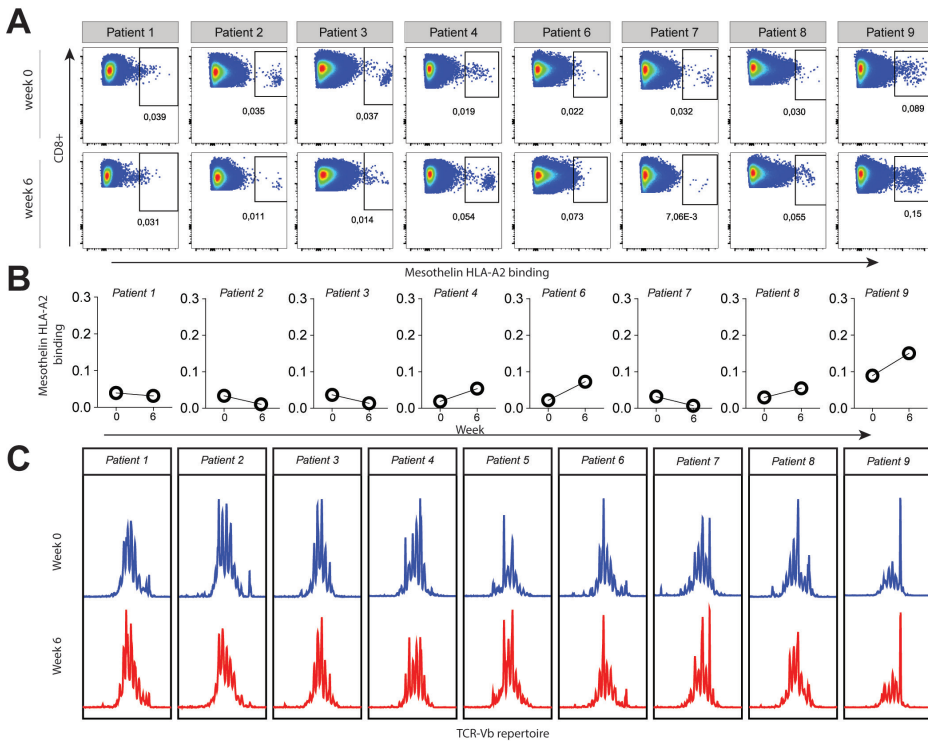


**Figure 2.** Mesothelin-specific CD8 T cells in HLA-A2 positive patients are measurable in pre- and post-vaccination samples. A) Peripheral blood samples were collected at baseline (week 0) and 2 weeks after the third vaccination (week 6). CD8 T cells were propagated in four culture cycles with mesothelin-peptide-B loaded aAPC, after which mesothelin-peptide B/HLA-A2 dextramers were used to detect mesothelin-specific CD8 T cells. Gating was based on the negative controls, FMO staining and the non-CD8 T cell population. All HLA-A2 positive patients are shown; patient 5 was excluded (haplotype HLA-A3/HLA-A68). B) Values of gated dextramer-binding CD8 T cells - as shown in panel A - presented as proportions of total CD8 T cells. C) Relative frequencies of complementarity determining region-3 (CDR3) lengths in pre- and post-therapy total T cells from PBMC samples of all patients. The Y-axis represents relative frequency as assessed by fluorescence intensity, with the various CDR3 lengths on the X-axis. A polyclonal repertoire would follow a normal distribution.

In summary, these findings show that following autologous DC therapy in mesothelioma patients the frequencies of circulating CD4 T cells expressing HLA-DR, PD-1 or ICOS, as well as CD8 T cells expressing the co-inhibitory receptor LAG3 are significantly increased.



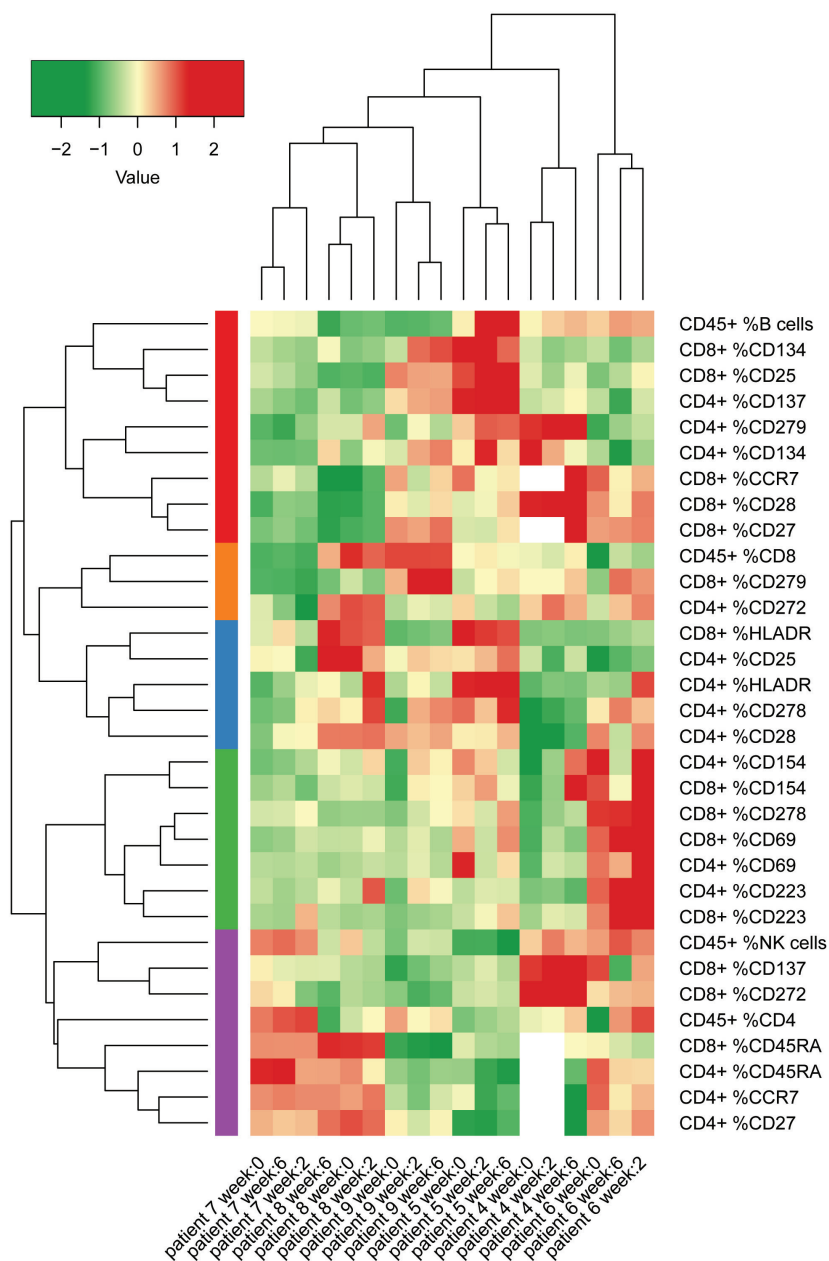


**Figure 3.** Heatmap of percentages of several different lymphocyte subsets and T cell surface markers in peripheral blood from patients in cohort 2 and 3 (MCV004 – MCV009). Columns represent different patient samples at week 0, week 2 and week 6 after start of treatment. Rows represent the proportions of CD4 T cell, CD8 T cell and CD45 lymphocyte populations that express defined markers. Two of the co-inhibitory molecules in our panel, CTLA-4 and TIM 3 were expressed at too low frequencies to yield reliable values. Therefore, we removed these markers from further analysis. Percentages were normalized according to mean values of all measurements and were clustered by non-hierarchical clustering.

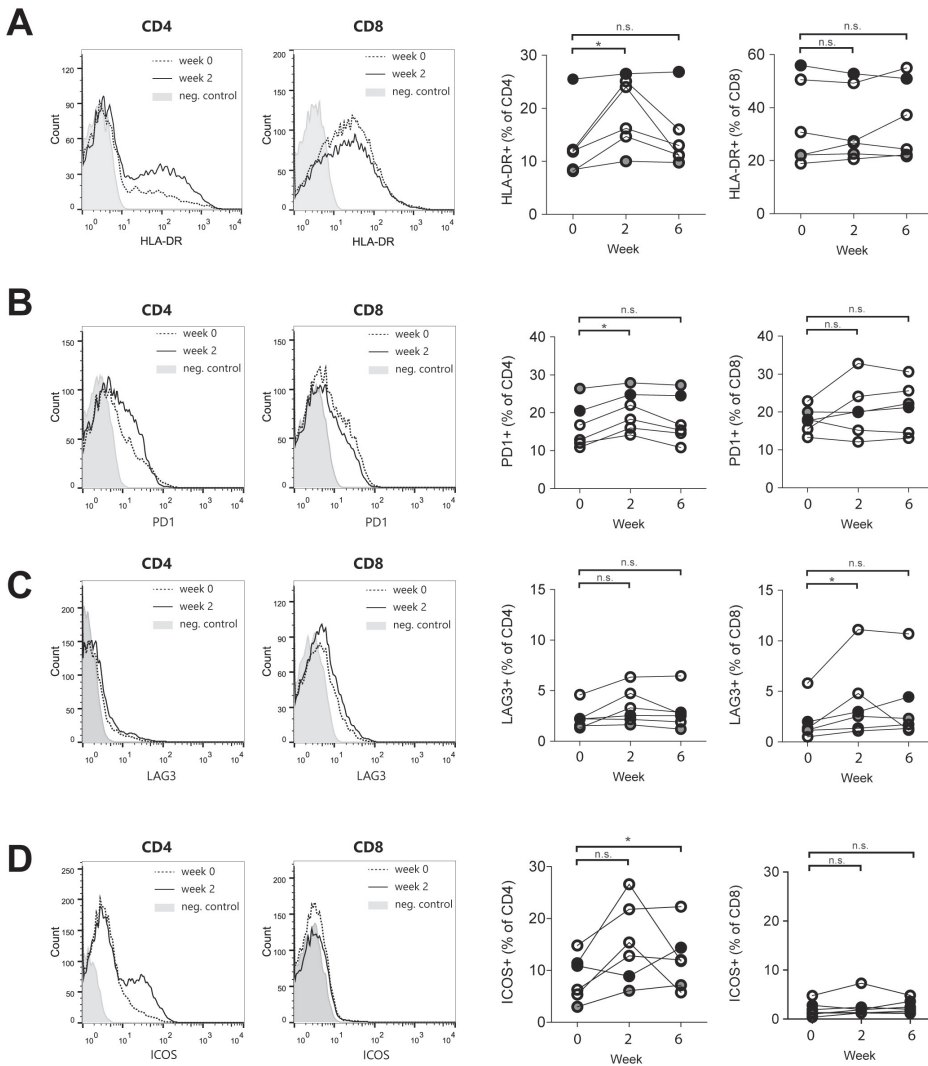


**Figure 4.** T cell activation and co-stimulatory molecule expression changes induced by DC immunotherapy. Representative histograms of flow cytometry data (left) and quantification for patients 4 to 9 at week 0, week 2 and week 6 after start of treatment (right). A) Proportions of HLA-DR-positive CD4 and CD8 T cells. B) Proportions of PD-1-positive CD4 and CD8 T cells. C) Proportions of LAG-3-positive CD4 and CD8 T cells and D) Proportions of ICOS-positive CD4 and CD8 T cells. \*  $p < 0.05$  - Wilcoxon paired signed-rank test, n.s. = not significant.

## DISCUSSION

Here we document on the effects of treatment of MPM patients with DC immunotherapy – autologous dendritic cells loaded with an allogeneic tumor lysate prepared from five human MPM cell lines – on blood immune composition. The clinical outcomes of this first-in-human clinical trial have been published previously, and showed feasibility of the therapy, as well as promising clinical responses [9].

We used flow cytometry to analyze peripheral blood and observed an increase in absolute numbers of B cells, and CD4<sup>+</sup> and CD8<sup>+</sup> T cells, suggesting induction of both a cellular and humoral immune response. Additionally, we found a significant increase of HLA-DR, PD-1, and ICOS-positive CD4<sup>+</sup> T cells, and an increase of LAG3-positive CD8<sup>+</sup> T cells after treatment with DC vaccination therapy.

As previously shown, a vaccine-induced delayed-type hyperreactivity skin response was observed in all patients after treatment [9]. Here, we confirmed that vaccine-reactive T cells were induced in the peripheral blood in three patients (two of whom receiving the lowest dose of ten million DCs). The DC immunotherapy was designed to induce a broad immune response towards multiple tumor antigens present in the tumor cell lysates. Nevertheless, for monitoring purposes that are independent of the availability of tumor material or pulsed DCs we analyzed mesothelin-specific T cells in peripheral blood during treatment. Since mesothelin was determined to be present in the tumor lysate, and expressed on the tumor cells of the patients, it was regarded to be a relevant antigen in this setting. Interestingly, after mesothelin-derived peptide-driven *in vitro* T cell propagation, CD8<sup>+</sup> T cells that bind mesothelin peptide/HLA-A2 complexes could already be detected in baseline blood samples of the majority of patients, suggesting that a mesothelin-specific immune response was already present in these patients prior to therapy. However, DC vaccination did not induce changes in frequencies of the mesothelin-specific T cells in peripheral blood. Additionally, as a measure of T cell clonality, we analyzed the TCRB CDR3 length in pre- and post-treatment blood samples, which indicated that no major repertoire shifts occurred.

Both the skin responses against the vaccine in all patients after therapy, and the confirmation of these result by *in vitro* experiments in three patients, show that a vaccine-specific T cell response is induced. Furthermore, the increase in CD4<sup>+</sup> and CD8<sup>+</sup> T cells at week 6, in absence of a change of detectable dominant T cell clones (by TCRB CDR3 length analyses) in peripheral blood suggest that these T cell responses are of a polyclonal nature. Indeed, it has been reported that DC immunotherapy broadens, rather than skews the diversity of the T cell repertoire. In melanoma patients, not only the number of neoantigen-specific

T cells increased, but also the number of clonotypes per antigen increased, indicating a further diversification of the repertoire [17].

In contrast, in studies employing vaccination with DCs pulsed with specific peptides, dominant T cell clone expansions were observed in peripheral blood [18, 19]. Increases in the frequency of tumor-specific T cells were determined by IFN- $\gamma$  ELISPOT [18] or HLA-A2 MHC multimers [19]. The use of specific peptides to pulse DCs in these studies likely resulted in a more easily detectable clonal expansion of T cells, as compared to our strategy using complete tumor cell lysate. In one study monitoring T cells specific for a single antigen after DC vaccination using allogeneic tumor lysate increased frequencies of MART-1-specific CD8<sup>+</sup> T cells were found after treatment in 3 out of 21 patients. In line with our findings, detectable numbers of these T cells were already present at baseline in 2 out of these 3 patients [20]. Furthermore, as the T cells activation and the co-culture experiment showed the highest response two weeks at the start of treatment, we might have missed detectable changes in peripheral blood that took place before week six. In conclusion, monitoring TCR-specificity against a single tumor-antigen (mesothelin) may support the presence of tumor-specific responses, but does not provide information on the repertoire of the tumor-specific T cell response.

Whereas a vaccine-specific response was reported to be induced in all nine patients in our clinical study [9], it remains unknown whether this response was also reactive against the autologous tumor. In previous studies with DC vaccination in mesothelioma using autologous tumor material, we found significantly increased cytotoxicity against the tumor after treatment, showing induction of a tumor-specific response by DC immunotherapy [7]. In the current study, no tumor material was collected for ethical reasons, but we anticipate a comparable induction of a tumor-specific immune response based on the clinical outcomes in our patient cohort. Two partial responses were reported after DC immunotherapy, of which one remarkable response of 70% tumor reduction in a treatment-naïve patient within six weeks which lasted for two years [9].

As shown here and by others, monitoring of specific T cells in peripheral blood upon immunotherapy with a broad antigen repertoire, is challenging due to the unknown antigen composition and low frequency of individual T cell clones, and requires either very immunogenic antigens like NY-ESO-1 or MART-1 [21, 22] or *in vitro* enrichment steps, which makes it less attractive for future use in clinical practice. The current study did not address whether changes occurred in T cell reactivity in the local compartment. However, removal of tumor can be harmful in MPM due to a substantial risk of local tumor outgrowth at the intervention site [23], precluding the analysis of local tumor material for monitoring

purposes. Next to T cell specificity, we investigated T cell phenotype, using extended multiplex flow cytometry. We demonstrated that treatment-related differences were most notable for CD4<sup>+</sup> T cells, with an increase in surface expression of ICOS, PD-1 and HLA-DR after treatment. This signifies T cell activation, because T cells upregulate HLA-DR [24], ICOS [25] and PD-1 [26] after (TCR) stimulation.

Interestingly, both HLA-DR<sup>+</sup> CD4 T cells and ICOS<sup>+</sup> CD4 T cells have been described to increase after treatment with ipilimumab (anti-CTLA-4 monoclonal antibody) [27]. Moreover, an increase of ICOS<sup>+</sup> CD4 T cells is suggested as a possible pharmacodynamic biomarker for response to this checkpoint inhibitor [28-30]. Notably, the best responding patient (#5) in our study showed the highest numbers of HLA-DR<sup>+</sup> CD4<sup>+</sup> and ICOS<sup>+</sup> CD4<sup>+</sup> T cells. Our flow cytometry panels did not allow analysis of co-expression of ICOS and HLA-DR. Others have demonstrated that ICOS<sup>+</sup> T cells also expressed CD45RO [25], indicating that T cells bearing high levels of ICOS may be in an advanced maturation phase. This would be in concordance with the low proportions of CCR7 and CD27-positive T cells in our patient (#5), which are markers of less matured T cells. In the current study patient numbers are too low to correlate the immune monitoring data with clinical outcome. Yet, our findings suggest that the ICOS<sup>+</sup> CD4<sup>+</sup> T cell subset may have value in the immune monitoring of future trials with DC immunotherapy. Furthermore, Fan and colleagues have described a functional role for ICOS in the anti-tumor immune response [31], providing a rationale for the combination of DC immunotherapy and engagement of ICOS-signaling in future treatments.

In conclusion, vaccination with a broad spectrum of antigens (as is the case with the allogeneic lysate used in the current study) in MPM patients, induced an increase in T cell and B cell numbers in peripheral blood. No evidence was found for a mono- or oligo-clonal T cell expansion, thus suggesting broad activation of the T lymphocytes after therapy. Additionally, changes in the frequencies of defined immune cell markers, in particular the increase of T cell activation markers in CD4<sup>+</sup> T cells, demonstrated treatment-associated changes that we would propose as parameters to be included in the monitoring of DC vaccination treatments. Future studies with larger patient groups should evaluate their relation with treatment efficacy.

## REFERENCES

1. Yap, T.A., et al., *Novel insights into mesothelioma biology and implications for therapy*. Nat Rev Cancer, 2017. **17**(8): p. 475-488.
2. Damhuis, R.A., et al., *Treatment patterns and survival analysis in 9014 patients with malignant pleural mesothelioma from Belgium, the Netherlands and England*. Lung Cancer, 2015. **89**(2): p. 212-7.
3. Lieveense, L.A., et al., *Checkpoint Blockade in Lung Cancer and Mesothelioma*. Am J Respir Crit Care Med, 2017.
4. Coussens, L.M., L. Zitvogel, and A.K. Palucka, *Neutralizing tumor-promoting chronic inflammation: a magic bullet?* Science, 2013. **339**(6117): p. 286-91.
5. Ujiie, H., et al., *The tumoral and stromal immune microenvironment in malignant pleural mesothelioma: A comprehensive analysis reveals prognostic immune markers*. Oncoimmunology, 2015. **4**(6): p. e1009285.
6. Cornwall, S.M., et al., *Human mesothelioma induces defects in dendritic cell numbers and antigen-processing function which predict survival outcomes*. Oncoimmunology, 2016. **5**(2): p. e1082028.
7. Hegmans, J.P., et al., *Consolidative dendritic cell-based immunotherapy elicits cytotoxicity against malignant mesothelioma*. Am J Respir Crit Care Med, 2010. **181**(12): p. 1383-90.
8. Cornelissen, R., et al., *Extended Tumor Control after Dendritic Cell Vaccination with Low-Dose Cyclophosphamide as Adjuvant Treatment in Patients with Malignant Pleural Mesothelioma*. Am J Respir Crit Care Med, 2016. **193**(9): p. 1023-31.
9. Aerts, J.G., et al., *Autologous dendritic cells pulsed with allogeneic tumor cell lysate in mesothelioma: From mouse to human*. Clin Cancer Res, 2017.
10. Van de Griend, R.J., et al., *Rapid expansion of human cytotoxic T cell clones: growth promotion by a heat-labile serum component and by various types of feeder cells*. J Immunol Methods, 1984. **66**(2): p. 285-98.
11. Butler, M.O., et al., *A panel of human cell-based artificial APC enables the expansion of long-lived antigen-specific CD4+ T cells restricted by prevalent HLA-DR alleles*. Int Immunol, 2010. **22**(11): p. 863-73.
12. Lamers, C.H., et al., *CD4+ T-cell alloreactivity toward mismatched HLA class II alleles early after double umbilical cord blood transplantation*. Blood, 2016. **128**(17): p. 2165-2174.
13. van Dongen, J.J., et al., *Design and standardization of PCR primers and protocols for detection of clonal immunoglobulin and T-cell receptor gene recombinations in suspect lymphoproliferations: report of the BIOMED-2 Concerted Action BMH4-CT98-3936*. Leukemia, 2003. **17**(12): p. 2257-317.
14. Langerak, A.W., et al., *EuroClonality/BIOMED-2 guidelines for interpretation and reporting of Ig/TCR clonality testing in suspected lymphoproliferations*. Leukemia, 2012. **26**(10): p. 2159-71.
15. Thomas, A.M., et al., *Mesothelin-specific CD8(+) T cell responses provide evidence of in vivo cross-priming by antigen-presenting cells in vaccinated pancreatic cancer patients*. J Exp Med, 2004. **200**(3): p. 297-306.
16. Laheru, D., et al., *Allogeneic granulocyte macrophage colony-stimulating factor-secreting tumor immunotherapy alone or in sequence with cyclophosphamide for metastatic pancreatic cancer: a pilot study of safety, feasibility, and immune activation*. Clin Cancer Res, 2008. **14**(5): p. 1455-63.
17. Carreno, B.M., et al., *Cancer immunotherapy. A dendritic cell vaccine increases the breadth and diversity of melanoma neoantigen-specific T cells*. Science, 2015. **348**(6236): p. 803-8.
18. Lee, J.H., et al., *A phase I/IIa study of adjuvant immunotherapy with tumour antigen-pulsed dendritic cells in patients with hepatocellular carcinoma*. Br J Cancer, 2015. **113**(12): p. 1666-76.
19. Trepikas, R., et al., *Vaccination with autologous dendritic cells pulsed with multiple tumor antigens for treatment of patients with malignant melanoma: results from a phase I/II trial*. Cytotherapy, 2010. **12**(6): p. 721-34.
20. Palucka, A.K., et al., *Dendritic cells loaded with killed allogeneic melanoma cells can induce objective clinical responses and MART-1 specific CD8+ T-cell immunity*. J Immunother, 2006. **29**(5): p. 545-57.

21. Grnjatic, S., et al., *NY-ESO-1: review of an immunogenic tumor antigen*. Adv Cancer Res, 2006. **95**: p. 1-30.
22. Kawakami, Y., et al., *Identification of the immunodominant peptides of the MART-1 human melanoma antigen recognized by the majority of HLA-A2-restricted tumor infiltrating lymphocytes*. J Exp Med, 1994. **180**(1): p. 347-52.
23. Agarwal, P.P., et al., *Pleural mesothelioma: sensitivity and incidence of needle track seeding after image-guided biopsy versus surgical biopsy*. Radiology, 2006. **241**(2): p. 589-94.
24. Arva, E. and B. Andersson, *Kinetics of cytokine release and expression of lymphocyte cell-surface activation markers after in vitro stimulation of human peripheral blood mononuclear cells with Streptococcus pneumoniae*. Scand J Immunol, 1999. **49**(3): p. 237-43.
25. Hutloff, A., et al., *ICOS is an inducible T-cell co-stimulator structurally and functionally related to CD28*. Nature, 1999. **397**(6716): p. 263-266.
26. Xing, K., et al., *Dexamethasone enhances programmed cell death 1 (PD-1) expression during T cell activation: an insight into the optimum application of glucocorticoids in anti-cancer therapy*. BMC Immunol, 2015. **16**: p. 39.
27. Weber, J.S., et al., *Ipilimumab increases activated T cells and enhances humoral immunity in patients with advanced melanoma*. J Immunother, 2012. **35**(1): p. 89-97.
28. Tang, D.N., et al., *Increased frequency of ICOS(+) CD4 T-cells as a pharmacodynamic biomarker for anti-CTLA-4 therapy*. Cancer immunology research, 2013. **1**(4): p. 229-234.
29. Chen, H., et al., *Anti-CTLA-4 therapy results in higher CD4+ICOShi T cell frequency and IFN-gamma levels in both nonmalignant and malignant prostate tissues*. Proc Natl Acad Sci U S A, 2009. **106**(8): p. 2729-34.
30. Vonderheide, R.H., et al., *Tremelimumab in combination with exemestane in patients with advanced breast cancer and treatment-associated modulation of inducible costimulator expression on patient T cells*. Clin Cancer Res, 2010. **16**(13): p. 3485-94.
31. Fan, X., et al., *Engagement of the ICOS pathway markedly enhances efficacy of CTLA-4 blockade in cancer immunotherapy*. J Exp Med, 2014. **211**(4): p. 715-25.

## SUPPLEMENTARY DATA

**Table S1:** Patient characteristics\*

Patient	Pretreatment (chemo)	DC dose (per vaccination)	Number of vaccinations	Best response (RECIST)	HLA haplotype	Msln expression diagnostic biopsy#	Skin responses to DCK, DC and lys †			Presence Msln-specific T cells in skin biopsy ‡	
							DCK	DC	lys	Msln peptide A	Msln peptide B
1	No	10 million	5	SD	A1/A2	++	+	-	-	-	-
2	No	10 million	5	SD	A2/A68	++	+	+	+	+	+
3	Yes	10 million	5	SD	A2/A2	++	+	-	-	-	-
4	Yes	25 million	5	PR	A1/A2	++	+	-	-	ND	ND
5	No	25 million	5	PR	A3/A68	++	+	+	-	ND	ND
6	Yes	25 million	5	SD	A1/A2	++	+	+	-	-	-
7	No	50 million	4	SD	A2/A24	ND	+	+	-	+	+
8	Yes	50 million	5	SD	A2/A24	++	+	+	-	+	+
9	Yes	50 million	4	SD	A2/A32	+	+	+	-	+	+

\* Patient characteristics are further detailed Aerts et al (2017)

Abbreviations: DCK, DC's pulsed with lysate and keyhole limpet hemocyanin (KLH); DC, DC's pulsed with lysate only; lys, tumor lysate; Msln, mesothelin; ND, not determined; SD, stable disease; PR, partial response.

# ++ = >75% positive tumor cells; + = 25-75% positive tumor cells;

† positive (+) if induration > 2 mm 48 hours after injection.

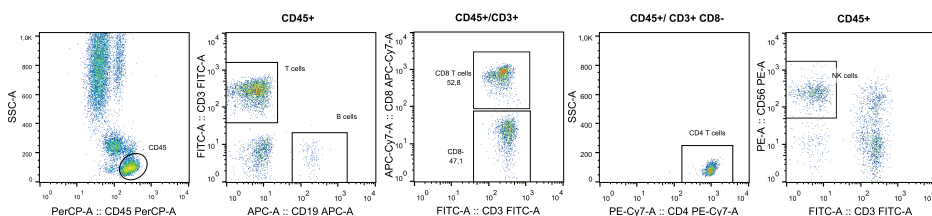
‡ positive (+) when dextramer-binding CD8 T cell frequency  $\geq 2x$  negative controls



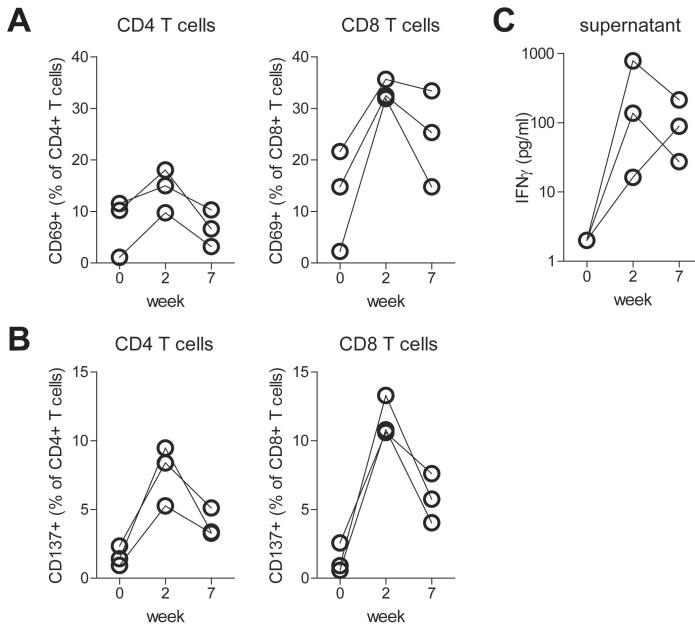
**Table S2:** List of antibodies used for multiplex flow cytometry

MARKER	LABEL	SUPPLIER	CAT.NO	CLONE	PANEL*
<b>CD3</b>	FITC	BD Biosciences	345764	SK7	1
<b>CD3</b>	Pacific Blue	BD Biosciences	558117	UCHT1	2,3,4,5
<b>CD4</b>	PE-Cy7	BD Biosciences	348809	SK3	1
<b>CD4</b>	BV510	BD Biosciences	560769	RPA-T4	2,3,4,5
<b>CD8</b>	APC-Cy7	BD Biosciences	348813	SK1	1
<b>CD8</b>	PerCP	BD Biosciences	345774	SK1	2,3,4,5
<b>CD19</b>	APC	eBioscience	17-0199-42	HIB19	1
<b>CD25</b>	APC	BD Biosciences	340907	2A3	3
<b>CD27</b>	APC-Cy7	BD Biosciences	560222	M-T271	2
<b>CD28</b>	APC	BD Biosciences	559770	CD28.2	2
<b>CD45</b>	PerCP	BD Biosciences	345809	2D1	1
<b>CD45RA</b>	PE-Cy7	BD Biosciences	337186	L48	2
<b>CD56</b>	PE	Dako	R7251	C5,9	1
<b>CD57</b>	FITC	BD Biosciences	333169	HNK-1	2
<b>CD69</b>	PE-Cy7	BD Biosciences	335792	L78	3
<b>CD127</b>	PE	BD Biosciences	557938	hIL-7R-M21	3
<b>CD134 (OX40)</b>	FITC	eBioscience	11-1347-42	ACT35 (ACT-35)	5
<b>CD137 (4-1BB)</b>	PE	eBioscience	12-1379-42	4B4 (4B4-1)	5
<b>CD152 (CTLA-4)</b>	APC	BD Biosciences	555855	BNi3	4
<b>CD154 (CD40L)</b>	APC-Cy7	Biolegend	310822	24-31	5
<b>CD223 (LAG3)</b>	PE-Cy7	eBioscience	25-2239-42	3DS223H	4
<b>CD272 (BTLA)</b>	PE	Biolegend	344506	MIH26	4
<b>CD278 (ICOS)</b>	PE-Cy7	eBioscience	25-9948-42	ISA-3	5
<b>CD279 (PD-1)</b>	APC-Cy7	Biolegend	329922	EH12.2H7	4
<b>CD366 (TIM-3)</b>	FITC	eBioscience	11-3109-42	F38-2E2	4
<b>CCR7</b>	PE	R&D	FAB197P	150503	2
<b>HLA-DR</b>	APC-Cy7	BD Biosciences	335831	L243	3
<b>TCRγδ</b>	FITC	BD Biosciences	347903	11F2	1

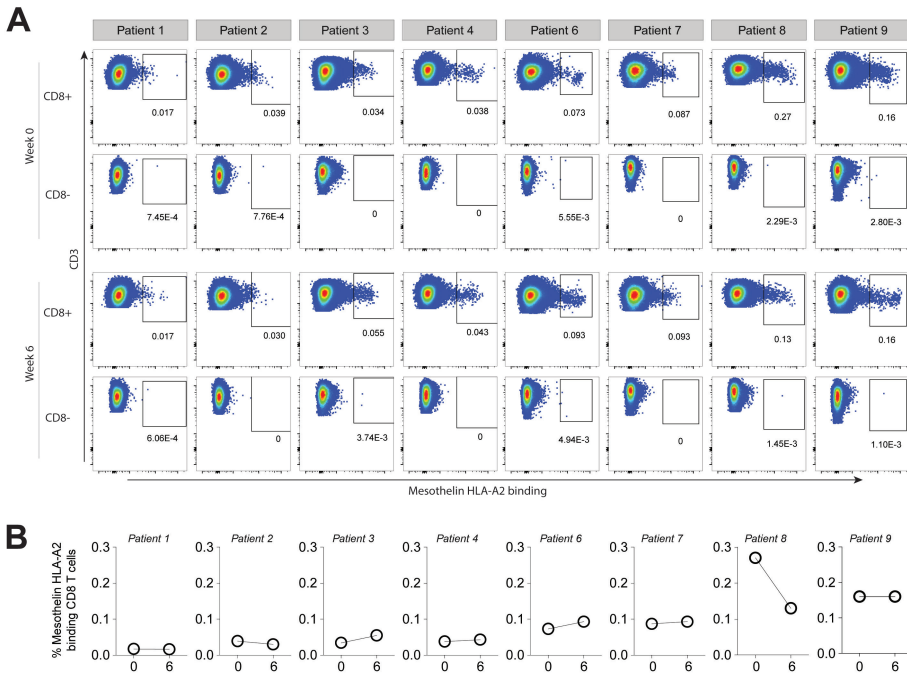
\*Panel 1: Absolute numbers, Panel 2: Maturation, Panel 3: Activation/Tregs, Panel 4: Co-inhibitory markers, Panel 5: Co-stimulatory markers



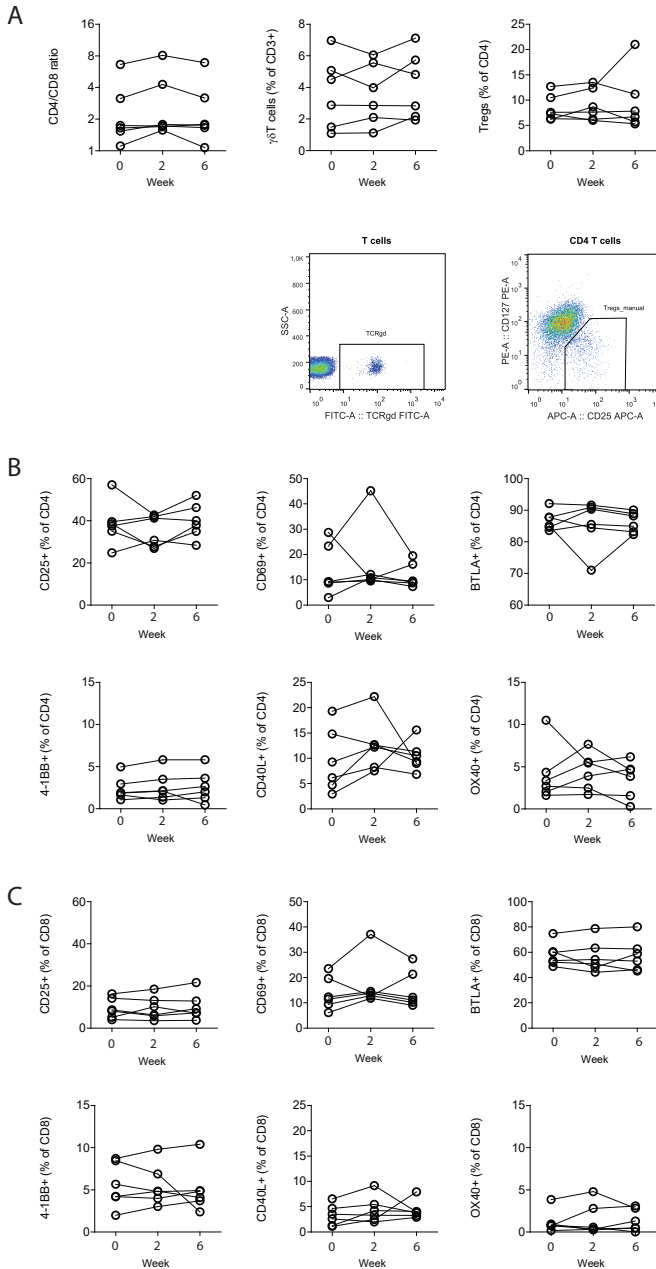
**Supplementary figure S1:** Example of gating strategy preceding the enumeration of immune cell populations. Lymphocytes were defined as CD45<sup>+</sup>, SSC-A<sup>low</sup> (plot1); from CD45<sup>+</sup>, SSC-A<sup>low</sup> lymphocytes, T cells (CD3<sup>+</sup>CD19<sup>-</sup>) and B cells (CD19<sup>+</sup>CD3<sup>-</sup>) were defined (plot 2). T cells were further subdivided in CD8<sup>+</sup> T cells, and CD4<sup>+</sup> T cells (plot3 and 4). Within the CD45<sup>+</sup>, SSC-A<sup>low</sup> lymphocytes, NK cells were defined as CD56<sup>+</sup>CD3<sup>-</sup> (plot 5).



**Supplementary figure S2:** Activation of post-therapy T cells after co-culture with lysate-pulsed DCs. Lysate-pulsed DCs were co-cultured for 24h with autologous PBMC obtained at week 0, 2 or 7. A) Proportions of CD4 and CD8 T cells expressing CD69, as determined by flow cytometry. B) Proportions of CD4 and CD8 T cells expressing CD137, as determined by flow cytometry. C) Concentration of IFN $\gamma$  in the culture supernatant after 24h, as determined by ELISA.

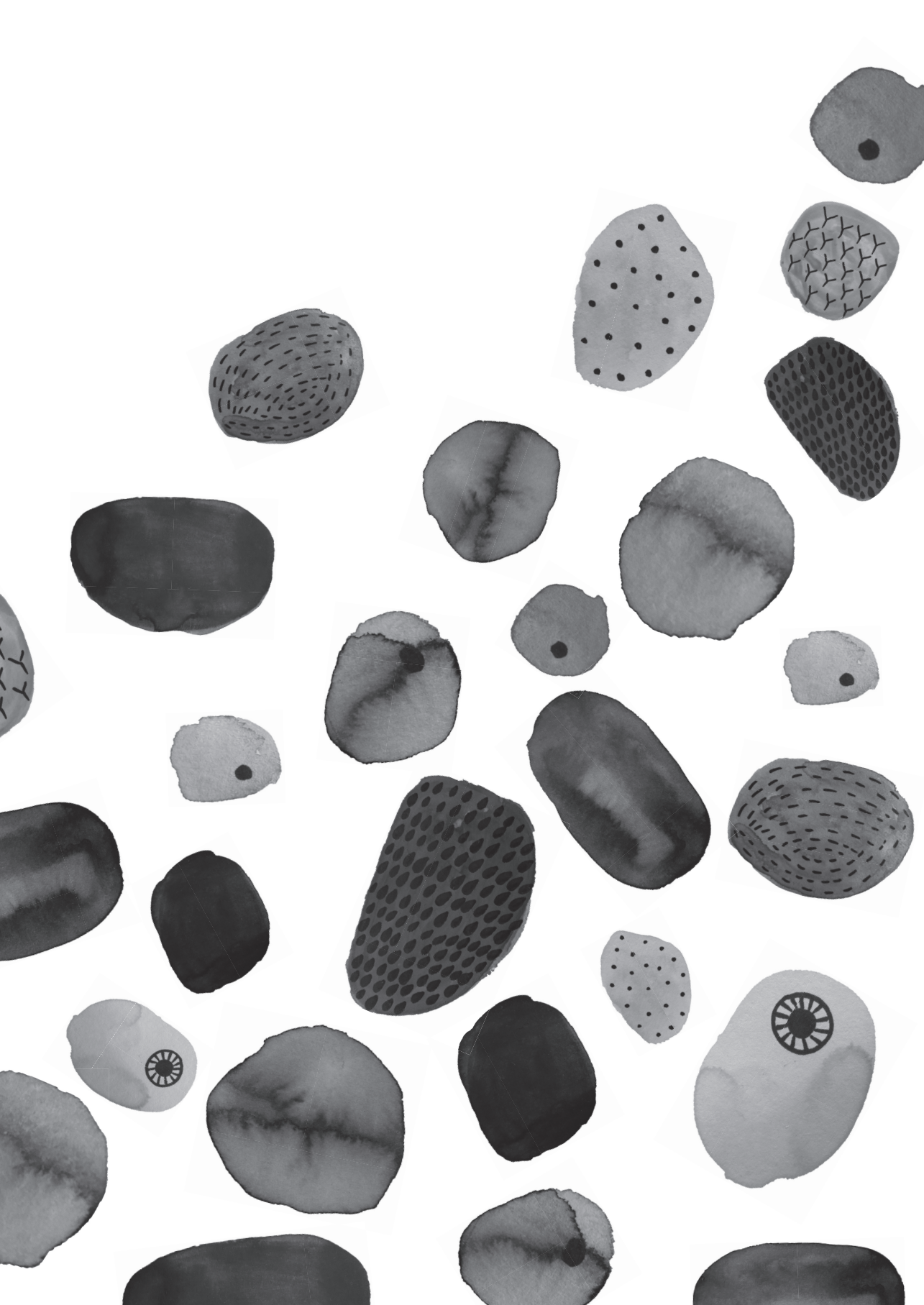


**Supplementary figure S3:** Mesothelin peptide A-specific CD8 T cells in HLA-A2 positive patients. A) Peripheral blood samples were collected at base line (week 0) and 2 weeks after the third vaccination (week 6). CD8 T cells were propagated in four culture cycles with mesothelin-peptide loaded aAPC after which mesothelin-peptide/HLA-A2 dexamers were used to detect mesothelin specific CD8 T cells. B) Values of gated dextramer positive CD8 T cells - as shown in panel A - presented as proportions of mesothelin-B HLA-A2-binding cells of total CD8 T cells. Gating was based on the negative controls: FMO staining and the non-CD8 T cell population. All HLA-A2 positive patients are shown; patient 5 was excluded (haplotype HLA-A3/HLA-A68).



**Supplementary figure S4:** Additional frequencies of T cell populations or ratios, as well as expression of cell surface markers, showing no change between week 0, 2 and 6. A) CD4/CD8 T cell ratio,  $\gamma\delta$ T cells and regulatory T cells (Treg) percentages (upper panels) and representative flow cytometry plots (lower panels;  $\gamma\delta$ T cell and Treg). B) CD4 T cells positive for CD25, CD69, CD272 (BTLA), CD137 (4-1BB), CD154 (CD40L) and CD134 (OX40). C) CD8 T cells positive for CD25, CD69, CD272 (BTLA), CD137 (4-1BB), CD154 (CD40L) and CD134 (OX40)





# CHAPTER

**GENERAL DISCUSSION**

8

## REVERSE TRANSLATIONAL RESEARCH AND IMMUNE MONITORING

The aim of translational research or translational medicine is to use fundamental scientific insights to develop and create new treatments to improve health. In the field of tumor immunology, this means that a solid understanding of tumor biology and immunology are needed to develop improved or novel strategies to treat and eventually cure cancer patients. Typically, translational research goes from bench to bedside. New drug targets and the effect of their modulation are first studied *in vitro* and subsequently tested in *in vivo* studies, using animal models that increasingly reflect the physiological situation in patients. Finally, new treatments are tested in clinical trials in patients. Unfortunately, no model fully reflects the complexity of the situation in the patient, and consequently new therapies may fail during development. Moreover, as each patient's condition is different, we do not know on beforehand which patients will respond to certain therapies and which patients will not. Besides efficacy of a certain drug, the right patient population should be determined for optimal treatment.

Whereas translation from bench to bedside is common practice in the field, less attention is given to translation the other way around: from bedside to bench. Much is to be learned by studying patient data from clinical trials; knowledge that can be used in improving the therapies in development. Immune monitoring in patients is an important part in this reverse translational research, providing insights in the mechanisms of action of certain therapies or defining patient groups with a differential sensitivity to certain treatments. Moreover, it can increase our understanding of the role of the several components of the immune system in cancer progression and prognosis.

The research described in this thesis focusses on monitoring immune cells and components in the peripheral blood of patients with thoracic malignancies. Immune monitoring can serve a clinical or a more fundamental objective:

1. From a clinical perspective, we aimed to predict an individual patient's response to treatment or chance of (long-term) survival in a way that can be implemented in clinical practice.
2. From a translational perspective, we aimed to increase our knowledge about the mechanism of action of several cancer therapies, which will benefit the design and improvement of novel treatment strategies, the discovery of drug targets, or a rationale for potential combination strategies.



Our main findings are that in early stage non-small cell lung cancer (NSCLC), radiotherapy induces an activation of T cells in the majority of patients, characterized by increased proportions of PD1+ and Ki67+ T cells. Furthermore, we showed that chemotherapy is able to induce activation markers on T cells, although this does not translate to an increased clinical response. Surgery does not increase T cell activation in early stage NSCLC patient. In malignant pleural mesothelioma (MPM) patients, we showed that dendritic cell (DC) immunotherapy is a promising treatment and induces immune responses accompanied by an increase in activation markers on CD4 T cells in peripheral blood.

## IMMUNE MODULATORY EFFECT OF CANCER TREATMENT

In **chapters 3, 4 and 7** we studied the immune modulatory effects of different treatments in patients with thoracic malignancies during conventional or experimental treatments. An overview of the immune modulatory effects of the different treatments studied in these chapters is presented in Table 1. All these measurements were performed in peripheral blood, as this is an ideal source for serial sample collection that is minimally invasive to the patient. The limitation is, however, that we do not know how well this reflects immune populations in the tumor and thus these data only inform us on systemic immune responses.

### Conventional therapy

In early stage lung cancer, patients are treated generally with surgery or ablative radiotherapy. Radiotherapy is mainly used in patients unfit for treatment or with a tumor on a location that is difficult to reach. In **chapter 3** we showed that in a subset of patients receiving stereotactic ablative body radiation (SABR), T cell activation is induced in the peripheral blood. This was characterized by increased proportions of proliferating T cells and increased PD1+ T cells. Patients receiving surgery did not show T cell activation. Instead, we observed that surgery induced a temporal increase in myeloid derived suppressor cells (MDSC) (additional data, not discussed in chapter 3). These findings may have implications for the use of immunotherapy in these patients. Currently, PD-1/PD-L1 inhibition has been EMA/FDA approved for NSCLC only at an advanced stage, but presently, in several large randomized phase III studies, the role of adjuvant PD-1/PD-L1 is being established, and consequently these treatments might be administered also at an earlier stage in the future [1]. As a pre-existing anti-tumor immune response is required for PD-1 blockade to reinvigorate T cells, we hypothesize that radiotherapy might increase sensitivity to PD-1 blockade by inducing immunogenic cell death and thereby priming this immune response. Current clinical trials are investigating this hypothesis [2, 3]. Another question for further

research, is whether the increase in T cell activation after SABR is predictive of a response to checkpoint inhibition.

In **chapter 4**, we monitored immune dynamics in patients with an advanced stage of NSCLC that were treated with chemotherapy and anti-VEGF combination. This combination treatment is an approved regimen in stage IV NSCLC. In these patients, an increase in proliferating CD8+ T cells was observed in the first six weeks after treatment. The increased proliferation occurred in T cells of the effector subtype that expressed PD-1. Similar to SABR-treated patients, this chemotherapy anti-VEGF combination might increase sensitivity to PD-1/PD-L1 inhibition, because increased CD8 proliferation in peripheral blood is associated with a better response [4, 5]. As with SABR, chemotherapy might therefore be combined with immunotherapy to increase efficacy.

We cannot conclude from our data to which of the components of the PCB treatment – paclitaxel, carboplatin or bevacizumab – these immune modulatory effects can be ascribed. Moreover, several studies have shown that different types of chemotherapy have a variable capacity to induce immunogenic cell death, capable of inducing an immune response [6-8]. Therefore, a direct comparison between the different chemotherapeutic regimens in combination with immunotherapy would be useful. The combination of paclitaxel and carboplatin as studied in this thesis, is one of the most frequently used regimens for advanced stage NSCLC. Interestingly, an indirect comparison of PD-1/PD-L1 inhibition treatment, chemotherapy treatment and the combinations thereof in a meta-analysis, suggested improved clinical outcomes of the combination therapy compared to PD-1/PD-L1 inhibition alone, indicating an additional benefit of chemotherapy [9]. Whether this is due to synergy of the two treatment effects in the same patients or separate patient groups that respond to either of the treatments and thus an increased response rate, remains to be elucidated.

### **Dendritic cell Immunotherapy**

Whereas the main mechanism of action of the conventional treatments radiotherapy and chemotherapy relies on the direct killing of tumor cells by interfering with their capacity to proliferate, immunotherapy is designed to induce or enhance the anti-tumor immune response. New insights into the role of the immune system in cancer progression and response to cancer treatment has led to the development of novel immunotherapeutic strategies. DC-based immunotherapy has been one of these strategies. Preclinical development of DC immunotherapy and subsequent development of MesoPher treatment for mesothelioma, an autologous DC treatment consisting of DCs pulsed with an allogeneic tumor cell lysate, has been described in **chapter 6**. MesoPher DC immunotherapy has

shown clinical promise with low toxicity and two clinical responses in patients with malignant mesothelioma.

In **chapter 7**, we studied the immune modulatory effects of MesoPher, as determined in peripheral blood. We studied various molecules on T cells to assess their activation. Classical T cell activation markers include CD25 and HLA-DR [10]. Furthermore, many co-inhibitory receptors such as PD-1, CTLA4 and LAG3 are also upregulated upon activation. However, upon prolonged antigen exposure, T cells can accumulate multiple inhibitory receptors and turn into a dysfunctional state called T cell exhaustion [11]. Interestingly, the immune modulatory effect of DC immunotherapy was most pronounced for CD4 T cells, with an increase in expression of HLA-DR, PD1 and ICOS. The upregulation of these markers – the activation marker HLA-DR, the co-inhibitory molecule PD-1 that is upregulation upon activation, and ICOS, a co-stimulatory molecule on T cells – together indicate activation of CD4 T cells after therapy. On CD8 T cells on the other hand, only a small increase in LAG3 expression was observed. As PD-1 was the only upregulated co-inhibitory molecule on CD4 T cells and LAG-3 the only co-inhibitory molecule upregulated on CD8 T cells, these changes are unlikely to reflect an exhausted state. Unfortunately, with the small number of patients in this study, we could not correlate these changes to clinical outcome. The value of these markers as biomarkers and predictors of clinical outcome will be investigated in subsequent clinical trials for this therapy. Another immunological outcome in this study was the delayed-type hypersensitivity (DTH) skin test, in which an immune reaction – redness and thickening – of the skin is assessed upon injection in the skin, in this case of the lysate-pulsed DCs. Six weeks after the first vaccination, all patients had a positive response on this skin test, showing a functional immune reaction against the vaccine (**chapter 6**). The timing of the response, 48h after injection, is indicative of a T cell response. Moreover, we detected specificity to the mesothelioma-related antigen mesothelin these skin-infiltrating T cells. However, this finding does not guarantee that these T cells reach the tumor.

These studies may guide the further development of DC immunotherapy for instance towards the optimal combination immunotherapy. We are currently eagerly awaiting clinical and translational results of the ongoing phase III clinical trial that will show whether the treatment is efficacious in pleural mesothelioma patients. Nevertheless, we can already speculate on ways to further improve the treatment. For example, pre-clinical studies show that depletion of immune suppressive cells in the tumor microenvironment can improve efficacy of DC immunotherapy, and another logical combination would be DC immunotherapy and anti-PD1/PDL-1 checkpoint inhibition [12]. The latter might be effective because DC immune therapy induces increased PD-1 expression on CD4 T cells but might also boost CD8 T cells simultaneously for an optimal immune response.

*In vivo* experiments in mice with allogeneic lysate-pulsed autologous DC showed induction of a tumor-specific CD8 T cell response (**chapter 6**), but immune monitoring of patient blood showed mainly activation of CD4 T cells. While this might be due to differences between the preclinical and clinical setting, it would be of interest to further investigate the contribution of CD4 T cell activation in DC immunotherapy efficacy. Depletion of either CD4 or CD8 T cells in animal models could show the contribution of these subsets in the efficacy of DC immunotherapy. Furthermore, it would be of interest to investigate to which extent the individual CD4 T cell subsets (Th1, Th2, Th17, Tfh, Treg) are activated by DC immunotherapy, for example by studying the cytokine profile of these T cells. The cytokine IFN $\gamma$  plays a key role in the anti-tumor immune response [13], therefore activation of the Th1 subset is expected to be most beneficial.

**Table 1.** Overview of main results of longitudinal immune monitoring data as reported in chapters 3, 4 and 7 of this thesis.

Ch.	Cancer	Treatment	Cell numbers	CD4 T cells	CD8 T cells	Immune suppressive cells
3	NSCLC early stage	Surgery	N.D.	No changes	No changes	Temporary increase in MDSC
3	NSCLC early stage	SABR	N.D.	Increased proliferation	Increased proliferation	No changes
4	NSCLC late stage	Chemotherapy + anti-VEGF	N.D.	No changes	Increased proliferation	Temporary increase in MDSC
7	Mesothelioma	DC immunotherapy	Increase in total B cells, CD4 T cells, CD8 T cells	Upregulation of PD1, HLA-DR, ICOS	Upregulation of LAG3 expression	No change in MDSC

### Immune monitoring in peripheral blood

Altogether, we showed that several immunological changes can be measured in the peripheral blood of cancer patients, whereby these changes are different across treatment strategies. Overall, there is a large variation between patients, but samples of an individual patient taken at different time points are strongly correlated. Proportions of the immune subsets (B cells, monocytes, T cells, CD4/CD8 T cell ratio and the various differentiation stages of T cells) remain surprisingly stable over time. However, changes in the activation status of T cells can be detected by increased proportions of T cells positive for markers such as Ki67 (associated with cell division), PD-1, HLA-DR and ICOS. In recent years, changes in peripheral blood Ki67<sup>+</sup> CD8 T cells have shown to be a marker of clinical response to checkpoint inhibition, which has been corroborated by several studies [4, 5, 14]. We have observed an increase in Ki67<sup>+</sup> CD8 T cells after both SABR and chemotherapy, which indicates that this is a more common response to cancer treatment. Unfortunately, Ki67

expression was not measured in the immune monitoring of the DC immunotherapy clinical trial, so whether this extends also to other immunotherapies remains to be determined.

In **chapter 7**, we monitored the specificity of T cells (i) by assessing the diversity in the length of complementarity-determining region 3 (CDR3) of the T cell receptor (TCR), which is the region that is responsible for recognizing antigens, and (ii) by assessing changes in the number of mesothelin-specific T cells, in which mesothelin was chosen as a model antigen for mesothelioma. However, no significant changes were observed in these patients after treatment. The used method of determining CDR3 length diversity is suitable to detect prominent clonal expansions. In addition, others have found that DC or whole tumor cell vaccination increases the diversity of T cells clones [15, 16]. Expansion of specific T cell clones after therapy is mainly reported in combination with clones identified in the tumor [17-19]. Immunotherapy using DCs that are pulsed with whole-cell lysates is not designed to induce a mono- or oligoclonal T cell response. Therefore, monitoring alterations in the repertoire of T cells is not recommended for immune monitoring in peripheral blood in future studies. However, more sensitive techniques such as next-generation sequencing will be useful to compare the T cell receptor repertoire in blood and tumor T cells or to explore changes induced by DC immunotherapy. Instead of monitoring T cell receptor repertoires, a general picture of the activation state of the immune system can be obtained by studying the different subpopulations and their activation markers in peripheral blood.

## THE IMMUNE PROFILE AS BIOMARKER FOR CLINICAL OUTCOME

### Myeloid-derived suppressor cells in advanced stage NSCLC

The NVALT 12 study was a Dutch national study investigating the role of adding a nitroglycerin patch to a standard chemotherapy regimen in a non-blinded randomized setting. The chemotherapy regimen carboplatin paclitaxel was combined with the anti-VEGF antibody bevacizumab, and the additional effect of the nitroglycerin patch on progression free survival was studied. The hypothesis that the vascular dilation caused by the nitroglycerin would improve chemotherapy delivery to the tumor potentiating its effect was not confirmed in this study. Within the NVALT12 study, blood samples were collected from a cohort of over 200 NSCLC patients, which allowed for analysis the immune profile in relation to the survival of these patients. We have shown in **chapter 2** that elevated numbers of MDSC are associated with worse survival in NSCLC patients. This means that in general, MDSC are disadvantageous for (lung) cancer patients, which is in line with other published research. Furthermore, we investigated expression of immunoglobulin-

like transcript 3 (ILT3), also called LILRB4. This molecule is expressed on monocytes and professional antigen-presenting cells (APCs) and confers an inhibitory signal via its immunoreceptor tyrosine-based inhibitory motif (ITIM) domain. We showed that ILT3 is expressed by MDSC and correlates with a worse survival. ILT3 expression might signify an even more suppressive state of MDSC and might thereby be an interesting target for therapy. Besides tolerogenic DCs and MDSC, recent literature has shown that ILT3 can also be expressed on tumor cells. For example, ILT3 is expressed on acute myeloid lymphoma (AML) cells and negatively impacts T cells [20]. Furthermore, colorectal carcinoma cells can express ILT3, which is negatively correlated with immune infiltration and survival [21]. This makes ILT3 an interesting target for therapy, which might affect tumor cells and MDSC simultaneously. In fact, a chimeric antigen receptor (CAR) T cell therapy against ILT3 for treatment of AML is currently being developed [22].

### Combining multiple markers

Accumulating evidence exists for a prognostic and/or predictive role for various immune cells either in the tumor microenvironment or in the peripheral blood (see also **chapter 1** of this thesis). In **chapter 2** we provided additional evidence for the negative impact of elevated MDSC proportions on survival of NSCLC patients. As the immune system involves many specialized cells each having their effect on the tumor, we hypothesized that the combination of immunological markers as a more complete immune profile would be a better predictor of clinical outcome than a single cell marker.

In **chapter 5** we used the flow cytometry data of the MDSC staining from **chapter 2** and the T cell stainings from **chapter 4**, to create a prediction model for clinically meaningful outcome, such as progression free and overall survival based on all possible marker combinations in these stainings, using the FloReMi pipeline [23]. Semi-automatic gating could be used to create a huge number of features for the model, encompassing all possible combinations of markers and thus immune subsets, given the markers that were measured. With advancing technology, the need for bioinformatic analysis methods is increasing. Multidimensional data such as flow cytometry and mass cytometry data require more sophisticated analysis than the two-dimensional plots that can be analyzed manually. (Semi)-automatic gating can be very useful for data sets with a large number of samples, such as clinical trials. Although reliable populations were extracted with automatic gating, the performance of the final prediction model was only moderate. Importantly however, usage of features extracted with the FloReMi pipeline resulted in a better prediction of survival compared to manually gated populations. In future research, the FloReMi, or other comparable approaches could be applied to other clinical cohorts in which a stronger effect of the peripheral blood immune profile on clinical outcome is expected, for example

immunotherapy trials. The selected features of the model can hold valuable information on immune populations and their effect on clinical outcome and may be hypothesis-generating.

### **Biomarkers - Correlation versus prediction**

As described, a statistical difference in survival between patients with normal or elevated proportions of MDSC has been observed in the NVALT12 study. Sensitivity and specificity are not high enough with this difference in median survival time to be used in clinical practice to predict an individual patient's survival chance. Similarly, with a concordance index of 0.67, the prediction model derived from the FloReMi pipeline is not robust enough to be used in clinical practice, although it does correlate significantly with the observed overall survival. In the search for biomarkers for response to (immuno)therapy, often correlations with overall clinical outcome are reported. Yet, a biomarker that can be used for clinical decision making requires a much greater sensitivity and specificity. PD-L1 expression in the tumor is currently the only approved biomarker available for PD1 blockade therapy, although also here specificity is not high enough to really guide clinical decision making [24], because patients with PD-L1 negative tumors can still respond to therapy, albeit with a lower response rate. Therefore, in most cases patients with PD-L1-negative tumors will still be treated with this therapy. With the present knowledge, to improve prediction of clinical outcome in cancer patients during certain treatments a combination of multiple factors should be employed. These may include clinical characteristics, immunological biomarkers in peripheral blood and in the tumor microenvironment, as well as tumor characteristics such as mutational burden.

## **IMPLICATIONS FOR FUTURE RESEARCH AND TRIAL DESIGN**

In the era of emerging immunotherapies, studying clinical parameters and molecular characteristics of the tumor is not sufficient for a full understanding of treatment response. When the immune system is actively targeted and is therefore the main mode of action of a treatment, immunological responses should be evaluated. On the other hand, the immune modulatory effects of conventional therapy might be more indirect and should be considered as well, especially when designing combination treatments. Furthermore, monitoring anti-tumor immune responses may provide information on the response status earlier after treatment. For example, an anti-tumor immune response can prevent recurrences which only become apparent after years. However, further research is needed to confirm this hypothesis in clinical settings, for example in the patient cohort of **chapter 3**, when recurrences have occurred. A discussion issue remains how to study the immune activation induced by these therapies. Is it essential to study the effects in the tumor tissue,

which is hampered by the limited availability of tissue both before the start of treatment and during or after treatment? Does peripheral blood, being easily accessible for longitudinal follow up, serve as a surrogate for tumor tissue or does the peripheral blood have a function on its own in the anti-tumor immune response? Evidence for the latter has been provided by Spitzer and colleagues, who studied the role of a systemic immune response during effective or ineffective treatment in murine tumor models and showed that a systemic immune response is crucial for tumor rejection [25]. This systemic immune response was characterized by sustained T cell proliferation in blood; a finding which is at least partly translated to the human setting, since increased T cell proliferation is correlated to response to checkpoint blockade in patients [4, 5, 26]. Some factors obviously cannot be studied in peripheral blood, such as tissue-resident immune cells and spatial localization of immune cells. However, given the limitations of studying tumor samples – inter-organ differences when studying primary tumor and metastases, intra- and inter-tumor heterogeneity within a patient – peripheral blood may be a suitable source to study, especially to capture the complete dynamics of the response by assessing multiple time points.

Based on the results presented in this thesis, the following marker combinations are advised to be included in future immune monitoring efforts. First, markers to define the major immune cell subsets (monocytes, B cells, CD4 and CD8 T cells, NK cells) in peripheral blood mononuclear cells (PBMC) should be included. Furthermore, markers to distinguish Treg from T helper cells (e.g. FoxP3, CD45RA, CD25, CD127) should be included. For T cell activation, PD-1, Ki67, HLA-DR and ICOS can be included. CD69, TIM3 and CTLA4 had a very low expression on peripheral blood T cells and determination of these markers is therefore only recommended when combined with other markers to specifically analyze a subset with higher expression, for example Tregs. MDSC are a population that is clinically relevant in peripheral blood and can be monitored, as well as classical and non-classical monocyte subsets that can be distinguished with the same set of markers. To avoid complex staining panels, the combination of HLA-DR and CD33 may be used.

There is an increasing number of anti-cancer drugs on the market and in (pre)clinical development. However, although these treatments improve survival rates of cancer patients, many of these will not lead to cure in an advanced stage disease. To improve cancer treatments, different therapies may be combined, but with the number of possible combinations there is a need for rational design. It would be simply too much to test all combinations in clinical trials. A proper rationale and preclinical evidence for certain combination is needed. Furthermore, with reverse translation we can make use of very valuable insights gained from clinical practice and clinical trials to shape and redesign our treatments, select the appropriate patient groups or combination strategies. Therefore, it is

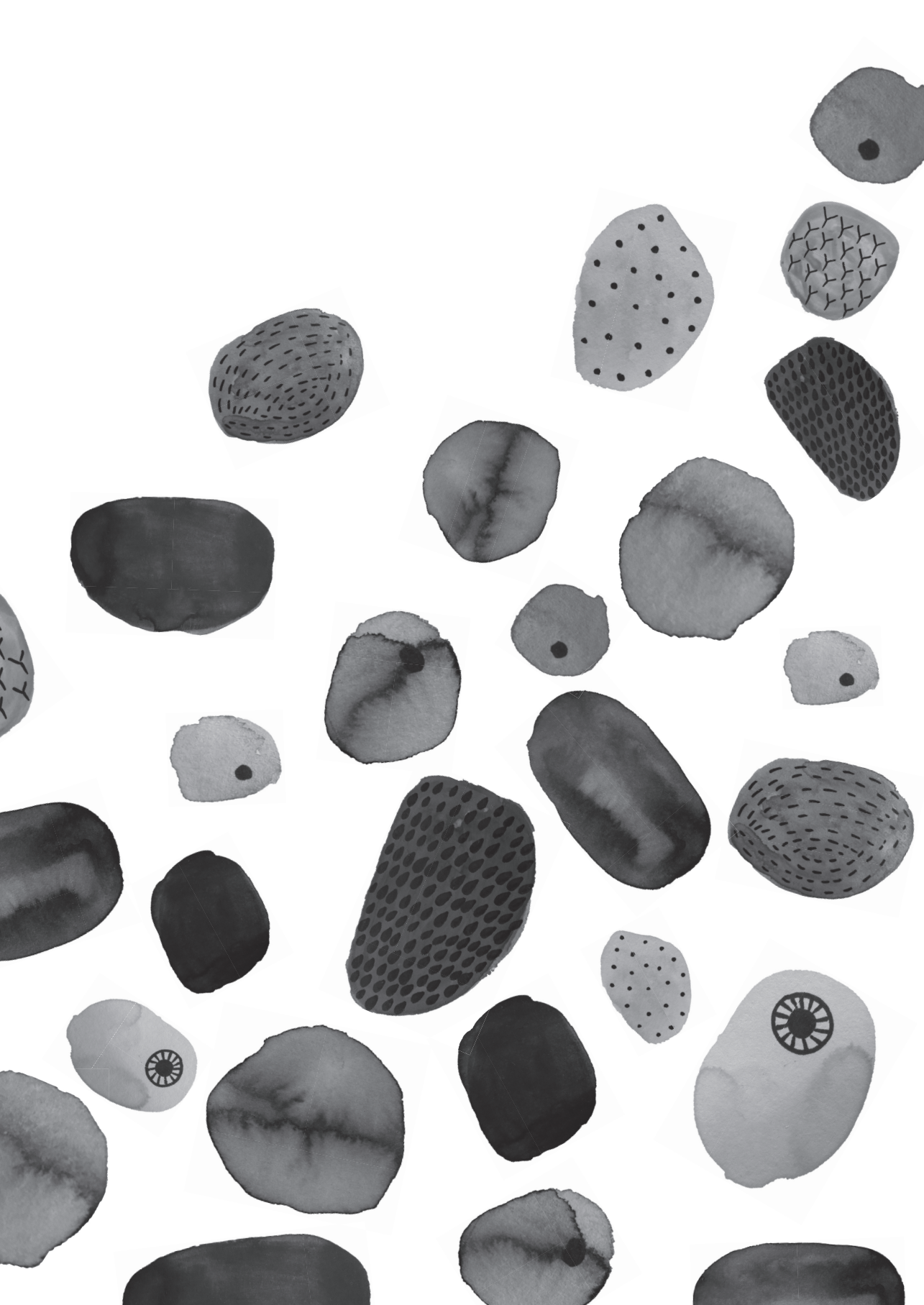


crucial to implement patient sample collection for immune monitoring in future clinical trials. Despite its limitations, peripheral blood has proven to be a valuable source for immune monitoring, especially for the markers as discussed above. Taking into account the rapid developments in technologies such as multi-color flow cytometry, mass cytometry and single cell RNA sequencing and the bioinformatic data analysis methods, as well as our rapidly expanding knowledge in the tumor immunology and immune monitoring field, this will greatly benefit reverse translation and is expected to lead to substantial improvement of patient-centered cancer therapy.

## REFERENCES

1. Yeh, J., K.A. Marrone, and P.M. Forde, *Neoadjuvant and consolidation immuno-oncology therapy in stage III non-small cell lung cancer*. *J Thorac Dis*, 2018. **10**(Suppl 3): p. S451-S459.
2. De Wolf, K., et al., *A phase II trial of stereotactic body radiotherapy with concurrent anti-PD1 treatment in metastatic melanoma: evaluation of clinical and immunologic response*. *J Transl Med*, 2017. **15**(1): p. 21.
3. Takamori, S., et al., *Combination Therapy of Radiotherapy and Anti-PD-1/PD-L1 Treatment in Non-Small-cell Lung Cancer: A Mini-review*. *Clin Lung Cancer*, 2018. **19**(1): p. 12-16.
4. Kamphorst, A.O., et al., *Proliferation of PD-1+ CD8 T cells in peripheral blood after PD-1-targeted therapy in lung cancer patients*. *Proc Natl Acad Sci U S A*, 2017. **114**(19): p. 4993-4998.
5. Huang, A.C., et al., *T-cell invigoration to tumour burden ratio associated with anti-PD-1 response*. *Nature*, 2017. **545**(7652): p. 60-65.
6. Obeid, M., et al., *Calreticulin exposure dictates the immunogenicity of cancer cell death*. *Nat Med*, 2007. **13**(1): p. 54-61.
7. Kroemer, G., et al., *Immunogenic cell death in cancer therapy*. *Annu Rev Immunol*, 2013. **31**: p. 51-72.
8. Pol, J., et al., *Trial Watch: Immunogenic cell death inducers for anticancer chemotherapy*. *Oncoimmunology*, 2015. **4**(4): p. e1008866.
9. Liang, H., et al., *PD-(L)1 inhibitors vs. chemotherapy vs. their combination in front-line treatment for NSCLC: An indirect comparison*. *Int J Cancer*, 2019.
10. Murphey, K. and C. Weaver, *Janeway's Immunobiology, 9th edition*. 2016: Ww Norton & Co.
11. Wherry, E.J. and M. Kurachi, *Molecular and cellular insights into T cell exhaustion*. *Nat Rev Immunol*, 2015. **15**(8): p. 486-99.
12. Dammeijer, F., et al., *Depletion of tumor-associated macrophages with a CSF-1R kinase inhibitor enhances antitumor immunity and survival induced by DC immunotherapy*. *Cancer Immunol Res*, 2017.
13. Kaplan, D.H., et al., *Demonstration of an interferon gamma-dependent tumor surveillance system in immunocompetent mice*. *Proc Natl Acad Sci U S A*, 1998. **95**(13): p. 7556-61.
14. Kim, K.H., et al., *The First-week Proliferative Response of Peripheral Blood PD-1(+)/CD8(+) T Cells Predicts the Response to Anti-PD-1 Therapy in Solid Tumors*. *Clin Cancer Res*, 2019. **25**(7): p. 2144-2154.
15. Carreno, B.M., et al., *Cancer immunotherapy. A dendritic cell vaccine increases the breadth and diversity of melanoma neoantigen-specific T cells*. *Science*, 2015. **348**(6236): p. 803-8.
16. Hopkins, A.C., et al., *T cell receptor repertoire features associated with survival in immunotherapy-treated pancreatic ductal adenocarcinoma*. *JCI Insight*, 2018. **3**(13).
17. Formenti, S.C., et al., *Radiotherapy induces responses of lung cancer to CTLA-4 blockade*. *Nat Med*, 2018. **24**(12): p. 1845-1851.
18. Wieland, A., et al., *T cell receptor sequencing of activated CD8 T cells in the blood identifies tumor-infiltrating clones that expand after PD-1 therapy and radiation in a melanoma patient*. *Cancer Immunol Immunother*, 2018. **67**(11): p. 1767-1776.
19. Hsu, M., et al., *TCR Sequencing Can Identify and Track Glioma-Infiltrating T Cells after DC Vaccination*. *Cancer Immunol Res*, 2016. **4**(5): p. 412-418.
20. Deng, M., et al., *LILRB4 signalling in leukaemia cells mediates T cell suppression and tumour infiltration*. *Nature*, 2018. **562**(7728): p. 605-609.
21. Liu, J., et al., *Expression of ILT3 predicts poor prognosis and is inversely associated with infiltration of CD45RO+ T cells in patients with colorectal cancer*. *Pathol Res Pract*, 2018. **214**(10): p. 1621-1625.
22. John, S., et al., *A Novel Anti-LILRB4 CAR-T Cell for the Treatment of Monocytic AML*. *Mol Ther*, 2018. **26**(10): p. 2487-2495.
23. Van Gassen, S., et al., *FloReMi: Flow density survival regression using minimal feature redundancy*. *Cytometry A*, 2016. **89**(1): p. 22-9.

24. Havel, J.J., D. Chowell, and T.A. Chan, *The evolving landscape of biomarkers for checkpoint inhibitor immunotherapy*. *Nat Rev Cancer*, 2019. **19**(3): p. 133-150.
25. Spitzer, M.H., et al., *Systemic Immunity Is Required for Effective Cancer Immunotherapy*. *Cell*, 2017. **168**(3): p. 487-502 e15.
26. Das, R., et al., *Combination therapy with anti-CTLA-4 and anti-PD-1 leads to distinct immunologic changes in vivo*. *J Immunol*, 2015. **194**(3): p. 950-9.



# CHAPTER

**ENGLISH SUMMARY**  
**NEDERLANDSE SAMENVATTING**  
**AUTHOR AFFILIATIONS**  
**DANKWOORD**  
**PHD PORTFOLIO**  
**ABOUT THE AUTHOR**

9

## ENGLISH SUMMARY

Cancer develops when normal cells of the body acquire mutations that lead to uncontrolled cell division and invasion of surrounding tissues. In the early stages of cancer, the tumor is confined to one local site, but it can progress to advanced stage, metastatic disease in which other organs are affected. Survival rates decrease drastically with an advancing stage of cancer. Various types of cancer exist, depending on the cell of origin. This thesis focuses on the thoracic malignancies non-small cell lung cancer (NSCLC) and mesothelioma. Non-small cell lung cancer has the higher cancer mortality world-wide and derives from cells in the lung. Mesothelioma is a cancer of the pleural lining of the lungs and is induced by asbestos exposure. Although several effective cancer treatments have been developed over the last century, most patients are still incurable.

The immune system plays a very important role in the protection against cancer. Described as the cancer immunity cycle, tumor antigens that are released in the tumor microenvironment are taken up by dendritic cells (DC) and presented to T cells in the lymph nodes. T cells specific for these tumor antigens are then activated and expand, upon which they travel to the tumor, recognize the tumor and are able to induce tumor cell death. However, cancer cells employ several mechanisms to evade or suppress this anti-tumor immune response.

Immunotherapy aims to enhance this anti-tumor immune response, for example by blocking inhibitory receptors on T cells (checkpoint inhibition) or by administering autologous immune cells (DCs or T cells) that are modulated and/or expanded *ex vivo*. Over the last decade, immunotherapy has revolutionized cancer treatment and showed unprecedented clinical responses. Checkpoint inhibitors have quickly moved to first- or second-line treatment in several cancer types, and many more immunotherapeutic strategies are showing promise in clinical trials. In addition, conventional cancer treatments such as radiotherapy and chemotherapy, may also have immune modulatory effects that play an important role in their efficacy.

Not all patients respond equally well to cancer treatment, and there is still a large fraction of patient that does not respond. Currently, a great challenge in cancer treatment is to determine the right therapy for the right patient. Biomarkers for response and solid data for rational combination strategies are highly needed to improve outcomes. In this thesis we aimed to increase our understanding of the role of the immune system and its clinical value in patients with thoracic malignancies during treatment (**chapter 1**).

We used flow cytometry to examine the immune profile in the peripheral blood of cancer patients. In **chapter 2** we studied a cohort of over 200 stage IV NSCLC patients from a randomized controlled trial that were treated with paclitaxel, carboplatin and bevacizumab (PCB) with or without additional nitroglycerin patch (the NVALT12 study). There was no difference in progression-free survival (PFS) or overall survival (OS) between the two treatment arms. In these patients, we assessed proportions of myeloid-derived suppressor cells (MDSC) and the expression of the inhibitory receptor immunoglobulin-like transcript (ILT) 3. MDSCs are a heterogeneous population of immune cells that play an important role in immune suppression and are elevated in many cancer patients. ILT3 may be expressed on DCs, where it plays a role in immune tolerance. It can interact with a still unidentified ligand on T cells and thereby induce T cell anergy, regulatory T cells or T suppressor cells. We showed that pretreatment proportions of circulating MDSCs are correlated to worse survival. Moreover, we showed for the first time that ILT3 is expressed by a subset of MDSCs, and that this expression is correlated with reduced overall survival in patients with increased proportions of MDSCs. Expression of ILT3 indicates an additional immune suppressive mechanism employed by MDSCs, that is relevant for clinical outcomes in stage IV NSCLC patients and may be an attractive target for treatment.

In early stage NSCLC, patients are mostly treated with surgery or stereotactic ablative body radiotherapy (SABR). We hypothesized that these different treatments would have a distinct effect on the immune system. In **chapter 3**, we compared T cell activation in peripheral blood of 13 patients that were treated with surgery and ten patients treated with SABR. We collected blood samples before treatment, and 1, 2, 3 and 6 weeks after start of treatment. In the flow cytometry analysis, several activation markers of T cells were included, as well as markers to define T cell subsets (CD8, CD4, FoxP3). Patients treated with surgery showed a small and temporary increase in proliferating T cells (characterized by Ki67 expression). In SABR treated patients, we observed a significant increase in proliferation of CD4 and CD8 T cells that remained up to week 6 and was accompanied by an increase in programmed death receptor-1 (PD-1) expression, which is a co-inhibitory surface molecule upregulated on T cells upon antigen recognition. Interestingly, within the SABR group, the majority of patients showed T cell activation, while other patients did not. It remains to be investigated whether this is related to recurrence-free survival in these patients. The increase in T cell activation and in particular PD-1 expression after treatment with SABR provides a rationale to combine radiotherapy with PD-1 blockade, to further enhance or prolong T cell activation.

In **chapter 4** we assessed the immune modulatory effect of the PCB combination in the NVALT12 study. This treatment is a standard treatment for stage IV non-squamous NSCLC patients. With immunotherapy as a new treatment modality for this group of patients

and the possibility of combination of the different treatment modalities, it is important to understand the immune modulatory effect of this chemotherapeutic regimen. We interrogated the peripheral blood immune profile of these patients before and during treatment at week 0, 3 and 6. We assessed proportions of T cells, B cells and monocytes, and measured several activation markers on T cells by flow cytometry. We observed a significant increase in Ki67-expressing, proliferating CD8 T cells after treatment. These proliferating CD8 T cells were mainly of the effector memory phenotype and had an increased expression of the inhibitory receptors PD-1 and CTLA4. Interestingly, a similar subset of proliferating CD8 T cells has been shown to be induced by PD-1/ PD-1 ligand 1 (PD-L1) inhibitors in NSCLC and melanoma patients. In melanoma, the ratio of proliferating CD8 T cells over tumor burden, was positively associated with a response to treatment. Increases in proliferating T cells in our study, did not correlate to improved overall survival, but may increase sensitivity to checkpoint inhibition.

Most immune monitoring efforts focus on the relation of a specific immune subset to response to therapy or patient survival. In **chapter 5**, we hypothesized that the combination of several of these factors would improve prediction of clinical outcome. Flow cytometry is the most frequently used technique to investigate immune populations and this technique is continuously improving, for example with an increasing number of markers that can be measured simultaneously on a single cell. To use the flow cytometry data to study the relation between the pretreatment immune profile and survival of NSCLC patients, a suitable data analysis pipeline should be used. We used the FloReMi pipeline, which is a recently developed semi-automatic analysis pipeline that extracts features from flow cytometry data and uses machine learning to build a prediction model using the most relevant features. From three flow cytometry panels with 12-16 markers each, over 60 thousand features were extracted from the raw data, reflecting frequencies and mean fluorescence intensity values (MFIs) of each possible subset based on the available markers. Automatically extracted populations were highly correlated to manually gated populations. A random-forest survival (RFS) model with the selected non-redundant features was trained and evaluated using five-fold cross-validation. The RFS model derived from the FloReMi pipeline showed a better performance than a model trained with manually obtained features, and its prediction was significantly associated with actual overall survival. The top feature that was associated with survival, was the frequency of HLA-DR<sup>+</sup>CD33<sup>+</sup> myeloid cells. We showed that FloReMi is a useful method to extract large numbers of reliable features from flow cytometric data that can be used to predict survival. However, the accuracy of prediction is too low to be used in clinical practice. Rather, this method may be used for more exploratory purposes and identify novel immune subsets with clinical relevance.



In **chapter 6** of this thesis we set out to improve immunotherapy for patients with malignant pleural mesothelioma (MPM). In the past, our research group has developed DC vaccination as a novel treatment for MPM. Autologous *ex vivo* cultured DCs pulsed with tumor cell lysate can activate tumor-specific T cells leading to an effective anti-tumor immune response. This treatment has been shown to be safe in patients. However, one of the main limitations of this treatment was the limited amount or quality of tumor material that could be obtained, which led a majority of patients being excluded for treatment. In **chapter 6** we used allogeneic tumor cell lysates derived from cell lines as an alternative source for pulsing the DCs. Using two mesothelioma mouse models, we studied survival and induction of a tumor-specific T cell response and showed comparable efficacy between allogeneic and autologous tumor cell lysates. Subsequently, a first-in-human clinical trial was initiated in which nine patients were treated with increasing doses of MesoPher treatment, consisting of autologous monocyte-derived DCs pulsed with lysate of five human mesothelioma cell lines. No dose-limiting toxicities were identified in any of the cohorts treated with 10, 25 or 50 million DCs. Median PFS was 8.8 months and median (OS) was not reached with a median follow up of 22.8 months. Two patients in the 25 million DC cohort showed a partial response. These findings show the safety and feasibility of MesoPher treatment. The next step will be the evaluation of efficacy in a subsequent phase III clinical trial.

In **chapter 7** we monitored immune responses in the peripheral blood of MPM patients treated with MesoPher during the first-in-human clinical trial to increase our understanding of the mechanism of action of DC immunotherapy and to identify markers that are suitable for immune monitoring in upcoming clinical trials. Peripheral blood was collected before start of treatment, and after each of the first three doses of DC immunotherapy. We determined the number and relative proportions of T cells, B cells and monocytes, and further characterized T cell subsets with several activation markers, and expression of co-stimulatory and co-inhibitory molecules. Furthermore, mesothelin-specific T cells were monitored as an indicator of tumor-reactive T cells and T cell receptor (TCR) diversity was evaluated by TCRb gene PCR assays. An increase in the number of total B cells, CD4 and CD8 T cells was observed in patients six weeks after the start of treatment. No changes were seen in mesothelin-specific T cells or TCRb diversity. CD4 T cells showed increased expression of human leukocyte antigen (HLA)-DR and PD-1 after two weeks, and increased expression of inducible T cell co-stimulator (ICOS) after 6 weeks, indicating an induction of T cell activation. CD8 T cells showed a slightly increased expression of lymphocyte-activation gene (LAG)-3 after two weeks. Our findings indicate that systemic immune activation is induced by DC immunotherapy, which is mainly reflected by an increased activation of CD4 T cells. These markers may be incorporated in immune monitoring efforts in future clinical trials to evaluate their predictive potential and use as biomarker for response.

Immune monitoring in peripheral blood provides insights in the immune modulatory effects of cancer treatment. There are considerable differences in the immune modulatory effects of surgery, radiotherapy, chemotherapy and immunotherapy and various immune subsets impact clinical outcomes in patients with thoracic malignancies, as described in **chapters 2-7**. While peripheral blood as a source for immune monitoring certainly has limitations, it provides a relatively non-invasive approach for serial collection of immune cells to study immune activation. Immune monitoring should be implemented as much as possible in future clinical trials to allow for reverse translation with a focus on the role of the immune system, which is needed to design and improve novel treatment strategies and combination, especially in the current era of emerging immunotherapies (**chapter 8**).

## NEDERLANDSE SAMENVATTING

Kanker ontwikkelt zich als normale cellen van het lichaam mutaties ondergaan die leiden tot ongecontroleerde celdeling en invasie van de omliggende weefsels. In vroege stadia van kanker bevindt de tumor zich nog slecht op één locatie, maar kan zich verder ontwikkelen tot een verder stadium met metastaseringen waarbij de kanker zich ook naar andere organen verspreidt. De overlevingskansen van een patiënt verminderen drastisch naarmate de kanker in een verder stadium komt. Er bestaan verschillende types kanker, afhankelijk van de oorsprong van de in kanker veranderde cel. Dit proefschrift focust zich op de thoracale maligniteiten niet-kleincellig longcarcinoom en mesothelioom. Niet-kleincellig longcarcinoom zorgt wereldwijd voor de hoogste kanker-gerelateerde sterfte en komt voort uit cellen van de long. Mesothelioom is een kanker van het longvlies en wordt veroorzaakt door blootstelling aan asbest. Ondanks de verscheidene behandelingen die over de laatste decennia zijn ontwikkeld, kunnen de meeste patiënten met longkanker en mesothelioom niet genezen worden.

Het immuunsysteem speelt een erg belangrijke rol bij de bescherming tegen kanker. Tumor-antigenen die vrijkomen in het tumor micromilieu kunnen opgenomen worden door dendritische cellen (DCs) en gepresenteerd aan T-lymfocyten in de lymfeklieren. De T-cellen die specifiek deze tumorantigenen kunnen herkennen worden hierdoor geactiveerd en gaan zich vermeerderen om vervolgens naar de tumor te reizen waar zij deze kunnen herkennen en celdood kunnen induceren. Kanker gebruikt echter verschillende methoden om aan het immuunsysteem te ontsnappen of deze anti-tumor immuunrespons te onderdrukken.

Het doel van immuuntherapie is om deze anti-tumor immuunrespons te versterken, bijvoorbeeld door remmende moleculen op de T-cellen te blokkeren (ook wel 'checkpoint inhibitie' genoemd) of door autologe immuuncellen (DCs of T-cellen) die buiten het lichaam zijn gemodificeerd, terug te geven aan een patiënt. In de laatste decennia heeft immuuntherapie een revolutie teweeggebracht in de behandeling van kanker, met nog niet eerder vertoonde klinische responsen. Checkpoint inhibitors hebben zich in rap tempo een weg gebaan naar eerste- of tweedelijns therapie bij verscheidene soorten kanker, en nog veel meer immunotherapeutische strategieën laten veelbelovende resultaten zien in klinische studies. Daarnaast hebben de conventionele kankertherapieën zoals radiotherapie en chemotherapie ook een effect op het immuunsysteem wat een belangrijke rol kan spelen in hun effectiviteit.

Niet elke patiënt reageert even goed op kankertherapie en er is nog steeds een grote groep patiënten die niet reageert. Momenteel is een grote uitdaging in de behandeling van kanker

het kiezen van de juiste therapie voor de juiste patiënt. Biomarkers voor respons en solide data voor het rationeel combineren van verschillende medicijnen zijn hard nodig voor het verbeteren van de behandelingsuitkomst voor patiënten. In dit proefschrift hebben we als doel gesteld beter te begrijpen wat de rol van het immuunsysteem en de klinische waarde hiervan is in patiënten met thoracale maligniteiten tijdens hun behandeling (**Hoofdstuk 1**).

We hebben flowcytometrie gebruikt om het immuunprofiel te bestuderen in het bloed van kankerpatiënten. In **hoofdstuk 2** onderzochten we een cohort van meer dan 200 patiënten met stadium IV niet-kleincellig longcarcinoom van een gerandomiseerd gecontroleerde studie, waarbij de patiënten behandeld waren met paclitaxel, carboplatine en bevacizumab (PCB) met of zonder additionele nitroglycerinepleister (de NVALT12 studie). Er was geen verschil in progressievrije overleving of algehele overleving tussen de behandelarmen. In deze patiënten hebben we de relatieve aantallen van myeloïde suppressorcellen (MDSC) bepaald, en de expressie van de inhibitorische receptor immunoglobulin-like transcript (ILT) 3. MDSCs zijn een heterogene groep immuuncellen die een belangrijke rol spelen in immuunsuppressie en verhoogd zijn in veel kankerpatiënten. ILT3 kan tot expressie komen op DCs waarbij het een rol speelt in immuuntolerantie. Het kan een interactie aangaan met een nog onbekende ligand op T-cellen waarbij het T-cel anergie, regulatoire T-cellen of T suppressorcellen kan stimuleren. We hebben laten zien dat de relatieve aantallen circulerende MDSCs voor de start van behandeling gecorreleerd zijn met een verminderde overleving. Daarnaast hebben we voor het eerst aangetoond dat ILT3 tot expressie gebracht wordt door een subset van MDSCs en dat deze expressie gecorreleerd is aan verminderde overleving, in de patiënten met verhoogde aantallen MDSCs. Expressie van ILT3 wijst op een additioneel immunosuppressief mechanisme dat gebruikt wordt door MDSCs en relevant is voor de klinische uitkomst in stadium IV longkankerpatiënten. ILT3 zou een aantrekkelijk target kunnen zijn voor een nieuwe therapie.

Vroeg stadium niet-kleincellig longcarcinoom wordt meestal behandeld met een operatie of met stereotactische bestraling (radiotherapie). Onze hypothese was dat deze behandelingen een verschillend effect hebben op het immuunsysteem. In **hoofdstuk 3** vergeleken we de activatie van T-cellen in bloed van dertien patiënten die geopereerd werden en tien patiënten die bestraald werden. We verzamelden bloed voor de start van behandeling en 1, 2, 3 en 6 weken na start van de behandeling. In de analyses middels flowcytometrie werden verschillende markers van T-cel activatie meegenomen, naast de markers die T-cel subsets definiëren (CD8, CD4, FoxP3). Bij de patiënten die geopereerd waren, was een kleine en tijdelijke stijging in delende T-cellen (gekaracteriseerd door Ki67 expressie) te zien. In de bestraalde patiënten zagen we een significante toename in deling van CD4 en CD8 T cellen die stabiel bleef tot week 6 en die samenging met een toegenomen

expressie van programmed death receptor-1 (PD-1), een co-inhibitoir oppervlaktemolecuul dat opgereguleerd wordt nadat de T-cel een antigeen herkent. Binnen de groep van bestraalde patiënten liet de meerderheid van patiënten T cel activatie zien, terwijl dit in een aantal andere patiënten niet geobserveerd werd. Het moet nog onderzocht worden of dit gerelateerd is aan het ontstaan van recidieven in deze patiënten. De toename in T-cel activatie en met name de expressie van PD-1 na bestraling biedt een motivering om radiotherapie te combineren met PD-1 remmers, om deze T-cel activatie te versterken of te verlengen.

In **hoofdstuk 4** bestudeerden we het immunomodulerende effect van de combinatiebehandeling PCB in de NVALT12 studie. Deze behandeling is een standaardbehandeling voor patiënten met stadium IV niet-kleincellig longcarcinoom dat niet van het plaveiselcelsubtype is. Nu er met immuuntherapie een nieuwe behandelmodaliteit beschikbaar is gekomen en daarbij meer mogelijkheden tot combinatietherapie, is het belangrijk om de immunomodulerende eigenschappen van deze chemotherapie te begrijpen.

We bestudeerden het immuunprofiel van deze patiënten in bloed vooraf en gedurende de behandeling op week 0, 3 en 6. We bepaalden relatieve aantallen T cellen, B-cellen en monocytten en verscheidene activatiemarkers op T-cellen door middel van flowcytometrie. We observeerden een significante toename in delende (Ki67-positieve) CD8 T cellen na behandeling. Deze delende CD8 T cellen waren met name van het effector memory subtype en hadden verhoogde expressie van de co-inhibitoire receptoren PD-1 en CTLA-4. Het is eerder aangetoond dat een vergelijkbare subset van delende CD8 T cellen toeneemt na behandeling met PD-1 en PD-1 ligand 1 (PD-L1) remmers in longkanker en melanoom patiënten. Bij melanoom is een verhoogde ratio van delende CD8 T cellen over tumorgrootte, geassocieerd met betere respons op therapie. De toegenomen delende T-cellen in onze studie waren niet gecorreleerd met een verbeterde overleving, maar zou hierdoor wel de gevoeligheid voor checkpointremmers kunnen verhogen.

De meeste immunomonitorstudies concentreren zich op de relatie tussen een specifieke immuunsubset en de respons op therapie of overleving van de patiënt. In **hoofdstuk 5** hadden we de hypothese dat een combinatie van meerdere van deze factoren een verbeterde voorspelling zou kunnen geven op de klinische uitkomst. Flowcytometrie is de meest gebruikte techniek om immuunpopulaties te bestuderen en deze techniek ontwikkelt zich snel, wat zich onder andere uit in een toenemende hoeveelheid markers die tegelijkertijd gemeten kunnen worden op een individuele cel. Om flowcytometriedata te gebruiken om de relatie tussen het immuunprofiel voor behandeling en de overleving

van longkankerpatiënten te onderzoeken is een geschikte data-analysemethode nodig. We gebruikten de recent ontwikkelde FloReMi methode, wat een semiautomatische analysemethode is waarbij variabelen uit flowcytometriedata geëxtraheerd worden en machine learning wordt toegepast om een predictiemodel te genereren die gebruik maakt van de meest relevante variabelen. Van drie sets ruwe flowcytometriedata met elk 12-16 markers, werden meer dan 60 duizend variabelen verkregen, die een afspiegeling waren van de percentages en gemiddelde fluorescentie-intensiteiten (MFIs) van elke mogelijke subset gebaseerd op de beschikbare markers. Deze automatisch verkregen variabelen waren sterk gecorreleerd met de handmatig geanalyseerde variabelen. Een random-forest survival (RFS) model met geselecteerde niet-overlappende variabelen werd getraind en geëvalueerd met een vijfvoudige crossvalidatie. Het RFS-model uit de FloReMi methode presteerde beter dan een RFS-model getraind met handmatig verkregen variabelen en de predictie was significant gecorreleerd aan de daadwerkelijke algehele overleving van patiënten. De meest voorspellende variabele was het percentage HLA-DR<sup>+</sup>CD33<sup>+</sup> myeloïde cellen. We hebben laten zien dat FloReMi een bruikbare methode is om grote aantallen betrouwbare variabelen uit flowcytometriedata te halen, die gebruikt kunnen worden voor de predictie van overleving. De accuraatheid van deze predictie is echter te laag om in de klinische praktijk gebruikt te worden. Deze methode kan dus beter gebruikt worden voor exploratieve doeleinden en het identificeren van nog onbekende immuunpopulaties met klinische relevantie.

In **hoofdstuk 6** van dit proefschrift stelden we ons tot doel om immuuntherapie voor patiënten met maligne pleuraal mesotheliom (MPM) te verbeteren. In het verleden heeft onze onderzoeksgroep een DC-vaccinatie ontwikkeld als nieuwe therapie voor MPM. Autologe gekweekte DCs die zijn beladen met tumorcellysaat kunnen tumor-specifieke T-cellen activeren en daarbij zorgen voor een effectieve anti-tumor immuunrespons. Het is aangetoond dat deze behandeling veilig is voor patiënten. Eén van de grootste limitaties van deze behandeling was echter de beperkte hoeveelheid of kwaliteit van het tumormateriaal dat verkregen kon worden, waardoor veel patiënten uitgesloten werden voor behandeling. In **hoofdstuk 6** gebruikten we allogene tumorcellysaat afkomstig van cellijnen als een alternatieve bron om de DCs mee te beladen. We onderzochten de overleving en het ontstaan van een tumor-specifieke T-celrespons in twee verschillende muismodellen voor mesotheliom, en lieten hierbij zien dat het gebruik van allogene materiaal voor een vergelijkbare effectiviteit zorgde als het gebruik van autologe cellysaten.

Vervolgens startten we een fase I klinische studie waarbij de therapie MesoPher voor het eerst getest werd in mensen. Negen patiënten werden behandeld met een toenemende dosis MesoPher, bestaande uit autologe, vanuit monocyt gekweekte, DCs beladen met de

lysaten van vijf humane mesothelioomcellijnen. Er werden in geen van de cohorten van 10, 25 en 50 miljoen DCs dosis-limiterende toxiciteit gevonden. De mediaan van progressievrije overleving was 8,8 maanden, en de mediaan van algehele overleving werd niet bereikt met een gemiddelde opvolging van 22,8 maanden. Twee patiënten die een dosis van 25 miljoen DCs ontvingen, ondergingen een partiele respons. Deze resultaten bevestigen de veiligheid en haalbaarheid van behandeling met MesoPher. De volgende stap zal zijn de effectiviteit van deze behandeling te bepalen in een opvolgende fase III klinische studie.

In **hoofdstuk 7** monitorde we de immuunresponsen in bloed van de MPM-patiënten die behandeld waren met MesoPher in de fase I klinische studie om tot een beter begrip te komen van het werkingsmechanisme van DC-immunotherapie en om markers te identificeren die geschikt zijn om te monitoren in de toekomstige klinische studies. Perifeer bloed werd verzameld voorafgaand aan de behandeling, en na de eerste drie doses van DC-immunotherapie. We bepaalden de absolute en relatieve aantallen T cellen, B-cellen en monocytten, en karakteriseerden de verschillende T-cel subsets door de expressie van verschillende activatiemarkers en co-stimulatorische en co-inhibitorische receptoren. Daarnaast monitorde we de aanwezigheid van mesotheline-specifieke T-cellen als een indicator van tumor-reactieve T-cellen, en bepaalden we T-cel receptor (TCR) diversiteit door een TCRb PCR-analyse. Zes weken na de start van de behandeling zagen we een toename in de absolute aantallen B cellen en CD4 en CD8 T cellen. Er waren geen veranderingen in de mesotheline-specifieke T-cellen en de TCRb diversiteit. Er was een toegenomen expressie van human leukocyte antigen (HLA)-DR en PD-1 na twee weken en een toegenomen expressie van inducible T cell co-stimulator (ICOS) na zes weken, wat wijst op toegenomen T-cel activatie. CD8 T cellen lieten een lichte verhoging zien in de expressie van lymphocyte-activation gene (LAG)-3 na twee weken. Deze bevindingen duiden erop dat DC-immunotherapie zorgt voor een systemische immuunactivatie die zich met name uit in activatie van CD4 T cellen. Deze markers zouden gebruikt kunnen worden voor het immunomonitoren in toekomstige klinische studies om hun voorspellende waarde en bruikbaarheid als biomarker voor respons te evalueren.

Immunomonitoren in bloed kan inzichten geven in de immunomodulerende effecten van kankerbehandeling. Er bestaan aanmerkelijke verschillen tussen de immunomodulerende effecten van operatie, radiotherapie, chemotherapie en immunotherapie en de verschillende immuunpopulaties hebben een effect op de klinische uitkomst van patiënten met thoracale maligniteiten, zoals beschreven in de **hoofdstukken 2-7**. Al kent perifeer bloed als bron voor immunomonitoren zeker zijn beperkingen, het biedt ook een relatief niet-invasieve manier om op meerdere momenten in de tijd immuuncellen te verkrijgen om immuunactivatie te bestuderen. Immunomonitoren moet daarom zo veel mogelijk geïmplementeerd

worden in klinische studies om ervoor te zorgen dat we, met een focus op de rol van het immuunsysteem, klinische gebeurtenissen kunnen vertalen naar wetenschappelijke kennis die nodig is om nieuwe en verbeterde (combinatie)therapieën te ontwikkelen, vooral in het huidige tijdperk van opkomende immuuntherapieën.



## AUTHOR AFFILIATIONS

Authors are listed in order of appearance. Affiliations of authors are at the time of publication of the chapter.

Koen Bezemer

*Erasmus MC Cancer Institute, Department of Pulmonary Medicine, Rotterdam, The Netherlands*

Marlies E. Heuvers

*Erasmus MC Cancer Institute, Department of Pulmonary Medicine, Rotterdam, The Netherlands*

Anne-Marie C. Dingemans

*Maastricht University Medical Center, Department of Pulmonary Medicine, Maastricht, The Netherlands,*

*Present: Erasmus MC Cancer Institute, Department of Pulmonary Medicine, Rotterdam, The Netherlands*

Harry J.M. Groen

*University of Groningen and University Medical Center Groningen, Department of Pulmonary Medicine, Groningen, The Netherlands,*

Egbert F. Smit

*VU University Medical Center, Department of Pulmonary Medicine, Amsterdam, The Netherlands, Present: Netherlands Cancer Institute, Department of Thoracic Oncology, Amsterdam, The Netherlands,*

Henk C. Hoogsteden

*Erasmus MC, Department of Pulmonary Medicine, Rotterdam, The Netherlands,*

Rudi W. Hendriks

*Erasmus MC, Department of Pulmonary Medicine, Rotterdam, The Netherlands,*

Joachim G.J.V. Aerts

*Erasmus MC Cancer Institute, Department of Pulmonary Medicine, Rotterdam, The Netherlands*

Joost P.J.J. Hegmans

*Erasmus MC Cancer Institute, Department of Pulmonary Medicine, Rotterdam, The Netherlands*

Cynthia Waasdorp

*Erasmus MC Cancer Institute, Department of Pulmonary Medicine, Rotterdam, The Netherlands  
Present: Academic Medical Center, Laboratory for Experimental Oncology and Radiobiology,  
Amsterdam, The Netherlands*

Merel T.B. Schram

*Erasmus MC Cancer Institute, Department of Pulmonary Medicine, Rotterdam and Amphia  
Hospital, Department of Pulmonary Medicine, Breda, The Netherlands*

Margaretha E.H. Kaijen-Lambers

*Erasmus MC Cancer Institute, Department of Pulmonary Medicine, Rotterdam, The Netherlands*

Mark de Mol

*Erasmus MC Cancer Institute, Department of Pulmonary Medicine, Rotterdam and Amphia  
Hospital, Department of Pulmonary Medicine, Breda, The Netherlands*

Koen J. Hartemink

*Netherlands Cancer Institute-Antoni van Leeuwenhoek Hospital, Department of Surgical  
Oncology, Amsterdam, The Netherlands*

Joost J.M.E. Nuyttens

*Erasmus MC, Department of Radiation Oncology, Rotterdam, The Netherlands*

Alexander P.W.M. Maat

*Erasmus MC, Department of Cardio-thoracic Surgery, Rotterdam, The Netherlands*

Suresh Senan

*VU Medical Center, Department of Radiation Oncology, Amsterdam, The Netherlands*

Myrthe Poncin

*Erasmus MC Cancer Institute, Department of Pulmonary Medicine, Rotterdam, The Netherlands*

André Kunert

*Erasmus MC Cancer Institute, Department of Pulmonary Medicine and Department of Medical  
Oncology, Rotterdam, The Netherlands*

Sofie van Gassen

*VIB Center for Inflammation Research and Ghent University, Department of Applied Mathematics, Computer Science and Statistics*

Yvan Saeys

*VIB Center for Inflammation Research and Ghent University, Department of Applied Mathematics, Computer Science and Statistics*

Robin Cornelissen

*Erasmus MC Cancer Institute, Department of Pulmonary Medicine, Rotterdam, The Netherlands*

Cor H. van der Leest

*Erasmus MC Cancer Institute, Department of Pulmonary Medicine, Rotterdam, The Netherlands  
Present: Department of Pulmonary Diseases, Amphia Hospital, Breda, The Netherlands*

Niken M. Mahaweni

*Department of Pulmonary Medicine, Erasmus MC Cancer Institute, Rotterdam, The Netherlands.*

*Present: Department of Transplantation Immunology, Maastricht University Medical Center, Maastricht, the Netherlands*

Ferry A.L.M. Eskens

*Department of Medical Oncology, Erasmus MC Cancer Institute, Rotterdam, The Netherlands.*

Eric Braakman

*Department of Hematology, Erasmus MC Cancer Institute, Rotterdam, The Netherlands.*

Bronno van der Holt

*Department of Hematology, Erasmus MC Cancer Institute, Rotterdam, The Netherlands.*

Arnold G. Vulto

*Hospital Pharmacy, Erasmus MC, Rotterdam, The Netherlands.*

Yarne Klaver

*Erasmus MC Cancer Institute, Department of Medical Oncology, Rotterdam, The Netherlands*

Anton W. Langerak

*Erasmus MC, Department of Immunology, Rotterdam, the Netherlands*

Heleen Vroman

*Erasmus MC Cancer Institute, Department of Pulmonary Medicine, Rotterdam, The Netherlands*

Cor H. Lamers

*Erasmus MC Cancer Institute, Department of Medical Oncology, Rotterdam, The Netherlands*

Reno Debets

*Erasmus MC Cancer Institute, Department of Medical Oncology, Rotterdam, The Netherlands*

## DANKWOORD

Dit proefschrift was niet tot stand gekomen zonder de hulp van een heel aantal mensen. Soms heel direct door medewerking aan dit proefschrift, soms meer indirect door mij de omgeving en steun te bieden die het mogelijk maakte dit onderzoek succesvol uit te voeren. Graag wil ik mijn dank uitspreken naar de volgende mensen.

Allereerst mijn promotoren prof.dr. J.G.J.V. Aerts en prof.dr. R.W. Hendriks. Beste Joachim, bedankt dat ik onder jouw leiding dit promotieonderzoek mocht uitvoeren. Je klinische blik in combinatie met je passie voor wetenschappelijke ontwikkeling is zeer waardevol en inspireren en ik bewonder hierin je ambitie. Met altijd de patiënt in gedachten breng je wetenschappelijke kennis naar de klinische praktijk, met als belangrijkste voorbeeld natuurlijk de DC immunotherapie. Beste Rudi, bedankt voor de begeleiding met name in de tweede helft van mijn promotietraject. Je kritische wetenschappelijke blik en enorme immunologische kennis hebben mijn hoofdstukken elke keer naar een hoger niveau getild. Je enthousiasme en betrokkenheid zorgen er voor dat lab longziekten zo'n prettige plek is om te werken.

Beste Joost, bedankt voor de begeleiding tijdens het begin van mijn promotietraject. Je liet mij me direct op mijn plek voelen in het ThoRR team en introduceerde me in het veld van de tumor-immunologie. Je hebt me aangestoken met je enthousiasme voor immunotherapie, wat nog steeds mijn grootste drijfveer als wetenschapper is.

De vele uren op het lab heb ik gelukkig niet alleen hoeven besteden. Margaretha, jij bent van enorme waarde geweest voor het werk in de meeste van mijn hoofdstukken. Je jarenlange ervaring in het lab en binnen het ThoRR team was enorm waardevol en je hebt me veel kunnen leren. Maar daarnaast kon ik ook altijd bij je terecht voor een praatje, om even te ventileren of te filosoferen, wat heel fijn was en minstens zo belangrijk. Koen, jij leerde mij de belangrijkste techniek voor mijn onderzoek, flow cytometrie. Ook maakte je mij wegwijs in de NVALT12 studie, waar je voor mijn komst al heel wat werk aan had gedaan en wat maakte dat ik een soepele start kon maken aan het project. Daarnaast ook bedankt voor alle gezelligheid! Cynthia, de Hamletstudie was niet mogelijk geweest zonder jouw hulp. Het verzamelen en verwerken van alle bloedsamples was een hele klus, maar jij traceerde elk sample en hielp me met het opzetten van de kleuringen, wat tot een mooi resultaat heeft geleid! Yarne, bedankt voor de samenwerking bij de immuunmonitoring van de MM03. Het was fijn om samen te kunnen sparren over het project en of we nou optimistisch of pessimistisch waren over onze experimenten, was het altijd gezellig om samen in het lab te werken. Reno en Cor, bedankt voor de samenwerking bij dit project.

Ik stond op het punt me te verdiepen in de bioinformatica en om R te leren, en toen klopte er ineens een student aan met een interesse voor zowel labwerk als bioinformatica. Myrthe, ik ben blij dat ik je tijdens je dubbele stage heb mogen begeleiden, waarbij je een belangrijke bijdrage hebt geleverd aan twee hoofdstukken van mijn proefschrift. Maar je was vooral ook een labmaatje, Gentmaatje, R-maatje en niet te vergeten borrelmaatje, ook nadat je stage al was afgelopen en je als analist bij longziekten aan de slag ging.

Over R en bioinformatica gesproken: Sofie en Yvan, enorm bedankt voor de mogelijkheid om de FloReMi pipeline te leren en toe te passen in mijn onderzoek. Ik liep al een tijdje met het idee rond dat er uitgebreidere data-analyses nodig waren voor de complexe en grote datasets die ik genereerde, maar jullie waren het die dit daadwerkelijk konden en beter nog, het mij konden leren. Sofie, bedankt voor al je geduld en hulp en het oplossen van vele errors! Ik ben ook blij om te zien dat onze samenwerking meer mensen bij longziekten heeft geïnspireerd om met R, FloReMi en FlowSOM aan de slag te gaan.

Een PhD traject zit vol pieken en dalen. Gelukkig zaten er meer mensen in hetzelfde schuitje, wat een belangrijke steun geeft en inspiratie biedt. Sanne en Sabine, vanaf mijn start in de ThORR groep kon ik bij jullie terecht met mijn PhD beginnersvragen. Bedankt voor de gezelligheid op de kamer gedurende onze overlappende ThORR tijd. Floris, bedankt voor je input op mijn projecten bij de vele werkbesprekingen, de gezelligheid in het lab en tijdens onze congres- en skiavonturen in Canada! Onderzoek is nooit klaar, dus ik ben blij met de volgende ThORR generatie. Sai Ping, Joanne, Bob en Mandy, succes met jullie onderzoek in het meest *exciting* onderzoeksveld. Heleen, fijn dat jij je na je PhD bij longziekten ook bij het ThORR team wilde voegen. Met je DC kennis en betrokken en geïnteresseerde aard ben je een hele waardevolle toevoeging aan het team! *André, thanks for the many conversations over coffee, your input on my projects but also the many discussions on career paths, which shaped my plans on what to do after my PhD.* Heleen en Denise, bedankt voor de vele koffietjes en goede gesprekken. Irma, Bobby, Tridib en Simar, bedankt voor alle gezelligheid, steun en inspiratie op vele momenten op werk maar ook buiten werk, vooral ook in de tijd dat ik nog op mijn proefschrift aan het zwoegen was maar niet meer op Ee22 rond liep en wel wat aanmoediging kon gebruiken. Irma, ik vind het super leuk dat je als paranimf aan mijn zijde staat!

Alle andere collega's van de afdeling longziekten die ik niet bij naam heb kunnen noemen wil ik ook bedanken voor de fijne tijd en gezelligheid op de afdeling!

Ik ben erg dankbaar dat ik voor mijn onderzoek gebruik heb kunnen maken van zo veel patiëntmateriaal. Mijn dank gaat dus ook zeker uit naar alle patiënten die mee hebben

gewerkt aan de verschillende klinische studies. Daarnaast ook veel dank aan de research consultants van de afdeling longziekten en de artsen die dit mogelijk hebben kunnen maken!

Intussen ben ik alweer een tijdje aan de slag bij mijn volgende baan. Lieve collega's van Genmab, bedankt voor een warm welkom en de ruimte die mij geboden is om de laatste hand aan mijn proefschrift te kunnen leggen. De voldoening die ik haal uit mijn huidige werk bevestigde opnieuw mijn keuze voor dit PhD traject.

Lieve vrienden, ik weet niet wat ik zonder jullie had ontmoeten. SH: Daisy, Fenna, Jorinde, Laura, Myora, Nina en Simone, jullie zijn geweldig! En het geeft zo veel kracht om te weten dat als ik jullie nodig heb, jullie nog dezelfde avond allemaal bij me op de stoep zullen staan. Fenna, wij hebben al zo ontzettend veel samen meegemaakt in ruim 18(!) jaar vriendschap. Ik ben blij dat ik daar mijn verdediging aan toe kan voegen, met jou als paranimf! Anita, Lianne, Suzanne, Vincent en Xiamyra, mijn Stockholm chicks. Van het delen van PhD-perikelen en wetenschappelijke (biomedische) discussies tot de minder subtiele gespreksonderwerpen. Dank voor het delen van vele wijntjes en de vriendschap! Inger, Marjolein en Yumke, Judith, Omar en de lieve smulcommeisjes: ook jullie hebben mij er op veel momenten doorheen gesleept. Tijdens een PhD kan je je soms een beetje te veel gaan identificeren met je project. Gezelligheid en goede gesprekken zijn zo belangrijk om te kunnen blijven relativeren!

Emma en Ludo, wat zijn jullie toch mooie mensen. Uit hetzelfde nest en in veel opzichten zo lijkend op mij maar toch ook zo verschillend. Ik ben trots op jullie en trots op ons als team! Dankjewel voor jullie steun. Emma, ik vind de omslag van mijn proefschrift echt fantastisch geworden, bedankt voor je creatieve ontwerp!

Papa en mama, ik word er verdrietig van dat ik jullie niet meer als eenheid aan kan spreken, maar dat zijn jullie voor mij nog steeds. De basis van wie ik ben en alles wat ik heb gedaan. De basis waar ik altijd op terug kon vallen. Mama, ik mis je zo onvoorstelbaar veel en het doet me pijn dat je mijn verdediging niet meer kan meemaken. Je bent me in mijn hele PhD traject zoveel tot steun geweest. Misschien snapte je inhoudelijk geen bal van mijn onderzoek, maar was toch zo geïnteresseerd. Je begreep als geen ander hoe ik in elkaar zat, wat mijn drijfveren en valkuilen waren, waardoor je me kon helpen en adviseren zonder ooit te oordelen of te sturen. Papa, mijn wetenschappelijke interesse heb ik voor zo'n groot deel aan jou te danken. Je leerde me eerst vele vogelnamen, toen alle planeten van het sterrenstelsel en we losten samen allerlei wiskundige puzzels op, nog voordat ik op de middelbare school zat. Je bracht me veel wijsheid, zelfstandigheid en een kritische blik

mee, belangrijke vaardigheden voor het volbrengen van een PhD. Ik voel me door jou altijd vertrouwd en gewaardeerd. Jouw steun zit hem meestal niet in woorden maar is daardoor zeker niet minder voelbaar!

Lieve Ewoud, jij hebt al mijn ups en downs van dichtbij meegemaakt en begreep door je eigen PhD traject ook precies wat ik doormaakte. Je hielp me de successen te vieren en moeilijke momenten te relativieren, en was eindeloos geduldig in het aanhoren van al mijn verhalen. Je laat me elke keer inzien wat er belangrijk is in het leven. Dank je voor jouw liefde en steun gedurende al die tijd.

Pauline



## PHD PORTFOLIO

**Name PhD student:** drs. P. L. de Goeje  
**Erasmus MC Department:** Pulmonary Medicine  
**Research School:** Molecular Medicine

**PhD period:** 2014-2019  
**Promotors:** Prof. dr. J. Aerts & prof. dr. R.W. Hendriks

	<b>Year</b>	<b>ECTS</b>
<b>General courses</b>	2014	2
Biomedical English Writing Course	2015	1
Research Management course		
Research Integrity		
<b>Specific courses</b>	2014	0.7
MolMed Course	2015	1.4
CE08: Repeated Measurements course (NIHES)	2015	
Coursera R Programming course	2015	1.4
MolMed course on R	2015	1
BD Horizon Tour 2.0	2016	3
Advanced Immunology course		
<b>Conferences and meetings</b>	2014	0.3
18 <sup>th</sup> MolMed day	2014	1
Longdagen (poster)	2014	1
CIMT	2014	1
NVVI Annual Meeting	2015	1
CIMT (poster)	2016	1
Daniel den Hoed day (oral presentation)	2016	1
MolMed day (oral presentation)	2016	1
CIMT (poster)	2016	1
NVVI-BSI Joint Meeting (poster)	2017	1
Keystone symposium "Cancer Immunology and Immunotherapy" (poster)	2017	1
MPM meeting Essen (oral presentation)	2018	1
T cell consortium meeting (oral presentation)		
<b>Teaching</b>	2015-2016	8
Supervision of Bachelor student graduation internship		

## ABOUT THE AUTHOR

Pauline Linda de Goeje was born on 30 July 1989 in Delft, as first child of Marius de Goeje and Juliaan van der Linden. She finished her high school (gymnasium) at Dalton Voorburg in 2007 and in the same year started here Bachelor studies Biomedical Sciences at the Leiden University Medical Center (LUMC). During her second year, she was selected for an Erasmus exchange program to study at Karolinska Institutet in Stockholm, Sweden for one semester. After an internship at the department of Molecular Epidemiology at the LUMC, she obtained her Bachelor's degree in 2011. She then continued with the Master Biomedical Sciences including an internship at the department of Thrombosis and Hemostasis at the LUMC, an elective internship at DKFZ Heidelberg, Germany and an internship at the Daniel Peeper lab at the Netherlands Cancer Institute under the supervision of dr. Renée van Amerongen. During both her Bachelor and Master studies she participated actively in several student societies, by joining several committees and board member functions. She graduated in September 2013 and her final thesis was published as a review in *Cancer Research* in 2014.

Her interest in both oncology and immunology came together in the PhD project that she started at the department of Pulmonary Medicine after returning from three months solo traveling in January 2014. She studied the role of the immune system in patients with thoracic malignancies, under the supervision of Joost Hegmans, Joachim Aerts and Rudi Hendriks. During her years as a PhD candidate, Pauline was also a board member of the Promeras and in this position member of Promovendi Netwerk Nederland (PNN), representing PhD candidates of the Erasmus MC and the Netherlands, respectively. In her research, Pauline investigated the role of several immune subsets on the clinical outcome in cancer patients, and the immune modulatory effect of several cancer treatments, of which the results are presented in this thesis. She started collaborations with VIB Ghent and with the department of Medical Oncology, both of which led to a chapter in this thesis.

In October 2018, Pauline joined Genmab where she is currently working as a scientist at the New Antibody Products Research department.



